PRESENT STATUS OF VEPP-2000*

Dmitry Shwartz, Dmitry Berkaev, Alexander Kirpotin, Ivan Koop, Alexander Lysenko, Igor Nesterenko, Evgeny Perevedentsev, Yury Rogovsky, Alexander Romanov, Petr Shatunov, Yuri Shatunov, Alexander Skrinsky, Ilya Zemlyansky BINP SB RAS, 630090 Novosibirsk, Russia

Abstract

VEPP-2000 electron-positron collider has been completed in the Budker INP in 2007. First beam was captured in a special lattice with switched off final focus solenoids. This regime is used for all machine subsystems test and calibration as well as vacuum chamber treatment by synchrotron radiation with electron beam current up to 150 mA. Another special low-beta lattice with solenoids switched on partially was used for the first test of the round beam option at the energy of 508 MeV. Studies of the beam-beam interaction were done in "weak-strong" and "strong-strong" regimes. Measurements of the beam sizes in both cases have indicated beam behaviour similar to expectations for the round colliding beams. Also the first collider energy calibration at the phi-meson resonance was performed with SND detector. Since the end of 2009 VEPP-2000 started first experimental work with both particle detectors SND and CMD-3 at the energies of 500-950 MeV range with the lattice mode close to project. The precise energy calibration via resonant depolarization method is in progress.

INTRODUCTION

At BINP for more than quarter of century the electron-positron collider VEPP-2M has been operated in the energy range of 0.4 ÷ 1.4 GeV. For a long time its results were the main source of information about hadrons production in this energy range. On the other hand, a whole number of events collected by different experimental groups in the energy span above VEPP-2M (up to 2 GeV) doesn't exceed 10 % of the data accumulated by VEPP-2M. These motivations caused a decision to create instead of VEPP-2M collider a new machine with higher luminosity (up to 10^{32} $cm^{-2}s^{-1}$) and the beam energy up to 2×1 GeV.

To achieve the final goals (luminosity and energy), the Round Beam Concept was applied in design of the machine optics [1]. The main feature of this concept is rotational symmetry of the kick from the round opposite beam. Together with the x – z symmetry of the betatron transfer matrix between the collisions, it results in particle's angular momentum conservation ($M = xz' - zx' = const$). As a consequence, it yields an enhancement of dynamical stability, even with nonlinear effects from the beam-beam force taken into account.

Computer simulations of the beam-beam interaction in "weak-strong" and "strong-strong" situations confirmed these expectations [2, 3].

*Work supported by RFBR grant, project No. 09-02-01060-a

COLLIDER OVERVIEW

The accelerator complex consists of VEPP-2000 collider itself and injection system including 900 MeV booster of electrons and positrons BEP and injection channels also designed for energy of 900 MeV.

Magnetic structure of VEPP-2000 [4] has the 2-fold symmetry. It includes two (3 m long) experimental straight sections, two straights (2.5 m) for beams injection and RF cavity and 4 short technical straights with 4 triplets of quadrupole magnets. Each triplet together with two 2.4 T bending magnets forms an 90° achromat.

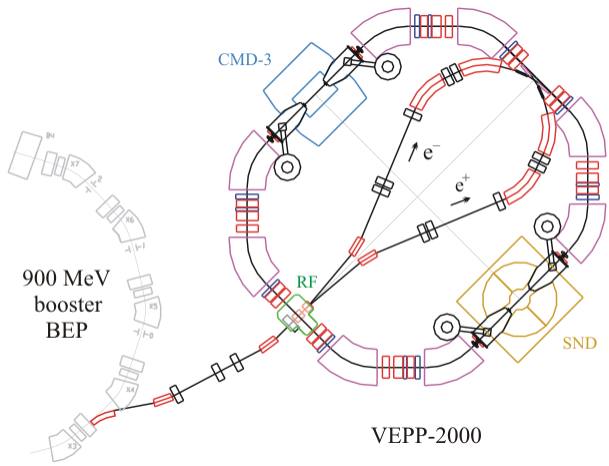

Figure 1: VEPP-2000 layout.

The RBC at VEPP-2000 was implemented by placing into Interaction Regions two pairs of superconducting solenoids symmetrically with respect to collision points.

Table 1: VEPP-2000 Main Parameters (at $E = 1$ *GeV*)

Parameter	Value
Circumference, Π	24.39 m
Betatron functions at IP, $\beta^*_{x,z}$	10 cm
Betatron tunes, $\nu_{x,z}$	4.1, 2.1
Beam emittance, $\varepsilon_{x,z}$	1.4×10^{-7} m rad
Momentum compaction, α	0.036
Synchrotron tune, ν_s	0.0035
Energy spread, $\sigma_{\Delta E/E}$	6.4×10^{-4}
RF frequency	172 MHz
RF harmonic number, q	14

CRAB WAIST APPROACH: FROM DAΦNE TO SUPERB

M. Zobov, INFN LNF, Frascati, Italy
on behalf of the DAΦNE Collaboration Team* and the SuperB Accelerator Team#

Abstract

The crab waist collision scheme (CW) was proposed and successfully tested at the Φ-factory DAΦNE. At present this scheme is considered to be most attractive for the next generation lepton factories. In particular, the novel scheme is a key element of the SuperB project, a new SuperB-factory with luminosity about two orders of magnitude higher than that achieved at the present B-factories (KEKB and PEPII). In this paper we summarize the results achieved at DAΦNE after implementation of the CW collision scheme and discuss the status of the SuperB project.

INTRODUCTION

Pushing the luminosity of storage-ring colliders to unprecedented levels opens up unique opportunities for precision measurements of rare decay modes and extremely small cross sections, which are sensitive to new physics beyond the Standard Model.

Present generation lepton factories have been very successful in achieving their design luminosity performances [1]. However, new ideas were required in order to achieve a further substantial luminosity increase. Indeed, several novel collision concepts and new collision schemes have been proposed to provide such a qualitative step in the luminosity increase. The most known are the following: round beam collision preserving an additional integral of motion [2]; crab crossing [3, 4]; collision with large Piwinski angle [5] ("superbunch" in hadron colliders [6, 7]); longitudinal strong RF focusing [8]; collision with travelling waist [9]; crab waist collision [10, 11].

Now the crab waist collision scheme is considered to be most prominent for the next generation factories since it holds the promise of increasing the luminosity of the storage-ring colliders by 1-2 orders of magnitude beyond the current state-of-art, without any significant increase in beam current and without reducing the bunch length.

The CW scheme has been successfully tested at the electron-positron collider DAΦNE [12], the Italian Φ-factory operating at the energy of 1020 MeV in the center of mass. After an upgrade including the implementation of this novel collision scheme, the specific luminosity at low beam currents has been boosted by more than a factor of 4, while the present peak luminosity, 4.53×10^{32} $cm^{-2}s^{-1}$, is a factor of 3 higher than the maximum value obtained with the original configuration based on the standard collision scheme. The achieved peak luminosity is close (within 10%) to the design value in good agreement with numerical simulations [13].

The successful test has provided the opportunity to continue the DAΦNE Physics program. Moreover, advantages of the CW collision scheme have triggered several collider projects exploiting its potential [14, 15, and 16]. In particular, an international collaboration is pursuing the SuperB project [14] aiming at constructing in Italy a very high luminosity asymmetric collider at the Y(4S) energy in the center of mass. The new SuperB factory is expected to reach a luminosity as high as 10^{36} $cm^{-2}s^{-1}$, i.e. 2 orders of magnitude higher than that achieved at present B-factories (KEKB and PEPII).

In the first section of this paper we discuss the basic concept and advantages of the CW scheme. In the following section we briefly describe results of the CW experimental test at DAΦNE. Finally, we overview the status of the SuperB accelerator project.

CRAB WAIST COLLISION SCHEME

The CW scheme can substantially increase collider luminosity since it combines several potentially advantageous ideas: collisions with a large Piwinski angle, micro-beta insertions and suppression of beam-beam resonances using dedicated ("crab waist") sextupoles. Let us consider two bunches colliding under a horizontal crossing angle θ (as shown in Fig. 1a). Then, the CW principle can be explained, somewhat artificially, in three basic steps.

*DAΦNE Team: D.Alesini, M.E.Biagini, C.Biscari, A.Bocci, R.Boni, M.Boscolo, F.Bossi, B.Buonomo, A.Clozza, G.O.Delle Monache, T.Demma, E.Di Pasquale, G.Di Pirro, A.Drago, A.Gallo, A.Ghigo, S.Guiducci, C.Ligi, F.Marcellini, G.Mazzitelli, C.Milardi, F.Murtas, L.Pellegrino, M.A.Preger, L.Quintieri, P.Raimondi, R.Ricci, U.Rotundo, C.Sanelli, M.Serio, F.Sgamma, B.Spataro, A.Stecchi, A.Stella, S.Tomassini, C.Vaccarezza, M.Zobov (LNF INFN); M.Schioppa (INFN,Cosenza); M.Esposito (La Sapienza); P.Branchini (INFN, Rome 3); F.Iacoangeli, P.Valente (INFN,Rome); E.Levichev, P.Piminov, D.Shatilov, V.Smaluk (BINP); N.Arnaud, D.Breton, L.Burmistrov, A.Stocchi, A.Variola, B.F.Viaud (LAL); S.Bettoni (CERN); K.Ohmi (KEK); D.Teytelman (Dimtel Inc.).

#SuperB Team: M.E.Biagini, R.Boni, M.Boscolo, B.Buonomo, T.Demma, A.Drago, S.Guiducci, G.Mazzitelli, L.Pellegrino, M.A.Preger, P.Raimondi, R.Ricci, C.Sanelli, M.Serio, A.Stella, S.Tomassini, M.Zobov (LNF INFN); K.Bertsche, A.Brachmann, A.Chao, R.Chestnut, M.Donald, C.Field, A.Fisher, D.Kharakh, A.Krasnykh, K.Moffeit, Y.Nosochkov, A.Novokhatski, M.Pivi, J.Seeman, M.K.Sullivan, A.Weidemann, J.Weisend, U.Wienands, W.Wittmer, M.Woods (SLAC); A.Bogomiagkov, I.Koop, E.Levichev, S.Nikitin, I.Okunev, P.Piminov, S.Siniyatkin, D.Shatilov, P.Vobly (BINP); F.Bosi, S.Liuzzo, E.Paoloni (Pisa University); J.Bonis, R.Chehab, O.Dadoun, G.Le Meur, P.Lepercq, F.Letellier-Cohen, B.Mercier, F.Poirier, C.Prevost, C.Rimbault, F.Touze, A.Variola (LAL); B.Bolzon, L.Brunetti, A.Jeremie (LAPP, Annecy); M.Baylac, O.Bourrion, J.M.DeConto, Y.Gomez, F.Meot, N.Monseu, D.Tourres, C.Vescovi (LPSC, Grenoble); A.Chancé, O.Napoly (CEA Saclay); D.P.Barber (DESY, Cockcroft Institute, Universty of Liverpool); S.Bettoni, D.Quatraro (CERN).

ACCELERATOR ASPECTS OF THE PRECISION MASS MEASUREMENT EXPERIMENTS AT THE VEPP-4M COLLIDER WITH THE KEDR DETECTOR *

Sergei Nikitin† for the VEPP-4 Team, BINP SB RAS, Novosibirsk

Abstract

Two methods for particle energy measurement are realized at the electron-positron collider VEPP-4M: one based on the resonant depolarization technique and another using the Back Compton Scattering. KEDR detector measurements of the J/Psi-, Psi' mesons and the tau-lepton masses performed with the help of these methods is better in accuracy now in the world. Peculiarities of the beam energy calibraton as well as of the mass measurement experiments are represented in the viewpoint of requirements on beam parameters and accelerator systems.

INTRODUCTION

The VEPP-4 accelerator facility with electron-positron colliding beams is known by the experiments on high precision calibration of the fundamental mass scale since the early eighties [1]. In 2002, the new series of similar experiments was started at VEPP-4M, the modernized collider ring, with the KEDR versatile magnetic detector. We improved the J/ψ and $\psi(2s)$ mass accuracy by a factor of 3-4 as compared with the world average one which had been based on our resuts of 80s. Owing to this fact, the J/Psi and Psi(2s) meson masses are now among the ten most accurate elementary particle masses measured over the entire history of physics. The measurement of the tau-lepton mass at its production threshold performed at the VEPP-4M collider is most accurate to date [2]. We obtained the D^0- and $D^{\pm}$-meson mass values (the second and the best results in accuracy, respectively) matching with the world average data.

The following activities at VEPP-4 contributed to so high precise results:
- the beam polarization measurement and beam energy monitoring methods including the new ones were developed and applied;
- the problems on accuracy of energy calibration by spin precession frequency were studied at new level;
- the questions on optimal tuning of VEPP-4 systems and operation modes for obtaining and application of beam polarization in mass measurements were set and resolved.

* Work was supported in a part by RFBR 01-02-17477, 04-02-16745, 07-02-00426, 04-02-16665, 07-02-00661

† nikitins@inp.nsk.su

BEAM ENERGY CALIBRATION

Resonant Depolarization technique

The Resonant Depolarization (RD) technique for measuring the beam energy was proposed and implemented for the first time at BINP [3]. This approach was widely used thereafter both at the BINP and in other laboratories throughout the world.

In an ideal storage ring with the planar orbits, the average energy of electrons in a beam E is related to the average spin precession frequency Ω by the simple equation

$$E = mc^2\gamma = mc^2 \cdot \frac{q_0}{q'} \cdot \left(\frac{\Omega}{\omega_0} - 1\right) = 440.64843(3) \cdot \nu,$$

with q' and q_0, the anomalous and normal parts of the gyromagnetic ratio; ω_0, the revolution frequency; $\nu = \gamma q'/q_0$, the spin tune parameter. Limiting accuracy of the energy determination by the spin frequency $\delta E/E \approx 7.8 \cdot 10^{-8}$ is due to errors in knowledge of the fundamental constants. To measure Ω one needs to have a polarized beam in a storage ring, a system to observe the beam polarization as well as a system for enforced beam depolarization at the external spin resonance.

State of the VEPP-4M beam polarization at energies up to 2 GeV is observed by comparison of the Touschek electron/positron counting rate from the polarized and unpolarized bunches separated by a half turn ("two bunch method") [4]. The system of scintillation counters installed at several azimuths and put into the dynamic aperture provides a total counting rate $\sim$ 1 MHz/mA at the distance of counters to the beam orbit $\approx$ 1 cm. The relative counting rate experiences a jump $\sim$ 1% at the moment of depolarization proportional to squared level of polarization.

The two matched striplines of the VEPP-4 kicker are used to create a TEM wave propagating towards the beam. The signal source is a frequency synthesizer with a minimal frequency step of 0.35 mHz [4]. Scan rate and the TEM wave amplitude are tuned to provide the depolarization time $\sim$ 1 second. The reference frequency signal for the synthesizer as well as for the VEPP-4M RF system is generated by the rubidium frequency standard (10^{-10}). Typical behavior of the measured effect in a time and the depolarization jump are shown in Fig.1. Absolute energy RD calibration accuracy is of a record level: $\delta E/E \sim 10^{-6}$. It is determined by the spin tune spread $\delta\nu/\nu \sim 5 \cdot 10^{-7}$ due to quantum diffusion of particle trajectories taking into account a quadratic non-linearity of the VEPP-4M guide field. To date more than 3000 RD calibrations has been performed.

PROJECT OF THE NUCLOTRON-BASED ION COLLIDER FACILITY (NICA) AT JINR

G. Trubnikov, N. Agapov, V. Alexandrov, A. Butenko, E. Donets, A. Eliseev, V.V.Fimushkin, Yu. Filatov, A.Govorov, V.Karpinsky, T. Katayama, V. Kekelidze, H. Khodzhibagiyan, V. Kobets, S.Kostromin, A. Kovalenko, O. Kozlov, A. Kuznetsov, I. Meshkov, V. Mikhaylov, V. Monchinsky, V. Shevtsov, A. Sidorin, A. Sissakian, A. Smirnov, A. Sorin, V. Toneev, V. Volkov, V. Zhabitsky, O. Brovko, JINR, Dubna, Russia

Abstract

The Nuclotron-based Ion Collider fAcility (NICA) is the new accelerator complex being constructed at JINR aimed to provide collider experiments with heavy ions up to uranium at the center of mass energy from 4 to 11 GeV/amu. It includes 6 MeV/amu heavy ion linac, 600 MeV/amu booster, upgraded Super Conducting (SC) synchrotron Nuclotron and collider consisting of two SC rings, which provide average luminosity of the level of 10^{27}cm^{-2}s^{-1}.

INTRODUCTION

The goal of the NICA project is construction at JINR of the new accelerator facility that consists of (see Fig.1)

- cryogenic heavy ion source of Electron String type (ESIS),
- source of polarized protons and deuterons,
- the existing linac LU-20,
- a new heavy ion linear accelerator (HILAc) [1],
- a new SC Booster-synchrotron (that will be placed inside the decommissioned Synchrophasotron yoke),
- the existing proton and heavy ion synchrotron Nuclotron (located in the basement of the Synchrophasatron building) [2],
- two new SC storage rings of the collider,
- a new system of beam transfer channels.

The facility will have to provide ion-ion (1÷4.5 GeV/amu of the ion kinetic energy), ion-proton collisions and polarized proton-proton (5÷12.6 GeV) and deuteron-deuteron (2÷5.8 GeV/amu) beams collisions.

As a result of the project realization, the potential of the Nuclotron accelerator complex will be sufficiently increased in all the fields of its current physics program. The fixed target experiments with slow extracted Nuclotron beams are presumed the experiments with internal target as well. The Booster will be equipped with a slow extraction system to perform radio-biological and applied researches using heavy ion beams.

The collider will have two interaction points. The Multi Purpose Detector (MPD), aimed for experimental study of hot and dense strongly interacting QCD matter and search for possible manifestation of signs of the mixed phase and critical endpoint in heavy ion collisions, is located in one of them. The second one is used for the Spin Physics Detector (SPD).

Main goal of the NICA facility construction is to provide collider experiment with heavy ions like Au, Pb or U at luminosity above $1\cdot10^{27}$ cm$^{-2}\cdot$s^{-1} at the energy of 3.5 GeV/amu. It was decided to choose the Gold nuclei $^{197}Au^{79+}$ as the reference particles for the heavy ion collider mode. In the collisions of polarized beams the luminosity above $1\cdot10^{31}$ cm$^{-2}\cdot$s^{-1} is planned to be achieved in the total energy range.

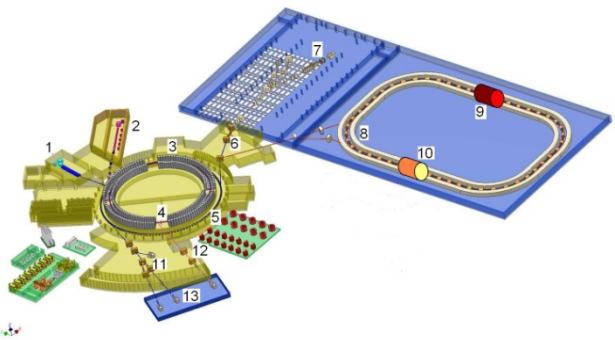

Fig. 1. Scheme of NICA facility: 1 – light and polarized ion sources and "old" Alvarez-type linac; 2 – ESIS source and new RFQ linac; 3 – Synchrophasotron yoke; 4 – Booster; 5 – Nuclotron; 6 – beam transfer line; 7 – Nuclotron beam lines and fixed target experiments; 8 – Collider; 9 – MPD; 10 – SPD; 11, 12 – transfer lines; 13 – new research

The essential features of the project permitting to minimize its cost, the construction period and to realize a wide experimental program are the following:

- Collider facility does allow independent carrying out the fixed target experiments;
- The facility can be used for collider experiments with light and middle weight ions including polarized deuterons;
- The required modifications of the Nuclotron ring including development of the ion sources are realizing within the project of the Nuclotron upgrade, which will be completed in 2010 [3];
- Choice of optimal Booster design based on a few possible versions made before;
- Application of recent world data obtained at BNL, CERN and GSI for achievement of a high collider luminosity;
- Wide co-operation with JINR Member State

OPTICS DESIGN FOR NICA COLLIDER

S.Kostromin, O.Kozlov, I.Meshkov, V.Mikhailov, A.Sidorin, G. Trubnikov, JINR, Dubna
V.Lebedev, S.Nagaitsev, FNAL, Batavia, Illinois, USA, Yu.Senichev, IKP, Juelich, Germany

Abstract

The Nuclotron-based Ion Collider fAcility (NICA) [1] is a new accelerator complex being constructed at JINR. It is designed for collider experiments with ions and protons and has to provide ion-ion (Au^{79+}) and ion-proton collisions in the energy range 1÷4.5 GeV/n and collisions of polarized proton-proton and deuteron-deuteron beams.

Collider conceptions with constant γ_{tr} and with possibility of its variation are considered. The ring has the racetrack shape with two arcs and two long straight sections. Its circumference is about 450m. The straight sections are optimized to have β^*~35cm in two IPs and a possibility of final betatron tune adjustment.

INTRODUCTION

NICA collider lattice development has a number of challenges which must be overcome in the design process. The requirements set by physics goals are: changeable energy of the Au-ions collision in the range 1÷4.5 GeV/n, operation with different ion mass (Au^{79+}, deuterons and protons), the peak luminosity up to $5\cdot10^{27}$ $cm^{-2}s^{-1}$ at 4.5 GeV/n, and, additionally, the collider rings must fit into existing JINR infrastructure.

The ring lattice is based on super-ferric magnets with 2T bending field. The technology of fabrication of such magnets operating at 4.5K with hollow composite NbTi cable is well established in JINR.

The main luminosity limitation is set by the direct space charge tune shift. In this case the luminosity is proportional to the beam emittance and, consequently, to the collider acceptance. Thus, good optics for NICA implies that in addition to the standard requirement of small beta-function in IP, β^*, there is a requirement of maximizing the machine acceptance.

INTRA-BEAM SCATTERING STUDY

The intra-beam scattering (IBS) is one of the main factors which have to be taken into account in a collider ring design. For operation below transition IBS is significantly reduced if the local beam temperatures averaged over the ring are equal. In this case the emittance growth rate due to IBS is equal to zero for a perfectly smooth lattice. Beta-function and dispersion variations destroy this thermal equilibrium resulting in an emittance growth in all three planes: larger variations excite faster emittance growth.

First, the IBS rates were computed for the ideal rings (without straight sections) constructed from ODFDO - and FODO -cells [2]. For the same number of particles the beam emittances were adjusted to have the same growth rates for all planes (thermal equilibrium) and to have the same vertical space charge tune shift (bunch density). Due to"smother" optics the IBS heating rate, τ_{IBS}^{-1}, for the ring based on the triplet cells is ~5 times smaller than for the singlet cells ring with the same phase advance per cell. Therefore the ODFDO-cell ring was chosen as a reference for the collider optics.

A transition from the ideal ring to the collider optics with low-β straight sections increases β-function and dispersion variations and yields an increase of IBS rates. Finally, the collider ring lattice based on FODO-cells has only ~1.5 times larger rates: the growth time of ~890 s versus ~1350 s for the luminosity of $6\cdot10^{27}$ $cm^{-2}s^{-1}$.

Table 1: Main parameters of the collider rings optics

Beam species and energy	Au^{79+}, 4.5 GeV/n
Ring circumference	454 m
Gamma-transition, γ_{tr}	6.22
Betatron tunes	9.46 / 9.46
Particles per bunch (of 20 bunches)	$5.3\cdot10^{9}$
Acceptance	40 π mm mrad
Longitudinal acceptance, Δp/p	+/- 0.0125
RMS emittance, $\varepsilon_x/\varepsilon_y$	1.1/0.6 π mm mrad
Beta function at IP, β^*	35 cm
Rms bunch length	60 cm
IBS growth time	1350 s
Luminosity (for Au^{79+} 4.5 GeV/n)	$6\cdot10^{27}$ cm^{-2} s^{-1}

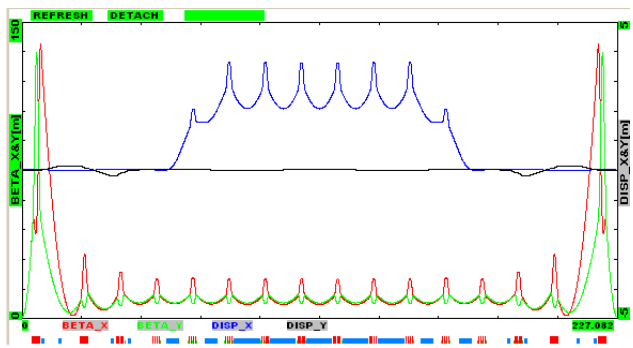

Figure 1: β-function & dispersions for half of the ring.

COLLIDER RING OPTICS STRUCTURE

Two main options of the NICA optics were considered.

Triplet based racetrack with γ_{tr}=6.22

This option was considered in Ref. [3] (see Fig.1). The objectives for the optics design are: (1) small β*, (2) an operation near thermal equilibrium where IBS rates can be minimized, (3) large transverse and momentum acceptances, (4) small circumference, (5) optimal location of collider tune and (6) two IPs. That determined the following design choices: (1) mirror symmetric racetrack with IP in each straight section, (2) triplet focusing through the entire machine (including IPs), (3) phase

MUON COLLIDER DESIGN STATUS*

Y. Alexahin, FNAL, Batavia, IL 60510, U.S.A.

Abstract

Muon Collider (MC) - proposed by G.I. Budker and A.N. Skrinsky a few decades ago [1, 2] - is now considered as the most exciting option for the energy frontier machine in the post-LHC era. A national Muon Accelerator Program (MAP) is being formed in the USA with the ultimate goal of building a MC at the Fermilab site with c.o.m. energy in the range 1.5-3 TeV and luminosity of ~1-5·10^{34} $cm^{-2}s^{-1}$. As the first step on the way to MC it envisages construction of a Neutrino Factory (NF) for high-precision neutrino experiments. The baseline scheme of the NF-MC complex is presented and possible options for its main components are discussed.

INTRODUCTION

As was already clear in 60s [1, 2] muons provide an intriguing alternative to electrons and positrons in TeV energy range: due to practical absence of synchrotron radiation the collider ring can be very compact fitting on existing laboratory sites, the collision energy spread is significantly smaller due to negligible beamstrahlung and can be made as small as a few units by 10^{-4} by applying a monochromatization scheme. Another obvious advantage is by $(m_\mu/m_e)^2$ times larger *s*-channel cross-section which makes muon collider potentially a more effective tool in search for scalar particles, such as the Higgs boson.

However, short lifetime of muons – 2.2 μsec in the rest frame – makes a muon collider very challenging technologically. In his talk at Morges seminar in 1971 [2] A.N.Skrinsky briefly outlined four major requirements to render such a machine feasible: high-intensity proton driver, efficient muon production and collection scheme (so-called front-end), ionization cooling channel and, finally, fast acceleration of muons.

In a later paper [3] devoted to various cooling techniques (including the ionization cooling) it was proposed to use cooled muon beams also as the source of neutrino beams for high-precision neutrino experiments – a concept which became later known as the Neutrino Factory. The modern look at physics possibilities at a NF and MC is presented in [4].

Since mid-90s there has been some theoretical and experimental effort in the framework of international Neutrino Factory and Muon Collider Collaboration (NFMCC) which lead to successful completion of MERIT experiment at CERN on pion production in Hg jet target [5] and launching of the Muon Ionization Cooling Experiment (MICE) now under construction at RAL [6].

A significant technological progress which was achieved during the past decade and better understanding of the underlying accelerator physics made the muon collider idea look more realistic and resulted in formation of a national Muon Accelerator Program (MAP) [7] on the basis of the American part of NFMCC and the Fermilab Muon Collider Task Force created in 2006. The goal of MAP is to provide by 2015 a Design Feasibility Study Report (DFSR) which would lay the groundwork for a full-scale project aimed at the MC construction at the Fermilab site in 2020s.

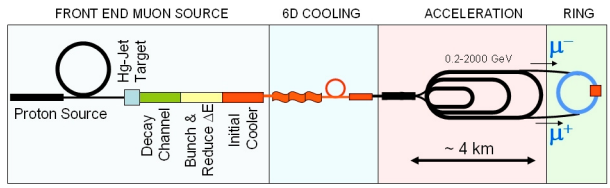

Figure 1: Schematic view of the Muon Collider complex.

GENERAL SCHEME

A simplified scheme of a Muon Collider is shown in Fig. 1. The high-power proton beam for pion production will be provided by a chain of accelerators including those to be constructed under the Fermilab Project-X [8]. A 3 GeV 1mA CW beam from Project-X accelerators will be accumulated and re-bunched in a ring for further acceleration to 8 GeV in a pulsed linac or even up to 21 GeV if a Rapid Cycling Synchrotron option will be adopted. A possibility is also considered to accelerate the proton beam in the Main Injector up to 60 GeV to substantially reduce the required number of protons per bunch.

The accelerated proton beam should then be longitudinally compressed in another ring to be finally delivered to the pion production target with the repetition rate of the complex (10-15Hz). The pions are confined transversely by strong longitudinal magnetic field (20T at the target) lowering to 1.5-2 T in the decay channel.

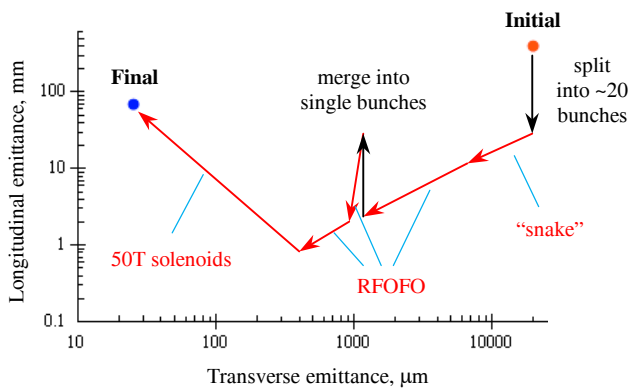

Figure 2: Evolution of muon beam emittance.

* Work supported by Fermi Research Alliance, LLC under Contract DE-AC02-07CH11359 with the U.S. DOE.
# alexahin@fnal.gov

CONCEPTS FOR RASING RF BREAKDOWN THRESHOLD BY USING MULTI-MODED CAVITIES

S.V. Kuzikov#, M.E. Plotkin, A.A. Vikharev, Institute of Applied Physics, Russian Academy of Sciences, Nizhny Novgorod, 603950, Russia.
J.L. Hirshfield, Omega-P, Inc., New Haven, CT 06510, U.S.A.
S.Yu. Kazakov, Fermi National Accelerator Laboratory, Batavia, 60510 IL, U.S.A.
Y. Jiang , Yale University, New Haven, 06520 CT, U.S.A.

Abstract

Multi-mode accelerating structures aimed at increasing accelerating gradient are described. Such structures operating in several resonant, equidistantly-spaced, axisymmetric, TM-like eigenmodes allow reduction of exposure time to surface fields, reduction of high-field areas and reduction of those fields which are responsible for electron emission. These effects are planned for use in studying the physics of RF breakdown phenomenon with the goal of designing new high-gradient accelerating structures.

ACCELERATION IN A STRUCTURE OF MULTI-FREQUENCY CAVITIES

Because rf breakdown is a strong limiting factor towards increase acceleration gradient, one needs first of all to prevent the initiation of breakdown. To follow this aim, let us consider a particle beam to be accelerated as a periodic sequence of tight bunches that move along a straight path with a velocity close to the speed of light. High accelerating fields need exist only during the narrow time intervals when test bunches traverse the cavities that comprise the accelerator structure. During time intervals between bunches, fields in each cavity should preferably be as small as possible. In each cavity, fields localized in space should periodically move between the structure axis when a bunch to be accelerated arrives, and at other times to move away from the axis and generally weaken (Fig. 1a) [1]. This principle automatically requires that cavity should contain equidistant spectrum of modes. The ideal electric field seen by bunches along the structure is sketched in Fig. 1b (curve 1—in green), in comparison with field behaviour in a single-frequency structure (curve 2—in red). In the case of a limited number of modes the resulted field would look like that in curve 3—in blue. It is widely accepted that thresholds increase for rf breakdown and thermal fatigue, as one decreases the exposure time to intense rf. It is thus natural to anticipate that a cavity in which the peak fields are present only during transit of the bunches - rather than during a substantial fraction of the interbunch period - should be capable of sustaining higher peak. An acceleration structure based on these main principles can be built either as a sequence of rectangular copper cavities driven in two-beam scheme [2-3], or as a sequence of axisymmetric cavities operated with alternating drive and accelerated bunches [4, 6].

#kuzikov@appl.sci-nnov.ru

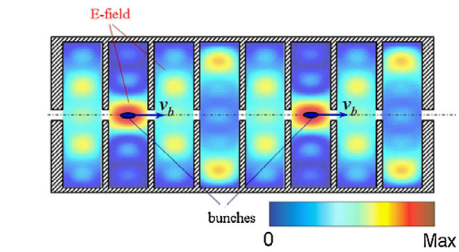

a)

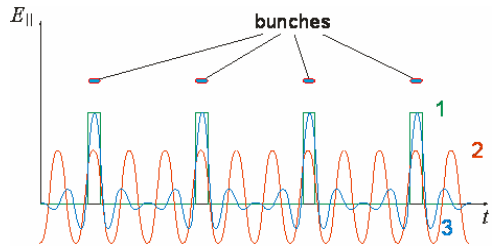

b)

Figure 1: Principles of acceleration of moving periodic bunches in multi-mode structure. a - accelerating structure scheme, b - time dependence of fields: in ideal multi-mode structure (curve 1 in green), in single-frequency structures (curve 2 in red), in a multi-mode structure operating in a limited number of modes (curve 3 in blue).

CRITERIA OF RF BREAKDOWN TRIGGERING

RF breakdown is a complicated, multi-stage phenomenon, which can be viewed as a continuous sequence of several stages. A modern theory is based on priority of electron field emission, describing how RF electric field produces electrons to tunnel from metal, surface heating causes growth of the protrusions and surface material evaporation [7-8]. Experimental data obtained for many accelerating structures show that the breakdown probability I is dependent on electric field threshold E and also on exposure time τ by the scaling law [8]:

$$I \sim E^6 \cdot \tau. \qquad (1)$$

Second, new experimental results obtained recently show that breakdown probability may depend by the rf magnetic field, i.e. by the surface temperature rise [9-10]. The model underlying (1) does not explain why magnetic

ACCELERATOR COMPLEX U70 OF IHEP: PRESENT STATUS AND RECENT UPGRADES

S. Ivanov, on behalf of the U70 staff[#]
Institute for High Energy Physics (IHEP), Protvino, Moscow Region, 142281, Russia

Abstract

The report overviews status of the U70, accelerator complex of IHEP-Protvino comprising four machines (2 linear accelerators and 2 synchrotrons). Particular emphasis is put on the recent upgrades implemented since the previous conference RuPAC-2008.

GENERALITIES

Layout and technical specification of the entire Accelerator complex U70 of IHEP-Protvino was specified in the previous status report [1] whose general part remains up-to-date.

On December 30, 2009, the Russian Federal Government issued an executive order enrolling the complex into the national List-Register of Unique Nuclear-Physics Facilities. It constitutes a prerequisite for an awaited revision of a funding scheme to maintain special and general-purpose engineering infrastructure of the IHEP facilities.

Efforts were continued to attain the following goals:

1. to ensure stable operation and high beam availability during the regular machine runs,
2. to improve proton beam quality,
3. to implement a program to accelerate light ions with a charge-to-mass ratio q/A = 0.4–0.5, and
4. to put forward a sound long-range option to diversify and develop accelerator and experimental facilities on the IHEP grounds, with a bias towards fixed-target research beyond elementary particle physics.

ROUTINE OPERATION

Since RuPAC-2008, the U70 complex worked for four runs in total. Table 1 lists their calendar data (end of the text). The first run of a year is shorter and solves, mainly, developmental and methodological tasks.

Dedicated machine development (MD) activity is split into two sessions per a run. One takes about a week prior to delivering beam to experimental facilities. Another (2-day long) occurs amidst the fixed-target physics program, under conditions of a smooth sustained operation of the machines thus facilitating R&D on beam physics.

Fig. 1 shows beam availability data during MDs and a fixed-target experimental physics program (XPh) with averages over 2002–10. Run 2009-2 has set a record with experimental facilities acquiring the extracted beam with its availability exceeding 90%.

During the runs, all the beam extraction systems available in the U70 were engaged — fast single-turn, slow 3rd-order resonant, internal targets, and deflectors made of bent silicon crystals. Fig. 2 demonstrates a period of smooth operation of the U70. Fig. 3 presents operation of slow extraction system.

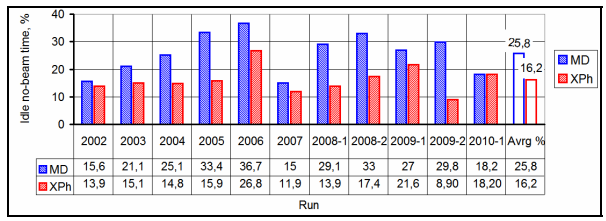

Figure 1: Beam availability statistics.

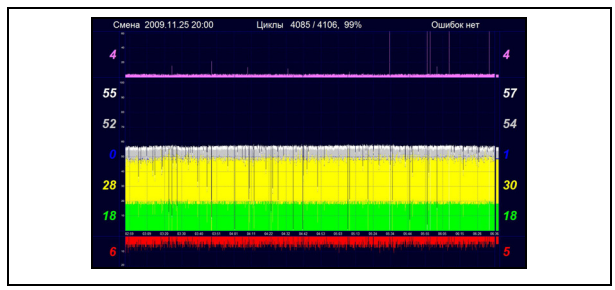

Figure 2: Screenshot of the on-line monitoring over the U70 operation. Time interval (abscissa) extends over 3 hr, or 1000 cycles of acceleration. Yellow trace slows intensity of stochastic extraction, green trace — operation of internal targets. Red (inverted) trace indicates spent beam remains damped onto internal absorber.

MACHINE DEVELOPMENT

This Section reports on recent updates in equipment.

New Septum Magnet SM26

In 2008, a new septum magnet SM26, manufactured at IHEP workshops, was installed in 4.9 m long straight section SS#26 of the U70 lattice, see Fig. 4. It was a step in upgrade of the slow extraction system aimed at enlarging vertical gap for extracted beam from 25 to 35 mm.

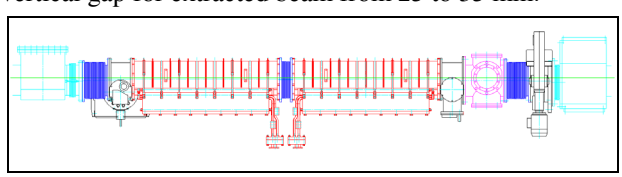

Figure 4: Layout of equipment in SS26 of the U70.

SM26 is sectioned into 2 identical units. Other auxiliary equipment housed in SS#26 (beam diagnostics, vacuum pumps and valves, bellows) was rearranged to a new configuration which also accommodated an universal 3-port docking box (right block in Fig. 4) suitable for inserting diagnostics devices or, say, bent-silicon-crystal deflectors.

[#] Yu. Fedotov, A. Minchenko, A. Afonin, E. Ludmirsky O. Lebedev, D. Demihovskiy, A. Ermolaev, Yu. Milichenko, I. Tsygankov, I. Sulygin, N. Ignashin, S. Sytov, O. Belyaev, V. Zenin, S. Pilipenko, Yu. Antipov, D. Khmaruk, V. Dan'shin and G. Kuznetsov.

MAINTENANCE OF ITEP-TWAC FACILITY OPERATION AND MACHINE CAPABILITIES DEVELOPMENT

N.N.Alexeev, P.N.Alekseev,V.A.Andreev, A.N.Balabaev,V.I.Nikolaev,A.S.Rjabtsev, Yu.A.Satov, V.S.Stolbunov,V.A.Schegolev, B.Yu.Sharkov, A.V.Shumshurov, V.P. Zavodov, ITEP, Moscow, Russia,

Abstract

The ITEP-TWAC facility operation with proton and heavy ion beams for ~4000 hours per year in several modes of beam acceleration and accumulation is determined by present-day demands of different beam users in the frame of current machine resources. Displacement of state interests from fundamental research to strictly-practical tasks as the spirit of the time stimulates multimode operation of accelerators with tendency of beam using for applications on the basis of modern beam technologies development. Mastering of Ag^{19+} ions acceleration in the UK ring up to the energy of 100 MeV/u and Fe^{26+} beam stacking in the U-10 ring at the energy of >200 MeV/u in addition to routine operation with C^{6+} beam at energy of 200-400 MeV/u with fast and slow extraction of circulating beam clear the way to beam using for a lot of applications requiring extension of the facility experimental area. Development of laser ion source (LIS) technology takes aim at high current and high charge state ions generation to get ratio of Z/A up to 0.4 for elements with A ~ 60 to be effectively stacked in the U-10 ring with multiple charge exchange injection technique at the beam energy of ~700 MeV/u. The machine maintenance efforts and current results of activities aiming at both subsequent improvement of beam parameters and extending of beam applications are presented.

INTRODUCTION

The ITEP-TWAC Facility consisting of main synchrotron-accumulator U-10 with 25 MeV proton injector I-2 and linked to U-10 ring booster synchrotron UK with 4 MV ion injector I-3 runs now in several operation modes accelerating protons in the energy range of 0.1-9.3 GeV, accelerating ions in the energy range of 0.1-4 GeV/u and accumulating nuclei at the energy of 200-300 MeV/u. Accelerated beams are used in several modes: secondary beams generated in internal targets of U-10 ring are transferred for experiments to Big experimental hall (BEH); beams extracted from U-10 ring in one turn are transferred to Target hall (TH); and proton beam bunch extracted from U-10 ring is transferred to Biological research hall (BRH). Some of secondary beam transfer lines are used now for transferring of slow extracted beams from U-10 ring.

MACHINE OPERATION

Next year will be 50-th anniversary of ITEP Ring Accelerator was started for operation that continues up today in parallels with machine modernization.

Statistic of ITEP-TWAC operation time is shown on Fig.1. The total machine run time of near 4000 hours per year is divided between three operation modes: acceleration of protons (~50%), acceleration of ions to relativistic energy (~10%) and nuclei stacking (~40%). Statistic of beam using for different research fields shows the tendancy of machine operation time increase for applications as proton and ion beams using in biology, medicine and radiation treatment of electronics for cosmic apparatus. The required beam time for users exceeds the possible one by factor of two. This discrepancy has to be cardinally reduced in a result of machine infrastructure development and extension of its experimental area.

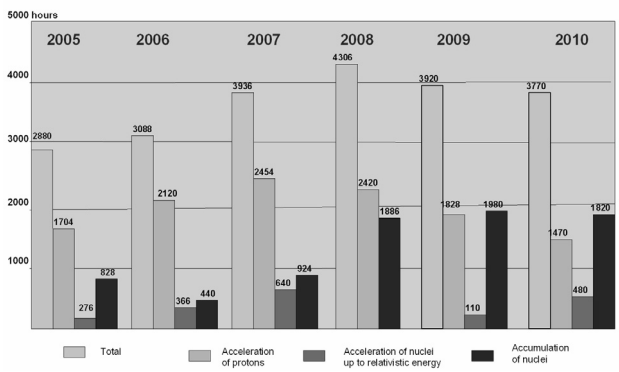

Fig.1. Statistic of ITEP-TWAC operation time

New modes of Fe-nuclei acceleration up to the energy of 3.6 GeV/u and of Ag^{19+}-ions acceleration up to the energy of 100 MeV/u realized in 2008-2009 are illustrated by oscillograms in Fig.2 and Fig.3. In the mode of Ag^{19+}-ions acceleration from very low level of injection energy as 0.7 MeV/u at vacuum in the beampipe as $1x10^{-9}$ Torr, particle losses at acceleration exceeds 90%.

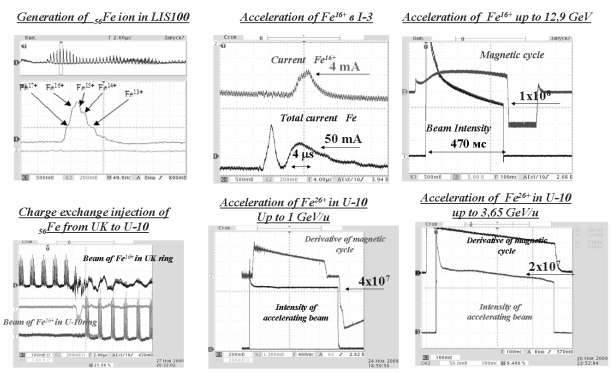

Fig.2. Acceleration of Fe-nuclei up to relativistic energy

COMPENSATION OF NONLINEARITIES IN NICA COLLIDER OPTICS

S.Kostromin, O.Kozlov, I.Meshkov, V.Mikhailov, A.Sidorin, JINR, Dubna, V.Lebedev, S.Nagaitsev, FNAL, Batavia, Illinois, USA, Yu.Senichev, IKP, Juelich, Germany

Abstract

The Nuclotron-based Ion Collider fAcility (NICA) [1] is a new accelerator complex being constructed at JINR. It is designed for collider experiments with ions and protons and has to provide ion-ion (Au^{79+}) and ion-proton collisions in the energy range 1÷4.5 GeV/n and collisions of polarized proton-proton and deuteron-deuteron beams.

Different chromaticity correction schemes involving several families of sextupoles are considered for two collider conceptions: with constant γ_{tr} and with changeable one.

INTRODUCTION

The collider rings has the racetrack shape and consist from two arcs and two long dispersionless straight sections with two IPs. The normalized chromaticity reaches a high value ~4.

Therefore the quite strong chromatic sextupoles magnets on arcs are required which in turn bring significant non-linear distortions in beam dynamics.

Different schemes involving several families of sextupoles and are tested. Optimization of the chromaticity correction scheme was carried out to increase the dynamic aperture.

CHROMATICITY CORRECTION SCHEMES

Triplet based racetrack with γ_{tr}=6.22

This option was considered in Ref. [2] (see Fig.1).

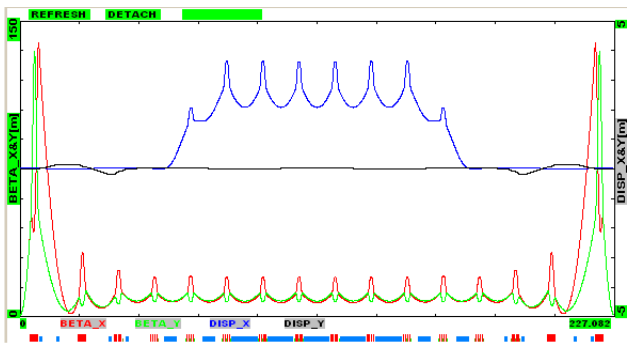

Figure 1: β-function & dispersions for half of the ring.

A chromaticity correction includes 4 families of sextupoles (2 focusing and 2 defocusing ones). It allows one to correct both the tune chromaticity and the beta-function chromaticity excited by IP quadrupoles. Sextupoles of each family are located with 180° betatron phase advances for their nonlinearity compensation. The dependence of the collider tune on Δp/p is shown in Fig. 2. It is very nonlinear due to large β^* which excites large tune and β-function chromaticity.

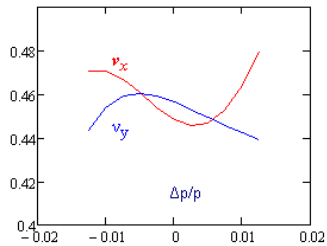

Figure 2: Tune dependence on the momentum offset.

The natural chromaticity of the ring are: ξ_x=-27.1, ξ_y=-23.2 ($\Delta\xi_{x,y}$ ~ −17 from two IPs). Corrected chromaticities are: ξ_x = −1.54, ξ_y = −1.50. The sextupole strength is ~0.35 kG/cm^2. A non-linear dependence of tunes and β-functions on Δp/p and the optics smoothness requirement do not allow the perfect chromaticity correction. However sextupole settings making reasonably good compensation were found (see Fig. 3).

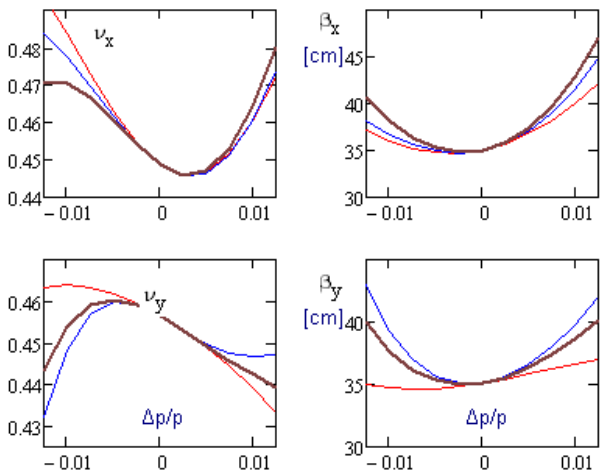

Figure 3: Dependence of the tune and β^* on Δp/p with different sextupoles strength.

That allowed us to avoid adding octupoles. Note also that the nonlinearity of tunes is actually profitable. It allows us to have large tune chromaticity required for transverse instabilities suppression with moderate tune variation across the momentum aperture.

FODO-cell based racetrack with changeable γ_{tr}

To meet the NICA requirements of operation with different magnetic rigidity beams, Au-ions in range 1÷4.5 GeV/u and with proton 6÷13 GeV lattice with changeable transition energy was considered.

1. *Au 4.5 Gev/u mode (see Fig. 4)*

Only sextupoles located in two central superperiods (without dispersion supressors) plus four additional sextupoles (instead of multipole correctors) are used for correction (see Fig. 5).

STUDY OF EFFICIENCY OF BEAM COLLIMATION AT U-70 ACCELERATOR BY USE OF CRYSTAL TARGETS

A.G. Afonin, V.T. Baranov, S. Belov, V.N. Chepegin, Yu. Chesnokov, P.N. Chirkov, A. Ermolaev, V. Gorlov, I. Ivanova, D. Krylov, V. Maisheev, D. Savin, E. Syshikov, V. Terekhov, I.A. Yazynin
IHEP Protvino, Russia.

Abstract

New crystal technique – bent crystal array and veer – type reflector based on straight crystals were used like first stage in collimation system at U-70 accelerator. Efficiency of collimation was enhanced up to 90% in two-stage collimation system which included first crystal stage and long steel absorber like second stage. For data taking and analysis of information modified modern beam diagnostic system was applied.

INTRODUCTION

The phenomenon of deflection of a charged particle beam in a bent crystal is well investigated and successfully applied at energies of about 10 GeV and higher [1,2,3]. However, the task of bending and extraction of charged particles with energies below 1 GeV presents a big practical interest, for example for the production of ultra stable beams of low emittance for medical and biological applications. There exists a big experimental problem in steering such energy beams, which is connected with the small size of the bent crystal samples. Potentially suitable tools in this case can be the bent quasimosaic crystals such as in [5], or thin straight crystals [6,7], but in both these cases it is necessary to increase a deflection angle of particles in some times.

CRYSTAL DEVICES

In this article we propose a novel crystal technique, which can effectively work in a wide energy range and is especially perspective for low energy below 1 GeV.

The first option is based on use of array of shot bent channeling crystals (Fig.1) with sub – millimeter length (special thin silicon wafers about 100 micron thickness were used for the production of such samples). Thus the bend of array occurs also, as a bend of the single well investigated silicon strip [8].

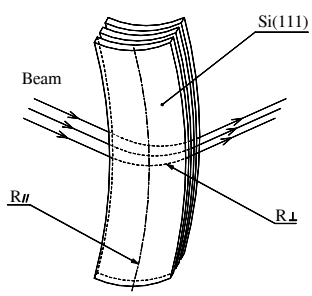

Figure 1: The array of bent silicon strips for beam deflection due to channeling.

The second option is based on the reflection of particles on very thin straight crystal plates with thickness, which is equal to an odd number of half-lengths of channeling oscillation waves $L = (2n+1)/2\times\lambda$, where $\lambda = \pi d/\theta_c$, $d = 2.3A^0$ – interplanar distance in silicon. It means, for example, that the optimum length of a crystal should be 10 microns for particles with energy 50 GeV. For the enhancement of the deflection angle, a few aligned plates placed like a veer are foreseen (Fig.2).

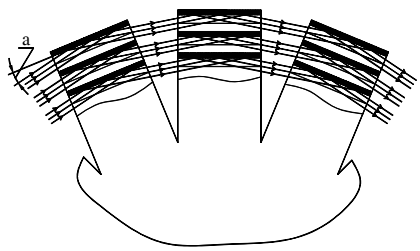

Figure 2: Veer-type reflector for bending of particle beam with use of thin straight crystals.

For an optimum deflection of a beam in this design each following crystal is unwrapped on angle $2\theta_c$. Then the total bend angle of beam can reach the value $2\theta_c \times N$, where N – is the amount of crystal plates. If the unwrap of a fan and thickness of plates are not optimal, the lower bend of particles occurs, and this picture is more difficult for interpretation. On Fig.3 for understanding the process of Monte Carlo calculations for unitary passage of a beam through a fan are submitted at its different parameters.

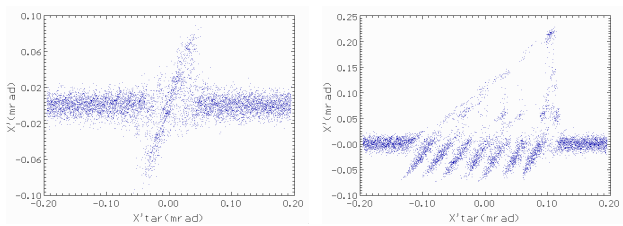

$dx' = 0\,\mu rad,\ L = 10\,\mu m,$ $dx' = 30\,\mu rad.$

Figure 3: Distribution of protons with energy 50 GeV on scattering angles after passage of a crystal fan from seven plates depending on its angular orientation X'tar with respect to the beam. The parameter dx' means a turn of the next plates of a fan in microradians.

Three different devices have been prepared for accelerator experiment: a usual crystal strip (the technology is described in [8]), a crystal array (Fig. 1),

SUPERCONDUCTING MAGNETS FOR THE NICA ACCELERATOR COMPLEX IN DUBNA

H. Khodzhibagiyan, P. Akishin, A. Bychkov, A. Kovalenko, O. Kozlov, G. Kuznetsov, I. Meshkov, V. Mikhaylov, E. Muravieva, A. Shabunov, A. Starikov, and G. Trubnikov, JINR, Dubna, Russia

Abstract

NICA is the new accelerator complex being under design and construction at JINR. The facility is aimed at providing collider experiments with heavy ions up to Uranium in a center of mass energy range from 4 to 11 GeV/u and an average luminosity up to 10^{27} cm-2s-1.The facility includes a new superconducting Booster synchrotron, the existing 6A·GeV superconducting synchrotron – Nuclotron, and the new superconducting Collider .The status of the design and construction of the full size model magnets for the Booster synchrotron as well as for the NICA Collider is presented.

INTRODUCTION

The flagship of the Joint Institute for Nuclear Research in Dubna is now the NICA/MPD project [1, 2] started in 2007. The general goal of the project is to start experimental study of hot and dense strongly interacting quantum chromodynamics matter in the coming 5-7 years. This goal is proposed to reach by: 1) upgrade of the existing superconducting synchrotron – the Nuclotron [3] as a basis for generation of intense beams over the atomic mass range from protons to uranium and light polarized ions; 2) design and construction of the facility to provide collider experiments with heavy ions like Au, Pb or U at luminosity of 10^{27} cm-2·s-1 at the kinetic energy range of 1 - 4.5 GeV/amu; 3) design and construction of the Multi Purpose Detector (MPD). The NICA facility (see Figure 1) includes two injector chains, a new 600MeV/u superconducting Booster synchrotron, the 6A·GeV superconducting synchrotron – Nuclotron, and the new superconducting Collider consisting of two rings of about 500m circumference each.

MAGNETIC SYSTEM OF THE BOOSTER SYNCHROTRON

The main goals of the Booster [4] are the following: accumulation of $4 \cdot 10^9$ Au^{32+} ions; acceleration of the heavy ions up to the energy of 600 MeV/u that is sufficient for stripping the Au ions up to the highest charge state of 79+; forming of the required beam emittance with an electron cooling system. The present layout makes it possible to place the Booster having 211 m circumference and a four fold symmetry lattice inside the yoke of the Synchrophasotron (shut down in 2002). Four large straight sections of the Booster will be used for injection from the linac, single turn extraction to transfer the beams into the Nuclotron, placing of the acceleration cavity and the electron cooler. With a maximum dipole field of 1.8 T, energy of above 600 MeV/u can be reached allowing the stripping of heavy ions up to the bare nucleus state. The magnetic system of the Booster consists of 4 quadrants and each of them has 10 dipole magnets, 6 focusing and 6 defocusing lenses. The multipole

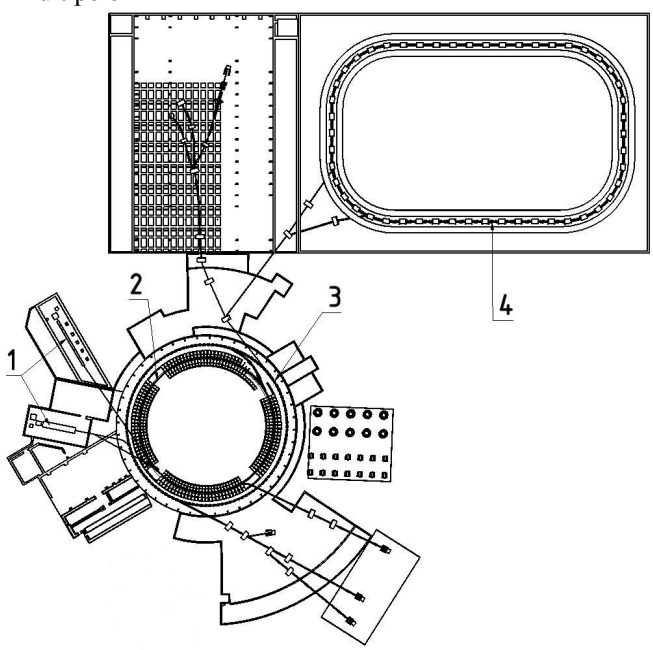

Figure 1: Schematic view of the NICA accelerator complex: 1 - injector chains; 2 - Booster synchrotron; 3 - existing superconducting accelerator Nuclotron; 4 – Collider with two superconducting rings.

correctors are also used to compensate the errors of both the main (dipole, quadrupole) and higher (sextupole, octupole) harmonics of the magnetic field. The required magnetic field in aperture is 1.8 T at the maximum rigidity. The increased aperture of both the lattice dipole and quadrupole magnets is one of the main design features.

The Nuclotron-type design [5] based on a window frame iron yoke and a saddle-shaped superconducting winding has been chosen for the Booster magnetic system. The Nuclotron magnets include a cold (4.5K) window frame iron yoke and a superconducting winding made of a hollow NbTi composite superconducting cable cooled with a two-phase helium flow.

Further development of the technology was proposed [6] to increase the efficiency of the magnetic system. A cross-section view of the Booster dipole and quadrupole magnets is shown in Figs. 2 and 3, correspondingly.

A 12 GHZ PULSE COMPRESSOR AND COMPONENTS FOR CLIC TEST STAND

A.A. Bogdashov, G.G. Denisov, S.V. Kuzikov#, A.A. Vikharev, Institute of Applied Physics, Russian Academy of Sciences, Nizhny Novgorod, 603950, Russia.
K.M. Schirm, I. Syratchev, CERN, 1211 Geneva 23, Switzerland.

Abstract

The X-band power test stand needed for preprocessing and testing of key CLIC RF components is being installed in the test facility CTF3. The test stand includes several 12 GHz XL5 klystrons (50 MW, 1.5 μs) and a pulse compressor (PC) of the SLED-I type to obtain over 120 MW peak power at 230 ns pulse length. A compact compressor of this type based on TE_{01}-TE_{02} beating wave in high Q-factor compressor's cavities has been designed, produced, and tested at low power level. For testing accelerating structures and so-called "CLIC recirculation principle" of its operation several -3 dB couplers, tuneable phase shifters, and variable power attenuators were also produced and tested.

DESIGN OF SLED-I PC

In order to provide at 12 GHz an efficient compression of rf pulses with parameters P_{inp}=50 MW, τ_{inp}=1.5μs, aimed to obtain P_{out}=120 MW, τ_{out}=230 ns, it is proposed to use a compact SLED-I pulse compressor [1]. The scheme of the well-known SLED-I is to be modified in order to provide necessary Q-factor of a storage cavity ($Q_l \approx 25 \cdot 10^4$, $Q_0 \approx 1.5 \cdot 10^5$), because Q-factors of spurious modes in an oversized cavity could be comparable with that for operating mode. The compressor of such modified scheme consists of two identical cavities coupled by -3 dB couplers [2], each cavity is based on TE_{01}-TE_{02} beating wave waveguide which starts from single-mode TE_{01} waveguide and finishes by a waveguide of a big enough radius which is necessary in order to provide the mentioned high Q-factors (Fig. 1). The use of the beating wave due to inserted absorbers allows simple solutions for spurious mode suppression. Indeed, these absorbers made of ceramics are placed out of the operating mode field while spurious mode fields are to penetrate perhaps in these absorbers. The design also naturally solves a problem of pumping ports which also play a role of selective elements and do not spoil Q-factor of the operating TE_{01}-TE_{02} mode (Fig. 2). Similar principle based on beating wave was used in 30 GHz TE_{01} mitre bends produced several years ago for CTF3 [3].

The beating wave (to provide deep modulation of surface field) consists of approximately 80% of the TE_{01} mode and only 20% of the TE_{02} mode. This mode mixture is produced sequentially by TE_{10} – TE_{01} "serpent-like" mode converter [3], and then the resulted TE_{01} mode is converted into the desired mode mixture by specially profiled horn (Fig, 3) which provides excitation level of other than TE_{01} and TE_{02} axisymmetric modes less than -30 dB (Fig. 3a). Mutual phase of the TE_{01} and TE_{02} modes at horn output is zero (this corresponds to flat phase front of a field localized out of waveguide wall) as it is seen in Fig. 3b.

The cavities in each channel are based on ∅100 mm copper waveguides. Length of each cavity corresponds to 3 beating periods (~600 mm).

The mentioned pumping port consists of a ring vacuum vessel which has a set of the 24 circular holes to pump a whole volume of the PC. The mentioned vessel is also partially filled by absorbers.

Fine frequency tuning in each of two channels is organized by means of independent, electric, stepping motors which allowed also manual control.

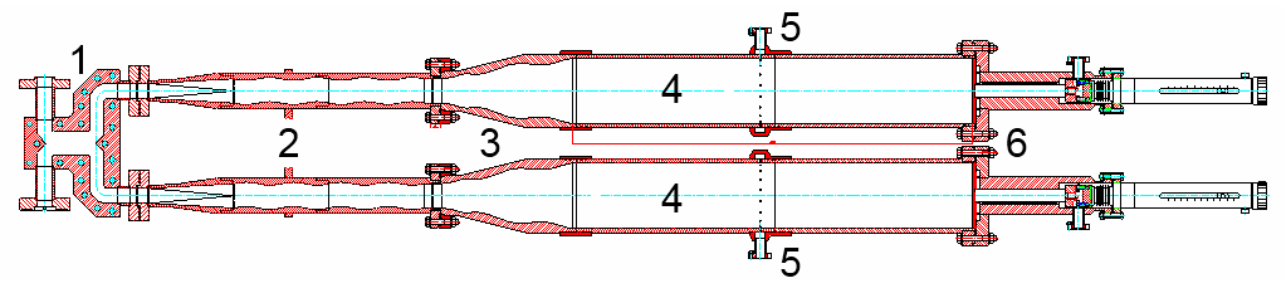

Figure 1: Technical drawing of 12 GHz PC: 1 - -3 dB coupler, 2- TE_{10} rectangular waveguide to TE_{01} of circular waveguide mode converters, 3 - TE_{01} to TE_{01}+TE_{02} mode converters (horns) with coupling irises in the beginning, 4 - circular waveguide cavities, 5- pumping ports, 6- plungers with stepping motors.

#kuzikov@appl.sci-nnov.ru

EXPERIMENT ON RF HEATING OF THE COPPER CAVITY – THE IMITATOR OF THE CLIC HIGH-GRADIENT ACCELERATING STRUCTURE*

S.N.Sedykh, E.V.Gorbachev, A.K.Kaminsky, N.I.Lebedev, E.A.Perelstein, N.V.Pilyar, T.V.Rukoyatkina, V.V.Tarasov, JINR, Dubna, Russsia
S.V.Kuzikov, N.Yu.Peskov, M.I.Petelin, A.A.Vikharev, IAP RAS, N.Novgorod, Russia

Abstract

The facility for joint experiments of JINR-IAP RAS has been commissioned to investigate the lifetime dependence of the CLIC high-gradient accelerating structure on the surface damage by repetitive high-power RF pulses. The facility is based on the 30 GHz JINR free-electron maser, which uses an electron beam of the induction linear accelerator LIU-3000.

Intermediate optical observations of the central ring allowed us to control the process of the damage evolution. The first damage of the copper surface have been observed after $1.6*10^4$ pulses with the pulse heating of 250ºK. After $6*10^4$ pulses the damage of the surface of the oxygen-free copper cavity became strong enough to cause regular breakdowns inside the test cavity.

INTRODUCTON

The project of the compact electron-positron collider CLIC with room-temperature accelerating structure is now developed by international collaboration headed by CERN [1]. The damage of the wall of the accelerating structure due to very intensive cyclic heating by short high-power RF pulses can be one of the most severe limits on the accelerating gradient or serve as a criterion for choice the materials for structure manufacturing [2]. Several experimental groups around the world have started investigations of this effect using different methods. Collaboration of JINR and IAP RAS has developed the experimental facility creating the RF pulse heating with temperature rise more than 200ºK. The expected lifetime of the copper cavity at such high temperatures was not more than $2*10^5$ pulses.

EXPERIMENTAL FACILITY

The facility is based on the 30 GHz 20 MW free-electron maser (FEM), which uses an electron beam of the induction linear accelerator LIU-3000 [3]. Radiation spectrum width does not exceed 10 MHz at pulse duration of 180 ns, repetition rate is 0.5-1 pulse per second.

The Gaussian wave beam from the FEM output waveguide is passing through the thin diagnostic film to the symmetrical two-mirror quasi-optical transmission line. After the oversized waveguide with an input vacuum window the radiation is transformed by the input horn from the Gaussian distribution into the TE_{11} mode and then – into TE_{01} mode by a specialized mode converter. After the output horn the radiation is monitored by a detector with a dielectric waveguide and then it is fully accepted by the calorimeter (figure 1).

A specially designed test cavity- imitator of the CLIC accelerating structure - operates at the mode TE_{011} with zero electric field near the wall to prevent the inner discharge. It consists of two diaphragms and the inner ring with a rather thin edge. The most heated area is the inner edge of the ring. The quality factor of the cavity is 1500. The precise frequency matching of the cavity with the FEM oscillator can be achieved by changing the distance between the diaphragms. The test cavity module has its own vacuum system.

DATA ACQUISITION AND CONTROL SYSTEM

The distributed data acquisition system was constructed several years ago [4, 5] and it demonstrates her versatility and reliability. Recently the some new possibilities were added. The automatic stabilization sub-system [6], being exploited in test regime with local control during 1 year, is now installed inside the accelerator hall and completely switched to the remote control. The electron beam focusing system consists of 12 magnetic lenses along the accelerator and beam-line. Each magnetic lens is fed by individual stabilized current supply. Controller is connected to the PC and current supplies by means of RS-485 protocol, allowing controlling the individual lenses currents. Another new feature of the control system is an active automatic start-times control for the modulators of the induction linear accelerator. It means the local feedback between the synchronization sub-system (which was operating previously only in human-controlled regime) and modulator pulse control sub-system. The hardware core of the pulse control subsystem is a set of fast ADC with memory buffers and input multiplexors. The server program is now supplied by a module of pulse shape recognition, which calculates a time when a flat top of pulse is started. TCP server module of this subsystem is ready to send this data to the client module in synchronization subsystem. The synchronization program calculates the difference between measured value and desired one, and then sends the correction to the synchronization channel connected with corresponding modulator. The list of channels taking part in this regime can be corrected by the operator in on-line regime.

*Work is partially supported by RFBR grants: # 06-02-16418-a, # 07-02-00617-a, # 09-08-00743-a.

THERMAL BALANCE OF MULTILAYERED TUNABLE DIELECTRIC LOADED WAKEFIELD ACCELERATING STRUCTURE*

I.L. Sheynman#, Saint-Petersburg ElectroTechnical University «LETI», Saint-Petersburg, Russia
I. Ya. Sheynman, St. Petersburg State Polytechnic University, St. Petersburg
A. Kanareykin, Euclid TechLabs, LLC, Solon, Ohio, U.S.A.

Abstract

Thermal balance of a cylindrical tuneable multilayer dielectric-filled accelerating structure is considered. One ceramic layer of the structure possesses ferroelectric properties, which allow the waveguide frequency spectrum to be tuned by varying the permittivity of the ferroelectric layer. Dielectric and induction losses in ferroelectric layer and a metal shell leads to a structure warming up and increasing temperature of the ferroelectric layer. Because of a temperature sensitivity of dielectric permittivity of ferroelectric layer this effect may detune the accelerating structure. On the basis of the analysis of a thermal regime of multilayered wakefield structure the medium and pulse temperature deviations are determined. A repetition rate of electronic bunch series should be chosen to limit temperature detuning.

INTRODUCTION

The method of dielectric wakefield acceleration of electrons is one of perspective directions of creation high gradient structures of modern linear accelerators. The methods based on the concept of wakefield acceleration in structures with dielectric filling, are now one of the most perspective in sense of possibility of creation высокоградиентных accelerating structures for the future generation of linear colliders. These structures which are object of intensive studying last years, can be excited both a high current electronic bunch, and an external source of powerful microwave radiation. At wakefield acceleration method high current (as a rule, 20–80 nC), short (1–4 mm) the leading electronic bunch, moving in the vacuum channel of the dielectric wave guide concluded in spending metal cover, generates TM01 mode of Vavilov-Cherenkov radiation which is used for acceleration of an electronic bunch of high energy, moving behind a leading bunch on the distance, corresponding to an accelerating phase of a wave.

In work [1] the structure analysis of wake fields and also induction losses in a metal cover was spent with reference to single-layered dielectric structure with the vacuum channel of rectangular geometry. In [2, 3] it is resulted experimental demonstration of tuneable structure with two-layer filling (a dielectric with dielectric permeability ε = 10 and a ferroelectric material with ε =500), and the maximum observable shift of frequency has made 160 MHz for accelerating TM01 fashions with frequency of 11.424 GHz. The analysis of losses of energy and a method of their decrease in structure is resulted in [4]. Research of possibility of creation of tuneable waveguides is conducted in work [5] with ferroelectric layers of cylindrical geometry.

Introduction of a ferroelectric layer between dielectric ceramic plates and a metal surrounding cover in a wave guide leads to management possibility its frequency spectrum. For the appendix of an external field operating a ferroelectric material the electrode serves. The choice of parameters of the ferroelectric layer – dielectric permeability and a thickness – is defined demanded for compensation of technological and temperature shifts by controllability of base frequency of a waveguide. Last is $\delta f = 2\Delta f / f_0$, where Δf – the greatest possible deviation of base frequency from settlement frequency f_0.

Presence located between a dielectric and a metal cover the ferroelectric layer with high value of dielectric permeability ε and rather big tangent of dielectric losses angle results as in increase of a share of the energy disseminated in the ferroelectric layer, and to additional induction losses in a metal cover of structure.

Last fact is caused by sharp growth tangential components of intensity of a magnetic field on a surface of a metal cover of the wave guide caused by rather high values of dielectric permeability of a ferroelectric material. As a result the contribution ferroelectrics and induction losses in the general losses of energy in system appears defining, and losses sharply accrue with growth of dielectric permeability of a ferroelectric material that limits an admissible thickness ferroelectric layer and limits possibilities of operative adjustment of frequency of accelerating structure with dielectric filling.

Total capacity of dielectric losses of energy in a ferroelectric material and a dielectric, and also the Joule losses connected with prompting of induction currents in a metal cover, can be presented as

$$w_s = \omega\varepsilon \tan\delta \int_V \mathbf{E}\cdot\dot{\mathbf{E}}\, dV + \frac{1}{2\sigma_m \Delta} \oint_{S_m} H_\tau^2 ds,$$

where $\varepsilon, \tan\delta, V$ are dielectric permeability, tangents of corners of dielectric losses and volumes of the dielectric and the ferroelectric material, H_τ is a tangential component of intensity of a magnetic field on border with an area S_m conductor, and depth of a skin-layer $\Delta = c/\sqrt{2\pi\omega\mu\sigma_m}$ is defined by frequency of an electromagnetic field ω and conductivity of metal σ_m, the point means complex interface.

INTERBUNCH ENERGY EXCHANGE IN THE ACCELERATING SCHEME WITH UNIFORM CHARGE DISTRIBUTION*

I. Sheynman#, Saint-Petersburg ElectroTechnical University «LETI», Saint-Petersburg, Russia
A. Kanareykin, Euclid TechLabs, LLC, Solon, Ohio, U.S.A.

Abstract

The efficiency of energy transformation in multi bunch accelerating schema with uniform charge distribution is considered. The transmitted energy to accelerated bunch taking into account driving bunch exit of relativism and settling them on the walls of the waveguide is determined. It is shown that accounting losses charge of generator beam increases passed accelerated bunch energy by eliminating exhaust bunches.

INTRODUCTION

The method of dielectric wakefield acceleration of electrons is one of perspective directions of creation high gradient structures of modern linear accelerators.

The basic element of a wakefield accelerator represents the cylindrical metal waveguide filled inside with a dielectric with the vacuum channel along an axis. The short electronic bunch with the big charge and concerning small energy of particles at flight on the vacuum channel generates a Cherenkov radiations TM01 mode with longitudinal component of electric field up to 100 MV/m. Following for it with a delay selected from the requirement of the coordination with the accelerating phase of a wake field, the accelerated bunch with a small charge is accelerated by it wake field. The given principle of acceleration has been successfully experimentally shown in Argonne National laboratory of the USA (ANL) and now intensively develops in a number of laboratories [1, 2].

The size of a charge of a driving bunch which can be passed through a waveguide, is limited by technical possibilities of the photoinjector, a created by a bunch spatial charge a Coulomb field and the sizes of the vacuum channel of a waveguide. In this connection to increase in an accelerating field in a waveguide instead of a single bunch apply a chain of electronic bunches. The accelerating scheme with a flat profile of bunches sequence (flat bunch train – FBT) is used for coherent addition of fields of separate bunches and increase in a total accelerating field.

Increase of efficiency of the accelerator is connected with increase in a share of energy of a driving bunch which is transferred to particles of an accelerated bunch [3] – [6]. The factor of transformation of energy R is defined as the ratio of the maximum increment of energy electron in an accelerated bunch to the maximum decrease of energy of driving bunches $R = \Delta W^{+} / \left(\max \left| \Delta W^{-} \right| \right)$.

For maximization of factor of transformation of energy R the accelerating scheme with a triangular profile of a chain Gaussian bunches with the sequence period $d = m\lambda + \lambda/2$, where λ – base frequency of accelerating structure (Ramped Bunch Train – RBT) is used. Charges in a chain a profiled so that the first bunch in sequence possesses the least charge, and last – the greatest. All driving bunches in a chain are affected identical on amplitude concerning the small braking field E_z^-, however the accelerating field behind a chain E_z^+ – is considerable above. This factor provides high efficiency of transmission of energy from driving bunches sequence to an accelerated bunch that reflects numerically increase in factor of transformation which ideally one mode regime excitation of a waveguide, exact positioning of bunches and exact selection of charges can reach values $R = 2N$ where N – the number of driving bunches in a chain. High efficiency of transmission of energy from a chain of driving bunches to a field in a RBT-method is reached by considerable range of flight on which there is a selection of energy from driving bunches.

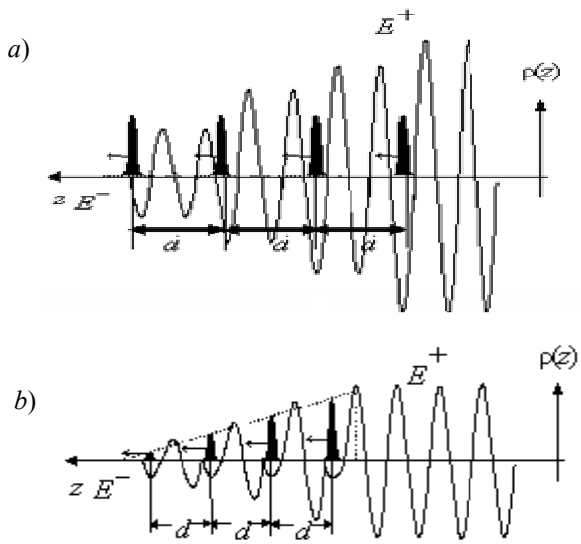

Figure 1: Multibunch acceleration schemes:
(a) FBT, (b) RBT

THE ANALYSES OF FBT

*Work supported by Ministry of Education and Science of the Russian Federation, the program "Scientific and scientific-pedagogical personnel of innovative Russia" and the Russian Foundation for Basic Research (09-02-00921)
#isheinman@yandex.ru

ATTOSECOND AND FEMTOSECOND ELECTRON BUNCHES OBTAINABLE UPON FIELD EMISSION IN A COMBINED QUASI-STATIC AND LASER ELECTRIC FIELD

V. A. Papadichev*
Lebedev Physical Institute, RAS, Leninsky Prospect 53, Moscow 119991, Russia

Abstract

Short pulses of electrons of femtosecond and attosecond duration are necessary for numerous applications: studying fast processes in physics, chemistry, biology and medicine. Heating of spikes for single-pulse regime is several degrees and therefore it is possible to generate a sequence of electron bunches (up to 100–500 pulses). They can be used in diffractometry and after acceleration to 3–4 MeV for generation of short pulses of VUV and soft X-ray radiation in periodic fields or as a relativistic mirror.

INTRODUCTION

Modulation of electron beams at optical frequencies is promising for numerous applications in physics, chemistry, and biology [1-5]. As it was shown earlier [6 - 9], placing a needle cathode biased with a quasi-static potential into the laser focus permits to obtain a train of electron bunches of femtosecond and attosecond duration at the frequency of the laser (e.g., carbon dioxide or neodymium lasers).

The number of bunches in the train can be varied from one to dozens or hundreds by changing the envelope of the laser pulse. Such electron bunches can be used for time-resolved diffraction analysis of expansion, deformation and destruction of solids under high-power thermal and mechanical loads [4].

After additional acceleration, electron bunches can be applied for generation of tunable, coherent UV and X-ray electromagnetic radiation in the periodic structure of the electromagnetic field.

Moreover, such trains of electron bunches could serve as a relativistic mirror [5]. Interacting with a counter-propagating pulse of electromagnetic radiation (even wide-band), the mirror will select radiation at resonant frequencies and reflect it with frequency multiplication of $4\gamma^2$, where γ is a relativistic factor of accelerated electrons.

Small longitudinal dimensions of bunches (nm) and negligible energy spread $10^{-4} - 10^{-3}$ allow to obtain tunable, coherent UV and X-ray radiation of acceptable power for experiments with micro- and nanoscale objects.

It was shown in previous papers [6 - 9] that it is possible to obtain ≈ 10 as pulses with a laser of 1 μm wavelength if space-charge forces are negligible . Currents of 10 mA to 10 A can be obtained from single-spike cathode and upto 10 kA with a multi-spike cathode. Further bunching occurs due to velocity modulation in the bunch by laser electric field. In this paper, electron dynamics is analyzed more thoroughly for various emission velocities as the main cause of dispersion. Quasi-static and laser fields and emission velocity influence phase distribution of electrons in a bunch so their strengths were varied to reveal it.

Bunch evolution in a space-charge dominated regime was also studied for two cases: a plane (sheet) bunch and a spherical one corresponding to multi-spike and single-spike cathodes respectively.

CATHODE GEOMETRIES AND REGIMES OF OPERATION

Wide known Fowler-Nordheim formula was used to calculate currents one can obtain from needle cathode. In the field strength range $3 \cdot 10^7 - 2 \cdot 10^8$ V/cm the density of current from the cathode follows the Fowler-Nordheim law quite well and in the case of a copper cathode for the given field strength range is $1 - 7 \cdot 10^8 A/cm^2$. The formula was obtained for static field but can be applied for variable fields as well if the time of electron tunneling is much less than a period of a periodic electric field [10]. In the case of a combined quasi-static and variable electric field obtaining the exact solution of the Schrödinger equation is very difficult, but the criteria of validity of Fowler- Nordheim formula is the same: the tunneling time of electron should be much less than duration of variable field period.

Evaluating the field strength for copper cathode (barrier height 4.3 eV) and carbon dioxide laser ($\lambda = 10\mu m$) gives $E_{sum} > 10^8$ and $E_{sum} > 10^9$ for neodymium laser ($\lambda = 1\mu m$).

It should be noted that real applied laser fields may be much lower because of field enhancement on the spike tip with small radius of curvature [11].

Fig. 1, 2 and 3 are schematic representation of three types of devices. In 1 a single spike device: a cathode having a spike with a curvature radius ρ_c is at the focus of a laser. A quasi-static voltage V_0 is applied to the cathode. This creates at the spike a high-intensity electric field $E_{0n} \approx V_0/\rho_c$, where E_{0n} is the field perpendicular to the cathode surface (the distance between the cathode and the anode here is considered to be much greater than the curvature radius ρ_c).

* papadich@sci.lebedev.ru

HOLLOW PHOTOCATHODE CONCEPT FOR E-GUN

M. A. Nozdrin#, N. I. Balalykin, V. Ph. Minashkin, E. M. Syresin, G. V. Trubnikov, G.D. Shirkov,
JINR, Dubna, Russia
J. Huran, IEE SAS, Bratislava, Slovakia

Abstract

Photocathodes are the key devices for high-quality electron bunches generation. Such bunches are needed as initial electron source in contemporary linear accelerators. In all cases there are several important parameters: fast response time, quantum efficiency, long lifetime, low thermal emittance, minimal effect on RF properties of the accelerating system. In this paper the new concept of the photocathode is proposed – hollow (absolutely transparent for the laser beam) photocathode. Such cathode geometry allows quantum efficiency rising due to surface photoelectric effect which is concerned with normal to material surface wave electric field multiplier. Usability investigation experimental results for both hollow photocathodes made of bulk materials (Nb, Cu) and by thin-film technology (CsITe and diamond-like carbon as film on copper substrate) are given. After Nb hollow photocathode irradiation by a laser beam (λ = 266 nm, τ_{pulse} = 15 ns, frequency 1 Hz) a charge of 64nC was extracted. Backside irradiation radically simplifies laser beam targeting on emitting surface, accelerator equipment adjustment and allows photocathode working surface laser cleaning.

INTRODUCTION

Despite that fact that today considerable results in effective photocathodes (RF, SRF, DC) development and creation are achieved, the work on this line is underway [1, 2, 3].

Progress in basic photocathode parameters is possible by optimal usage of photoemission initializing laser beam potential.

Response time and emittance of electron beam increase upon thermoemission current appearing and rising, so there are several signatures that distinguish photoemission from thermoemission.

- Since upon photoelectric effect electron output is inertialless so current pulse lateness relative to laser pulse is absent. At that, for one-photon process, current pulse length is equal to laser pulse length. Lateness is absent at intensities less than 4 MW/cm^2 [4]. At intensities above 4 MW/cm^2 lateness is observed and photocurrent pulse broadening occurs, what is evidence of thermoemission process appearing. For impulses shorter than 10^{-11} s coverage of the photoelectric effect against a background of thermoemission can be expanded to intensities of 10÷100 GW/cm^2 [4, 5]. In the picosecond range of pulse duration thermoemission nature changes severely. With such durations electron subsystem is isolated out of the lattice and in view of small thermal capacity warms up nearly inertialless. So, for thermoemission under the picosecond pulses influence, current lateness against laser pulse is absent. Such thermoemission almost can not be observed separately from photoemission but can cause emittance increasing.
- As is well known, surface photoelectric effect is a typical vector phenomenon. Current magnitude is concerned with normal to surface wave electric field multiplier and dramatically depends on laser beam hade and polarizing angle. From the other side, thermoemission current completely depends on metal surface temperature which depends on accepted power.

It is interesting to investigate the following questions:

- Thermoemission minimization degree by cathode accepted power decreasing (by close to 90° laser beam to work surface hade using).
- Quantum efficiency increasing due to normal to cathode work surface electric field multiplier.

HOLLOW HOTOCATHODE AND EXPERIMENTAL RESULTS

Investigations were done by a stand [6] (Fig. 1) with a chamber vacuum of 2•10^{-9} torr and gun anode voltage of 6 kV.

Monopulse YAG:Nd3+ (yttrium-aluminium garnet alloyed with neodymium) laser was used for cathode irradiation. Wavelength of generated UV-radiation was 266 nm, beam Ø6 mm, pulse energy less than 15 mJ.

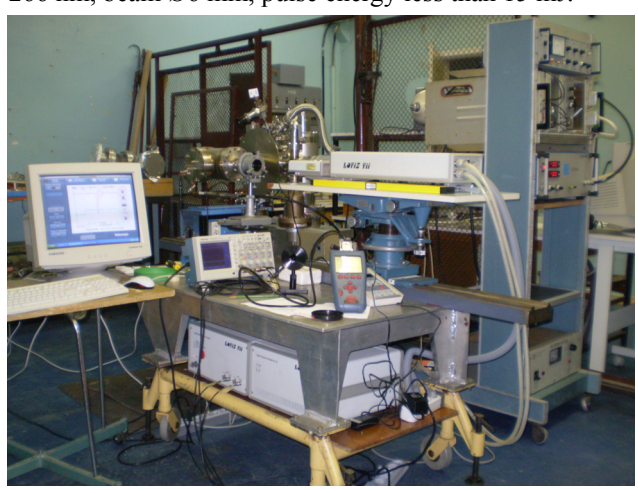

Figure 1: Photocathode stand overview

#nozdrin@sunse.jinr.ru

TBA SCHEME WITH ION/PROTON DRIVING BEAM

E.G. Bessonov, FIAN LPI, Moscow, Russia
A.A.Mikhailichenko#, Cornell University, LEPP, Ithaca, NY 14853, U.S.A.

Abstract

We are considering a two-beam accelerator (TBA) scheme with ion or proton beam as a driver. By comparison of the proposed scheme and the one with electron driver, we concluded, that TBA with ion/proton driver beam looks preferable. Existence of big proton accelerators in a few laboratories gives a boost for reconsideration of the baseline for post-LHC era. These Labs are FERMILAB, BNL, CERN and IHEP at Protvino, Moscow region. Protvino could emerge as one advantageous location and get stimulus for recovering the 600*GeV*-proton synchrotron in the existing~20*km*-long tunnel. This synchrotron was planned as a booster for 3x3*TeV* storage ring.

OVERVIEW

Many authors have developed TBA during the last decades [1]. CLIC is the mostly advanced representative of this kind [2]. The CLIC team does not give up even after International Technology Recommendation Panel made their decision in a favour of SC technology in August 2004. This is a good indication that some positive aspects are present in this idea. Obvious difficulty of TBA scheme associated with generation of electron driving beam (which forced recent change of CLIC operational frequency, by the way). To be useful for excitation of accelerating structure, the driving beam should have maximal content of spectral component of the driving current at the operational frequency. To some extent, TBA scheme with electron beam as a driver uses low impedance beam for transferring its energy to a high impedance one.

On the other hand, an idea of energy accumulation in a beam circulating in a storage ring and further usage of it for excitation of RF structure is an old one, discussed by G.I.Budker [3]. Later the idea to use the proton beam for excitation of the accelerating structure of electron linac was revealed in [4]. Here the proton beam excites *the same structure*, which is used for acceleration of electrons (or positrons). Naturally, this narrows the freedom of optimization of RF generation and further transferring it to the accelerating beam, as the transfer structure should take only a small fraction of power from the drive beam, while the accelerating structure should deliver as much power to the beam as possible. Usage of different structures for extraction of energy and for acceleration, linked together by the waveguides solves this problem.

The proton/ion drive beam is more advantageous, than the electron one is as follows: first advantage of the ion/proton beams is associated with their much lower emittance. These beams (or plans to have them) already exist–that is another advantage. Other positive moment associated with lower gamma factor γ for the same energy $\sim mc^2\gamma$. Lower gamma factor allows easier manipulation of the beam in a longitudinal phase space, $\sim 1/\gamma^2$. High stored energy in the proton beam (up to few *MJ*) is more than enough for excitation of RF structure. For fixed radius of accelerator the intensity of synchrotron radiation $\sim \gamma^2$, which excludes the losses associated with SR for protons. These losses prohibit usage of electron beam with high-energy as a driver. On the other hand, the energy of proton beam is high, so the ratio of impedances of the driving beam to the main beam is closer to unity for the proton/ion driver. The longitudinal component of the transport current is the only important parameter in a process of RF generation in a transfer structure. Lower γ makes bunching with chicane easier $\sim 1/\gamma^2$ and decreases the longitudinal mass $\sim m\gamma^3$.

Basically, we raise the question for revision of TBA scheme in a favour of proton/ion driver beam. We shall use 30GHz-CLIC parameters as the reference ones [11]. All components developed for this project can be used for our scheme, delivering substantial savings.

PRINCIPAL SCHEME

Principal scheme of TBA driven by the Ion/Proton beams is represented in Fig.1.

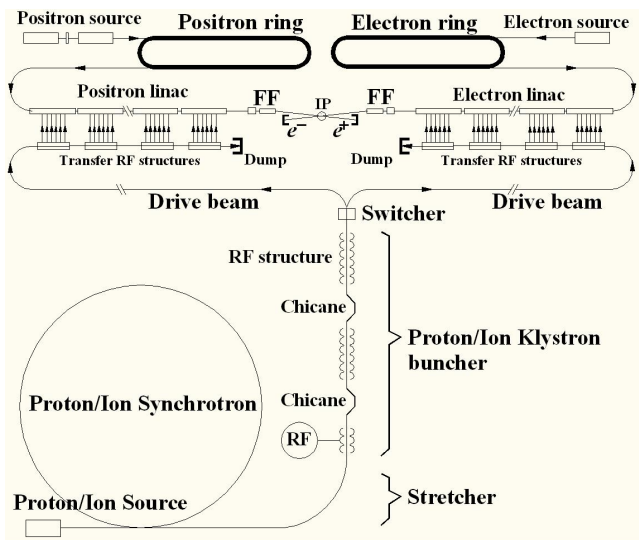

Figure 1: Principal scheme of the Complex proposed. FF stands for the Final Focus, IP-interaction point. RF stands for the RF generator feeding the first bunching structure.

Positron source with undulator could be easily introduced here in the same style as the one for ILC [5]. We consider the possibility of stacking polarized

#aam10@cornell.edu

THE CDS PARAMETERS FOR PROTON LINAC WITH MODERATE HEAT LOADING

V.V. Paramonov*
Institute for Nuclear Research of the RAS, Moscow, Russia

Abstract

The Cut Disk Structure (CDS) was originally proposed for high energy linac in L-band or S-band frequency range. CDS combines simultaneously high coupling coefficient, high efficiency and small transverse dimensions. For lower particle velocity ($\beta < 1$) the structure loses in the effective shunt impedance Z_e value due to relatively thick partition with internal cooling channels. For moderate heat loading internal cooling is not necessary and partition thickness is limited only by mechanical rigidity. The structure equalizes in Z_e value with another bi-periodical structures and original CDS advantages come in front. Calculated CDS parameters for proton linac are presented.

INTRODUCTION

For high energy part ($\beta \geq 0.4$) of proton linac such well known normal conducting accelerating structures as Side Coupled Stricture (SCS) [1], Disk and Washer Structure (DAW), Annular Coupled Structure (ACS) [2] are realized. Topologically these structures can be considered as External Coupling Cell (ECC) structures, Fig. 1a with coupling cells removed from the beam axis. The septum thickness t_1 between adjacent accelerating cells is defined by structure rigidity and placement of cooling channels.

The Cut Disk Structure (CDS) has been proposed [3] initially for electron $\beta \approx 1$ linac with S-band and L-band operating frequency to join both high Z_e and coupling coefficient k_c values. Topologically initial CDS is the structure with Internal Coupling Cells (ICC), Fig. 1b. The coupling cell with the length l_{cc} is placed in the septum between accelerating cells. Cooling of the drift tube region is required for intense linacs with high heat loading at the structure. If internal cooling channels are required, the effective septum thickness $\frac{2t_2}{\beta\lambda}$ is still high for $(\beta \sim 0.4 \div 0.5)$ and CDS loses in Z_e value with respect to another structures.

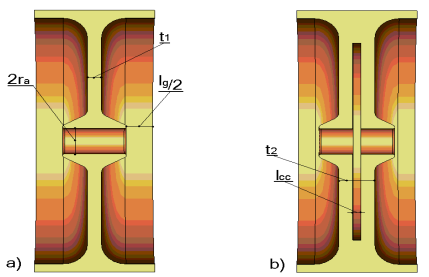

Figure 1: Accelerating cells in structures with External (a) and Internal (b) Coupling Cells - ECC and ICC.

Further CDS development [4] has shown preference of the four windows CDS option (CDS4W, Fig. 2c), as compared to two (CDS2W, Fig. 2b) or three windows - sufficient $k_c \approx (10 \div 15)\%$ value, a higher vacuum conductivity, a simpler cooling scheme, slightly higher Z_e value, absence of transversal field for coupling mode, strongly reduced possibility of multipactor discharge in coupling cells. For lower operating frequency $f_0 \geq 700MHz$ the relative septum thickness becomes smaller and CDS with internal cooling is competitive with another structures [5] in Z_e value and has big advantage of small transverse dimensions.

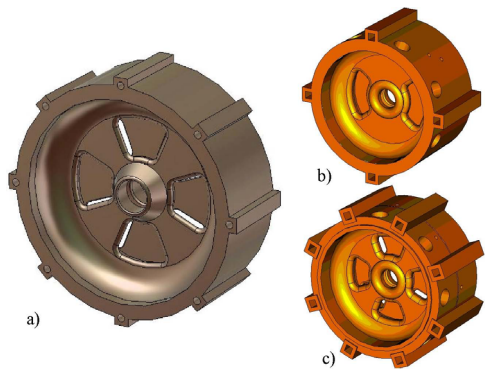

Figure 2: CDS structure for proton linac (a) and for electron intense linac, (b) - CDS2W, (c) -CDS4W.

With the moderate average heat loading to the structure $\sim 3kW/m$ internal cooling is not strongly necessary. The septum thickness in CDS can be reduced.

CDS RF PARAMETERS FOR THIN SEPTUM

The CDS RF parameters were calculated for operating frequency $f_0 = 991MHz$ with aperture radius $r_a = 17mm$ and septum thickness $t_2 = 14mm$ for particle velocity range $0.4 \leq \beta \leq 0.8$. Results are plotted in Fig. 3. The CDS coupling value $k_c \approx (14 \div 17)\%$ appears naturally, due to original concept [3] and is well balanced with respect DAW coupling $k_c \approx 50\%$ and SCS-ACS one, $k_c \approx 5\%$.

Comparison with another structures in Z_e value is presented in Fig. 4. Coupling windows in CDS4W are placed in the region of the maximal magnetic field for accelerating mode, resulting in th surface decreasing and related

* paramono@inr.ru

DESIGN OF THE NUCLOTRON BOOSTER IN THE NICA PROJECT

Andrey Butenko, Nikolay Agapov, Alexey Eliseev, Viktor Karpinsky, Hamlet Khodzhibagiyan, Alexander Kovalenko, Grigory Kuznetsov, Igor Meshkov, Vladimir Mikhaylov, Valery Monchinsky, Anatoly Sidorin, Alexander Smirnov, Grigoriy Trubnikov, Bogdan Vasilishin, JINR, Dubna, Russia

Abstract

NICA is the new complex being constructed on the JINR aimed to provide collider experiments with ions up to uranium at energy of 3.5x3.5 GeV/u. The NICA layout includes Electron String Ion Source, 6.2 Mev/u linac, 600 MeV/u booster synchrotron, upgraded Nuclotron and ion collider with average luminosity of 10^{27} cm^{-2} s^{-1}. The main goals of the Booster are the following: accumulation of $4 \cdot 10^9$ Au^{32+} ions; acceleration of the heavy ions up to energy required for effective stripping; forming of the required beam emittance with electron cooling system. The present layout makes it possible to place the Booster having 211 m circumference and four fold symmetry lattice inside the yoke of the Synchrophasotron (shut down in 2002). The features of this booster, the requirement to the main synchrotron systems and their parameters are presented in this paper.

INTRODUCTION

General challenge of the NICA facility is to achieve a high luminosity level of heavy ion collisions in a wide energy range starting with about 1 GeV/u. To reach this goal the NICA injection chain has to deliver a single bunch of fully stripped heavy ions (Au^{79+}) at intensity of about $1 \div 1.5 \cdot 10^9$ ions [1]. An effective stripping of the ions before injection into the Nuclotron requires their preliminary acceleration to an energy of a few hundreds of MeV/u. Therefore, realization of the NICA project presumes design and construction an intermediate booster synchrotron as new element of the NICA collider injection chain.

Before injection into the collider ring the Nuclotron RF system has to provide compression of the accelerated bunch. The beam parameters providing by linac-injector do not permit to realize the bunch compression with required efficiency. Thus a beam cooling at some stage of its acceleration is necessary. The Nuclotron ring has no convenient straight sections for location of the cooling system. Therefore the booster is only the place where the beam cooling can be realized. Additionally, the larger beam energy at the injection simplifies requirements to vacuum conditions in the Nuclotron beam pipe.

Correspondingly, the main functions of the intermediate heavy ion synchrotron, the Booster of the Nuclotron, are the following:

- Accumulation of $4 \cdot 10^9$ Au^{32+} ions that necessary to have after acceleration and stripping the beam intensity of $1 \div 1.5 \cdot 10^9$ ions ;
- Decrease of the ion beam longitudinal emittance at the energy of 100 MeV/u approximately by application of the electron cooling;
- Acceleration of the ions up to energy of 600 MeV/u that is sufficient for stripping of the Gold ions up to the charge state of 79+;
- Simplification of the requirements to the vacuum conditions in the Nuclotron owing to higher energy and charge state of the injected ions.

MAIN PARAMETERS OF THE BOOSTER

The huge yoke of the Synchrophasotron – the old 10 GeV proton synchrotron that was decommissioned in 2002, after the magnet winding is removed, gives a free tunnel of 4 x 2.3 m. The present layout of the Nuclotron and existing injection and extraction systems make it possible to place the Booster having 211 m circumference and four fold symmetry inside the yoke (Fig. 1).

Four large straight sections of the Booster will be used for injection from the linac, single turn extraction to transfer the beams into the Nuclotron, placing of the acceleration cavity and electron cooler. At the maximum field of dipole magnets of 1.5 T one can reach for heavy ions the energy of above 600 MeV/u that is sufficient for stripping of the ions up to the bare nucleus state (Table 1).

Table 1. Main parameters of the Booster

Ions	Au^{32+}
Circumference, m	211 m
Fold symmetry	4
Quadrupole periodicity	24
Injection/extr. energy Au^{32+}, MeV/u	6.2/600
Magnetic rigidity, T·m	2.2 ÷ 25.0
Dipole field, T	0.17 ÷ 1.8
Pulse repetition rate, Hz	0.25
Magnetic field ramp, T/s	1.2
Beam Injection type	Twice repeated, single turn
Beam extraction type	Single turn
Injection store duration, s	0.02
Vacuum, Torr	10^{-11}
Au^{79+} beam intensity, ions per pulse	1.5×10^9
Transition energy, GeV/u	3.98

INJECTOR COMPLEX OF THE NICA FACILITY

A.O.Sidorin, A.V.Butenko, E.E.Donets, E.D.Donets, A.I.Govorov, V.V.Kobets, V.A.Monchinsky, I.N.Meshkov, G.V.Trubnikov, V.V.Fimushkin, JINR, Dubna, Russia, A.Belov, INR, Moscow, Russia, O.K.Belyaev, A.P.Maltsev, Yu.A.Budanov, I.A.Zvonarev, IHEP, Protvino, Russia, V.V.Kapin, MEPhI, Moscow, Russia

Abstract

The injector complex of the NICA facility consists of existing Alvarez-type linac LU-20 and new heavy ion linac HILac. The LU-20 is under modernization now, the HILac will be constructed during coming years. Parameters of the accelerators are presented.

INTRODUCTION

General goal of the NICA/MPD project under realization at JINR is to start in the coming 5÷7 years an experimental study of hot and dense strongly interacting QCD matter and search for possible manifestation of signs of the mixed phase and critical endpoint in heavy ion collisions. The Nuclotron-based Ion Collider fAcility (NICA) and the Multi Purpose Detector (MPD) are proposed for these purposes. The NICA collider is aimed to provide experiment with heavy ions like Au, Pb or U at the kinetic energy range from 1 to 4.5 GeV/u with average luminosity of 10^{27} $cm^{-2}\cdot s^{-1}$ and to provide collisions of light ions in the total energy range available with the Nuclotron.

The goal of the NICA project is construction at JINR of the new accelerator facility that consists of [1]:

- cryogenic heavy ion source of Electron String type (ESIS),
- source of polarized protons and deuterons,
- the "old" linac LU-20,
- a new heavy ion linear accelerator (HILac),
- a new superconducting Booster-synchrotron,
- the existing proton synchrotron Nuclotron,
- two new superconducting storage rings of the collider,
- new set of transfer channels.

Two acceleration and stacking chains of heavy ions and polarized protons and deuterons are pressumed:

- ESIS → HILac → Booster → Nuclotron → Collider
- Source of polarized ions → LU-20 → Nuclotron → Collider

The main elements of the NICA injection complex (source of polarized ions, LU-20, ESIS and HILac) are described in this paper.

POLARIZED ION SOURCE

Presently the maximum achieved intensity of polarized beam in the Nuclotron is about $2\cdot10^{8}$ particles per cycle. The main direction of work aimed at increase of the intensity is connected with the design and construction of a new high current polarized ion source with charge-exchanged plasma ionizer (IPSN) based on the equipment of CIPIOS polarized proton and deuteron source transferred to Dubna from Bloomington (Indiana University, USA) [2]. The work is carried out in collaboration with INR (Troitsk). Some parts of suitable equipment for the new source were presented by DAPHNIA (Saclay). The IPSN will provide the output beam current up to 10 mA of $\vec{d}^{+}$ and $\uparrow p$ ions. $\vec{d}^{+}$ ion polarization of 90% of the nominal vector mode +/-1 and tensor mode +1,-2 is expected. That will result in increase of the accelerated polarized beam intensity at the Nuclotron up to above 10^{10} part/cycle.

ALVAREZ-TYPE LINAC LU-20

LU-20 Linac Status

At present time, the injector of the Nuclotron is the Alvarez-type linac LU-20 (Fig. 1), which was built in 1974 as a proton injector with output energy of 20 MeV. Main parameters of LU-20 were presented in paper [3]. LU-20 was originally designed as so-called the $L = \beta\lambda$ Alvarez drft-tube linac (DTL).

Fig. 1. Inner view of LU-20 resonator.

It can also operate in the second harmonic mode as the $L = 2\beta\lambda$ DTL allowing acceleration of light ions with output energy of 5 MeV/u, it was experimentally proved that it is also possible to accelerate ions with $Z/A \geq 1/3$ ions at increased levels of RF field. In the middle of nineties, the front part of the LU-20 was upgraded in order to ensure acceleration of ions with

STOCHASTIC COOLING SYSTEM PROTOTYPE FOR NUCLOTRON

I. Meshkov, V. Seleznev, N.Shurkhno, A. Sidorin, G. Trubnikov, JINR, Dubna, Moscow Region
R.Stassen, IKP FZ Juelich, Germany

Abstract

Joint Institute for Nuclear Research (JINR) initiated the creation of a new and unique heavy-ion collider – Nuclotron-based Ion Collider Facility (NICA), which is planned to be operational in 2016 [1]. The luminosity in the colliding beams of Au^{79+} ions is expected to reach 10^{27} $cm^{-2}s^{-1}$. By met estimates it will mainly be determined by the intra-beam scattering effect. To suppress one, it was proposed to use the cooling of the beam. For the medium and high-energy heavy ions, such as NICA collider, stochastic cooling will be more efficient, then electron cooling, so this system will be used in the collider. In the coming years it's planned to build stochastic cooling system prototype at presently working accelerator Nuclotron to test different working modes at an early stage of NICA project. Main results of the development of stochastic cooling system at Nuclotron are presented.

INTRODUCTION

The Veksler and Baldin Laboratory of High Energy Physics (VB LHEP) of JINR is a pioneer in designing, constructing and commissioning the world first fast cycling synchrotron based on low-field iron dominated electromagnets with superconducting coils. This accelerator named Nuclotron was commissioned in 1993 [2]. Superconductive ring of 251,5 m in circumference is located in the tunnel with a cross-section of 2,5x3 m that was a part of the Synchrophasotron infrastructure. Since 1993 it was performed 41 beam runs at the accelerator. Presently the Nuclotron delivers ion beams for experiments on internal targets and for fixed target experiments using slow extraction system. Achieved energy of protons is 5.7 GeV, deuterons – 3.8 GeV/u and nucleons - 2.2 GeV/u.

The Nuclotron lattice is typical for a strong-focusing separated function synchrotron. It contains 8 superperiods. Each superperiod consists of three regular FODO cells. The fourth cell has not a dipole magnet. The regular cell includes F- and D-quadrupole magnets, four dipole magnets and two small drift spaces for the installation of correcting magnets, beam monitors, etc. In total the ring contains 96 dipole, 64 quadrupole, 32 correcting multipole SC-magnets. The betatron tunes are $Q_x \sim Q_y \approx 6.75$.

There are two straight sections on the direct opposite sides of the ring (Fig.1) where the pick-up and kicker can be installed.

The main argument to have operating stochastic cooling system prototype at Nuclotron - is to test different working modes of the machine. The first stage includes longitudinal cooling of the coasting deutron or light ion (lithium, carbon) beam using notch filter technique [3] for the cooling.

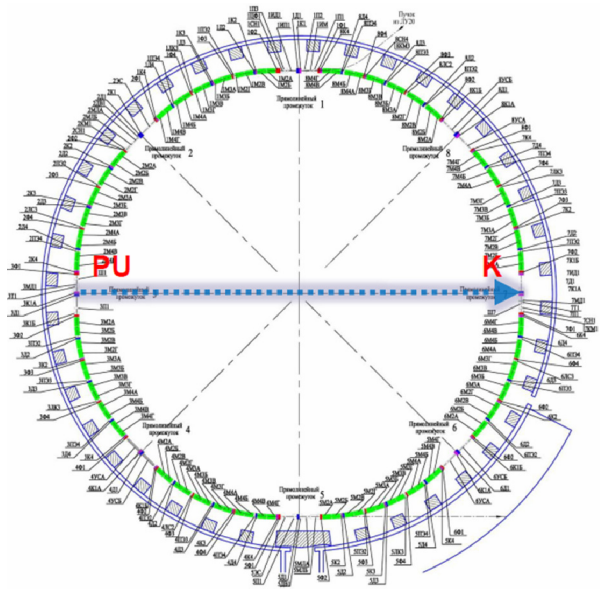

Figure 1. Nuclotron ring configuration.

Regular operation cycle duty of the machine is from 5 to 10 seconds, the flat-top time is around 80% of the duty cycle, therefore period available to get effect of the stochastic cooling process is limited to characteristic flat-top time. Main parameters of the accelerator summarized in Table 1.

Table 1. Nuclotron ring parameters

Circumference, m	251.5
Ions	up to A = 124
Energy, GeV/u	6
Rev.frequency, MHz	1.2
Vacuum, Torr	10^-10
Intensity	10^11(p)-10^9(C12)
dp/p	10^-3
Ring slippage factor	0.0322

SCHEME OF THE PROPOSED STOCHASTIC COOLING SYSTEM

The first step in realization of stochastic cooling experiment is longitudinal cooling of the coasting beam.

PROJECT OF JINR SUPERCONDUCTING SYNCHROTRON FOR HADRON THERAPY

E.M. Syresin#, V.A. Mikhaylov, A.V. Tuzikov, N.N. Agapov, A.V. Eliseev,
G.G. Khodzhibagiyan, V.N. Karpinsky, A.D. Kovalenko, A.I. Malakhov, I.N. Meshkov,
A.G. Olshevsky, G. D. Shirkov, S.G. Shirkov, G.V. Trubnikov,
Joint Institute for Nuclear Research, Dubna, Russia

Abstract

The project of the medical carbon synchrotron at maximal ion energy of 400 MeV/n was developed in JINR. The project goal is accumulation of the superconducting technology at construction of the carbon synchrotron with a circumference of 65 m on basis of the Nuclotron type magnet elements. For injection of the carbon ions it is proposed to use IH linac of C^{4+} at energy 4 MeV/n. The superconducting gantry is developed for patient treatment at a weight of 150 t.

INTRODUCTION

Today, the cancer is the second highest cause of death in developed countries. Its treatment still presents a real challenge. Protons and carbon ions allow depositing the radiation dose more precisely in a cancer tumor, reducing greatly the amount of dose received by healthy tissue surrounding the tumor with respect to electrons. But in addition to the ballistic accuracy of protons, the carbon ion beams have an extra advantage in radiation therapy: they have a different biological interaction with cells and are very effective even against some type of cancerous cells which resist to usual radiations. That is why the last years have seen increasing interest in particle therapy based on $^{12}C^{6+}$ ions. A project of the medical superconducting synchrotron dedicated for the carbon therapy has been designed in JINR.

The basis of this medical accelerator is the superconducting JINR synchrotron – Nuclotron [1,2] (Fig.1).

Figure. 1: JINR superconducting synchrotron- Nuclotron.

The Nuclotron type straight dipole magnets [2] (Fig.2) were adopted for the optic of the medical synchrotron and beam delivery system. The superconducting magnets permit to reduce the accelerator electrical consumption, the size and weight of the accelerator. Especially the superconducting technology is important at design of the carbon gantry. A superconducting gantry was developed for tumor treatment at a weight of 150 t.

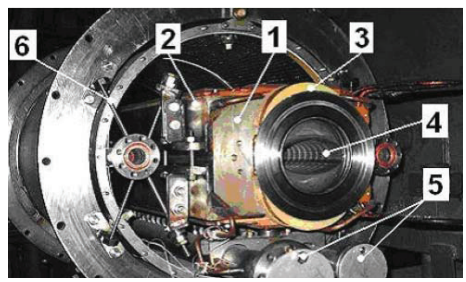

Figure. 2: The Nuclotron type dipole magnets

INJECTION

The superconducting electron string ion source [3] is planed to use for $^{12}C^{4+}$ injection in the carbon linac. Additionally this source can applied for formation of primary radioactive carbon ion beams $^{11}C^{4+}$ in ISOLDE scheme. The intensive primary radioactive $^{11}C^{4+}$ ion beams can be used simultaneously for cancer treatment and on-line PET. The compact IH linac [4] (Table 1) will applied as synchrotron injector. The injection channel consists from two sections: the discharge section, where accelerated in IH linac ions C^{4+} are discharged to ions C^{6+}, and the section of injection of ions C^{6+} in the synchrotron.

Table 1. Parameters of carbon IH linac.

Parameters	RFQ	IH-DTL
Injection energy, MeV/u	0.01	0.61
Extraction energy, MeV/u	0.61	4
Operation frequency, MHz	200	200
Charge-mass ratio	1/3	1/3
Cavity length, m	2.5	3.4
Cavity outer diameter, m	0.42	0.44
Power, kW	120	360
Normalized 90% emittance, π·mm·mrad	0.85	1.1
Normalized 90% longitudinal emittance, π·ns·keV/n	1	1.2
Energy spread,%		±0.4
Maximal beam current, eμA	392	390

#syresin@nusun.jinr.ru

INTERCATION OF THE BIOMOLECULAR IONS WITH THE ELECTRON TARGET IN THE ELECTROSTATIC STORAGE RING

Syresin E.M., Shirkov S.G.,
Joint Institute for Nuclear Research, Dubna, Russia

Abstarct

A nanostructure of the radiation damages is formed at an interaction of carbon ions with DNA molecules at hadron therapy. A local interaction of the ion beam with the bimolecular structures in the human cells is defined mainly by parameters of the ion tracks. The track core is connected with ionization properties of the charged ion, its cross-section sizes are defined by the delta-electrons. The delta-electron energy varies statistically from several eV to few keV therefore they lead to substance ionization along their trajectory on a distance several nanometers from that point where they were produced.

Interaction of the delta-electrons with DNA molecules and other biological structures is one of the important mechanisms realized in process of the hadron therapy. A study of interaction of the accelerated biomolecular ions with an electron target in the electrostatic storage ring was performed for modeling of an input of the delta-electrons in processes of the hadron therapy.

INTRODUCTION

The realization of carbon therapy on a microscopic level is connected with a nanostructure of local radiation damages produced along trajectories of ions with a characteristic cross dimension of a few nanometers and a root-mean-square distance between the damages several hundred nanometers (Fig. 1), covering the structure of DNA molecules in the tumor cells with a probability around of 80%. The arising two-strand breaks of DNA molecules are irreversible because of high linear energy transfer (LET) for particles stopped in the tumor, while the structure of radiation damages in normal tissues at low LET ensures less than 10–20% probability of complications in these tissues, producing damages (predominantly single-strand DNA breaks) that allow cell functioning to be restored after irradiation.

At carbon therapy the ions produce the double-strand breaks of DNA molecules by the direct ionization. The delta-electrons are formed also at this ionization. It leads to additional DNA breaks along the electron trajectories. As a result, the radiation damages arise in the region of ion track with the lateral dimensions of the order of nm comparable with the DNA transverse dimensions. Majority of the delta-electrons have energy lower 30 eV.

The interaction of the electrons with an energy of 0.5-100 eV with the biomulecular ions at a mass of 1000-66000 a.m. accelerated up to energy of 30 keV/Z in the KEK (Japan) electrostatic ring is discussed below.

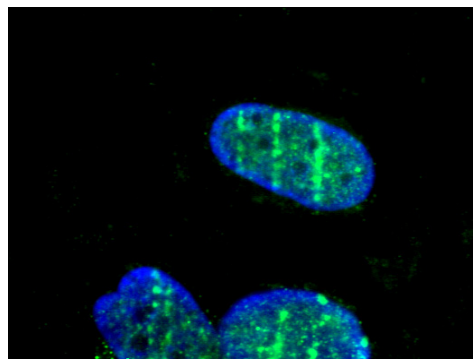

Fig.1. Photo of irradiated human cells taken at the fluorescent microscope. Fluorescent markers demonstrate nanostructured double-strand breaks of the DNA molecules caused by the carbon ions.

ELECTROSTATIC STORAGE RINGS

The magnetic rigidity Bρ of the ion storage ring is determined by the ion mass M: $B\rho=(2E_iM/q_i^2)^{1/2}$, where E_i and q_i is ion energy and charge. Consequently, the biomolecular ions of proteins, amino acids or DNA ions with a mass of 10^3-10^6 a.m. can not accelerated in the ion storage rings with a magnetic structure. In this regard, in recent years a new class of electrostatic storage rings [1-4] was constructed. The rigidity of electrostatic ring Eρ does not depend on ion mass: $E\rho=2E_i/q_i$. These storage rings were effectively used for the formation and accumulation of the biomolecular ion beams [1-4].

The circumference of the KEK electrostatic ring is equal to 8.1 m. The accumulated current of biomolecular ions was 50-500 nA. The lifetime of biomolecular ions with masses up to 66 000 in the KEK electrostatic storage ring is 10-20 s at a pressure of $(3\text{-}5)\times10^{-11}$ Torr. The ring acceptance corresponds to 50 π·mm·mrad. The emittance of stored ion beam is equal to 15 π·mm·mrad, the ion beam diameter is about 6 mm in the electron target. The relative momentum spread corresponds to 10^{-3}.

The biomolecular ions are produced in the electrospray ion source [2]. Then they are stored in the ion trap to increase by one order of magnitude the

POWER SUPPLY AND PROTECTION SYSTEM OF THE NUCLOTRON BOOSTER IN THE NICA PROJECT

A. Kudashkin, V. Karpinsky, H. Khodzhibagiyan, A. Sidorin, JINR, Dubna, Russia

Abstract

The Nuclotron Booster in NICA project [1] is aimed to accelerate heavy ions up to 600 MeV/u to provide effective stripping before injection into the Nuclotron. The Booster power supply system consists of one powerful unit, providing maximum current of 12 kA and field ramp up to 1.2 T/s, and two additional units, that are used for the ring working point adjustment. The quench protection system is based on thyristor switches. Structure and parameters of the power supply system are presented.

THE SYSTEM STRUCTURE AND DESTINATION

The Nuclotron-type design based on a window-frame iron yoke and a saddle-shaped superconducting winding is chosen for the Booster. The Nuclotron magnets include a cold (4.5K) window frame iron yoke and a superconducting winding made of a hollow NbTi composite superconducting cable cooled with two-phase helium flow at T = 4.5 K [2]. A further development of the technology was proposed [3] to increase the efficiency of the magnetic system. In accordance with this proposal the single-layer winding bent dipole will be built to reduction the magnet cross section and AC losses in comparison with the straight double-layer winding dipole at the same aperture budget by means of the doubled structural current density in a winding.

At design of the Booster power supplies system (fig. 1) the requirement of consecutive connection of structural dipole magnets (total inductance 16.4 mH), quadrupole focusing (total inductance 0.6 mH) and defocusing (total inductance 0.6 mH) lenses is accepted for a basis. The main powerful source of the power supply system forms a demanded current (up to 12.1 kA) with the required magnetic field ramp of 1.2 T/s in the general chain according to a demanded cycle.

The powerful power supply source consists of connected in parallel thyristor rectifiers PS1, 2, powered from a high-voltage net 6 kV. Each of sources “PS” is a 12 phase rectifier with nominal parameters of 180 V x 6.3 kA, and phase shift between voltages of 15 degree. Together PS1, 2 form 24 phases regulated thyristor rectifier with nominal output parameters 180 V x 12.6 кА, that allows to receive the magnetic field ramp of 1.2 T/s. The peak power of a source is 2.5 MW.

Two additional power supply sources of essentially smaller power are intended for flexible adjustment of an working point of the accelerator. One of them allows to change simultaneously a field gradient in focusing and defocusing lenses, another only in defocusing ones.

The power supply system includes also equipment of regulation, management and diagnostics.

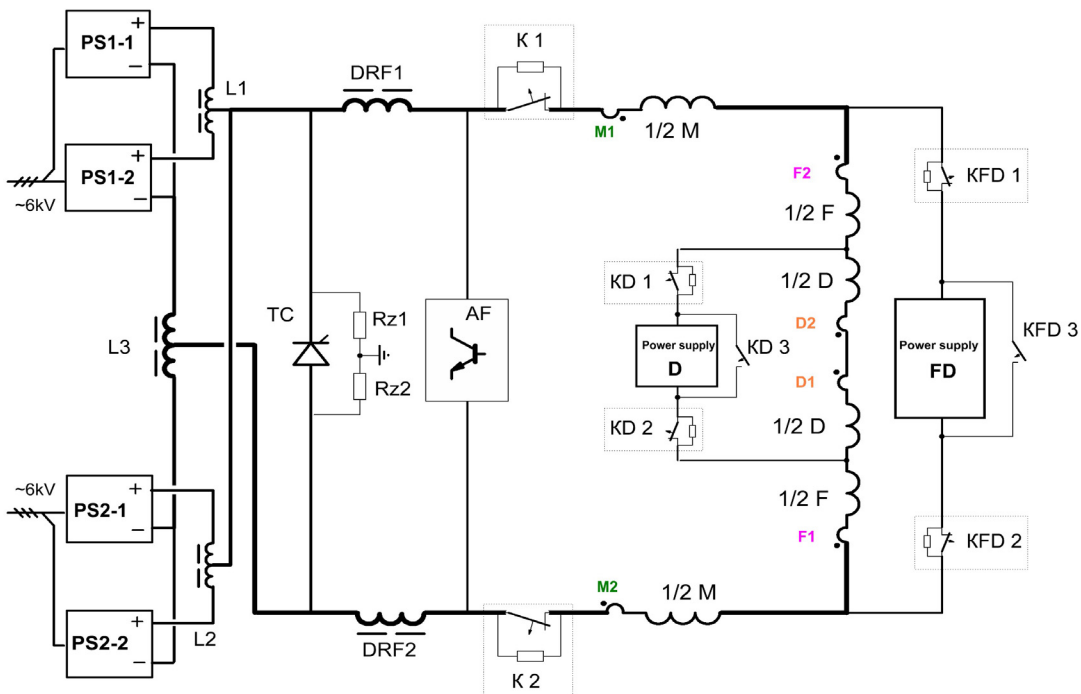

Fig. 1. The schematic diagram of the Booster power supply system (the explanation in the text).

DEVELOPMENT OF INJECTOR FOR ITEP HEAVY ION SINCHROTRON BASED ON LASER PLASMA GENERATOR

N. Alekseev, A. Balabaev, A. Belokurov, I. Khrisanov, A. Vasilyev,
Yu. Satov, B. Sharkov, A. Shumshurov, *ITEP, Moscow, 117259, Russia.*

Abstract

A schematic diagram of heavy ion injector based on laser ion sources is described. Two different basic laser configurations used in ITEP synchrotron. First laser excels in simplicity and consists of CO_2 free-running laser that is applied for carbon target plasma heating and ionization at laser power density $q=3\cdot10^{12}W/cm^2$ to create high current C^{4+} ion beam. Second master oscillator-amplifier laser configuration intends for production super high laser intensity at a target to provide considerable charge state in a plasma of heavy elements (Al, Fe, Ag etc). This laser configuration is founded on original physical principle* that simplifies the installation and ensures high reliability for long term operation.

Laser characteristics for the different laser scheme and ion current for injector outlet beam of C^{4+} and Ag^{+19} are shown in this paper. The latter was accelerated in synchrotron for energy up to 100 MeV/u.

* K. N. Makarov et al. Quantum Electronics (Russian), 2001, 31 (1), pp. 23÷29

INTRODUCTION

The fundamental knowledge of the high charge state ion generation with lasers was obtained in the frame of laser-plasma interaction researches. In Russia such investigations were carried out in leading physical institutes with different types of laser. In particular, it was shown that high intensity laser radiation focused on the material allows creation of high temperature powerful stream of plasma having small phase volume. The following separation of electron and ion components produces a pulsed ion source with superior luminosity. Basing on known in literature laser-plasma investigation publications one might say that there are no crucial distinctions for laser-plasma ion generators using different types (different wavelength) of lasers. Nevertheless, CO_2 lasers are mainly used in the practice due to their high output energy with comparative technical simplicity for the repetition rate operation, cheapness of the installation and ecological compatibility. These preferences of CO_2 lasers ensure adapting them in a laser-plasma ion source for an ion accelerator injector. The use of such injectors in a heavy ion synchrotron simplifies the accelerator scheme due to momentary (by a single pulse) ring filling by the particles of proper mass and charge state number.

The investigations of the ion generation from plasma produced by CO_2 laser pulses with a target power density q up to $q\leq5\cdot10^{13}$ W/cm^2 and the laser-plasma generators (LPG) development were realized by ITEP-CERN-TRINITI collaboration [1-9]. In the frame of lead ion generation measurements it was shown that, in particular:

1. The total ion current is proportional to the laser pulse energy while the other parameters remain unchanged.
2. The average ion charge state number is proportional to logarithm of the laser flux at a the target, at least, for the case of ionization of external atomic shells.
3. For an effective laser-plasma heating it is necessary to use the laser pulse duration τ_p less than the characteristic plasma expansion time τ_{exp} ($\tau_p < \tau_{exp}$). The latter is defined by the ion velocity and the characteristic plasma thickness which depend finally on the target laser pulse density. Otherwise, the process of laser-plasma interaction for long high power density pulses is complicated due to the refraction of the laser beam in the plasma corona, self-focusing of laser radiation and generation of shock waves distorting the expanding plasma flow. As a result, the laser heating efficiency drops and useful part of ions near expansion axis is decreased.

The experimental data allow choosing the laser driver scheme with such general considerations. It is known, for example, that the free-running CO_2 generator provides the laser pulses with duration $\tau_p \leq 40$ns. That allows to use efficiently such a laser for ion generation up to $q\leq10^{11}\div10^{12}$W/cm^2 and, correspondingly, for the plasma expansion velocity $V_{exp}<10^6$cm/s. In these conditions the plasma extension is not to be significant during the laser heating $V_{exp}\cdot\tau_p < 0.4$mm. The ion generation for a higher laser flux requires using more complicate optical laser scheme such as master-oscillator power amplifier (MOPA) configuration. The shortest pulse duration is to be $\tau_p \approx 150$ ps correspondingly the amplification line width of 7GHz for the typical gas mixture of an atmospheric pressure CO_2 laser [10]. The ITEP heavy ion accelerator injector is based on both the free-running and the MOPA CO_2 lasers (LPG-1,2) to carry out scientific program devoted to fundamental researches and medical applications. Now the heavy ion acceleration program is basically founded on two laser systems: effective free-running generator "Malish" and wide aperture laser L-100 that operates in two modes, either a free-running generator [11] or a master oscillator-power amplifier configuration. The laser-plasma ion source with the MOPA scheme is directed to generate extremely ionized heavy particles, similar to Al, Fe, Ag, Pb, etc. The free-running CO_2 laser is used in the injector of carbon ions.

DEVELOPMENTS OF LPG-1 AND LPG-2

Laser plasma generator LPG-1 including the free-running laser "Malish" was developed to increase output laser intensity as a main parameter. The improvement consists of modernization of an electrical scheme for formation of volume discharge basing on the techniques described

SIMULATION OF Au^{32+} BEAM LOSSES DUE TO CHARGE EXCHANGE AND DYNAMIC VACUUM IN NUCLOTRON BOOSTER

A.V. Philippov[#], A.B. Kuznetsov , V.A. Mikhaylov , A.O. Sidorin , G.V. Trubnikov
JINR, Veksler and Baldin Laboratory of High Energy Physics Dubna, Russia
P. Puppel , P. Spiller
GSI Helmholtzzentrum für Schwerionenforschung GmbH, Darmstadt, Germany

Abstract

The StrahlSim code [1] was used to simulate the beam loss and the dynamic vacuum for the proposed Nuclotron booster [2]. The Nuclotron booster will accelerate Au32+ ions from 6.2 MeV/u to 600 MeV/u. The simulations have been carried out considering systematic injection (0% to 10%) and RF-capture losses (5% to 15%). Furthermore the influence of an ion catcher system on the beam loss has been investigated, in order to estimate, if such a system could stabilize the beam loss. Without an ion catcher system, zero systematic losses, and a static pressure of 10^{-11} mbar ($7.5\cdot10^{-12}$ Torr), the transmission was calculated to be 83%. The presence of an ion catcher system would stabilize the transmission at a considerably higher level than without such a system for all scenarios.

BOOSTER PARAMETERS LIST

The main functions of the Nuclotron booster are the following [2]:

- Accumulation of $4\cdot10^9$ Au^{32+} ions in the booster;
- Acceleration of the ions up to energy of 600 MeV/u that is sufficient for stripping the gold ions up to the charge state of 79+;
- Simplification of the requirements to the vacuum conditions in the Nuclotron owing to higher energy and charge state of the ions injected into the Nuclotron;
- Decrease of the ion beam longitudinal emittance at the energy of approximately 100 MeV/u by application of electron cooling.

The FODO lattice was considered for further investigation as the more preferable lattice design. The parameters for the booster are listed in tables 1, 2, and 3. A diagram of the booster cycle and a scheme of the booster vacuum system are shown in Fig. 1, 2.

SIMULATION SETUP

The acceleration ramp had to be divided into two parts, because StrahlSim is not capable of simulating a waiting time in the middle of the ramp, as it is foreseen in the Nuclotron booster cycle. The division of the simulation is shown in Fig. 1 (left and middle) and was used for all calculations. First part (red line): injection at 6.2 MeV/u, acceleration with 1 T/s to 100 MeV/u and 1 s waiting time (electron cooling) at this energy. Second part (green line): acceleration with 1 T/s to a beam energy of 600 MeV/u, followed by a fast extraction at this energy, and ramping down. The beam losses due to electron cooling were not simulated, because StrahlSim is unfortunately not able to consider these losses. So the simulated beam losses during the cooling time are only due to charge exchange processes, and therefore less than the beam loss that can be expected.

Table 1: Parameter list for the Nuclotron booster lattice.

Fold symmetry	4
Number of the FODO lattice cells per arc	6
Length of lattice cell, m	9
Length of straight sections per cell, m	4
Betatron tunes	5.8/5.85
Phase advance per cell	1.51
Amplitude of β-functions, m	17
Maximum dispersion function, m	2.9
Dipole	
Beam horizontal/vertical emittance, π·mm·mrad	10/10
Effective field length, m	2.2
Curvature radius, m	14
Quadrupole	
Bending angle, degree	9
Effective field length, m	0.4
Average aperture	
Chamber shape	elliptical
Vacuum chamber, m^2	0.065×0.032

Unfortunately there are no charge exchange cross sections for Au^{32+}. Therefore the cross sections for Au^{31+} have been used for all simulations discussed in this work. The differences between these cross sections are considered to be negligible.

Table 2: Parameter list for the Nuclotron booster.

Ions	Au^{32+}
Circumference, m	211
Injection/extraction energy, MeV/u	6.2/600
Magnetic rigidity, T·m	2.4÷25

[#]philippov@jinr.ru

RTS&T CODE STATUS

I.I. Degtyarev*, O.A. Liashenko , F.N. Novoskoltsev , I.A. Yazynin , IHEP, Protvino, Russia
A.I. Blokhin, IPPE, Obninsk, Russia

Abstract

The paper describes the main features of the RTS&T2010 the modern version of the RTS&T (Radiation Transport Simulation and Isotopes Transmutation problem) code system [1]. The RTS&T code performs detailed Monte Carlo simulations of many type of particles transport in complex spatial geometries with composite materials in the energy range from thermal energy up to 100 TeV. The RTS&T code considers interaction of low-, intermediate-, and high-energy particles with condensed matter, including hadron-nucleus interactions inside the target, generation and transportation of secondary particles, deposition of energy and production of radionuclides in the target. Recently, the transfer of ions was added and tested. The modern version of the RTS&T code supports a researches in the fields of accelerator and reactor technologies, radiotherapy, space radiation, and in many other fields which are related to particle and ion transport phenomena.

INELASTIC HADRONIC AND PHOTONIC INTERACTIONS

Inelastic hadronic and photonic interactions are simulated within RTS&T code by several energy-dependent models based on the different microscopic and macroscopic approaches (Fig. 1) [2].

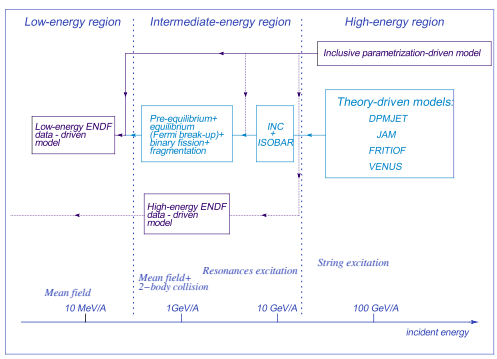

Figure 1: Inelastic hadronic and photonic interactions are simulated within RTS&T code by several energy-dependent models based on the different microscopic and macroscopic approaches.

High-Energy Region

To simulate of hadron(nucleus)-nucleus inelastic collisions at $E > 5$ GeV the modified versions of some micro-models (DPMJET-II/III, JAM, FRITIOF,VENUS, RQMD) or an inclusive parametrization-driven model can be used. These codes has been completed with a simulation of the nuclear destruction at fast stage of the interaction, with a calculation of the excitation energy of the nuclear residual nuclei and with a simulation of the nuclear relaxation stage in the framework of the statistical evaporation model to calculate the characteristics of the inelastic hadron-nucleus and nucleus-nucleus interactions at the energies higher 3-5 GeV per nucleon.

Intermediate-energy region

In the RTS&T calculations, the hadron-induced nuclear reaction process in the energy region about 20 MeV to 5 GeV is assumed to be a three-step process of spallation (intranuclear cascade stage), pre-equilibrium decay of residual nucleus and the compound nucleus decay process (evaporation/high-energy fission competition). To calculate the intranuclear cascade stage, the Dubna-version of intra-nuclear cascade model coupled with the Lindenbaum-Sternheimer isobar model for single- and double-pion production in nucleon-nucleon collisions and single-pion production in pion-nucleon collisions was provided. Recently, an addition of multiple-pion channels was included in code package to simulate up to 5 pions emission. The pre-equilibrium stage of nuclear reaction simulation is based on the exciton model. The initial exciton configuration for pre-equilibrium decay is calculated at the cascade stage of reaction or postulated in general input. The equilibrium stage of reaction (evaporation/fission processes competition) is performed according to the Weisskopf-Ewing statistical theory of particle emission and Bohr and Wheeler or Fong theories of fission. To calculate the quantities determining the total fission width, Atchison prescriptions are used.

Low-Energy Region

The RTS&T code uses continuous-energy nuclear and atomic evaluated data files to simulate of radiation transport and discrete interactions of the particles in the energy range from thermal energy up to 20/150/3000 MeV. In contrast with is a well-known and widely used Monte Carlo code MCNP [4, 5] for neutron, photon, and electron transport simulations, the ENDF-data driven model of the RTS&T code does access the evaluated data directly. In current model development, all data types provided by ENDF-6 format can be used in the coupled multy-particle radiation

* Igor.Degtyarev@ihep.ru

THE COMPACT FARADAY CUP FOR RADIOBIOLOGICAL RESEARCHES IN IHEP ACCELERATORS BEAMS

Yu. Antipov, N. Anferov, G. Dantsevich, A. Koshelev, A. Larionov, V. Seleznev, A. Sytin,
Institute for High Energy Physics, Protvino, Moscow region, Russia

Abstract

IHEP's experts are currently working on the creation of a medical irradiation centre with beams of protons and carbon ions on the basis of IHEP acceleration complex. Already existing IHEP accelerators I-100 - U-1,5 - U-70 are forming a complete chain capable of accelerating not only protons, but also, due to certain modifications, light ions: deuterons and carbon. The compact autonomic Faraday cup which works in the atmospheric environment has been developed to measure currents in the accelerators beams. The device has a good electromagnetic protection. It is compact and allows to make measurements on any (from 600 mm long) open site of a beam line. Vacuum tests and work with biological samples on a beam of protons of I-100 accelerator have proved that the Faraday cup is meeting all the requirements.

INTRODUCTION

IHEP's experts are currently working on the creation of a medical irradiation centre with beams of protons and carbon ions on the basis of IHEP acceleration complex. Already existing IHEP accelerators I-100 - U-1,5 - U-70 are forming a complete chain capable of accelerating not only protons, but also, due to certain modifications, light ions: deuterons and carbon.

In collaboration with scientists of the Medical radiological scientific centre (MRSC, Obninsk, Kaluga region), IHEP experts make biological researches in IHEP accelerators, with existing beams. Possible places of making researches on complex IHEP are shown on fig. 1 by red colour.

The parameters of beams in these sections [2] are shown in the Table 1.

Table 1: Parameters of beams at 3 points of IHEP accelerators

	Ions	Kinetic energy, MeV/u	Range in water, mm	Z/A	Pulse duration, current	
I-100 (point 1)	$_1H^{+1}$	72	43	1	1÷50 μs	1-50 mA
	$_2H^{+1}$	16,7	4	1/2	1÷50 μs	15 mA
	$_{12}C^{+6}$	16,7	1,0	1/2	3 μs	1.5 mA
U-1,5 (point 2)	$_1H^{+1}$	<1320	<4700	1	≈0.2 μs	400 mA
	$_2H^{+1}$	<440	<2000	1/2		80 mA
	$_{12}C^{+6}$	<440	<300	1/2		8 mA
U-70 (point 3)	$_1H^{+1}$	<1320	<4700	1	Slow extraction	
	$_2H^{+1}$	<440	<2000	1/2		
	$_{12}C^{+6}$	<440	<300	1/2		

CALIBRATION OF THE ELECTROSTATIC BEAM POSITION MONITOR FOR VEPP-2000

Yu. A. Rogovsky, I. N. Nesterenko, BINP SB RAS, 630090 Novosibirsk, Russia

Abstract

The basic requirement for the VEPP-2000 Beam Position Monitor (BPM) is the measurement of the beam orbit with 0.1 mm precision. To improve the measurement accuracy, the response of the electrostatic BPMs (pickups) were mapped in the laboratory before they were installed in the VEPP-2000 ring. The wire method for the sensitivity calibration and position-to-signal mapping is used. The test stand consists of high frequency coaxial switches to select each pickup electrode, movable antenna to simulate the beam, signal source, spectrum analyzer to measure the pickup signals, and analysis software. This calibration showed possibility of required accuracy. During calibration the electrical center of the different BPMs was measured with respect to the mechanical center. Conversion between the BPM signal and the actual beam position is done by using polynomial expansions fit to the mapping data within ± 6 mm square. Results for these portions of the calibration are presented.

INTRODUCTION

A beam position monitor system is operated for two kinds of orbit measurements, a relative measurement and an absolute measurement. The former is to measure the orbit displacement from the initial or standard orbit when some optics perturbation is applied. The latter case is to measure orbit position relative to the geometrical monitor center. This function will be essential for maintaining stable operations in a ring where the optics depends strongly on the orbit, particularly at nonlinear optics elements.

Closed orbit stabilization and correction is routine operation for VEPP-2000 ring [1, 2]. To stabilize the beam orbit, the absolute beam position should be measured. The output data from a position monitor system usually shows the orbit position relative to the electric monitor center, not the geometrical center. So we should calibrate each beam position monitor to know the location of the electric center with respect to geometrical one i.e. relative to the reference frame of each BPM.

Moreover the system needs calibrating not only because of pickup characteristics (center displacement, sensitivity and nonlinearity) caused by machining, installment, cable matching, and signal processing circuits, but in order to meet the requirements on the accuracy of the measured beam position.

Basically there are 4 BPMs installed in VEPP-2000 ring, but there is reserve one. In order to test characterize, align, and provide data for calibration, a general purpose test stand was designed and constructed in 2006. All BPMs needed for operations was calibrated and data analyzed in the same year, and last one was processed in 2009 because of some replacement actions.

CALIBRATION TEST STAND

BPM Block

The electrostatic BPM for VEPP-2000 ring consist of four 15 mm diameter button style electrodes are mounted on the diagonals of its housing and are centered symmetrically. Buttons orientation is 45 degrees to avoid the fan of synchrotron radiation. All parts precisely machined from solid stainless steel blocks, isolated the electrodes and feedthroughs with ceramic material. The electrode surface is smoothed with that of the vacuum chamber, so the impedance induced by the electrode may be reduced greatly. The vacuum chamber of VEPP-2000 is not the same along the ring. With exception of the bending magnets, it has approximately square form (35 mm inscribed circle diameter). The BPM is integral part of the quadrupole vacuum chamber of the technical strait section, which in turn is referenced to the magnet axis by means of supporting arms, and assembled on the vacuum chamber by welding, assuring no gas leak. To reduce the mechanical surveyment for the BPM with the same vacuum chamber dimensions, BPM housing has the same cross section form and dimensions, and coincides with the vacuum chamber within ± 0.2 mm. Fig. 1 shows a transverse section and common view of the pickup before assembling.

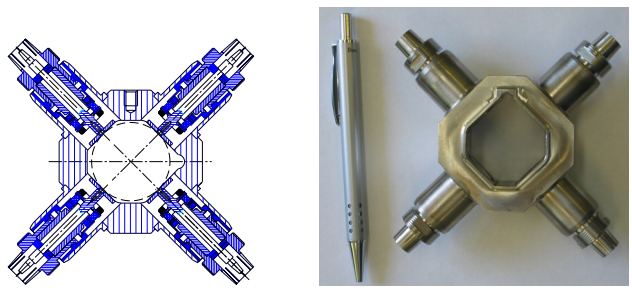

Figure 1: The electrostatic BPM for VEPP-2000 ring.

Test Stand and Data Collection

The approach used to determine the position of the electron beam is to treat the effect of the beam as a two dimensional electrostatic problem. An electron beam passing through a BPM induces a charge on the buttons, which uniquely depends on the position of the beam. Due to the lack of longitudinal variation, the electron beam appears to be essentially a line charge. Using the voltage on the buttons, one can solve for the position of the electron beam.

PICKUP BEAM MEASUREMEN SYSTEM AT THE VEPP-2000 COLLIDER

Yu. A. Rogovsky, E. A. Bekhtenev, BINP SB RAS, 630090 Novosibirsk, Russia

Abstract

This paper reviews the present state of electromagnetic beam position monitors (pickups) at VEPP-2000 collider. It includes descriptions of position monitors, typical interfaces for these monitors and their system characteristics (resolution, stability, bandwidth and problems or limitations) are discussed. The paper also reviews several types of diagnostic measurements using beam position monitors which are useful in improving accelerator operations.

INTRODUCTION

The new electron-positron collider VEPP-2000 ring is a part of VEPP-2000 complex [1, 2] at BINP has been successfully commissioned and has been delivering luminosity at energy close to 508 MeV since June 2007. VEPP-2000 is a new machine with luminosity up to 10^{32} cm^{-2}s^{-1} and the beam energy from hadron production threshold up to 2×1 GeV. Small ring size and sophisticated optics lay on limitation on beam quality and operations. Therefore such modern machines requires various beam diagnostics for perfect tuning and ask us to monitor the beam status quickly and accurately.

The measurement and control of the closed orbit is one of the basic functions of any accelerator beam instrumentation and control systems. A beam position monitor (BPM) system is operated for two kinds of orbit measurements, a relative measurement and an absolute measurement. The former is to measure the orbit displacement from the initial or standard orbit when some optics perturbation is applied. The latter case is to measure orbit position relative to the geometrical monitor center. This function will be essential for maintaining stable operations in a ring where the optics depends strongly on the orbit, particularly at nonlinear optics elements.

The VEPP-2000 electrostatic BPMs system is not only used to monitor the beam orbit and correct the closed orbit distortion (COD), but also used to perform the interaction point (IP) beam steering along the detectors, control and adjustment of the beam oscillation amplitude during the injection, measure the dispersion functions and the betatron frequencies.

SYSTEM HARDWARE

The VEPP-2000 collider ring is equipped with a system of beam position diagnostics based on 4 electrostatic BPMs, frontend electronics located near BPMs and readout electronics in CAMAC standard. A set of low loss coaxial cables brings up the BPM signals of each detector to the local control room where the signal readout and processing electronics is located. The lengths of cables vary from 15 to 25 meters depending on the locations of the detectors in the storage ring. Each BPM is placed in the center of the technical strait section surrounded with two quadrupole magnets, very close to them. Before installation, electrical zero point of pickup electrode for each BPM is calibrated by a calibration bench with a wire method [3].

BPM Block

The beam position monitor for VEPP-2000 ring consist of four 15 mm diameter button style pickups are mounted on the diagonals of its housing and are centered symmetrically. The button type electrodes, which are capacitive coupled to the beam, are most popular with electron-positron rings because they occupy very little longitudinal space and the coupling impedance is small. Buttons orientation is 45 degrees to avoid the fan of synchrotron radiation. All parts precisely machined from solid stainless steel blocks, isolated the electrodes and feedthroughs with ceramic material. The electrode surface is smoothed with that of the vacuum chamber, so the impedance induced by the electrode may be reduced greatly. Fig. 1 shows a transverse section and common view of the BPM before assembling.

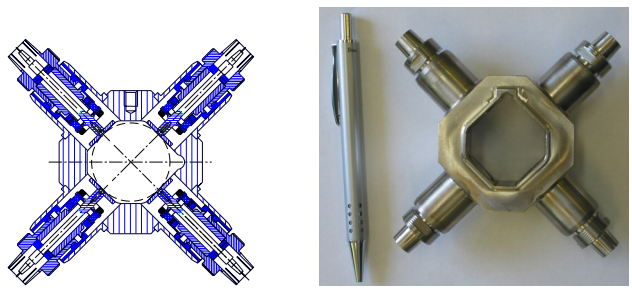

Figure 1: The beam position monitor for VEPP-2000 ring.

Electronics

The signals from four BPM electrodes are simultaneously processed with four channels of processing electronics. Each channel consist of LPF with cut-off frequency of 110 MHz, programmable gain amplifier and 12-bit ADC.

Time interval between electron and positron bunches is about 20 ns for each BPM. Analog electronics bandwidth of 110 MHz allows us to decrease the crosstalk of electron and positron bunches signals at level of 0.5 dB. Timing circuit provides ADC samples at the top of BPM signal. It is achieved by means of programmable delay of reference

* Work is supported by RFFBR, project 09-02-01060-a.

BEAM MEASUREMENTS WITH VISIBLE SYNCHROTRON LIGHT ON VEPP-2000 COLLIDER*

Yu. A. Rogovsky, D. E. Berkaev, A. N. Kyrpotin, I. N. Nesterenko,
A. L. Romanov, BINP SB RAS, 630090 Novosibirsk, Russia

Abstract

This paper describes beam diagnostics at VEPP-2000 collider, based on visible synchrotron light analysis. These beam instruments include: SR beamline and optics; acquisition tools and high resolution CCD cameras distributed around the storage ring to measure the transverse beam profile and its position in vacuum chamber; photomultiplier tubes (PMT) which enables beam current measurements; video system. Some applications of these measurement systems and their measurement results are presented.

INTRODUCTION

The new electron-positron collider VEPP-2000 ring is a part of VEPP-2000 complex [1, 2] at BINP has been successfully commissioned and has been delivering luminosity at energy close to 508 MeV since June 2007. VEPP-2000 is a new machine with luminosity up to 10^{32} cm^{-2}s^{-1} and the beam energy from hadron production threshold up to 2×1 GeV. Small ring size and sophisticated optics lay on limitation on beam quality and operations. Therefore such modern machines requires various beam diagnostics for perfect tuning and ask us to monitor the beam status quickly and accurately.

The measurement and control of the closed orbit is one of the basic functions of any accelerator beam instrumentation and control systems. A beam position monitor (BPM) system is operated for two kinds of orbit measurements, a relative measurement and an absolute measurement. The VEPP-2000 optical BPM system equipped with 16 CCD cameras registering beam synchrotron radiation have high precision of 1 μm, and used to monitor the beam orbit and correct the closed orbit distortion (COD), but hasn't absolute calibration.

BEAM ORBIT AND TRANSVERSE PROFILE MONITOR

SR acquisition system

Beam parameters in the VEPP-2000 collider measured by the Synchrotron Radiation (SR) at 8 points along the ring for both (e^+e^-) directions. Polished copper plates installed in the vacuum chamber, are used for output the SR from the bending magnets. The SR after passing through vacuum glass window comes to the optical diagnostics station and then is distributed by the half-transmitting mirrors Fig. 1-2.

Each station equipped with two CCD cameras (for positron and electron beams) for measurements the beam size and position. Because the SR outputs are located in orbital positions with very small dispersion function, four additional places are foreseen for dispersion and its symmetry control, and the beam position is measured in these points with pick-ups. In some stations the SR are used for beam current measurement (by the PMT) and will be used for the longitudinal beam sizes control in future (by the dissectors).

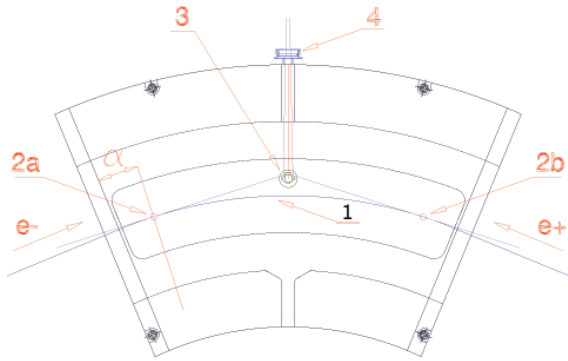

(a) 1-beam orbit, (2a, 2b)-radiation point of e^+e^- beams, 3-copper mirror, 4-output window, $\alpha = 4°47'$.

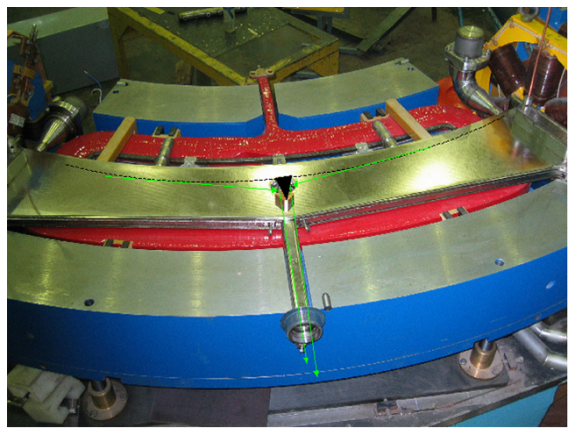

(b) Vacuum chamber and mirror after assembling. Additional mirror is placed in the center for comparison.

Figure 1: SR output in bending magnet.

CCD camera

Processing of optical part of the SR in circular accelerators allows one to obtain various beam parameters – vertical and radial sizes, axes tilt, position in a vacuum chamber. There is non-perturbative diagnostics that can work with super small beam currents. The essential nonlinearity (gamma correction) and low spatial resolution put some limitations on "TV camera + videograbber" system. In the case of a cheap digital TV camera the limitations ap-

* Work is supported by RFFBR, project 09-02-01060-a.

PROFILES AND INTENSITIES MEASUREMENTS IN THE DIAGNOSTIC SYSTEM OF THE EXTRACTED BEAMS OF THE U-70 ACCELERATOR

N. Ivanova, V.Kovaltsov, A.Koshelev, A.Lukyantsev, S.Makonin, A.Matyushin, V.Milyutkin, V.Seleznev, A.Sotnikov, IHEP, Protvino, Russia

Abstract

Diagnostic system for the extracted beams of the U-70 accelerator is a hardware-software complex with profilometers, intensimeters and electronic crates at the lower level, VME-crates with ADC-modules and MVME-167 processors (vxWorks operating system, basic EPICS tools, home made software) at the middle level, personal computers used as workstation at the upper level.

In this report we consider:

- The approaches to the system adaptation problems during the U-70 runs and solutions to these problems
- Data acquisition and hardware-sofware levels of data processing for non-standard profilometers
- The tools for the beam intensity measurement and presentation, the intensimeter calibration procedure.

INTRODUCTION

The diagnostic system for the extracted beams of the U-70 was operated since the 2001. The basic principles of the system and its original structure were described in [1].

The main tasks of the system are:

- the acquisition of beam related data and its primary processing;
- various on-line and off-line presentation of the information;
- data archiving and access to data.

The system does have a flexible adjustment mechanism, but it cannot solve all the problems. Since physicists and beam specialists are doing scientific research, an alteration of the software and hardware is sometimes needed. We will consider the ways of the non-standard measurement hardware integration into the system as well as the system adaptation to special operation modes.

LOWER AND MIDDLE LEVELS OF THE DIAGNOSTIC SYSTEM

The diagnostic system is a three-level hardware-software complex. The software for the upper and middle levels is based on the EPICS toolkit [2].

The layout of the middle and lower levels is shown in Figure 1. The signals related to beam particles are registered at the lower level. VME-crates with crate controllers and ADC-modules make up the middle level. This is the IOC (Input-Output Controller) in EPICS terms. In the considered configuration IOC consists of VTG, VSA, VCT modules and Motorola MVME-167 controller. VTG is the timing module, VSA is 12-bit ADC for 16 channels and VCT is 8-channel counter module.

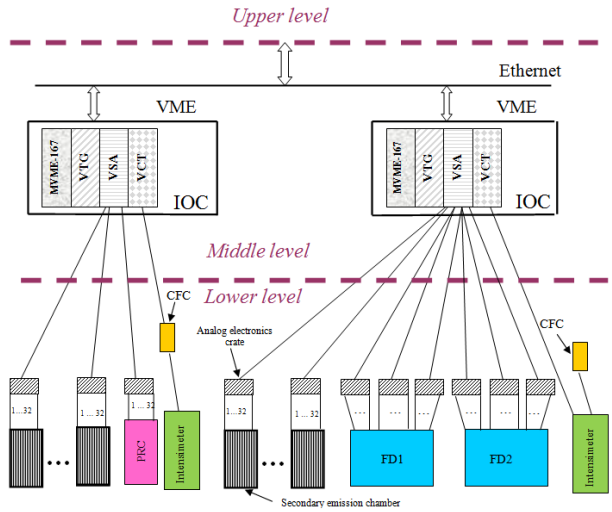

Figure 1: The layout of the lower and middle levels of the diagnostic system. The new components are marked by colors. PRC – the proportional chamber before beamstopper. FD1 and FD2 – the ionization chambers in the area of FODS setup.

IOC operates in the real time mode in accordance with the U-70 accelerator supercycles which are 8-9 seconds long. Within this time interval data should be acquired and processed and transferred to the upper level.

For IOC start-up one needs to load several files from the upper level via Ethernet. The files contain vxWorks operating system [3], EPICS base software, developed in IHEP special software and various setup parameters.

THE NONSTANDARD HARDWARE IMPLEMENTATION

All “standard” diagnostic system profilometers have 16 measurement channels in the horizontal plane and 16 – in the vertical one. The chambers are connected to the analog electronic crates.

The profilometer located before the beamstopper which is needed for OKA setup has a different structure. It is a proportional chamber with 32 signal electrodes in the particle separation plane. In order to make usage of this chamber as close as possible to the standard way the first 16 channels were connected to analog electronics as correspondent to the horizontal plane, and the other 16 channels – as correspondent to the vertical plane. This prevents any changes on the IOC level. The transfer of the information and its processing were the same as for the “standard” orthogonal chambers.

THE TNK BEAM POSITION MONITOR SYSTEM

E.A.Bekhtenev, G.V.Karpov, E.I.Shubin, Budker Institute of Nuclear Physics, Novosibirsk, Russia

Abstract

New second generation synchrotron radiation source TNK is being built in Zelenograd, Russia. The new FPGA-based beam position monitor (BPM) system for TNK has been developed and produced in BINP. The BPM system requirements for second generation light sources are not as severe as for the third generation light sources. Nevertheless the system is able to perform turn-by-turn measurements and has micron level accuracy. The TNK light source is intended for work both in multiple and in single bunch mode. In the second case the charge of one bunch can achieve the value of 60 nK, which results in high peak voltages at BPM electrodes. Design features of the BPM system, its parameters and testing results are presented in this paper.

INTRODUCTION

Second generation synchrotron radiation source TNK ("Zelenograd") is presently under construction in Zelenograd, Russia [1]. Storage ring main parameters are given in Table 1.

Table 1: Main parameters of the TNK storage ring

Beam energy	2 GeV
Revolution frequency F_0	2.59 MHz
RF frequency	181.3 MHz
Beam current in multiple bunch mode	300 mA
Beam current in single bunch mode	150 mA

For beam orbit measurements Beam position monitor (BPM) system has been designed and fabricated at BINP. The system includes 24 button-type Beam Position Monitors (BPMs) and BPM electronics. Requirements to BPM electronics are:

- possibility of turn-by-turn measurements
- measurements of injected beam trajectory (first turn)
- resolution for nominal beam currents not worse than 1-2 microns
- relative accuracy for nominal beam currents at ~10 microns
- measurement rate is ~10 Hz, fast data acquisition is not required.

Slow data acquisition (~10 Hz) will be used for slow orbit feedback. Fast orbit feedback is not planned at TNK.

SYSTEM STRUCTURE

One of the methods which combine turn-by-turn measurements with high accuracy is method based at the use of an array of switches [2]. We choose this method for our BPM electronics. One of the problems associated with the use of semiconductor switches was high peak voltages at pickup buttons. In single bunch mode the charge of one bunch can achieve the value of 60 nK which gives peak voltage of tens of volts after passing through Low Pass Filter with cut-off frequency of 500-600 MHz.

Acceptable solution of this problem is employment of RF band pass Filters (BPF) directly after pickup buttons [3]. For this purpose a special printed-circuit BPF with frequency 362 MHz (doubled RF frequency) had been developed at BINP. The measured parameter S_{21} of the filter is shown in Fig.1,2. The measured bandwidth is ~10 MHz, insertion loss is ~6 dB.

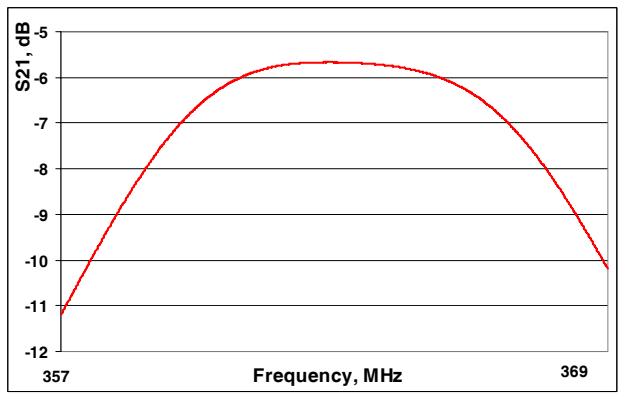

Fig.1. Measured S_{21} of BPF, narrow frequency span.

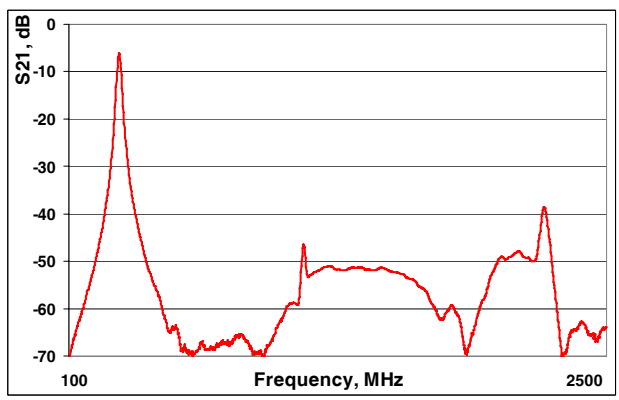

Fig.2. Measured S_{21} of BPF, wide frequency span.

Inequality of Band Pass Filters results in static measurement error therefore calibration of electronics is needed.

The structure of the BPM electronics is presented in Fig.3.

TRANSITION RADIATION DETECTOR WHICH USED DIHEDRAL ANGLE AS RADIATOR

A.V.Koltsov and A.V.Serov. P.N.Lebedev Physical Institute RAS

Abstract

The spatial distribution of the field of transition radiation generated by a relativistic particle flying into a dihedral angle formed by perfectly conducting plane surfaces is determined. The angular distributions of radiation intensity in dihedral angles of different values are calculated. It has been shown that the dependence of the angular distributions of radiation intensity in a dihedral angle on the energy and on the direction of motion of particles is stronger than a similar dependence in the case of transition radiation on a plane interface.

Transition radiation possesses certain properties that make this radiation useful for solving various problems [1]. One of the simplest and important particular cases in the theory of transition radiation is the radiation generated when a particle is incident on a perfectly conducting plane. This problem was considered in the first paper by Ginzburg and Frank on the theory of transition radiation [2]. They pointed out that the transition radiation on a perfectly conducting plane can be considered as radiation from two particles: a real particle with charge q and its image with charge $-q$.

The study of radiation on dihedral angle has shown that the spectral-angular distributions of radiation in this case exhibit new features that enhance the applicability of transition radiation. The properties of transition radiation generated when a particle passes through a dihedral angle have been investigated both theoretically [3-5] and experimentally [6].

In the present paper, we consider the specific features of transition radiation in a dihedral angle that enhance the applicability of this transition radiation to the measurement of the parameters of charged particles.

The geometry of the problem is shown in Fig.1. Let us introduce a cylindrical system of coordinates (ρ,φ,z).

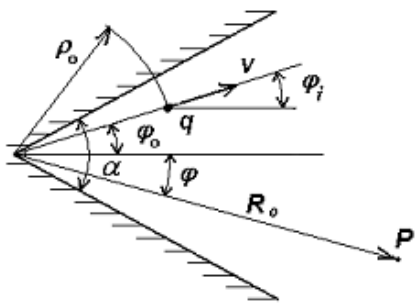

Figure1: Geometry of the problem.

The value of the dihedral angle is α. The z-axis is directed along the edge of the dihedral angle, and the planes that form the dihedral angle coincide with the planes $\varphi = \alpha/2$. The charged particle with charge q flies out from a point (ρ_0,φ_0) on the edge of dihedral angle and moves at constant velocity v. The velocity vector of the particle lies in the plane $z=0$ and is directed at an angle φ_t.

In this paper the method of images is used to describe transition radiation. Fig.2 illustrates the dispositions and velocity vectors of real and additional charges in dihedral angles of $\alpha = \pi/2$ and $\alpha = \pi/3$. The dihedral angles are shown in Fig.2 by solid lines, while the complementary angles are shown by dashed lines. The original charge q_1 moves on dihedral angle and additional image charges move on complementary angles.

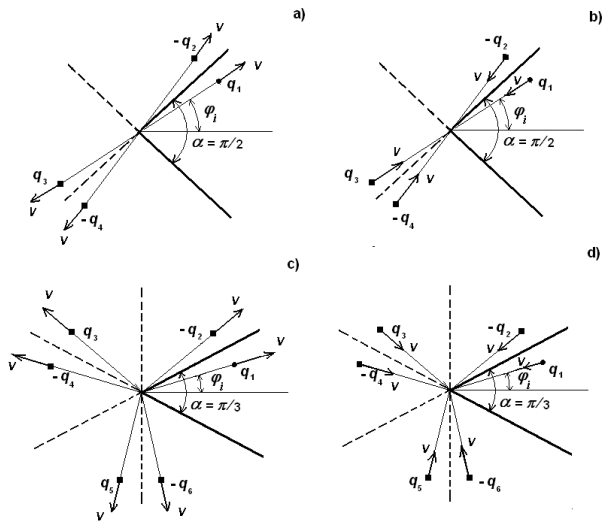

Figure2: The disposition and the velocity vector of the given and additional charges in dihedral angles of $\alpha = \pi/2$ and $\alpha = \pi/3$.

In the case of a dihedral angle of $\alpha=\pi/n$, where $n=0,1,2..$, Fourier component of the field of transition radiation can be expressed as

$$E_\omega = \frac{q\,v}{2\pi}\,\frac{\exp(-ikR_0)}{R_0}\sum_{j=0}^{n-1}\Big[\frac{\sin(\varphi-\varphi_t-2j\alpha)}{1-\beta\cos(\varphi-\varphi_t-2j\alpha)}\,x$$
$$\exp(ik\rho_0\cos(\varphi-\varphi_t-2j\alpha)) - \frac{\sin(\varphi+\varphi_t-(2j-1)\alpha)}{1-\beta\cos(\varphi+\varphi_t-(2j-1)\alpha)}\,x$$
$$\exp(ik\rho_0\cos(\varphi+\varphi_t-(2j-1)\alpha))\Big] \qquad (1)$$

where $k=2\pi/\lambda$, λ - wave length.

The angular distribution of the radiation intensity in the plane $z=0$ has been considered. Fig.3 shows the

DISTORTIONS OF PROTON BEAM 2-D IMAGES AND PROFILES DUE TO BEAM SPACE CHARGE

P. Reinhardt-Nickoulin[1#], S. Gavrilov[1,2], A. Feschenko[1,2], I. Vasilyev[1]
1) Institute for Nuclear Research of RAS, Moscow, Russia
2) Moscow Institute of Physics and Technology, Moscow, Russia

Abstract

The special residual gas ion cross section monitor is used at Proton LINAC INR RAS output to provide measurements of beam parameters. There are distortions and errors of measurements which are caused by various external and internal factors during the formation of beam cross section images. Below estimations of these distortions and results of numerical simulation of registration process of images are resulted, resolution of the detector and accuracy of measurements are discussed.

INTRODUCTION

Beam cross section monitor (BCSM) of accelerated protons is installed at an output of INR linac about in 4 m behind last accelerating resonator. It gives the possibility to observe the next beam parameters during adjustment and exploitation of the linac: form of beam cross section (BCS), form of current impulse, beam position and its displacement concerning linac axis. Besides due to computer processing of images BCSM allows to observe distribution of density of the accelerated particles in BCS and beam profiles. Double dimension distribution of accelerated beam particles in BCS is more informative characteristic in comparison with profiles of a beam [1].

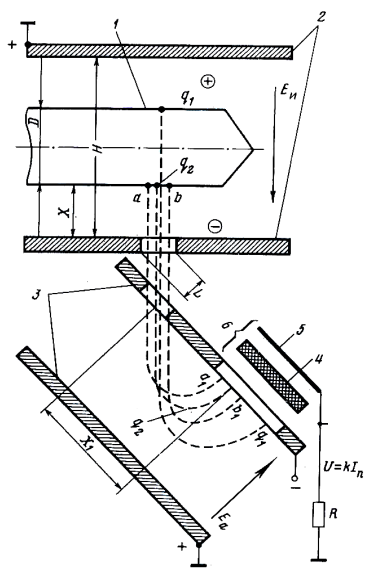

Fig. 1. Configuration design of the monitor:
1) Investigated beam 2) Condenser extracting ions
3) Analyzer of ions 4) Microchannel plates
5) Phosphor screen 6) Electro-optical converter

#petrrein@inr.ru

The beam of the accelerated protons moves in the vacuum chamber of the accelerator and ionizes residual gas. Formed positive ions are extracted by homogeneous field of flat electrostatic condenser (extracting condenser) through a special slit in lower electrode of the condenser (Fig. 1). Accelerated gas ions pass the slit and form the taped beam. Then ions are rotated by a field of electrostatic energy analyzer (analyzing condenser) which electrodes are placed under 45 degrees to a direction of extraction of ions and to the plane of the extracting electrode. After that ions get to a double microchannel plate (MCP) of the electro-optical converter (EOC) with the coordinates depending on coordinates of an ionization point, creating the image of beam cross section registered TV-camera. Calculation of ion motion trajectory in homogeneous electrostatic fields shows that all kinds of positive ions compose the image [2].

THEORETICAL DESCRIPTION OF IONS DYNAMICS

Indeed nascent positive ion is under the influence of several kinds of fields (Fig. 2):

1) electrostatic field of the extracting condenser $E_{ext} = 1{,}2$ kV/cm (force F_{ext})
2) electromagnetic field of the beam which consists of radial electric field E_b (force F_E) and azimuth magnetic field B_b (force F_B).

The vector of the resultant force F_{Ion} isn't perpendicular to axis Y that causes broadening of BCS image (ΔY) along this axis under the influence of the beam space charge. In addition it is necessary to take into account ΔY-errors because of the finite width of the slit and nonzero initial velocities of the ions.

In our case the proton beam coasts at the interval L and expands significantly (by several digits) in a longitudinal direction under the law $\Delta\varphi = \frac{360 \cdot L}{\lambda \cdot \beta \cdot \gamma^2} \frac{\Delta p}{p}$ because of different value of impulses of accelerated particles $\Delta p / p \approx \pm 2 \cdot 10^{-3}$.

Therefore the beam length σ_z is much large than the transverse radii σ_x and σ_y. The appropriate charge distribution in this case is a Gaussian distribution in two dimensions with the constant line number density n:

$$\rho(x,y) = \frac{nq}{2\pi\sigma_x\sigma_y} \exp\left(-\frac{x^2}{2\sigma_x^2} - \frac{y^2}{2\sigma_y^2}\right).$$

In case of such azimuthally symmetric beam with two-dimensional charge Gaussian distribution the approximate

SHAPES OF NUCLEAR INDUCTION SIGNALS UNDER INHOMOGENEOUS MAGNETIC FIELDS

B. Makarov, V. Ryzhov, Federal State Unitary Enterprise "The Moscow Radio Institute of the Russian Academy of Sciences", Moscow, Russia

INTRODUCTION

The shape of the nuclear induction signal is determined by structural types and dynamic processes in the analizable substance. It depends on the conditions of observation: temperature, a radio-frequency (RF) impulse sequence type, a spatial inhomogeneity of the RF field and so on [1, 2]. The magnetic polarizing field inhomogeneity exerts essential influence on nuclear induction signal parameters. The form and the orientation of the sample have also effect. F. Bloch equations describing the motion of the macroscopic nuclear magnetization vector have been solved in case of the homogeneous magnetic field. The inhomogeneity influence is taken into account under the assumption that the real distribution of the magnetic field is known [3 – 5].

SHAPES OF NUCLEAR INDUCTION SIGNALS

In the inhomogeneous magnetic field B_0 ($\vec{B}_0$ is axial $\vec{z}$) and the absence of the electromagnetic field ($\vec{B}_1 = 0$) the x-component (M_x) of the macroscopic nuclear magnetization vector $\vec{M}$ is

$$M_x(t) = M_x(0)\exp(-t/T_2)\cos(\omega_0 t), \quad (1)$$

where $M_x(0)$ – initial value of the transversal component of the magnetization vector, $\omega_0 = \gamma B_0$ the resonant value of the nuclear frequency in the field B_0, γ - gyromagnetic ratio, T_2 – the transverse relaxation time of nuclear spins.

The sample is divided into elementary volumes. The field inside of them is considered to be homogeneous. The signal from the elementary volume is a two-variable function: of time t and of $\Delta\omega_0 = \gamma\Delta B_0$ - a frequency deviation of a nuclear precession from its average value $\omega_0 = \gamma B_0$, where ΔB - induction deviation from its average value B_0 inside the volume element (the spot). In that case

$$M_x(t,\alpha) = M_x(0)\exp(-t/T_2)\cos(\omega^{\bullet} t), \quad (2)$$

here

$$\omega^{\bullet} = (1-\sigma)\omega == (1-\sigma)(\omega_0 + \Delta\omega) =$$
$$= (1-\sigma)(\omega_0 + \alpha) = \gamma(1-\sigma)(B_0 + \Delta B)$$

– a precessional frequency in the elementary volume taking into account the screening magnetic effect, σ - constant of the magnetic screening, α = Δω. Since field deviations from the average value B_0 are small value M(0) – a weak dependence function from inhomogeneity. This dependence is neglected.

The total precession signal from the simple is

$$F_x(t) = \int_{-\infty}^{+\infty} f(\alpha) M_x(t,\alpha)\, d\alpha = \quad (3)$$
$$= M_x(0)\exp(-t/T_2)\int_{-\infty}^{+\infty} f(\alpha)\cos\,\omega^*(\alpha) t\, d\alpha$$

In case of the exponential distribution

$$f(\alpha) = \frac{1}{2\beta}\cdot\exp(-|\alpha|/\beta) \quad (4)$$

the total signal with the initial amplitude normalized to unity is

$$F_N(t) = \frac{M_x(t)}{M_x(0)} = \frac{\exp(-t/T_2)}{\sqrt{1+(\beta^* t)^2}}\cdot\cos(\omega_0^* t + \phi), \quad (5)$$

where $\phi = arctg\ (\beta^* t)$, $\beta^* = (1-\sigma)\beta$, $\omega_0^* = (1-\sigma)\omega_0$, this and below index "x" is omitted. The phase of the induction signal is time-depended. Therefore the frequency of total precession signal is changing.

Selecting the field triangular distribution

$$f(\alpha) = \begin{cases} h(1+h\alpha) & by \quad -1/h < \alpha < 0 \\ h(1-h\alpha) & by \quad 1/h > \alpha > 0 \\ 0 & by \quad |\alpha| > 1/h \end{cases}, \quad h > 0$$

it is getting

$$F_N(t) = \left[\frac{\sin(h^* t)}{(h^* t)}\right]^2 \exp(-t/T_2)\cos(\omega_0^* t), \quad (6)$$

where $h^* = (1-\sigma)/2h$.

In case the Lorentz, the Gaussian, the triangular, the impulse (rectangular) field distributions the frequency is $\omega_0^* = const$. Amplitude expressions for the Lorentz, the Gaussian and impulse distributions published in [5] agree with those which we deduced in special case of $\sigma = 0$.

Let's examine the pulse distribution with finite acceleration time. If the leading edge curve changes by Lorentz law

$$f(\alpha) = \begin{cases} \dfrac{1}{pa} & by \quad |\alpha| \le \dfrac{a}{2} \\ \dfrac{(p-1)T_2'}{p\pi\{1+[(|\alpha| - \frac{a}{2})T_2']^2\}} & by \quad |\alpha| > \dfrac{a}{2} \end{cases},$$

$p \ge 1$

the nuclear induction signal is

$$F_N(t) = A\exp(-t/T_2)\cos(\omega_0^* t + \phi), \quad (7)$$

where

$$A = \frac{1}{p}\sqrt{B(B+C) + (p-1)^2 D},$$

ADVANCE OF MARGINAL OSCILLATOR

B. Makarov, V. Ryzhov, Federal State Unitary Enterprise "The Moscow Radio Institute of the Russian Academy of Sciences", Moscow, Russia

INTRODUCTION

The marginal oscillator is used for detecting nuclear magnetic resonance (NMR) signals. This scheme is convenient for search of resonant absorption of energy by atomic nuclei so it is prevalent in the NMR magnetometers. At present the valve and the transistor oscillators are developed [1 - 5].

In this article is briefly considered the theory of operation and concrete schemes of the marginal on basis of a field-effect transistor (FET).

BASES OF THEORY

A sample containing nuclear spins is placed in the coil of an oscillatory circuit of the marginal. In this case inductance of the coil is equal

$$L = \mu L_0 = L_0(1 + 4\pi\chi\xi), \quad (1)$$

where L_0 - self inductance of the coil, μ - magnetic permeability of substance of the sample, χ - dynamic nuclear susceptibility, ξ - factor of filling of the coil [2].

The impedance of the circuit is changed at the moment of the resonant absorption of the high-frequency energy by spins. The real component of the impedance of the parallel circuit is

$$\frac{\Delta R}{R} = 1 - \frac{1}{(1 + 4\pi\chi'\xi)(1 - 4\pi Q\chi''\xi)}, \quad (2)$$

and the phase angle is

$$tg\,\varphi = -\frac{4\pi Q\chi'\xi}{1 + 4\pi Q\chi''\xi}. \quad (3)$$

Here Q is the quality of the oscillatory circuit, χ', χ'' are the real and the imaginary parts of dynamic nuclear susceptibility $\chi = \chi' - j\chi''$.

The contribution to (2) by real part of the magnetic susceptibility approximately in Q times is less than the one of its imaginary part. Therefore only as a first approximation it is possible to consider that in the case amplitude detecting the marginal oscillators develop the signal proportional to the absorption. Simultaneously according to (3) the operating frequency is changed. Mainly this change is caused by the imaginary part of the dynamic susceptibility. Thereby the imaginary part of the nuclear susceptibility is responsible for absorption of energy of the radio-frequency circuit at the resonance, and phase and the frequency changes are caused by its real part.

Except the aforesaid staggering of the oscillatory circuit the phenomenon of frequency capturing is observed at changing (modulating) the invariable magnetic field through the resonant value analogous picking-up the oscillations in the tube or the transistor oscillator by external force. In this case the system of the nuclear magnetic moments acts like the external force. It is possible to consider it as the high-Q resonant circuit which interacts with the marginal oscillatory circuit. However, in this case there is no the perfect analogy. This interaction differs from that of two connected oscillatory circuits. Therefore frequency deviation connected with magnetic field change allows comparing this phenomenon with frequency capturing instead of frequency pulling observed in two connected oscillatory systems [6].

The marginal is an oscillator operating under the scheme of "an induction three-point (Hartley oscillator)" or of "a capacitor three-point (Colpitts oscillator)" [1 - 5] theory which is well developed [7, 8]. According to the theory for generating the self-oscillation a two-pole net with negative differential resistance is necessary to be connected to the oscillatory circuit

$$I(u) = S_1 u + S_3 u^3 + \ldots, \quad (4)$$

where $S_1 < 0$.

From this theory it also known that stable inherent oscillations arise at increase of factor of feedback β to some critical value β_{cr}, i.e. at

$$\beta > \beta_{cr} = \frac{R_0 C}{S_1 L_0} = \frac{1}{S_1 R}, \quad (5)$$

here R_0 and C - parameters of the parallel oscillatory circuit, R_0 - (real) resistance of the coil, R - entering (equivalent) resistance of the circuit at the resonance. (The expression (5) doesn't consider transistor influence.) As appears from (2) at the nuclear magnetic resonance equivalent resistance of the parallel circuit decreases. According to expression (5) it leads to increase in critical value of feedback factor β_{cr}. So for the value of feedback factor β_0 established in the generator the amplitude of oscillations will decrease.

And under the influence of destabilizing factors the self-oscillations in oscillators are the oscillations with random amplitudes and phases

$$u(t) = A(t)\cos(\omega t + \varphi(t)), \quad (6)$$

where $A(t)$ and $\varphi(t)$ are time stochastic functions.

The marginal scheme feature is that its sensitivity increases when the oscillation amplitude reduces [2, 7]

$$E(t) \approx \frac{dA(t)}{dS_1} \propto \frac{1}{A(t)}. \quad (7)$$

As consequence there are fluctuations of the sensitivity and the NMR signal amplitude.

The feature of the marginal is that it generates voltage with small amplitude (therefore it is still named the oscillator of small oscillations). In this operating mode even very small changes of parameters of an oscillatory circuit

HV ELECTRON COOLER FOR THE NICA COLLIDER

E.V.Ahmanova, A.G.Kobets**, I.N.Meshkov#, R.V.Pivin, A.U.Rudakov, A.V.Shabunov,
A.V. Smirnov, N.D.Topilin, Yu.A.Tumanova, S.L.Yakovenko, JINR, Dubna
A.A.Filippov, L.M.Fisher, M.M.Pashin, AREI, Moscow,

Abstract

The goal of the cooling system of the NICA collider is to meet the required parameters of ion beams in energy range of 1 ÷ 4.5GeV/u that corresponds to the 0.5 ÷ 2.5 of the electron MeV. The electron cooler is developed according to the available world practice of manufacturing of similar systems [1] The main peculiarity of the electron cooler for the NICA collider is use of two cooling electron beams (one electron beam per each ring of the collider) that never has been done. The acceleration and deceleration of the electron beams is produced by common high-voltage generator. The cooler consist of three tanks. Two of them contain acceleration/deceleration tubes and are immersed in superconducting solenoids. The third one contains HV generator. The scheme of the electron cooler, its main parameters and operation regime are presented.

CONCEPTUAL DESIGN OF THE COOLER

The electron cooler (Fig. 1) consists of three tank filled with SF6 gas under pressure of 8 at. Tanks 1 and 3 contain acceleration tube and electron gun for one of the electron beam and deceleration tube and electron collector for another one. The tank 2 houses the HV generator

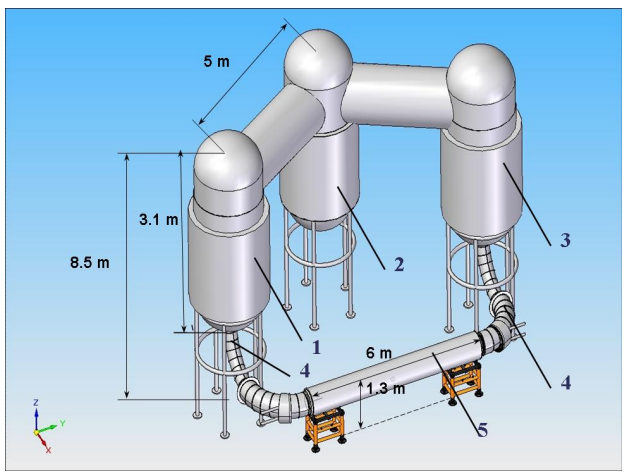

Fig.1. General view of the electron cooler. 1, 3 – tanks with electron gun and acceleration tube and deceleration tube + collector for electron beam of opposite direction, 2 – tank with HV generator, 4 – beam transportation solenoids, 5- electron cooling section.

The magnetic field is formed by a set of straight and toroidal superconducting solenoids. The solenoids forming the magnetic field in the region of acceleration/deceleration tubes are placed outside of the tanks that resolve the problem of HV insulation.

Table 1. Cooler parameters

Electron energy, MeV	0.5 ÷ 2.5
Electron beam current , A	0.1 ÷ 1,0
Beam diameter, cm	1,0
SC solenoid magnetic field, T	0.1 ÷ 0.2
HV PS current, mA	1
Collector PS, kW	2×2
HV PS stability	1×10^{-4}
SF6 gas pressure, at	5 ÷ 8

Both acceleration and deceleration systems consist of three main subsystems (Fig. 2): acceleration vacuum tube with electron gun or collector mounted on the upper end of the tube, high pressure tank, solenoid forming longitudinal magnetic field. Acceleration vacuum tube with electron gun or collector mounted on the upper end of the tube. Electron gun design (Fig.3) has three main elements: cathode with the Pierce electrode, control (steering) electrode, anode connected with first (upper) flange of acceleration tube. Electron collector (Fig.3) consists of three elements as well: collector anode connected with upper flange of deceleration tube, suppressor ("repeller") electrode, electron collecting vessel. The last one is cooled by water circulating at high potential. The design of collector cooling system is under construction.

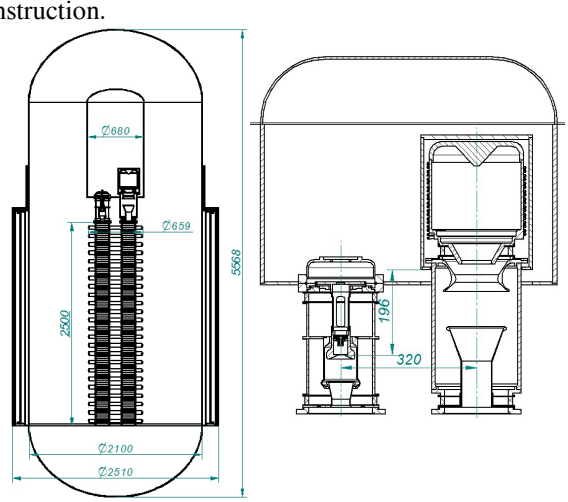

Fig.2. Acceleration and deceleration systems of two beams of opposite directions.

** Joint Institute for Nuclear Research, Russia,
Institute of Electrophysics and Radiation Technologies, Ukraine
meshkov@jinr.ru

STATUS OF THE NUCLOTRON

A. Sidorin, N. Agapov, V. Alexandrov, O. Brovko, V.Batin, A. Butenko, E.D. Donets, A. Eliseev, A.Govorov, V. Karpinsky, V. Kekelidze, H. Khodzhibagiyan, A.Kirichenko, A. Kovalenko, O. Kozlov, I. Meshkov, V. Mikhaylov, V. Monchinsky, S.Romanov, V. Shevtsov, V. Slepnev, I. Slepnev, A. Sissakian, G. Trubnikov, B.Vasilishin, V. Volkov,
JINR, Dubna, Moscow Region

Abstract

The "Nuclotron-M" project started in 2007 is considered as the key point of the first stage of the NICA/MPD project. General goal of the "Nuclotron-M" project is to prepare all the systems of the Nuclotron for its long and reliable operation as a part of the NICA collider injection chain. Additionally the project realization will increase the Nuclotron ability for realization of its current experimental program. Results of the last runs of the Nuclotron operation are presented.

INTRODUCTION

The project "Nuclotron-M" is considered as a key part of the first stage of the JINR general project NICA/MPD (**N**uclotron-based **I**on **C**ollider f**A**cility and **M**ulty **P**urpose **D**etector) [1]. The extension of JINR basic facility capabilities for generation of intense heavy ion and high intensity light polarized nuclear beams, including design and construction of heavy ion collider aimed at reaching the collision energy of $\sqrt{s_{NN}}$ = 4÷11 GeV and averaged luminosity of $1 \cdot 10^{27}$ $cm^{-2}s^{-1}$ is necessary for realization of the NICA/MPD.

The first stage of the NICA/MPD realization includes the following tasks:

- upgrade the Nuclotron facility (the "Nuclotron-M" project);
- elaboration of the NICA technical design report;
- development of the laboratory infrastructure aimed for long term stable operation of the accelerator complex and preparation for construction of the NICA elements;
- R&D works for MPD elements.

The "Nuclotron-M" program includes all necessary works on the development of the existing Nuclotron accelerator complex [2] to the facility for generation of relativistic ion beams over atomic mass range from protons to gold and uranium ions at the energies corresponding to the maximum design magnetic field (2 T) in the lattice dipole magnets. Realization of the project will make it possible to reach new level of the beam parameters and to improve substantially reliability and efficiency of the accelerator operation, renovate or replace some part of the equipment that have been under operation since 1992-93 as well.

As an element of the NICA collider injection chain the Nuclotron has to accelerate single bunch of fully stripped heavy ions (U^{92+}, Pb^{82+} or Au^{79+}) from 0.6 to about 4.5 GeV/u. The required bunch intensity is about $1 \div 1.5 \cdot 10^9$ ions. The particle losses during acceleration have to be minimized and do not exceed 10%. The magnetic field ramp has to be ≥ 1 T/s. To demonstrate the ability of the Nuclotron complex to satisfy these requirements, the general milestones of the project are specified as an acceleration of heavy ions (at atomic number larger than 100) and stable and safety operation at 2 T of the dipole magnet field. The project has been started in 2007. During the project realization almost all the Nuclotron systems were modernized and 5 runs of the Nuclotron operation were carried out. During the last run performed from 25 of February to 25 of March 2010 the Xe ions were accelerated and the magnetic system was operated at 1.8 T. Completion of the project is scheduled for the fall of 2010.

STATUS AND MAIN PARAMETERS OF THE NUCLOTRON

The first run at the Nuclotron (the superconducting synchrotron intended to accelerate nuclei and multi charged heavy ions) was performed in March 1993. Presently the Nuclotron delivers ion beams for experiments on internal targets and for fixed target experiments using slow extraction system. Achieved energy of protons is 5.7 GeV, deuterons – 3.8 GeV/u and nucleons - 2.2 GeV/u. The maximum achieved energy is limited by the system of the energy evacuation of the Nuclotron SC magnets and power supply of the lattice magnets.

Main elements and systems of the Nuclotron facility (Fig. 1) are the following:

1. superconducting synchrotron Nuclotron, which magnetic-cryostat system of the circumference of 251,5 m is located in the tunnel surrounding the Synchrophasotron basement;
2. cryogenic supply system consisting of two helium refrigerators KGU-1600/4.5 with required infrastructure for storage and circulation of the gaseous helium, liquid helium transfer lines, tanks for the liquid nitrogen storage and nitrogen tranfer lines for thermal screens of the Nuclotron lattice magnets;
3. the injection complex consisting of HV fore-injector and Alvarez-type linac LU-20. The fore-injector voltage up to 700 kV is produced by pulsed transformer. The LU-20 accelerates the protons up to the energy of 20 MeV and ions at Z/A ≥ 0.33 up to the energy of 5 MeV/u. The wide range of the ion species is provided by the heavy ion source "KRION-2", duoplasmatron ion source, polarized deuteron source

ACCELERATION OF DEUTERONS UP TO 23.6 GEV PER NUCLEON THROUGH I100, U1.5, AND U70 OF IHEP

S. Ivanov, on behalf of the U70 light-ion task team[#]
Institute for High Energy Physics (IHEP), Protvino, Moscow Region, 142281, Russia

Abstract

The paper reports on the recent progress en route of implementing the program of accelerating light ions in the Accelerator Complex U70 of IHEP-Protvino. The crucial milestone of guiding the deuteron beam through entire cascade of three accelerators available to a specific kinetic energy of 23.6 GeV per nucleon was accomplished in April 2010, which confirms feasibility of the project goal to diversify our main proton machine U70 to a light-ion synchrotron as well.

INTRODUCTION

The program to accelerate light ions with a charge-to-mass ratio q/A = 0.4–0.5 in the Accelerator complex U70 of IHEP-Protvino aims at diversification and development of our accelerator facilities. The ion mode of operation involves a sequence of Alvarez DTL I100, rapid cycled synchrotron U1.5, and the main synchrotron U70 proper.

Refs. [1, 2] reported on the first attempts of operation with a deuteron beam of a yet truncated cascade comprising I100 and U1.5. Since then, consisted efforts were continued to adapt and upgrade technological systems of the proton machines to better accommodate the ion beam. This report chronologically overviews the progress achieved since the previous conference RuPAC-2008.

RUN 2008-2

During this run, in the period of 10–12.12.08, acceleration of deuterons from 16.7 to 455 MeV per nucleon was accomplished for the second time in the U1.5 record of service (Fig. 1). Achieving this goal was hampered by improper vector adding at beam of RF voltages from 8 accelerating ferrite-loaded cavities whose start frequency is lowered from 0.747 (design value) to 0.563 MHz.

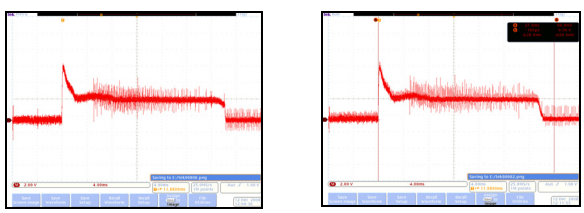

Figure 1: Deuteron beam in the U1.5 seen by a DCCT.

A bit earlier, while being in a proton mode, the U70 was trained to accept the ions. To this end, 1.32 GeV proton beam accumulation and circulation on flat-bottom was studied. The lattice magnets were powered a stand-alone DC power supply (131.1 A, 354 G). Coasting beam circulation (with RF off) and injection of bunches populated by as small as $3{\cdot}10^{10}$ ppb (imitation of a low-intensity deuteron bunch) were tried.

Attempts to transfer a full deuteron beam to the U70 ring and get a circulation there were not successful. Still, first deuterons in the U70 were observed with scintillating screen in straight section #10 indicating beam traversal through at least 4 of 120 combined-function magnets.

RUN 2009-1

In the closing days of this run (on April 25, 2010), the first ever stable circulation of a light-ion beam (ions of deuterium) at flat-bottom values of magnetic guide field of the main synchrotron U70 was obtained.

To start with, the Alvarez DTL I100 safely accelerated deuterons to 16.7 MeV per nucleon at the 4π-mode. The gas ion source yielded 16–17 mA of pulsed current at 40 μs pulse width with chopper off, and 15 mA; 5 μs with chopper on.

Specific kinetic energy was then ramped in the U1.5 ring from 16.7 to 448.6 MeV per nucleon. Overall in-out transfer efficiency through the machine amounted to 50%. The output intensity of $4.5{\cdot}10^{10}$ dpb complies with design expectations. Beam observation over the regime is shown in Fig. 2.

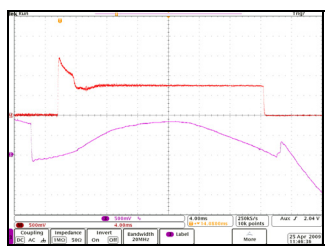

Figure 2: Ramping rate of the U1.5 guide field (lower trace) and deuteron beam intensity monitored with a DCCT (upper trace). Acceleration is accomplished in 26 ms. Compare with Fig. 1 to notice much improved performance of beam diagnostics made free of EM interferences.

Finally, the deuterons at 448.6 MeV per nucleon were transferred onto the waiting flat-bottom of the U70 ring (field 350.9 G, DC PSU current 128.4 A).

As a result, the U70 got a stable circulation of a coasting deuteron beam for about 7.5 s. This limit was imposed by an operational constraint in the existing timing system rather than by any physical reason. Momentum spread of the bunch injected is equal to $\pm 3.6{\cdot}10^{-3}$, bunch full length at base is about 100 ns, intensity is $4.5{\cdot}10^{10}$ dpb.

[#] O. Lebedev, A. Ermolaev, G. Hitev, V. Lapygin, Yu. Milichenko, V. Bezkrovnyy, V. Stolpovsky, I. Sulygin, E. Nelipovich, A. Bulychev, Yu. Antipov, S. Pilipenko, N. Anferov, D. Khmaruk, S. Semin, V. Dan'shin, N. Ignashin, S. Sytov, and G. Kuznetsov.

STATUS AND PROSPECTS OF THE NOVOSIBIRSK FEL FACILITY

N.A. Vinokurov#, E.N. Dementyev, B.A. Dovzhenko, A.A. Galt, Ya.V. Getmanov, B.A. Knyazev, E.I. Kolobanov, V.V. Kubarev, G.N. Kulipanov, L.E. Medvedev, S.V. Miginsky, L.A. Mironenko, V.K. Ovchar, B.Z. Persov, V.M. Popik, T.V. Salikova, M.A. Scheglov, S.S. Serednyakov, O.A. Shevchenko, A.N. Skrinsky, V.G. Tcheskidov, M.G. Vlasenko, P.D. Vobly, N.S. Zaigraeva, Budker INP, Novosibirsk, Russia

Abstract

Multiturn energy recovery linacs (ERL) looks very promising for making ERLs less expensive and more flexible, but have serious intrinsic problems. At this time only one multiturn ERL exists. This Novosibirsk ERL operates with two orbits and two free electron lasers now. The Novosibirsk terahertz radiation user facility provides 0.5 kW average power at 50 - 240 micron wavelength range. Different users work at six stations. Two another orbits and third free electron laser are under construction. The operation experience revealed specific problems of ERLs(especially, of multiturn ones). Some solutions were proposed recently.

THE FIRST ORBIT FEL

A source of terahertz radiation was commissioned in Novosibirsk in 2003 [1]. It is CW FEL based on an accelerator–recuperator, or an energy recovery linac (ERL). It differs from other ERL-based FELs [2, 3] in the low frequency non-superconducting RF cavities and longer wavelength operation range. The one-turn ERL (which is the first stage of the full-scale four-turn ERL) parameters are listed in Table 1, and its scheme is shown in Fig. 1.

Table 1: Parameters of the first stage of Novosibirsk ERL.

Beam energy, MeV	11
Maximum average electron current, mA	30
RF frequency, MHz	180.4
Maximum bunch repetition rate, MHz	22.5
Bunch length, ps	100
Normalized emittance, mm·mrad	30
Charge per bunch, nC	1.5
RF cavities Q factor	$4 \cdot 10^4$

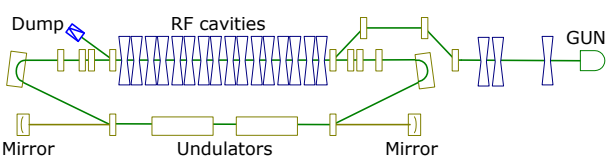

Figure 1: Scheme of the Novosibirsk terahertz free electron laser.

This first stage of the Novosibirsk free electron laser generates coherent radiation tunable in the range 120-240 micron as a continuous train of 40-100 ps pulses at the repetition rate of 2.8 - 22.5 MHz. Maximum average output power is 500 W, the peak power is more than 1 MW [4,5]. The minimum measured linewidth is 0.3%, which is close to the Fourier-transform limit. The third harmonics lasing was obtained recently. It was achieved by suppression of the first harmonics lasing using aperture-decreasing scrapers.

Five user stations are in operation now. Two other are in progress.

THE SECOND STAGE OF ERL AND FEL

Full-scale Novosibirsk free electron laser facility is to be based on the four-orbit 40 MeV electron accelerator-recuperator (see Fig. 2). It is to generate radiation in the range from 5 micrometer to 0.24 mm [6, 7].

Manufacturing, assembly, and commissioning of the full-scale four-turn ERL are underway. The orbit of the first stage with the terahertz FEL lies in the vertical plane. The new four turns are in the horizontal one. One FEL will be installed at the fourth orbit (40 MeV energy), and the second one is already installed and works at the bypass of the second orbit (20 MeV energy).

The bypass provides about 0.7 m lengthening of the second orbit. Therefore, when the bypass magnets are switched on, the deceleration of beam take place at the third passing through the accelerating system, and after that electrons come to the first orbit and, after the second deceleration, to the beam dump.

All 180-degree bends are achromatic. To reduce sensitivity to the power supply ripples, all magnets are connected in series. To simplify the mechanical design, all non-round (small) magnets are similar and parallel-edge. Water-cooled vacuum chambers are made from aluminium.

#vinokurov@inp.nsk.su

KURCHATOV SYNCHROTRON RADIATION SOURCE FACILITIES MODERNIZATION

M.Blokhov, V.Leonov, E.Fomin, G.Kovachev, V.Korchuganov, M.Kovalchuk, Yu.Krylov, V.Kvardakov, V.Moryakov, D.Odintsov, N. Smoliakov, S.Tomin, Yu.Tarasov, V.Ushkov, A.Valentinov, A.Vernov,Yu.Yupinov, A.Zabelin, RRC Kurchatov Institute, Moscow 123182, Russia

Abstract

Kurchatov Synchrotron Radiation Source (KSRS) operates in the range of SR from VUV up to hard X-ray. Technical modernization of KSRS systems is under way. It includes a replacement of the power supplies and the nano- and micro-second generators by the new ones, the installation of the new third RF accelerator cavity on 2.5 GeV storage ring SIBERIA-2. The projects of the feedback system for the longitudinal coherent multi-bunch instabilities dumping and of the new sensitive electronics for pick-up stations on Siberia-2 storage ring start in 2010. Three 7.5 T wiggler beam lines were mounted and tested with SR beam in December 2009. The 7.5 T (19+2) poles SC wiggler and new 3 RF cavities are doing the KSRS spectrum harder and intensive. The program tools for KSRS operation are introduced in accelerator control system with a new electronics. The new scheme of top-up energy injection placed outside of Siberia-2 storage ring tunnel is carried out. The report describes a statistics works and plans on KSRS facilities.

INTRODUCTION

The accelerator complex of KSRS consists of the linear accelerator and two storage rings [1]. Main parameters of the KSRS accelerator facilities are shown in Table 1.

Table 1: Parameters of KSRS facilities

Linac	**SIBERIA-1**	**SIBERIA-2**
E = 80 MeV	E = 80÷450 MeV	E = 0.45÷2.5 GeV
I = 0.2 A	I = 0.2÷0.3 A (singlebunch)	I = 0.1÷0.3 A (multibunch)
L = 6 m	C = 8.68 m	C = 124.13 m
DE/E = 0.005	B = 1.5 T	B = 1.7 T
ε_0=300 nm·rad	ε_{x0}=800 nm·rad	ε_{x0}=78÷100 nm·rad
T = 18 ns	T_0 = 29 ns	T_0 = 414 ns
f_{rep} = 1 Hz	T_{rep} = 25 s	τ =10÷25 hrs
	λ_c=61 Å , BMs	λ_c=1.75 Å, BMs λ_c=0.40 Å, SCW
Forinjector	Booster, VUV and soft X-ray source	Dedicated SR source 0.1-2000Å [1]

Possible number of photon beam lines from BMs equals to 24, SR sources like SC wigglers and warm wigglers (undulators) are planed to offer 6-8 SR beam lines from IR to hard X-ray radiation.

KSRS FACILITIES WORK

The work of SIBERIA-2 on experiments is carried out with use of SR from bending magnets in energy range of photons 4-40 keV and spectral flux (10^{13}-10^{11}) ph/s/mrad/0.1%BW during week runs in a round-the-clock mode. Within one week 9 working 12-hour shifts are presented.

Table 2 shows the integral time devoted for SR experimental work in 2005 - 2009 years. Fig.1 contains some statistics of the time which was spent on experiment, injection and tuning of SR source.

Table 2: SR Experimental time in 2005-2009 years

	2005	2006	2007	2008	2009
Siberia-1: experiment, hrs	238	236	205	471	634
Integral, A-hrs	16.1	21.1	13.4	41.7	67.4
Siberia-2: experiment, hrs	1292	2035	1629	1437	1527
Integral, A-hrs	94.9	165.5	126.2	56.3	77.5

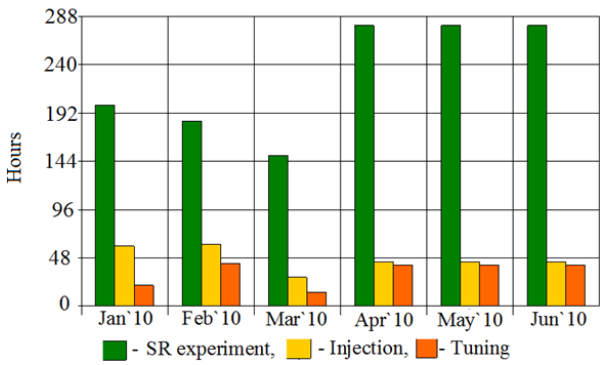

Figure 1: The Siberia-2 work in 2010.

MODERNIZATION OF 2008-2010

New septum-magnet of Siberia -1(KCSR-INP)

The new pulse septum-magnet was installed with aim to increase the effectiveness of electron beam ejection from Siberia -1 into the electron transport line - ETL-2. The new septum-magnet is the modified version of the old one that worked during previous 8 years. It has more homogeneous magnetic field distribution. The results are obtained: stable control of the pulse generator

RADIATION SOURCES AT SIBERIA-2 STORAGE RING

V.N. Korchuganov, N.V. Smolyakov, N.Yu. Svechnikov, S.I. Tomin,
RRC Kurchatov Institute, Moscow 123182, Russia

Abstract

In this report, two projects of radiation sources at Siberia-2 storage ring are considered. The first one is in-vacuum short period mini-undulator, which is intended for generation of bright X-ray beams. It is shown the feasibility of diffraction-limited in vertical direction X-ray source, which is to say that vertical emittance of the electron beam is equal to diffraction emittance of generated by undulator 2 KeV photon beam.

The second source will utilize edge radiation, which is generated in the fringe fields of the bending magnets. Numerical simulations show that the edge radiation is more intensive in infrared – ultraviolet spectral range as compared with standard synchrotron radiation (SR) from regular part of the same bending magnet.

INTRODUCTION

The magnetic system of Siberia-2 storage ring (electron beam energy of 2.5 GeV) consists of six mirror-symmetrical cells, each containing an achromatic bend and a gap with a zero dispersion function, see Fig.1 [1, 2]. The distance between the down- and upstream edges of the bending magnets is 5340 mm. The portion of straight section, suitable for insertion device loading, is about 3 m in length. The Siberia-2 lattice is so designed that the different requirements for wigglers and undulators are satisfied. So, the straight sections with small values of betatron functions, where electron beam has minimum sizes, provide optimum performance for wigglers, while the straight sections with large betatron functions, where the electron beam has small angular divergences, are optimum for undulators.

Now at Siberia-2 storage ring SR is mainly in use. Its flux is of the order of 10^{11}-10^{13} phot/s/mrad/(BW=0.1%) in 4 – 40 KeV spectral range. One superconducting wiggler with 7.5 T magnetic field amplitude is also installed. At the same time nearly all straight sections are planed to complete with different insertion devices in the nearest future, see Fig.1 and Table 1.

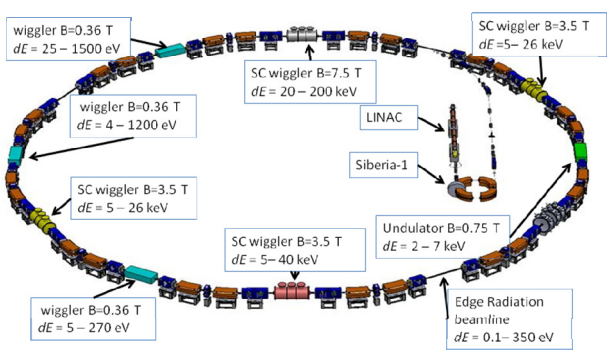

Fig.1 Siberia-2 layout with projected insertion devices.

#smolyakovnv@mail.ru

Table 1. Main parameters of insertion devices

	B_{max} T	λ_u, mm	Number of periods	Spectral range KeV
s/c wiggler	**7.5**	**164**	**10**	**20-200**
s/c wiggler	**3**	**44**	**35**	**5-40**
wiggler	**0.36**	**80**	**51**	**5.5-270 eV**
undulator	**0.75**	**7**	**300**	**2-7**
edge radiation	**-**	**-**	**-**	**0.1-350 eV**

UNDULATOR RADIATION

The most important feature of undulator radiation beam is its brilliance, which is mainly determined by the electron beam emittances and radiation diffraction phase volume, which is equel to $\lambda/4\pi$, where λ is radiation wavelength. A light source is called diffraction - limited if the electron beam emittance is smaller than that of the photon beam.

Nowadays a natural horizontal emittance of electron beam in Siberia-2 at 2.5 GeV is equal to 98 nm·rad [1]. Operating parameters of storage ring are listed in the Table 2. In addition to existing optical lattice new more brilliant lattice with horizontal emittance 18 nm·rad (at 2.5 GeV energy) has been developed (Table 2), The new lattice allows to obtain the horizontal emittance of 4.9 nm·rad at 1.3 GeV. Vertical emittance of electron beam is 49 pm·rad with a coupling factor of betatron oscillation k≈0.01 for Siberia-2. Thus, vertical emittance is equal to emittance of 2 keV photons. It is important to note that the new brilliant lattice can be obtained by changing of currents in lattice magnetic elements only.

Table 2: Siberia-2 Storage Ring Parameters

Lattice	**"standard"**	**"brilliance"**
Energy	2.5 GeV	1.3 GeV
Emittance	98 nm·rad	4.9 nm·rad
Beam size: σ_x/ σ_y	1500/78	363/17
Circumference	124.128 m	
Coupling	0.01	
Momentum compaction	0.0103	4.2×10^{-3}
Betatron tunes: Q_x/Q_y	7.775/6.695	9.707/5.622
R.m.s. energy spread	9.5×10^{-4}	5×10^{-4}
Damping times: τ_x, τ_y, τ_s	3.2; 3;1.5 ms	22;22;11 ms
Beam current	100-300 mA	

For generation of 2 KeV photons by 1.3 GeV electron beam, undulator should match rigid requirements, see Table 3. Undulator has very short 7 mm period and high peak field 0.75 T. Last years technology for undulators was greatly advanced [3, 4, 5]. It gives us a hope that production of the undulator with such record parameters will be possible.

REVIEW OF THE DIAMOND LIGHT SOURCE TIMING SYSTEM

Y. Chernousko, P. Hamadyk, M. T. Heron, Diamond Light Source Ltd, United Kingdom

Abstract

The Diamond Light Source timing system utilises a central event generator with distributed event receivers at the equipment being controlled for all accelerator and beamline subsystems. This provides distributed fiducials with resolution of 8 nsec and stability of 8 psec. It is based on commercial hardware from Micro-Research, Finland.

This paper describes the installed timing system and summarizes 5 years' operational experience of the system. It describes the hardware and software and the distributing network, and the achieved precision and stability of the system. Developments in the timing system to support additional operational functionality of Diamond, including top-up operation, are also discussed.

INTRODUCTION

Diamond Light Source is a 3 GeV third-generation light source with a 561 m storage ring (SR), a full-energy booster and a 100 MeV pre-injector Linac [1]. The photon output is optimised for high brightness from undulators and high flux from multi-pole wigglers. The current state includes 19 photon beamlines operational, with a further three beamlines in design and construction.

The Diamond timing system is based on commercial hardware from Micro-Research Finland Oy [2] and provides an integrated timing system across the three accelerators and the photon beamlines.

DIAMOND TIMING SYSTEM STRUCTURE

The Diamond timing system is based on a central event generator (EVG) which generates events from an internal sequencer and external sources. These events are distributed over fibre optic links to multiple event receivers (EVRs) [3]. The EVRs, which are located in the control system interface layer, decode the events as hardware triggers or software interrupts. Hardware triggers are connected directly to the equipment using copper or fibre optic connections or through a four-channel timer when greater timing resolution is required. For the Linac, the decoded events are further encoded by a gun transmitter and sent over a fibre link to the gun high voltage platform. The external event sources include astronomical time derived from GPS through a Symmetricom, XLi - Time & Frequency System and a 10 MHz clock from a rubidium generator, a 50 Hz trigger and a post-mortem trigger when the beam is lost. The event clock is derived from the 500 MHz master oscillator, so that it is locked to changes in the RF frequency. The structure is shown in Fig 1.

HARDWARE

Event Generator

The EVG issues event frames consisting of an 8-bit event code and an 8-bit distributed data bus, at a rate of 125 MEvents/sec. Events can originate from several sources which are: eight external trigger events, a sequence RAM, software events and events received from an upstream event generator. Events from different sources have different priorities which are resolved in a priority encoder. A block of RAM is used to store a sequence of events. The Booster revolution clock is used to count through the sequence memory, thereby transmitting events with a time resolution of ~500nsec The 8-bit distributed data bus signals are sampled simultaneously at the event clock rate and distributed to the event receivers. The EVG is realised as a VME module.

Event Receiver

The EVR recovers the event clock signal from the event stream and splits the event frame into the 8-bit event code and the 8-bit distributed data bus. The decoded events are mapped through RAM on to: four delayed pulse outputs, with programmable delay and width (16-bit pre-scaler from the event clock, 32-bit delay and a 32-bit width register), 14 pulse outputs with programmable delay and width (32-bit delay and 16-bit width) or seven set/reset flip-flop outputs. The processed events can produce hardware outputs or software interrupts and are time-stamped with a resolution of 1 μs. The hardware outputs are routed to connectors of the rear transition board, but any of them may also be multiplexed on to the front panel connectors. The EVRs are realised as both VME and PMC modules.

Linac Gun Driver

The Linac gun driver consists of two channels, providing single- and multi-bunch injection respectively, by driving separate gun triggers. It is realised as a gun transmitter in the Linac timing crate and a gun receiver which is placed on the gun HV platform. The gun transmitter accepts trigger signals from an EVR system, delays them with a resolution of 2 ns and generates modulated optical signals which are sent to the gun receiver, where they are decoded for driving the gun. A fine programmable delay is also available and allows adjustment of the triggering position with a resolution of 10 ps over a range of 10 ns.

PROGRESS WITH THE 2 MEV ELECTRON COOLER FOR COSY-JUELICH/ HESR

J. Dietrich#, V. Kamerdzhiev, FZJ, Juelich, Germany
M.I. Bryzgunov, A.D. Goncharov, V.V. Parkhomchuk, V.B. Reva, D.N. Skorobogatov, BINP, Novosibirsk, Russia

Abstract

The 2 MeV electron cooling system for COSY-Juelich was proposed to further boost the luminosity even in presence of strong heating effects of high-density internal targets. The project is funded since mid 2009. Manufacturing of the cooler components is in progress. The space required for the 2 MeV cooler was made available in the COSY ring during the summer 2010 shutdown. The design and construction of the cooler is accomplished in cooperation with the Budker Institute of Nuclear Physics in Novosibirsk, Russia. The 2 MeV cooler is also well suited in the start up phase of the High Energy Storage Ring (HESR) at FAIR in Darmstadt. It can be used for beam cooling at injection energy and is intended to test new features of the high energy electron cooler for HESR. Two new prototypes of the modular high voltage system were developed, one consisting of gas turbines the other based on inductance-coupled cascade generators. The technical layout of the 2 MeV electron cooler is described and the status of component manufacturing is reported.

INTRODUCTION

The new generation of particle accelerators operating in the energy range of 1-8 GeV/u for nuclear physics experiments requires very powerful beam cooling to obtain high luminosity. For example the investigation of meson resonances with PANDA detector requires an internal hydrogen target with effective thickness 4×10^{15} atoms per cm^2 and 10^{10} – 10^{11} antiprotons at 15 GeV circulating in the HESR. In this case the peak luminosities ranging from 2×10^{31} to 2×10^{32} $cm^{-2}s^{-1}$ are achievable. These experiments allow to observe meson resonances in proton-antiproton annihilations. Resolution of the experiments is limited by momentum spread in antiproton beam, which must be better than 10^{-4}.

The average momentum losses $\frac{dp}{pdt}$ on such a target (for 4 GeV antiprotons) will be about $4\cdot10^{-6}s^{-1}$ and the heating rate of momentum spread by fluctuation of ionization losses will be near $\frac{dp^2}{p^2dt} = 2\cdot10^{-9}\,s^{-1}$. To obtain momentum spread of 10^{-5} – 10^{-4} cooling time in the range $\tau_{cool} = 2(dp/p)^2/(dp^2/dt/p^2) = 0.1\div10s$ is needed. The 4 MeV electron cooler at the RECYCLER ring (FNAL) [1] achieves cooling time about 1 hour. The new cooler for COSY should provide a few orders of magnitude more powerful longitudinal and transverse cooling that requires new technical solutions. The basic idea of this cooler is to use high magnetic field along the orbit of the electron beam from the electron gun to the electron collector. In this case high enough electron beam density at low effective temperature can be achieved in the cooling section. For example the electron beam density of $2\cdot10^8$ cm^{-3} (6 mm beam diameter and 1.5 A of current) magnetized with longitudinal magnetic field of 2 kG will have $2.7\cdot10^6$ cm/s drift velocity in the beam reference frame. This velocity corresponds to a cooling time near 0.1 s for the low angular spread ($\Delta p_\perp / p = 10^{-5}$) beam.

#j.dietrich@fz-juelich.de

BASIC DESIGN FEATURES

The basic parameters for the COSY cooler are listed in Table 1. The length restrictions are given by the space available in the COSY ring. The height is limited to 7 m by the building.

Table 1: Basic Parameters and Requirements.

COSY 2 MeV Electron Cooler	Parameter
Energy Range	0.025 ... 2 MeV
High Voltage Stability	$< 10^{-4}$
Electron Current	0.1 ... 3 A
Electron Beam Diameter	10 ... 30 mm
Length of Cooling Section	2.69 m
Toroid Radius	1.00 m
Magnetic Field (cooling section)	0.5 ... 2 kG
Vacuum at Cooler	10^{-9} ... 10^{-10} mbar
Available Overall Length	6.39 m
Maximum Height	5.7 m
COSY Beam Axis above Ground	1.8 m

In Fig. 1 the layout of the COSY 2 MeV cooler is shown. The cooler HV terminal is installed inside the pressure vessel filled with SF_6 gas. The main features of the cooler are:

1. The design of the cooling section solenoid is similar to the ones of CSR (IMP) and LEIR (CERN) coolers designed by BINP [2, 3]. However, for the 2 MeV cooler the requirement on the straightness of magnetic field lines is so high ($\Delta\theta < 10^{-5}$) that a system for control of magnetic field lines in vacuum becomes necessary.
2. For suppression of high energy electron beam losses at IMP and LEIR coolers electrostatic bending was used [4]. The shape of the 2 MeV transport lines, however, dictates a different approach. The collector (inside the HV terminal) will be complemented by a Wien filter to suppress return flux.

DEVELOPMENT OF ELECTRON COOLER COMPONENTS FOR COSY

J. Dietrich, V. Kamerdzhiev, FZJ, Juelich, Germany
M.I. Bryzgunov, V.N. Bocharov, A.V. Bubley, V.G. Cheskidov, A.D.Goncharov, A.M. Kryuchkov, V.M. Panasyuk, V.V. Parkhomchuk, V.A. Polukhin, A.A. Putmakov, V.B. Reva, D.N. Skorobogatov, BINP, Novosibirsk, Russia

Abstract

The 2 MeV electron cooling system for COSY-Juelich was proposed to further boost the luminosity even in presence of strong heating effects of high-density internal targets. The project is funded since mid 2009. Manufacturing of the cooler components has already begun with collaboration efforts of two institutes BINP(Novosibirsk) and FZJ(Juelich). The high cooling rate requires using of the high intensity electron beam with strong magnetization at the cooling section. The 2 MeV cooler also well suits in the start up phase of the High Energy Storage Ring (HESR) at FAIR in Darmstadt. At the report experimental testing results of the prototypes of the cooler elements will be discussed.

INTRODUCTION

The new generation of particle accelerators operating in the energy range of 1-8 GeV/u for nuclear physics experiments requires very powerful beam cooling to obtain high luminosity. For example the investigation of meson resonances with PANDA detector requires an internal hydrogen target with effective thickness 4×10^{15} atoms per cm^2 and 10^{10} – 10^{11} antiprotons at 15 GeV circulating in the HESR. In this case the peak luminosities ranging from 2×10^{31} to 2×10^{32} $cm^{-2}s^{-1}$ are achievable. These experiments allow observe meson resonances in proton-antiproton annihilations. Resolution of the experiments is limited only by momentum spread in antiproton beam, which must be better than 10^{-4}.

The average momentum losses $(dp/dt)/p$ of ion on such a target (for 4 GeV antiprotons) will be about $4\cdot10^{-6}s^{-1}$ and the heating rate of momentum spread by fluctuation of ionization losses will be near $\frac{dp^2}{p^2dt} = 2\cdot10^{-9}s^{-1}$. To obtain momentum spread of 10^{-5} – 10^{-4} cooling time in the range $\tau_{cool} = 2(dp/p)^2/(dp^2/dt/p^2) = 0.1\div10s$ is needed. The 4 MeV electron cooler at the RECYCLER ring (FNAL) achieves cooling time about 1 hour. The new cooler for COSY [1] should provide a few orders of magnitude more powerful longitudinal and transverse cooling that requires new technical solutions. The basic idea of this cooler is to use high magnetic field along the orbit of the electron beam from the electron gun to the electron collector. In this case high enough electron beam density at low effective temperature can be achieved in the cooling section. For example the electron beam density of $2\cdot10^{8}$ cm^{-3} (6 mm beam diameter and 1.5 A of current) magnetized with longitudinal magnetic field of 2 kG will have $2.7\cdot10^{6}$ cm/s drift velocity in the beam reference frame. This velocity corresponds to a cooling time about 0.1 s for the low angular spread ($\Delta p_\perp / p = 10^{-5}$) beam.

BASIC DESIGN FEATURES

The basic parameters for the COSY cooler are listed in Table 1. The restrictions are given by the space available in the COSY ring. The height is limited to 7 m by the building.

Table 1: Basic Parameters and Requirements.

COSY 2 MeV Electron Cooler	Parameter
Energy Range	0.025 ... 2 MeV
High Voltage Stability	$< 10^{-4}$
Electron Current	0.1 ... 3 A
Electron Beam Diameter	10 ... 30 mm
Length of Cooling Section	2.69 m
Toroid Radius	1.00 m
Magnetic Field (cooling section)	0.5 ... 2 kG
Vacuum at Cooler	10^{-9} ... 10^{-10} mbar
Available Overall Length	6.39 m
Maximum Height	5.7 m
COSY Beam Axis above Ground	1.8 m

In Fig. 1 the layout of the COSY 2 MeV cooler is shown. The cooler HV terminal is installed inside the pressure vessel filled with SF_6 gas. The main features of the cooler are:

1. The design of the cooling section solenoid is similar to the ones of CSR (IMP) and LEIR (CERN) coolers designed by BINP [2,3]. However, for the 2 MeV cooler the requirement on the straightness of magnetic field lines is so high ($\Delta\theta < 10^{-5}$) that a system for control of magnetic field lines in vacuum becomes necessary.
2. For suppression of high energy electron beam losses at IMP and LEIR coolers, electrostatic bending was used [4]. The shape of the 2 MeV transport lines, however, dictates a different approach. The collector (inside the HV terminal) will be completed by a Wien filter to suppress return the electrons flux.

MAGNETIC SYSTEM

The magnetic system has the cooling section (1) (see fig.1), where electrons and protons move at common orbit and parallel to each other. At the 45^0 toroid magnets this beams are joined and separated (2). Magnetic dipoles (3) are installed along the proton orbit for compensation of

RESULTS OF ELECTRON COOLING BEAM STUDIES AT COSY*

C. Böhme, J. Dietrich, V. Kamerdzhiev#, FZJ, Jülich, Germany
M. Bryzgunov, V. Reva, BINP SB RAS, Novosibirsk, Russia
A. Kobets‡, I. Meshkov, A. Rudakov, N. Shurkhno, A. Sidorin, JINR, Dubna, Russia

Abstract

Beam studies dedicated to electron cooling and related problems were carried out at COSY in April 2010. The newly installed Ionization Profile Monitor was used to study the dynamics of longitudinal and transverse electron cooling. Friction force measurements were performed. Beam lifetime was measured for different injection parameters, electron currents and working points. Position and angle scans of the electron beam were also performed. Results of the recent beam studies are reported and the plans for future studies are discussed.

INTRODUCTION

The work was performed under the Helmholtz-Russia Joint Research Group (HRJRG) - HRJRG-106 "Development of a high energy electron cooler for hadron physics experiments at COSY and HESR". A long tradition of cooperation exists with the Budker Institut of Nucler Physics, Novosibirsk and the JINR Dubna in performing experiments at the low energy electron cooler at COSY Jülich.

The electron cooler was designed and constructed during the years 1989 through 1992. The design goal was a 4 A electron beam at 100 keV confined and guided in solenoidal magnetic field up to 0.15 T. Since the first cooling on May 1993 the cooler was mostly operated at injection energy of COSY, which corresponds to electron beam energy of 20 to 25 keV. Practically, electron currents up to 0.5 A are applied. Until recently the solenoid field was set to 0.08 T.

COSY INJECTION SCHEME

In this section, some of the operational features of the stripping injection into COSY are considered, see fig. 1 [1]. The stripper foil is located behind a dipole in the extraction arc, about 40 mm off the nominal orbit. For injection the COSY orbit is bumped to the edge of the foil so that it meets the incoming cyclotron beam position and direction. The injection is controlled by three main parameters, the macropulse length t_{macro}, the bumper ramp down time t_{ramp}, and the micropulsing factor f_{micro}. Controlled by a shutter at the cyclotron, H^- (or D^-) ions are delivered within a time interval t_{macro}. The orbit bumpers are de-energized in the same time. If requested, the cyclotron current I_{cycl} can be decreased by micropulsing, $f_{micro} = 1$ corresponds to 100% I_{cycl}. As injection proceeds, the betatron amplitude of the stored beam increases up to a value determined by the available horizontal acceptance. Multiscattering due to many repeated traversals through the foil and a possible mismatch of incoming and circulating beam angles with subsequent filamentation broaden the stored beam also vertically up to the available acceptance. With the standard values $t_{macro} = t_{ramp} = 20$ ms, no micropulsing, and typically 6 μA cyclotron current, the ring is filled with $(5 – 10)\cdot10^{10}$ protons, but at the expense of large emittances. Based on the aperture of the beam tubes, the optical functions, and the orbit distortions in COSY we estimate acceptances of $A_x = 80$ μm and $A_y = 20$ μm. The proton beam size (3σ emittances) is then larger than the electron beam diameter. If the macropulse is made shorter at constant ramp down time one may expect a beam with smaller emittance but also less stored beam intensity.

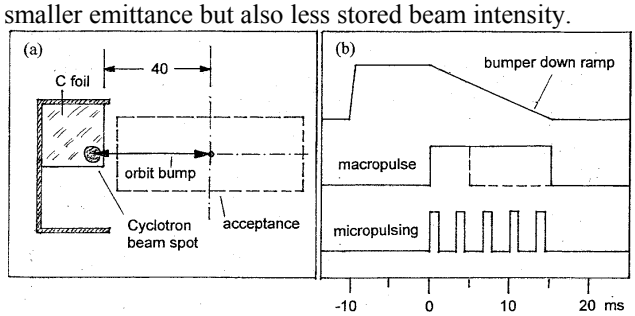

Figure 1: Principle of the stripping injection at COSY. H^- or D^- delivered by the cyclotron injector change their charge state in a carbon foil. Before injection the COSY orbit is bumped to the edge of the stripper foil (a). During the injection time, defined by the macropulse length, the orbit is moving back to its nominal position, coasting beam injection. Bumper ramp down time t_{ramp} and macropulse length t_{macro} are variable parameters (b). Micropulsing by chopping the macropulse allows to reduce the intensity I_{cycl} of the incoming cyclotron beam.

BEAM INSTRUMENTATION

Ionization Profile Monitor

The Ionization Profile Monitor (IPM), developed at GSI [2], is intended to provide fast and reliable non-destructive beam profile measurements at the future FAIR machines. The IPM was installed in COSY to test its performance and reliability and to provide routine non-destructive profile data for COSY.

The ionisation products are guided to a position sensitive detector by transverse electric field. An arrangement consisting of an MCP stack (100x48 mm^2), a luminescent screen, and a 656×494 pixel CCD camera is used to detect ions. High voltage electrodes provide the electric field for ion extraction. The IPM contains two identical units to provide simultaneous measurements in

*Work supported by HRJRG-106
#v.kamerdzhiev@fz-juelich.de
‡ Institute of Electrophysics and Radiation Technologies, Ukraine

ELECTRON COOLING EXPERIMENTS IN CSR*

Xiaodong Yang#, Guohong Li, Jie Li, Xiaoming Ma, Lijun Mao, Ruishi Mao,
Tailai Yan, Jiancheng Yang, Youjin Yuan , IMP, Lanzhou, 730000, China
Vasily V. Parkhomchuk, Vladimir B. Reva , BINP SB RAS, Novosibirsk, 630090, Russia

Abstract

The six species heavy ion beam was accumulated with the help of electron cooling in the main ring of Cooler Storage Ring of Heavy Ion Research Facility in Lanzhou(HIRFL-CSR), the ion beam accumulation dependence on the parameters of cooler was investigated experimentally. The 400MeV/u $^{12}C^{6+}$ and 200MeV/u $^{129}Xe^{54+}$ was stored and cooled in the experimental ring CSRe, the cooling force was measured in different condition.

INTRODUCTION

Heavy Ion Research Facility of Lanzhou(HIRFL)[1] is an accelerators complex with multi-purpose, its research field includes radioactive ion beam physics, heavy ion physics, high energy density physics, super-heavy elements synthesis, atomic physics, and cancer therapy. It consists of two cyclotrons, SFC and SSC, two synchrotrons, CSRm and CSRe. It can provide the ion beam with energy range from 10 MeV/u to 1GeV/u. The ion beam delivered from SFC or SSC was injected into CSRm, after accumulation with the help of electron cooling, and acceleration, and then delivered to cancer therapy terminal and other experimental terminals, or injected into CSRe. In CSRe, ion beam was cooled by electron cooling device, and various physics experiments were completed in this ring. The ion beam with higher energy in CSRe was stripped, and higher charge state ion beam will be decelerated to lower energy, in the case of low energy of higher charge state ion beam, atomic physics experiments will be performed in CSRe.

ELECTRON COOLING DEVICES

The electron cooling devices was equipped in each ring of CSR, the purpose of electron cooling in CSRm is ion beam accumulation, the cooler was adapted as the way to increase the stored particle number in CSRm, continuous electron cooling is applied to the stored ion beam for compensation of the heating by an internal gas jet target in CSRe, the most important feature is the ability to cool ion beam to highest quality for experiments with stored highly charged ions.

In CSRm, the electron cooling device plays an important role in the heavy ion beam accumulation at injection energy. The new state-of-the-art electron cooling device was designed and manufactured in the collaboration between BINP and IMP, it has three distinctive characteristics, namely high magnetic field parallelism in cooling section, variable electron beam profile and electrostatic bending in toroids.

Continuous electron cooling is applied to the stored ion beam for the compensation of the heating by various scattering in CSRe. The most important thing is the ability to cool the ion beams to the highest quality for physics experiments with stored highly charged ions. The electron cooling devices of HIRFL-CSR were reported in many conferences[2],[3],[4],[5],[6],[7],The previous results have been given in the COOL05-P02[8], COOL07-TUM1I02[9] and COOL09-FRM1MCIO02[10].

ION BEAM ACCUMULATION IN CSRM

In order to demonstrate the performance of HIRFL accelerators complex, and satisfy the requirements of different physics experiments, ion beam with different energy, different charge state were accumulated with the help of electron cooling in CSRm. During accumulation, two injection modes were applied, in the case of lighter ion beam, stripping injection was adapted, for heavier ion beam, repeated multi-turn injection was performed. Due to the injection beam intensity, ion beam was delivered by different injector, SFC or SSC. In the case of fixed energy, choose proper injection interval, partially hollow electron beam, the direction and position of electron beam and ion beam matched well, the maximum accumulation results can be achieved.

Commissioning procedure

The CSR commissioning procedure was described as following steps:

- Obtaining high transportation efficiency in beam line and maximal beam intensity at injection point.
- Correcting the position and angle of ion beam at the injection point, Obtaining the maximal injection intensity at first Faraday cup in the ring.
- Correcting the closed-orbit globally and locally, specially in the region of electron cooler, correcting work-point (without electron beam and with electron beam), improving ion beam lifetime in the ring.
- After turned on the cooler magnetic field, compensating the influence of cooler magnetic field, correcting the position and angle of ion beam entering cooler.
- Fine tuning the energy of electron, after observe accumulation, optimizing the electron beam current and the profile, improve the lifetime of ion beam in the present of electron beam.
- Optimizing injection interval, bump amplitude and time constant.
- Optimizing the ramping data, proper time setting of trigger for RF and kicker, acceleration to high energy

*Work supported by The National Natural Science Foundation of China, NSFC(Grant No. 10975166, 10905083, 10921504)
#yangxd@impcas.ac.cn

ADVANCE IN THE LEPTA PROJECT

E.Ahmanova , V.Bykovsky, M.Eseev[*], V.Kaplin, V.Karpinsky, A.Kobets[#,**],
V.Lokhmatov,V.Malakhov, I.Meshkov, V.Pavlov, R.Pivin, A.Rudakov,
A.A.Sidorin, S.Yakovenko, JINR, Dubna

Abstract

The Low Energy Positron Toroidal Accumulator (LEPTA) at JINR is close to be commissioned with circulating positron beam. The LEPTA facility is a small positron storage ring equipped with the electron cooling system and positron injector. The maximum positron energy is of 10 keV. The main goal of the project is generation of intensive flux of Positronium (Ps) atoms - the bound state of electron and positron, and setting up experiments on Ps in-flight. The report presents an advance in the project: up-grade of LEPTA ring magnetic system, status of the construction of positron transfer channel, and the electron cooling system, first results of low energy positron beam formation with ^{22}Na radioactive positron source of radioactivity of 25 mCi.

LEPTA RING DEVELOPMENT

The Low Energy Particle Toroidal Accumulator (LEPTA) is designed for studies of particle beam dynamics in a storage ring with longitudinal magnetic field focusing (so called "stellatron"), application of circulating electron beam to electron cooling of antiprotons and ions in adjoining storage electron cooling of positrons and positronium in-flight generation.

For the first time a circulating electron beam was obtained in the LEPTA ring in September 2004 [1]. First experience of the LEPTA operation demonstrated main advantage of the focusing system with longitudinal magnetic field: long life-time of the circulating beam of low energy electrons. At average pressure in the ring of 10^{-8} Torr the life-time of 4 keV electron beam of about 20 ms was achieved that is by 2 orders of magnitude longer than in usual strong focusing system. However, experiments showed a decrease of the beam life-time at increase of electron energy. So, at the beam energy of 10 keV the life time was not longer than 0.1 ms. The possible reasons of this effect are the magnetic inhomogeneity and resonant behaviors of the focusing system.

Magnetic and vacuum system improvements

During March-May 2009 new measurements of the longitudinal magnetic field at solenoids connections were performed. According to the measurement results water cooled correction coils have been fabricated and mounted. As result, the inhomogeneity has been decreased down to $\Delta B/B \leq 0{,}02$ (Fig.1).

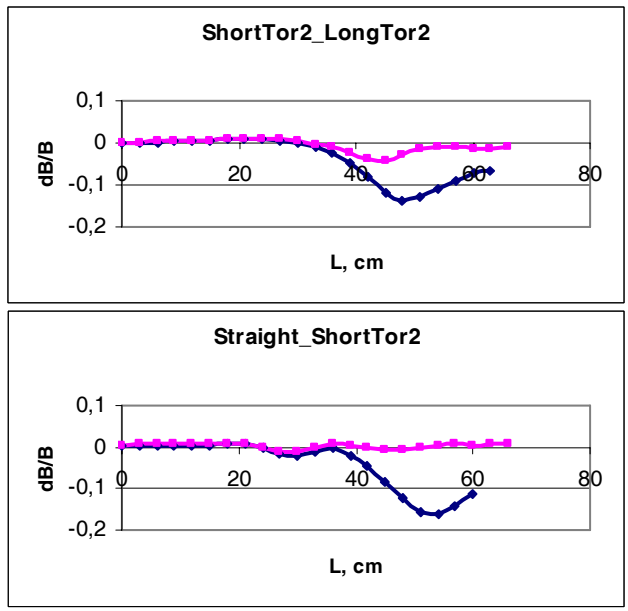

Figure 1: Magnetic field distribution along the toroidal solenoid axis.

The new water cooled helical quadrupole lens was designed and fabricated that allowed us to improve significantly the vacuum conditions in the straight section.

In old design the distance between kicker plates was off 32 mm that limited the aperture. New kicker design allows us to increase aperture up to 120 mm.

Testing after upgrading

After all the improvements and modifications the ring has been reassembled, the electron beam circulation has been obtained again and its life time has been remeasured. Typical life time dependence on electron energy, $\tau e(Ee)$, has two slopes (Fig.2). The left one, where τe increases with Ee, is defined by electron scattering on residual gas. The right slope, descending with Ee, relates to violation of electron motion adiabaticity on inhomogeneities of solenoid magnetic field.

The curves 1 and 2 were obtained in 2005, whereas the curves 3, 4 and the point 5 have been measured in June 2008. The curve 6 was measured in August 2009, after all modifications of the ring described above. One can see significant increase of the electron life time. Of the main importance is the increase of the life time (comparing with the values of the year 2005, 2008) in the energy range above 4 keV by 6÷10 times. It proves the necessity

[*] M.V.Lomonosov Pomor State University, Russia.
** Joint Institute for Nuclear Research, Russia,
Institute of Electrophysics and Radiation Technologies, Ukrain
[#] kobets@jinr.ru

ELECTROSTATIC STORAGE RINGS AT THE ULTRA-LOW ENERGIES RANGE

A.I.Papash, Max Planck Institute for Nuclear Physics, Heidelberg, Germany and
Joint Institute for Nuclear Research, Dubna, Russia
C.P.Welsch, University of Liverpool, UK and
The Cockcroft Institute for Accelerator Science and Technology, UK

Abstract

Electrostatic storage rings have proven to be invaluable tools for atomic and molecular physics at the ultra-low energy range from 1 to 100 keV/A. Due to the mass independence of the electrostastic rigidity, these machines are able to store a wide range of different particles, from light ions to heavy singly charged bio-molecules. A so-called "reaction microscope", incorporated into the ring is considered to be a powerful tool to study fundamental effects by multiple crossing of the stored ion beam with an ultrasonic gas jet. To enable the operation of such internal experiment, one needs to provide very short beam pulses in the 1-2 nanosecond range to pave the way for kinematically complete measurements of the collision dynamics of fundamental few-body quantum systems on the level of differential cross sections. However, earlier measurements at some rings showed strong limitations depending on beam intensity, probably linked to non-linear fields that cannot be completely avoided in such machines. In this contribution, we discuss common features of electrostatic storage rings and analyze the performance of such rings.

INTRODUCTION

Magnetic storage rings operates not only in high energy range but also at low energies. In particular, the LEAR ring at CERN was the first machine to store, cool and decelerate antiprotons down to only 5 MeV [1]. $^{4}He^{-}$ and $^{12}C_{70}^{-}$ ions have been stored at energies of 5 and 25 keV respectively in the ASTRID magnetic ring [2].

The first electrostatic ring was built in 1953 to act as an electron analogue of the Brookhaven AGS synchrotron [3]. Ions are stored in electrostatic traps at lowest energies [4,5]. Another type of storage device complinmentary to traps and developed in response to the needs of the astro-, atomic and molecular physics communities, are Electrostatic Storage Rings (ESR) [6]. As opposed to magnetic storage rings, ESR have no lower limit on the beam energy as well as no upper mass limit on the ion mass that can be stored. Due to the mass independence of the electric fields, massive particles such as clusters and bio-molecules can be stored at lowest energies. ESR were already used to study the following problems [4,6,7]:

- Collision phenomena and plasma properties of astrophysical objects i.e.molecular clouds, quasars;
- electron impact rotational and vibrational excitation of cold molecular ions;
- quantum reaction dynamics of cold molecular ions;
- gas-phase spectroscopy of biomolecular ions;
- ultra-cold (2 K) ESR will allow to store molecular ions in their rotational ground state;
- rotational effects in the process of dissociative recombination of molecular ions with low temperature electrons (<10 K);
- molecular dynamics - to achieve Coulomb cristallization for a fast strored beam and study phase transition to a cristalline beam;
- fundamental few body Coulomb problem for single as well as for multiple ionisation;
- measurements of single and multiple ionization cross-sections (total and differential) of antiprotons colliding with atoms of supersonic gas jet;
- ion-impact ionisation to benchmark theoretical predictions;
- anti-hydrogen studies by merging antiprotons with positrons;
- study of the lifetime of metastable atomic states;
- investigations of the single component plasma.

COMMON FEATURES OF ELECTROSTATIC STORAGE RINGS

ESR are in some way complimentary to ion traps and allow reducing the ion energy to almost ground state. In ESR, ions circulate in one direction while in ion traps there is no designated direction of motion. One can outline the following common features of all ES rings:

- ESR can store ions at keV energies and potentially even lower energies;
- Their fields are mass independent, i.e. –a wide range

Table 1. Electrostatic storage rings worldwide

Ring	ELISA [9,10]	ESR [11]	FRR [13]	DESIREE [14]	CSR [18,19,20]	USR [21,22,23]	AD-REC [24]
Location	Aarhus Univ. Danmark	KEK Tsukuba Japan	Frankfurt Univ. Germ	Stockholm Univ. Sweden	MPI Heidelberg Germany	FAIR-GSI Darmstadt Germany	ASACUSA CERN Switz
Ions	A ≤ 100	A ≤ 100	A ≤100	A ≤ 100	A ≤ 100	antiprotons	antiprotons
Energy, keV	(5–25)·Q	20·Q	50	(25-100)·Q	(300-20)·Q	300-20	3-30
Type	Racetrack	Race track	Race track	2 x Race tracks	quadratic	Achromat quadratic	Low beta racetrack
Symmetry	2	2	2	2 x 2	4	4	2
Perimeter, m	7.62	8.14	14.17	9.2 x 9.2	35.2	43	7.9
Revolution time, μs	3.5 (p) 93 (C_{60})	4 (p) 22 (N_2^+)	4.5 (p)	4–60	4–180	5.67–22	10–3
ES Deflectors	160°+10°	160°+10°	75°+15°	160°+10°	39°+6°	37°+8°	90°+90°
DeflRad mm	250	250	250	250	2000+1000	2000+1000	400
Deceleration/ acceleration	Drift tube	Drift tube	--	--	Drift tube 10 V	Drift tube 10 V	Pulsed injector
e-cool eV	NO	NO	NO	NO	10	10	NO
life time, s	10-30	12-20	--	--	10–100	~10	~20 ms
Operation modes	storage	Storage	D=0 at target	Colliding beams	Cooling storage	Short bunch Slow extr.	Low beta Low Disp.
Vac. mbar	10^{-11}	$5{\cdot}10^{-11}$	10^{-12}	10^{-12} (10°K)	10^{-15} (2°K)	10^{-11}	10^{-10}
Status	operate	operate	tested	Project	manufact.	Design	Manufact.

RESEARCH OF PHOTON EMISSION OF 120 GEV CHANNELING POSITRONS

V.A. Maisheev, Y.A. Chesnokov, P.N. Chirkov, I.A. Yazynin, IHEP, Protvino, Russia
D. Bolognini, S. Hasan, M. Prest, Università dell'Insurbia, Milano; E. Vallazza, INFN, Trieste, Italy

Abstract
The motion of positrons in the interplanar nonlinear potential of a straight thin Si crystal and radiation spectra are calculated.

INTRODUCTION

By this time the considerable number of experimental and theoretical works is devoted to researching the radiation at plane channeling of high energy positrons in monocrystals [1, 2, 3]. This radiation arises during the motion of a charged particle under a small angle in relation to a crystallographic plane and for positrons with energies up to ~20 GeV is monochromatic enough and is characterized by high intensity. At energies of positrons more than ~20 GeV monochromaticity of the radiation strongly degrades. In September, 2009 in CERN the experiment INSURAD devoted to research of radiation at various orientations of bent monocrystals has been made at energy of positrons of 120 GeV. The radiation type of a relativistic particle depends on the value of multipole parameter ρ. When $\rho << 1$ it corresponds to the interference type (dipole approximation) of the radiation formed along sufficiently large length of the crystal. The case with $\rho >> 1$ is close to the synchrotron radiation. At energies of positrons 100 GeV and more the parameter ρ can exceed 20 units for a considerable part of the particles.

In the given work we wish to receive the following results: to define characteristic parameters of motion of an ultrarelativistic particle in real plane potential of a monocrystal and to study the influence of its nonlinearities on ensemble of particles captured in a mode channeling; to calculate radiation spectrums of positrons with energies an order 100 GeV at their different entry initial conditions on an input in a monocrystal.

INTERPLANAR ONE–DIMENSIONAL MOTION OF CHANNALED POSINRONS

The motion of a charged ultrarelativistic particle in the interplanar electric field D of a monocrystal can be described by the following system of equations

$$\frac{E}{c^2}\frac{d^2x}{dt^2} = e\mathrm{D}(x),\quad \frac{d^2y}{dt^2} = 0,\quad \frac{ds}{dt} = c\left(1 - \frac{1}{2\gamma^2} - \frac{1}{2c^2}\left(\left(\frac{dx}{dt}\right)^2 + \left(\frac{dy}{dt}\right)^2\right)\right),$$

where: x, y, s - the Cartesian co-ordinates of a particle (the electric field D is directed along the axis x); E, e, γ - energy, charge and gamma factor of a particle, accordingly; t - time, c - velocity of light. The first equation describes periodic motion along x, the third equation reflects the influence of transverse motion on longitudinal one. From the above equations it is seen that the problem of finding the trajectory of a particle in three-dimensional space is reduced to finding the function $x(t)$.

We will consider periodic (generally nonharmonic) motion of positrons with energy of $E = 120$ GeV in the interplanar potential of a straight crystal Si with orientation (011). The interplanar potential is calculated for silicon at a room temperature as it is described in work [4]. The interplanar potential of interaction of a positron in a straight crystal is defined by expression [4, 5]

$$U(\xi) = -\frac{d}{2}\sum_{k=1}^{7}\frac{\alpha_k}{2k}\xi^{2k}, \qquad (1)$$

where:: $\xi = 2x/d$ - normalized interplanar coordinate, $\xi \in [-1,+1]$; $d = 1.92$ Å - interplanar distance in (011) channel; $\vec{\alpha} = (-32.21\ \ 13.86\ \ -443.78\ \ 2340.52\ \ -5315.05\ \ 4811.79\ \ -1375.13)$ in [eV/Å]; such values of $\vec{\alpha}$ provide $dU/d\xi = 0$ at $\xi = \pm 1$.

In a Fig. 1 the dependence of normalized frequency $\Omega(\xi_\mathrm{m}) = \omega(\xi_\mathrm{m})/\omega_\mathrm{o}$ on the amplitude of periodic motion is shown, where: $\omega_\mathrm{o} = (2|\alpha_1|c^2/Ed)^{1/2} \cong 5.013\times10^{13}$/sec - frequency of oscillations with small (zero) amplitudes in the potential hole $U(\xi)$. The maximum displacement of periodic motion is interpreted as amplitude ξ_m. The motion of a positron in normalized potential well $\widetilde{U}(\xi) = 2U(\xi)/|\alpha_1|d$ is described by the canonical equations

$$d\xi/d\tau = p \quad \text{и} \quad dp/d\tau = -d\widetilde{U}(\xi)/d\xi, \qquad (2)$$

where: $\tau = \omega_\mathrm{o}\, t$ - the dimensionless time (phase); $p^2/2 + \widetilde{U}(\xi) = \varepsilon$ - the transverse energy (integral of motion). Maximum deviation (amplitude) $\xi_\mathrm{m}(\varepsilon)$ is defined from equation $\widetilde{U}(\xi_\mathrm{m}) = \varepsilon$. The dependence of normalized frequency Ω on amplitude ξ_m is determined by

$$\Omega(\xi_\mathrm{m}) = 1/\frac{4}{2\pi}\int_0^{\xi_\mathrm{m}} d\xi/\sqrt{2(\widetilde{U}(\xi_\mathrm{m}) - \widetilde{U}(\xi))}.$$

The multipole parameter ρ is expressed through parameters of plane periodic motion of a particle as follows [1]: $\rho = 2\gamma^2 < (\upsilon_\mathrm{x}/c)^2 >$, where the averaging is taken over the motion period. For the channeled positron with the given ξ_m we have

$$\rho(\xi_\mathrm{m}) = \gamma^2\kappa^2\Omega(\xi_\mathrm{m})\frac{4}{\pi}\int_0^{\xi_\mathrm{m}}\sqrt{2(\widetilde{U}(\xi_\mathrm{m}) - \widetilde{U}(\xi))}\, d\xi,$$

where $\kappa = d\omega_\mathrm{o}/2c \cong 16.052\cdot10^{-6}$. In Fig. 2 (the continuous line) the exact dependence of multipole parameter on

JINR ACTIVITY IN FEL

O. Brovko, G. Chelkov, E. Ivanov, M. Kapishin, E. Matyushevskiy, N.Morozov, G. Shirkov, E. Syresin#, G. Trubnikov, M. Yurkov, Joint Institute for Nuclear Research, Dubna, Russia

Abstract

Different methods for diagnostic of ultrashort electron bunches are developed at JINR-DESY collaboration within the framework of the FLASH and XFEL projects. Photon diagnostics developed at JINR-DESY collaboration for ultrashort bunches are based on calorimetric measurements and detection of undulator radiation. The MCP based radiation detectors are effectively used at FLASH for pulse energy measurements. The new MCP detector for X-ray beam diagnostic for XFEL is under development now in JINR. The infrared undulator constructed at JINR and installed at FLASH is used for longitudinal bunch shape measurements and for two-color lasing provided by the FIR and VUV undulators. The JINR also participates in development and construction of Hybrid Pixel Array Detector on the basis of GaAs sensors. The JINR in collaboration with IAP RAN and DESY (Zeuthen) develops a project of laser system based on Nd laser with pulse shaper for formation of quasi 3D ellipsoidal laser pulses applied for a prototype of XFEL gun.

FLASH MCP-BASED PHOTON DETECTOR

The free electron laser FLASH has been in operation at DESY since the year 2000 [1,2]. The electron energy now reaches 1 GeV, rms bunch length is 50 μm, the FWHM radiation pulse duration is about 30 fs, the normalized emittance is 2 π·mm·mrad, the bunch charge is 1 nC, the peak power is up to 1 GW, the peak brilliance is of 10^{28} ph/s/mrad2/mm2/(0.1%bw).

Successful operation of FLASH strongly depends on the quality of the radiation detectors. The key issues are: the wide wavelength range 6-100 nm, the wide dynamic range (from the spontaneous emission level to the saturation level), and the high relative accuracy of measurements which is crucial for detection of radiation amplification and characterization of statistical properties of the radiation.

The key FLASH photon detector developed by the JINR-DESY collaboration is a micro-channel plate (MCP) detector intended for pulse energy measurements [3-5]. The MCP detector is used for measurement of statistical properties of the radiation allowing determination of the pulse length. Key element of the detector is a wide dynamic MCP which detects scattered radiation from a target. With four different targets and MCPs in combination with optical attenuators, the present FLASH detector covers an operating wavelength range 6 -100 nm, and a dynamic range of the radiation intensities, from the level of spontaneous emission up to the saturation level of SASE FEL.

#syresin@nusun.jinr.ru

The gold target is perfect for the wavelength range above 10 nm, however its reflectivity falls dramatically for shorter wavelengths, and different targets and geometries of the detector are used. We added three more targets to gold mesh: two iron meshes, and one copper mesh. This helps us to operate the detector in a range below 10 nm.

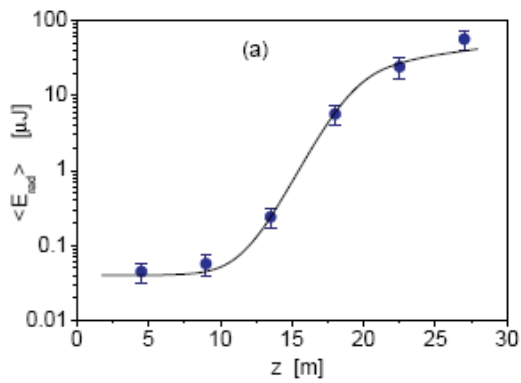

Figure. 1: Measured average energy in the radiation pulse versus the undulator length.

For tuning SASE at very short wavelengths we use movable MCPs directly facing photon beam. Light intensity variation by a factor of 50 is controlled by a mechanical attenuator of light located in the target unit. To have full control of light intensity in a wide range we installed a side MCP which detects radiation reflected by the iron mirror. The mirror serves for two purposes. One is to deflect the photon beam off- the axis, which allows placing the MCP in better background conditions.

The dependence of the measured average energy in the FLASH radiation pulse on the undulator length is shown in Fig. 1. In the saturation regime the average pulse energy is 40 μJ and the wavelength is 13.7 nm.

DEVELOPMENT OF XFEL MCP

The developed XFEL MCP-based detector consists of four main elements: attenuator, frequency filter, MCP equipped with anode as pulse energy monitor, and MCP imaging detector as a viewer of photon beam image (Fig.2). Frequency filter selects frequencies near the required harmonic of the radiation (fundamental, or higher). Technical realization of frequency filter and attenuator depends on the wavelength of interest. For operating wavelength band below 0.4 nm (fundamental harmonic of SASE1 and SASE2) Si (111) crystal (Bragg reflection) is used as a frequency filter, and attenuation is

PROPOSAL FOR AN ACCELERATOR COMPLEX FOR EXTREME ULTRAVIOLET NANOLITHOGRAPHY USING KW-SCALE FEL LIGHT SOURCE

E.Syresin , M. Yurkov, Y. Budagov, N. Balalykin, I. Lensky, A. Olshevsky, A. Sumbaev, G. Shirkov, G.Trubnikov, Joint Institute for Nuclear Research, Dubna, Russia.

Abstract

The project is aimed at construction of accelerator complex, based on a 0.7 GeV superconducting linear accelerator, for applications in nanoindustry, mainly for extreme ultraviolet lithography using kW-scale Free Electron Laser (FEL) light source. The project involves construction of a 0.7 GeV superconducting linear accelerator to produce coherent FEL radiation for extreme ultraviolet nanolithography at a wavelength of 13.5 nm and an average radiation power of 0.5 kW. The application of kW-scale FEL source permits realizing EUV lithography with 22 nm, 16 nm resolutions and beyond. The project for construction of an accelerator complex for EUV lithography is based on the technology realized on FEL FLASH (Free Electron Laser in Hamburg) facility at DESY (Hamburg).

INTRODUCTION

The project is aimed at construction of accelerator complex, based on a 0.7 GeV superconducting linear accelerator, for applications in nanoindustry, mainly for extreme ultraviolet lithography using kW-scale Free Electron Laser (FEL) light source. The project involves the following activities.

Construction of a 0.7 GeV superconducting linear accelerator to produce coherent FEL radiation for extreme ultraviolet nanolithography at a wavelength of 13.5 nm and an average radiation power of 0.7 kW.

Construction of a dedicated channel for extreme ultraviolet lithography with a few nanoscanners operating simultaneously in a processing line with 22 nm, 16 nm and beyond using FEL radiation at a wavelength 13.5 nm.

Medico-biological investigations using radiation with wavelengths ranging from 2.4 nm to 4.6 nm (3rd harmonic FEL) .

Research in magnetic materials using radiation with a wavelength of about 1.5 nm (5rd harmonic FEL).

Realization of the superconducting RF linear accelerator technology for the International Linear Collider.

.

EXTRIME ULTRAVIOLET LITHOGRAPHY

The development of the next generation lithography was started since the middle of 1990s. A target goal was to follow Moore's law in the reduction of a feature size by a factor of two in two years. During last two decades the progress in the feature size reduction has been provided by reducing the wavelength of lasers used. The conventional lasers operate at wave length of 193 nm. Immersion and photoresist technologies aiming to get feature size below λ/4 limit reached their boundaries as well.

The ASML TWINSCAN NXE platform [1] (Fig.1) is the industry first production platform for extreme ultraviolet lithography (EUVL) based on the laser source LPP [2] at wave length of 13.5 nm. The resolution of NXE:3100 corresponds to 27 nm (Table 1). The resolution of NXE: 33000B is 22 nm with conventional illumination and 18 nm with of-axis illumination.

Figure 1: ASML TWINSCAN NXE industry platform for EUVL with LLP at radiation wavelength of 13.5 nm.

Table 1. Parameters of SML EUV platform.

Parameter	NXE:3100	NXE: 33000B
NA	0.25	0.32
Resolution, nm	<27	<22 (18nm off-axis illumination)
Exposition field, mm	26×33	
Illumination sigma	0.8	0.2-0.9
Overlay, nm	4.5	3.5
Productivity, wph	>60	>125

The power of LPP sources now corresponds to 75 W [2]. The exposition power is equal to 20 W that provides

SELF-STIMULATED UNDULATOR RADIATION SOURSES

E.G Bessonov, M.V.Gorbunkov, A.L. Osipov, Lebedev Phys. Inst. RAS, Moscow, Russia
A.A.Mikhailichenko, Cornell University, LEPP, Ithaca, NY 14853, U.S.A.

Abstract

The phenomena of self-stimulation of incoherent radiation emitted by particles in a system of undulators installed in the linear accelerators or quasi- isochronous storage rings are investigated. Possible applications of these phenomena for light sources are discussed.

INTRODUCTION

A particle passing through an undulator emits an undulator radiation wavelet (URW), the length of which in the direction of its average velocity is $M\lambda_1$, where M is the number of undulator periods, and λ_1 is the wavelength of the first harmonic. In a system of N_u identical undulators, located along straight line, the particle radiates N_u URWs with a separation l; both l and λ_1 are defined by the Doppler effect, by an angle θ between the average particle velocity in the undulator and the direction to the observer, by the distance between the undulators l_0, by the period of the undulator λ_u and by the relativistic factor $\gamma = \varepsilon / mc^2 >> 1$, m_e is the rest electron mass, ε is the electron energy [1], [2]. In the forward direction ($\theta = 0$) they are: $l = l_0 / 2\gamma^2$ and $\lambda_1 \sim \lambda_u / 2\gamma^2$. The energy radiated by a particle in a system of N_u undulators becomes modified and is N_u times larger than one radiated in just a single undulator. The spectrum of radiation emitted in an arbitrary direction also changes, appearing as a line structure. The integrated spectrum does not change much however.

Self-Stimulated Undulator Radiation (SSUR) is a kind of undulator radiation (UR) emitted by a charged particle in a field of the downstream undulator in the presence of self-fields of its own wavelets emitted at earlier times in the same or upstream undulator. These wavelets focused back to the particle's position at the entrance of the downstream undulator with mirrors, lenses and passed through the optical delay lines [3]. Below we considering two schemes based on linear accele-rators and storage rings.

One way to increase the loss rate of a particle in a system of N_u undulators by the introduction of controlled delays in the motion of the particles between undulators relative to their URWs is shown on the Fig.1.

Delays are chosen so that a particle enters the following undulator in the decelerating phase at the front edge of its URW, which was emitted from preceding one. In this case the particle will experience deceleration in its self-field generated by its instantaneous motion in the field of the undulator as well as in the field of the URW from preceding undulators (stimulated radiation in field of a co-propagating URW). Under such conditions super-position of the wavelets occurs, which yields the electric field growth $\sim N_u$ and the growth of energy density in the emitted radiation becomes $\sim N_u^2$. Below we will name the linear system of undulators and optical elements by self stimulated undulator klystron (SSUK).

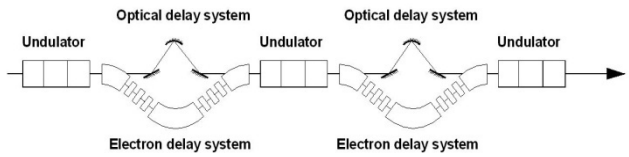

Figure 1: Schematic of the installation.

To be optimally effective, this system must use appropriate focusing elements such as lenses and/or focusing mirrors (see Figs. 1, 2). Mirrors and lenses are used to form a crossover in the middle of the undulators with the Rayleigh length of the order of the length of undulator $Z_R \cong M\lambda_u / 2$.

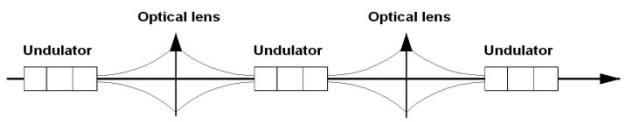

Figure 2: Equivalent optical scheme.

We considered here the case where the optical delays are tuned so that the wavelets emitted by the particle are congruent and all particles stay at the decelerating phase. For this the beam delay system must be isochronous.

Another way to increase the loss rate of a particle is the SSUR source based on a quasi-isochronous storage ring equipped with an undulator (or SSUK) installed in its straight section and the mirrors installed at both sides of the undulators outside of the closed orbits of electrons, circulating in the ring (Fig.3). So the mirrors set an optical resonator.

The scheme of the SSUR source has resemblance to the scheme of ordinary FEL with additional synchronicity condition: the oscillation period of the URW emitted by every electron in the undulator inside the optical cavity coincides with the revolution period of this electron in the storage ring in the limits of energy and transverse emittance of the beam. The URWs emitted by every electron are accumulated effectively in the optical resonator by the superposition one by another if theirs longitudinal shift per turn satisfies condition

$$\Delta\, l - n\lambda_m \,| \leq \lambda_m / F, \qquad (1)$$

where $\lambda_m = \lambda_1 / m$ is the wavelength of the UR emitted by the electron on the *m*-th harmonic in the direction of its average velocity, F is the finesse (quality factor) of the

LIGHT SOURCES IN RUSSIA

E.G.Bessonov, Lebedev Phys. Inst. RAS, Moscow, Russia

Abstract

Possible ways of development of Light Sources (LS) based on relativistic electron and ion beams in accelerators and storage rings in Russia are discussed.

INTRODUCTION

Progress in various fields of natural science, medicine, biology, chemistry and technology is closely connected with the development and use of LS based on relativistic electron and ion beams. One of the main motivations to build such sources is to have a very brilliant and bright source of monochromatic photon beams with smoothly varied frequency in a wide spectral region and varied kinds of polarization. This is achieved on one hand with the production of low emittance particle beams in accelerators and storage rings of differed energy, on the other hand with the use of a variety of undulators and on the third hand with the use of different kinds of the emitting particles (electrons, ions) which can be optimized to the special demands of a certain experiment.

By definition, the LS's are sources of powerful beams of IR to X-rays having high degree directionality, narrow bandwidth, tunability, variable photon energy and polarization. These sources are based on accelerators and storage rings and make possible basic and applied reseach in different fields that are not possible with more conventional equipment. They are UR sources, including Backward (or Inverse) Compton scattering (BCS) sources and possibly future Backward Rayleigh scattering (BRS) sources. These sources are both spontaneous incoherent UR sources, spontaneous coherent UR sources (prebunched fel's) and stimulated UR sources (fel's) [1]. Development of LS's go on in all these directions. 3 Generations of the LSs are developed. 4th Generation of LSs is in the process.

One of the main motivations to build new generation LS is to have more bright source of photons in a wide spectral region. Brightness and brilliance (*) are determined by the equations

$$B_{rn} = \frac{1}{\hbar\omega}\frac{\partial^2 W}{\partial\omega\partial o}\Delta\omega, \qquad B_{rl} = \frac{1}{\hbar\omega}\frac{\partial^2 W}{\partial\omega\partial o\partial s}\Delta\omega,$$

where adopted $\Delta\omega/\omega = 10^{-3}$, $\hbar$ is the Planck constant, ∂s is the effective source area [2].

If the emitted UR beam is focused onto the sample, then the figure of merit of the UR source is its brilliance. In this case the smaller the particle beam dimensions and divergence, the smaller the sport size and divergence of the photon beam at the sample. The figure of merit of the source for the unfocused UR beams is its brightness. The brilliance was chosen to be an absolute criterions for generations of LS's. But it can obscure essential distinctions between particular machines which determine if the machine is suited for a given application. Existing IR and optical FELs and future fully coherent monochromatic long duration x-ray FELs are not included in any generation of LSs. A full characterization of a LS involves specification of the brilliance, polarization, spectrum, coherence, and time structure of the emitted radiation. Third generation LSs based on storage rings can complement of forth generation LS's.

Third generation LSs based on storage rings are physically very large (~1000 meters in circumference) with a capability for 30 or more insertion-devices, and a comparable number of bend-magnets and beam lines. They are very expensive and occupy an area the size of a sports stadium. Can be such installation shrunk down to fit on the desk? Similar suggestions are discussed for a long time. Now the Compact LS (CLS) based on small storage ring (~20 – 100 MeV) and laser beam stored in high quality open resonator and propagated along a straight section of the storage ring with zero dispersion and low beta-function is developed. Radiative cooling of the electron beam in the storage ring by high intensity laser light permits to overcome the problem of intrabeam scattering and to maintain the low emittance of the stored beam and its cross section at the IP at the average beam current I > 10 mA which permits to produce brightness enough for many experiments. Experiments will show the limiting stored currents which are determined by the laser intensity at the interaction point.

BCS and BRS sources can be considered as UR sources. In this case electron trajectories both for free electrons and for electrons bounded by nuclei (in classical approach) are undulator ones. Electrons bounded by nuclei are a very high quality oscillators. The amplitude of oscillations of an electron bounded by nuclei at resonance is much higher then for electron in free space. That is why the cross-section of the Rayleigh scattering is much higher (~10-15 orders) then Compton one (†). Ion storage rings are much expensive then electron ones. At the same time BRS sources are fraught the ultimate in the capabilities both spontaneous and stimulatd radiation sources in X-ray and gamma-ray regions.

The energy of scattered photons is high. It can reach high value ~5 MeV at the electron energy ~ 500 MeV and the photon energy ~ 1 eV. In this case the electron will be lost at the walls of the storage ring after interaction with a laser photon. Cross section of Compton scattering is small. That is why the intensity and hardness of CLS is

(*) Flux refers to the number of photons/s/0.1percentBW, Brightness refers to: photons/s/unit solid angle/ 0.1percentBW and Brilliance refers to: photons/s/unit solid angle/0.1 percent BW/unit area. Forth generation LS will have average brilliance $>10^{22}$ and peak one $>10^{30}$ at photon energies > 1 KeV.

(†) Transition energies and equilibrium amplitudes (oscillator strengths) are calculated in the framework of the quantum theory.

THE EXPANDED PROGRAM TOOLS FOR KSRS OPERATION WITH ARCHIVATION OF DATA

E.Kaportsev, Yu.Krylov, V.Korchuganov, K.Kuznetsov, K.Moseev, L.Moseiko, N.Moseiko, Yu.Yupinov, RRC Kurchatov Institute, Moscow, Russia

Abstract

The running cycle of Kurchatov Synchrotron Radiation Source (KSRS) [1] includes the injection of electrons with energy 80 MeV from the linear accelerator in the booster storage ring Siberia-1, the accumulation of a electron current up to 400 mA and, then, electron energy ramping up to 450 MeV with the subsequent extraction of electrons in the main ring, storage ring Siberia-2, and accumulation there up to 300 mA, and at last the energy ramping up to 2.5 GeV. The control system is based on the distributed network of the processors operating technological systems of KSRS. The operational level of control system is realized as a local network of the personal computer.

The database describing logic channels of the control, modes of the technological systems and the script of the running cycle of accelerating facilities is developed. The database for preservation of the received parameters of a complex is developed, the program of an archiving received with ADC data is developed. Logic channels of the control are a basis for creation of the user interface. The examples of realization of the software used in operative work KSRS are given.

OPERATIONAL MANAGEMENT OF THE COMPLEX

Network operator's machine consists of workstations running Windows XP, in the local network Ethernet (Fig. 1). [2] Program Management and diagnosis of receiving information from the database server based on MS SQL Server, where it comes from the application server. In our case, the database server and application server are located within a single machine. All executable modules, ADC and DAC combined into a CAN-network. On the application server load management program and collect data from performing devices, sensors and diagnostic tools. These servers are only three: Application server, CAMAC messaging server and Vacuum server.

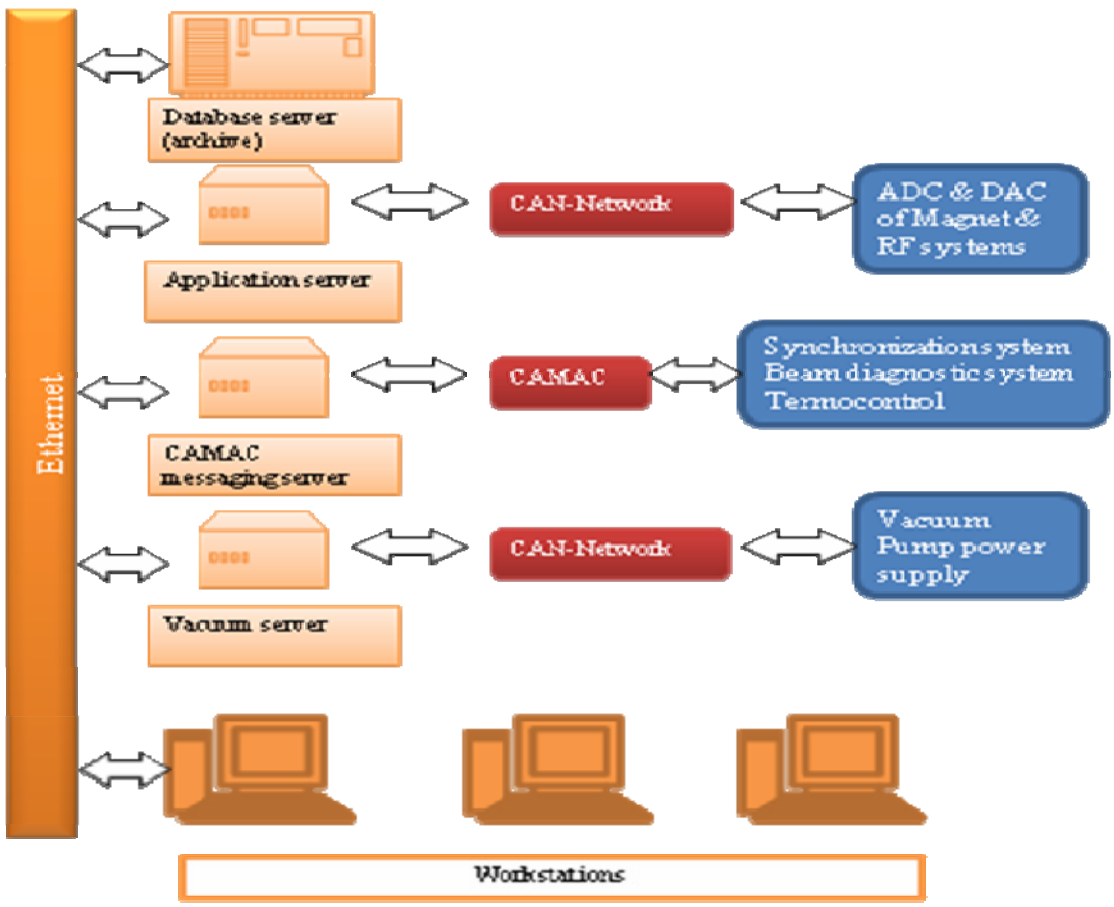

Fig. 1. Scheme of control system.

ACCELERATION OF HEAVY IONS IN SPACE PERIODIC QUADRUPOLE RF FOCUSING STRUCTURE

Yu.A.Budanov, O.K.Belyaev, I.A.Zvonarev, A.P.Maltsev,
State Research Center of Russia Institute for High Energy Physics,
142281, Pritvino, Moscow Region, Russia

INTRODUCTION

Accelerators with space uniform quadrupole radio-frequency focusing (RFQ) are used for a long time already for acceleration not only protons, but also almost all spectrum of accelerated ions. In IHEP the first-ever such accelerator has been implemented, and then various accelerators with RFQ [1] have been produced some more. However, their wide application is limited only by low energy area as an initial part of the accelerator. The effective utilization of radio-frequency focusing on higher energy demands application of accelerating structure with space periodic focusing (RFQ DTL) [1], it has been carried out successfully in IHEP Protvino. Application RFQ DTL is practically realized for acceleration of protons up to 30 MeV [1]. Acceleration of heavy ions with the help RFQ DTL was never carried out, though at acceleration of heavy ions in the first sections of the linear accelerators energetically favorably use of resonators with a longitudinal magnetic field. Essential feature of space periodic focusing is dependence of focusing properties of the channel on a phase of a high-frequency field. Thus, the bunch of particles after preliminary acceleration in RFQ should be enough small in phase size, it is quite provided at acceleration of such easy ions as protons and deuterons. However at acceleration of heavy ions the phase size of the bunches changes essentially more slowly, than for protons, and its remains rather big at the reasonable sizes RFQ, used for a preliminary grouping and acceleration.

In the given report it is offered the suitable device, developed in IHEP Protvino, and parameters of section RFQ DTL. That device will consist of buncher and quadrupole lenses which allow to solve the given problem and, in general, to improve the matching of all six phase variables. Correctors of beam position in transverse plane are proposed in this matching device also.

Numerical calculations are carried out with the example of gold ions Au_{197}^{+32} at working frequency 74 MHz. Energy of transition from RFQ in RFQ DTL 0.4 MeV/u and final energy in RFQ DTL section 2 MeV/u. Calculation of section parameters for the accelerator has preliminary been carried out, determined it acceptance and separatrix. Then parameters and dynamics of a beam in the matching device have been designed. The operating mode of the described devices: $10\,\mu s$ - duration of current pulses and frequency pulses up to 10 Hz is supposed.

PARAMETERS OF RFQ DTL SECTION

The scheme of the acceleration period for RFQ DTL section is presented on fig. 1.

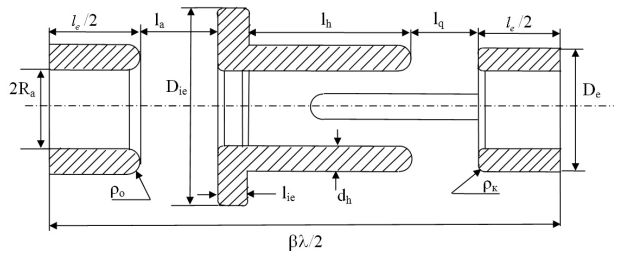

Figure 1: Acceleration period. $2R_a$ – diameter of an aperture, D_{ie} – external diameter of a space electrode, D_e – external diameter of an main electrode, d_h – diameter of a finger electrode, ρ_o – radius of a main electrode, ρ_k – radius of edges of electrodes, $\beta\lambda/2$ – length of the period of acceleration, $l_e/2$ – half of length of an main electrode, l_a – length of an axially-symmetrical gap, l_{ie} – length of an space electrode, l_h – length of a finger electrode, l_q – length of a gap between of a finger electrode and a next main electrode.

Parameters of the periods of acceleration should satisfy to a number of criteria, such as maintenance of electric strength of structure, maintenance of appropriate parameters of longitudinal and transverse movement and enough high rate of acceleration. At a choice of parameters of section RFQ DTL the special attention has been given transverse movement of particles. In this case the type of focusing FFDD has been chosen.

Acceleration and focusing of heavy ions is essentially concerned with acceptance of the channel. Dependence of focusing on phase RF field should be considered already at a preliminary stage. In this case by choice of lengths of quadrupole (focusing) electrodes l_h and lengths of axial (accelerating) gaps l_a it was possible to receive in all range of phases of acceleration such phase advance μ and the minimum value of frequency of transverse oscillation ν_{min} , which yield minimum changes μ and ν_{min} . These changes are not critical for the necessary interval phase of RF field (Fig. 2). This dependence was controlled on all length of the focusing RFQ DTL channel. It is necessary to note, that first and last period of the accelerating channel differs from the regular period (fig. 1).

METHOD TO ESTIMATE THE BEAM AND STRUCTURE PARAMETERS FOR THE DISPERSION ACCELERATOR PARTS

V.A.Moiseev , INR RAS, Moscow, Russia

Abstract

The beam dynamics parameters as the transverse emittance information, momentum spread and structure characteristics are determined by treatment of the small number of profile measurements for the dispersion accelerator parts. The reliability of measurements is estimated.

INTRODUCTION

For dispersion accelerator parts the qualitative transverse profile measurement treatment is important both for circular accelerators and aside beam lines of the linacs. On a measuring area the dispersion distorts the standard phase space ellipse description [1], where the particles with different longitudinal momentum have other transverse central orbits. For the dispersion plane the off momentum particles have a transverse moving over the central orbit defined by

$$x_c(s) = D(s)\cdot\delta \qquad (1)$$

where $D(s)$ – the dispersion function at an accelerator point s; δ – the relative particle longitudinal momentum deviation from the nominal value.

Later for simplicity it will be supposed that there is dispersion in the horizontal plane only. The calculations will be presented for this plane.

ASSUMPTIONS AND MATHEMATICAL FORMALISM

Let is proposed the measurement area is placed between the longitudinal coordinates s_0 and s_1 of an accelerator (Fig.1). At the end point a transverse beam profilometer is located.

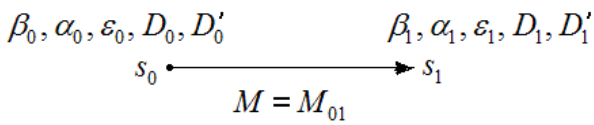

Figure 1: Measurement area

In Fig.1 at points s_0 and s_1 the $\beta_0, \alpha_0, \beta_1, \alpha_1$ are characteristic functions [1] for the beam particles with $\delta \sim 0$; ε_0 , ε_1 - rms unnormalized beam emittances of the beam particles with $\delta \sim 0$; D_0, D_0', D_1, D_1' – the values of dispersion and its derivations; M_{01} – (2×2) transfer matrix of a measurement beam line.

The basic formulas for further calculations are:

$$\overline{x^2}(s) = \overline{\xi^2}(s) + D^2(s)\cdot\overline{\delta^2} \;\; ; \;\; \overline{x}(s) = \overline{\xi}(s) \qquad (2)$$

where $\overline{x^2}(s)$ – the square of the rms beam profile measurements for the total beam particles; $\overline{\xi^2} = \beta(s)\cdot\varepsilon(s)$ is the standard beam phase space characteristic [1] for particles with $\delta \sim 0$. For Eq.2 the followed assumptions were done:

- the particles with deviation from nominal longitudinal momentum have the identical normalized distribution functions in transverse planes;
- the momentum distribution function is symmetrical.

For simplicity further we suggest that there are no accelerator elements and there are variation elements, for example quadrupole lenses, to change the transfer matrix M_{01} of the measurement area (Fig.1). Therefore the followed equations are valid [1]:

$$\begin{aligned} &\varepsilon_0 = \varepsilon_1 \\ &\beta_1 = m_{11}^2\beta_0 - 2m_{11}m_{12}\alpha_0 + m_{12}^2\cdot\frac{1+\alpha_0^2}{\beta_0} \\ &D_1 = m_{11}D_0 + m_{12}D_0' \\ &M = \begin{pmatrix} m_{11} & m_{12} \\ m_{21} & m_{22} \end{pmatrix} \end{aligned} \qquad (3)$$

By using the above formulas for the N_m profile measurement results the Eq.2 may be written in the followed form:

$$\overline{x_i^2} = \beta_i\varepsilon_0 + D_i^2\cdot\overline{\delta^2} \quad , \quad i = 1 \div N_m \qquad (4)$$

where index i is referred to the values at point s_1 for each measurement. In Eqs.4 there are six variables $\beta_0, \alpha_0, D_0, D_0', \varepsilon_0, \delta$. To exclude from any two Eqs.4 the variables ε_0, δ, for example by followed formulas

$$\varepsilon_0 = \frac{x_i - D_i^2\overline{\delta^2}}{\beta_i} \quad ; \quad \overline{\delta^2} = \frac{\overline{x_i^2}\beta_j - \overline{x_j^2}\beta_i}{D_i^2\beta_j - D_j^2\beta_i} \quad , \quad i \neq j \qquad (5)$$

and replace these values to any third equation from Eqs.4 the next form may be derived

$$\begin{aligned} &\overline{x_i^2}(\beta_j D_k^2 - \beta_k D_j^2) + \overline{x_j^2}(\beta_k D_i^2 - \beta_i D_k^2) + \\ &+\overline{x_k^2}(\beta_i D_j^2 - \beta_j D_i^2) = 0 \;\; , \;\; i \neq j \neq k \end{aligned} \qquad (6)$$

In Eqs.6 there are only four independent variables $\beta_0, \alpha_0, D_0, D_0'$. Because of the independence and equality of measurements to combine from N_m by three we get $N_1 = C_{N_m}^3$ equations like Eq.6. In Table 1 this number is presented. The equations like Eq.6 are strongly nonlinear due to the coupling in Eqs.3.

RECONSTRUCTION OF THE BEAM PARAMETERS AND STRUCTURE CHARACTERISTICS FOR INR ISOTOPE CHANNEL

V.Moiseev, S.Bragin, A.Feschenko, O.Grekhov, Yu.Kiselev, A.Mirzojan, O.Volodkevich,
INR RAS, Moscow, Russia

Abstract

The various treatments of profile measurements have been applied to estimate both the major beam parameters and structure functions for the INR isotope channel (IC). The main problem for beam dynamics reconstruction consists in the presence of a dispersion function along the beam line studied. The reliable results were obtained and used to form the beam on the target of INR isotope complex.

INTRODUCTION

Special proton beam extraction channel is used at INR linac for isotope production for the technical and medical purposes in wide energy range (100÷160 MeV) [1]. The qualitative beam behaviour control is needed to form the beam on the isotope target. The total beam line for monitoring and forming the desired beam parameters is presented in Fig.1a (linac part) and Fig.2a (isotope channel). The deflection of the proton linac beam is carried out in horizontal plane by two bending magnets BM1 and BM2 (Fig.2a) with the total bending angle 26º.

The profile measurements for linac part (Fig.1a) are made by two 2-wire scanners WS1 and WS2. In isotope channel two-coordinate multiwire profilometer MWP (Fig.2a) is used. The beam formation on the isotope target is made by all quadrupole doublets shown in Fig.1a and Fig.2a.

For simplicity the measurements and calculations will be discussed below only for the horizontal plane where the dispersion is taken place for the isotope complex beam line.

METHOD 1

This method is based on the measurements by the linac profilometers WS1 and WS2 only. Both monitors are operated simultaneously. The scanning time is ~ 3 min. For each space step multiple measurements are carried out over the beam pulse. The space step is determined by 1 Hz beam pulse repetition rate, whereas the time structure is sampled at 1 MHz frequency. Any time and space region of beam intensity distribution can be taken for further treatment [1].

For the accelerator part (Fig.1a) the method [2] was realized to determine the transverse beam phase space configuration. The current variations for doublets D15 and D16 (Fig.1a) were used. The well-known beam phase space characteristics (α, β, γ) and rms emittance ε may

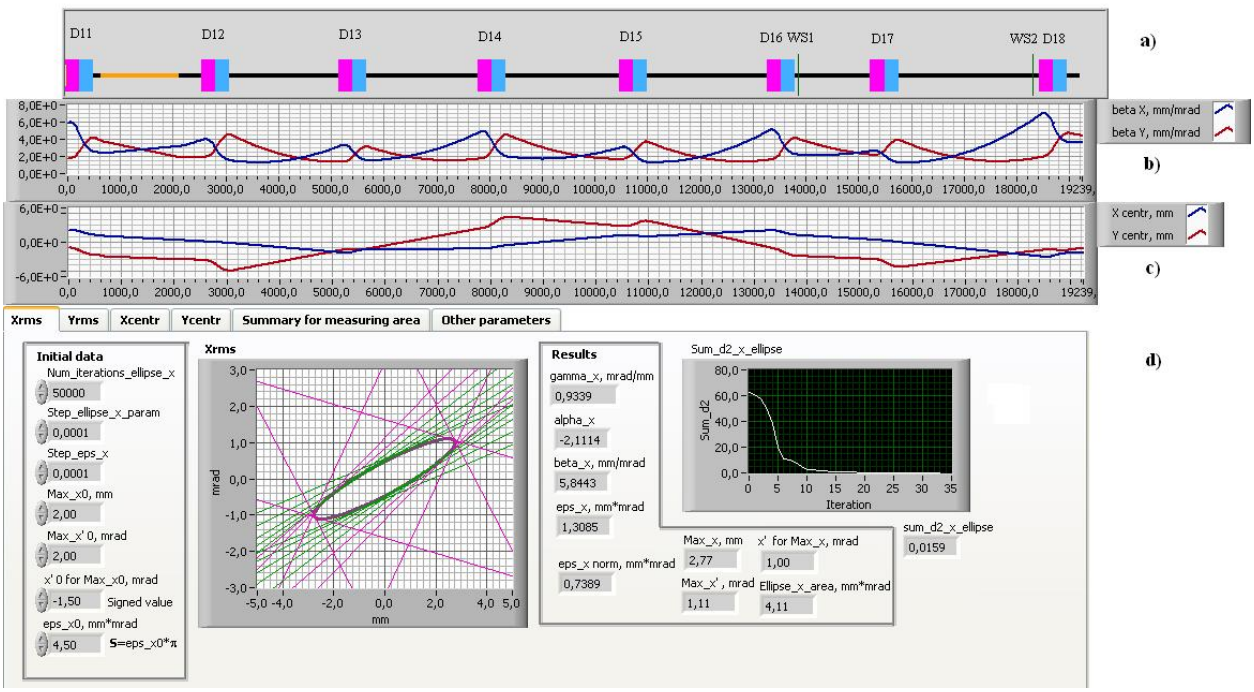

Figure 1: 160MeV beam measuring area: a) lattice: D11,…, D18 - quadrupole doublets; WS1, WS2 – 2-wire scanners; b) $\boldsymbol{\beta}$-function tracing; c) beam center tracing; d) inscribing of the beam phase ellipse and main parameters.

EXAMINATION OF CHARGED PARTICLE DYNAMICS THROUGH EMPLOYMENT OF THE FOURIER SERIES

O.E. Shishanin, Moscow State Industrial University, Moscow

Abstract

To explore a role of betatron oscillations in accelerators at the generation of synchrotron radiation it was necessary to have the continuous solutions for the Hill equation. In this case the transverse components of magnetic field were expanded in a Fourier series [1, 2]. This approach was usefully employed for the above-mentioned problem and later it has become evident that the same scheme is usable for storage rings. The procedure may even work for wigglers and undulators.

As an illustration let us consider three examples for axial betatron oscillations. The FOFDOD model can be treated as a strongfocusing system in accelerators. Here notations F and D mean focusing and defocusing magnetic fields, respectively, and symbol O is assigned to field-free section. The length L of single period successively consists of $a+l_1+a+a+l_2+a$, where a is the length of magnets, l_1 and l_2 are the extension of straight shifts. The path of orbit S is defined as

$$2\pi R + N(l_1 + l_2) = 2\pi R_0,$$

where

$$R_0 = R(1+k),\ k = (l_1+l_2)/4a,\ a = \pi R/2N,$$

N is the number of periods. Magnetic field gradient is equal to n at

$$\varphi \in (0, aT) \cup ((a+l_1)T, (2a+l_1)T),$$

where φ is the azimuth angle and $T = 2\pi/(LN)$. If

$$\varphi \in ((2a+l_1)T, (3a+l_1)T) \cup ((3a+l_1+l_2)T, 2\pi/N),$$

gradient will be $-n$. This periodic step function may be written after expansion as

$$n(\tau) = \frac{8n}{\pi}\sum_{\nu=1}^{\infty} g_\nu \cos\nu(\tau-\tau_1),$$

where $\tau = N\varphi$,

$$\tau_1 = (2a+l_1)\pi/L,\ g_\nu = \sin^2(\pi\nu a/L)\cdot\sin(\nu\tau_1)/\nu.$$

In the middle of the first magnet $\varphi = a\pi/LN$ and after summing $n(\tau) = n$. If take one-half of the second free section $\varphi = (2a+l_1+l_2/2)T$, then $n(\tau) = 0$. For the points with first-kind discontinuities the function $n(\tau)$ equals, by the Dirichlet theorem, $0, n/2, -n/2$. The field of single magnet H is given as br^{-n}, where b is the constant.

The equation of vertical oscillations in linear approximation takes the form

$$\frac{d^2z}{d\tau^2} + \frac{(1+k)^2}{N^2}n(\tau)z = 0. \qquad (1)$$

Setting $z = \exp(i\gamma_z\tau)\varphi_z(\tau)$, instead of (1) other equation for function $\varphi_z(\tau)$ may be derived as

$$\frac{d^2\varphi_z}{d\tau^2} + 2i\gamma_z\frac{d\varphi_z}{d\tau} + [\frac{(1+k)^2}{N^2}n(\tau) - \gamma_z^2]\varphi_z = 0.$$

Putting

$$\varphi_z = \varphi_0 + \sum_{i=1}^{\infty}\varphi_i/N^i,\ \gamma_z = \sum_{i=1}^{\infty}\gamma_i/N^i$$

and exclusive of secular terms one can sequentially obtain: $\varphi_0 = b,\ \varphi_1 = b_1$ (b and b_1 are the constants);

$$\gamma_1 = 0,\ \varphi_2 = bN^2S_1,\ \varphi_3 = b_1\varphi_2/b,$$

$$\gamma_2 = \pi n\sqrt{1+k}/2\sqrt{3},$$

where

$$S_1 = \frac{8n(1+k)^2}{\pi N}\sum_{\nu=1}^{\infty}\frac{g_\nu}{\nu^2}\cos\nu(\tau-\tau_1).$$

Then frequency is formed as $\nu_z = \gamma_z N$ and phase lag equals to well-known quantity

$$\mu_z = \pi^2 n\sqrt{1+k}/N^2\sqrt{3}.$$

The first terms of asymptotics can be written as follows:

$$z = B[(1+S_1)\cdot\cos\tau_z + \nu_z S_2\cdot\sin\tau_z], \qquad (2)$$

where $\tau_z = \nu_z\tau/N + \psi$,

$$S_2 = \frac{16n(1+k)^2}{\pi N^3}\sum_{\nu=1}^{\infty}\frac{g_\nu}{\nu^3}\sin\nu(\tau-\tau_1).$$

Here B and ψ have been interpreted as the amplitude of axial oscillations and the initial phase. It is significant that the solution (2) is the superposition of harmonic curves with modulated amplitudes. The small parameter is n/N^2. To ease the task of estimation of an angular velocity $\dot\varphi$, the guiding magnetic field H_0 may be averaged over the entire period and R_0 can be conceived of as a mean radius. After that it is believed that $\dot\varphi$ becomes

$$\dot\varphi = \frac{\omega_0}{1+k}[1 - \frac{\rho}{R_0} + \frac{3}{2}\frac{\rho^2}{R_0^2} +$$

SIMULATION OF CARBON ION EXTRACTION AND LOW ENERGY BEAM TRANSPORT SYSTEM FOR RFQ AT THE LINAC I-100

B.A. Frolov
State Research Centre of Russia Institute for High Energy Physics,
142281, Protvino, Moscow Region, Russia

Annotation

For the carbon ion injection into the radio frequency quadrupole, the laser ion source and the low energy beam transport (LEBT) system has to deliver 20 mA of C^{5}_{12} ion beam with 80 keV at the input of RFQ within normalized emittance of 0.39π mm·mrad. An extraction system and a low energy transport line should be optimized to reduce the beam emittance as much as possible. The results of computer simulation are presented for extraction and LEBT system: the combination of the tetrode extraction system and the electrostatic focusing lens from three electrodes with middle grid electrode negative voltage.

INTRODUCTION

In the last two decades the methods of ion radiation therapy have been investigated very dynamically. The proton and especially carbon ion beams are a superior tool in treating cancer. Proton-ion radiation therapies hospital medical centers are being actively built in Japan, Germany and Italy. In the nearest future the construction of such centers is planned in the USA, France, Austria and China. For today more than 5500 patients have already been treated with carbon-ion beam at Heavy Ion Medical Accelerator in Chiba (HIMAC), Japan. Patients' treatment was first implemented at Heidelberg Ion Beam Therapy Center (HIT), Germany 2008. The project of the proton-ion beam therapy center in SRC IHEP was developed in 1998-2000 [1]. In the course of experiments held in 2000-2001 stable acceleration of carbon ion was achieved in linac I-100 [2]. In the last few years a large volume of work has been done regarding the modernization of the linear accelerator I-100 and the circular accelerator (booster) U-1.5, the transportation channel of ion beam from I-100 in the booster was built and successfully tested. Experimental researches on acceleration and accumulation of protons and deuterium ions in the circular accelerator U-70 in 2008-2009 revealed the feasibility of using IHEP acceleration complex in medical purposes: for proton-ion radiation therapies [3].

Before 1985 the linear accelerator I-100 was used as a standard proton injector directly into the big synchrotron U-70. Currently I-100 is used as injector of light ions with the energy of 16.7 MeV/u and/or as a reserve injector of protons with the energy of 72.7 MeV/u into the synchrotron-booster U-1.5 [3]. To switch to the carbon ions acceleration mode the gas-discharge source of duaplasmatron type should be replaced with the laser ion source. It seems reasonable to keep the possibility of a fast switch from the proton or deuteron acceleration mode to the carbon ions acceleration and visa versa. The scheme of carbon ion injection into the linac I-100 with the help of radio frequency quadrupole (RFQ) accelerator which is fixed at an angle to the protons injections route was developed in IHEP. The carbon ions acceleration in I-100 happens at the second multiplicity. The switch to the second multiplicity determines the number of restriction at the ratio Z/A for the accelerated ions (where Z is ion charge, A – is its mass). The work [4] shows that the ions with the ratio Z/A=0.4-0.5 can be accelerated in I-100 because of the complex of few restrictions. The percentage of carbon with Z=6 generated by the laser ion source is small [2]. That's why the RFQ parameters calculation was done for the ions beam C^{+5}_{12} at the current of 20 mA and at the injection energy of 80 keV/u. To transport the ions from the source and to modify the beam parameters in accordance with the required at the input to the RFQ the ion-optic system (IOS) of beam matching is to be design.

OPTICAL SYSTEM SIMULATION

The matching of intensive beam of highly charged ions with the input of the linear accelerator is a complicated and not yet completely solved problem. To the large extent it is due to the strong effect of the space charge forces for the low energy region. IOS calculation is complicated by a full range of other important factors. The laser ion source is used to get the highly charged carbon ion beams. Such source was created in IHEP in 2000 [2]. The duration of multicharged ions formation is a few dozens of nanoseconds. The beam with the needed for future usage duration of a few microseconds is formed due to thermal spread of ions speed in plasma at the drift gap of L=1340 mm length from the laser focusing point till the extraction plane. The experimental investigations [2] showed that the output beam had a complicated time and charge structure. In the beam there are the ions from the first till the fifth charge inclusively. In the initial part of the current pulse (~ 5÷10 μs) mainly there are ions with the charge Z=5 and Z=4. During the pulse the profile together with the intensity of the beam with the given charge change. Also the ratio between the currents for ions with different Z changes. As a result of the given above features of the carbon ion beam generated by the

SPACE CHARGE SIMULATION USING MADX WITH ACCOUNT OF SYNCHROTRON OSCILLATIONS

V. Kapin, MEPhI, Moscow, Russia
Yu. Alexahin, Fermilab, Batavia, IL60510, USA

Abstract

Direct space charge forces can be simulated with the 6D beam dynamics code MADX using a number of 4D BEAMBEAM elements with Gaussian transverse profile for charge density. To take into account effects of synchrotron oscillations on space charge (s.c.) forces, the amplitude of BEAMBEAM elements is modulated according to the distance between a particle and the bunch center assuming Gaussian longitudinal profile. Parameters of every BEAMBEAM element (charge and sizes) are defined by local values of beta-function and dispersion, while they are updated according to the beam intensity and beam emittances at every turn. MADX script accomplishing this method has been written for the lattice of the existing Debuncher ring. The slow extraction at the 3rd order resonance with simultaneously varying the horizontal tune and the sextupole strength is considered as one of the options for Debuncher to be used in the "mu2e" project. Our MADX simulation results are compared with results obtained by V.Nagaslaev (FNAL) using the particle-in-cell ORBIT-code. The evolutions of the phase-spaces and the beam intensity within ten thousands turns have shown a good agreement between the MADX and ORBIT results.

INTDRODUCTION

Direct s.c. forces in beam dynamics codes can be represented analytically by the bunch with elliptical cross-section. This approach has been already used with several codes, e. g. FRANKENSPOT [1], MICROMAP [2] and MAD8 [3], where the beam with Gaussian distribution is usually assumed. With the MADX code [4], which is a successor of MAD8 code, the s.c. forces can be simulated using an arbitrary number of 4D BEAMBEAM elements with Gaussian transverse profile for charge density [5,6].

In Ref. [5], the MADX with 4D s.c. has been implemented for coasting beam. In Ref. [6], effects of synchrotron oscillations on s.c. forces have been simulated assuming a prescribed Gaussian modulation of the longitudinal profile for 4D-BEAMBEAM elements.

In this report, the MADX 6D-tracking is implemented and the amplitude of 4D-BEAMBEAM is a function of the distance between an arbitrary particle and the bunch center. The example MADX-script is written for the FNAL Debuncher taking into considerations turn-to-turn variations of the lattice parameters, beam intensity and emittances during a slow extraction process.

S.C. SIMULATIOS WITH MADX

A numerical realization of the s.c. calculations with MADX deals with the s.c. force created by thin elements, e.g., 4D-BEAMBEAM kicks, which are inserted around the ring according to some integration method. The method had been already implemented in other beam dynamics codes [1-3]. Our task is a step-by-step adaptation some of them to MADX, which is presently one of the most advanced code for nonlinear beam dynamics simulations without space-charge. The most of work is done using a language of MADX input scripts.

In our realization, s.c. kicks are inserted within every lattice thick element (e.g., BEND, QUADRUPOLE, DRIFT, etc.), according to the 2nd order ray tracing integrator [7]. At the beginning, the linear s.c. kicks represented with MATRIX elements are used for calculations of the beam sizes at the given transverse emittances, while an iteration procedure with TWISS command is used. Then, the nonlinear s.c. kicks represented with 4-D BEAMBEAM elements are inserted along the ring instead of s.c. MATRIX elements. The beam sizes of every BEAMBEAM are derived from calculations with MATRIX elements. The number of particles in every particular BEAMBEAM element is set up according to the formula presented in Ref. [3].

The benchmarking for the intense coasting beam in SIS-18 lattice has shown a good consistency with MICROMAP and SIMPSON codes [8]. The benchmarking with MADX assuming a prescribed Gaussian modulation of the longitudinal profile of 4D-BEAMBEAM elements is also showed good resuts [6,8].

6D-MADX tracking with 4D-BEAMBEAMs

To take into account effects of synchrotron oscillations on s.c. forces, the more realistic model is implemented in this report. 6D-MADX tracking determines the distance between an arbitrary particle and the bunch center. The amplitude of BEAMBEAM elements is modulated according to Gaussian longitudinal profile with a variance derived from the longitudinal emittance ε_{L} calculated according to a special fitting procedure [9] for the integral of distribution function $F(I)=1-\exp(-I/\varepsilon_{\mathrm{L}})$, where I is the action variable.

The beam sizes of 4-D BEAMBEAMs in bending magnets are corrected according to the relation $\sigma_{\mathrm{tot}}^2=\sigma_\beta^2+\left[D(s)\sigma_p\right]^2$, where $D(s)$ is the dispersion.

MADX-tracking in varying lattice

Normally MADX is used for multi-turn tracking in the lattice with constant parameters. The multi-turn tracking in the lattice with turn-by-turn varying parameters can be realized via multi-runs of the one-turn tracking (TURNS=1), while changing the lattice and beam

TRANSVERSE BUNCH DYNAMICS IN RECTANGULAR DIELECTRIC LOADED WAKEFIELD ACCELERATOR*

A.M. Altmark#, I.L.Sheynman, S.S. Baturin, St.Petersburg Electrotechnical University «LETI», St.Petersburg, Russia
A.D.Kanareykin, St.Petersburg Electrotechnical University «LETI», St.Petersburg, Russia, and Euclid Techlabs LLC, Solon, Ohio, USA

Abstract

Beam breakup (BBU) effects resulting from parasitic wakefields provide a potentially serious limitation to the performance of dielectric structure based accelerators. We report here on comprehensive numerical studies of transverse bunch dynamics in a rectangular dielectric loaded accelerating structure. The numerical part of this research is based on a particle-Green's function beam dynamics code (BBU-3000) that we are developing. The code allows rapid, efficient simulation of beam breakup effects in advanced linear accelerators. It is shown that the LSE modes make its main contribution to the transverse deflecting force causing beam breakup in rectangular DLA structures. Results of test simulations are presented.

INTRODUCTION

A new method of wakefield acceleration of charged particles using bunches passing through the dielectric waveguide structure, is currently the subject of intense experimental and theoretical studies [1-5].

Techniques based on the Dielectric Wakefield accelerator concept are some of the most promising to date in terms of their potential to provide high gradient accelerating structures for future generation linear colliders [2-4]. High-current electron bunches in accelerator structure generate electromagnetic fields with the amplitude of the longitudinal electric field component up to 100 MV/m at GHz frequency range [2-4] and up to ~ GV/m at THz [5], which is used to accelerate the subsequent low-current bunch. The accelerated structure is a dielectric loaded waveguide with an axial vacuum channel, Fig.1. A high charge, electron drive beam propagating through the waveguide vacuum channel generates electromagnetic Cherenkov radiation (wakefields) which is used to accelerate a less intense beam following the leading bunch at an appropriate distance.

The dynamics of the beam in structure-based wakefield accelerators leads to beam stability issues not ordinarily found in other machines [6]. In particular, the high current drive beam in an efficient wakefield accelerator loses a large fraction of its energy in the decelerator structure, resulting in physical emittance growth, increased energy spread, and the possibility of head-tail instability for an off axis beam, all of which can lead to severe reduction of beam intensity. Beam breakup effects resulting from parasitic wakefields provide a potentially serious limitation to the performance of dielectric structure based wakefield accelerators as well [6,13].

The purpose of this work is research on beam dynamic simulations in rectangular waveguide (Fig. 1), providing a number of technological and constructive advantages in comparison with a traditional for DLA cylindrical waveguide. We have implemented software for rapid, efficient simulation of beam breakup effects in this type of DLA structures [13].

WAKEFIELD IN RECTANGULAR WAVEGUIDE

Transverse deflecting force in a rectangular DLA structure is a vector sum of F_x and F_y components, which can be expressed as:

$$F_x = E_x - \beta H_y,\ F_y = E_y + \beta H_x \qquad (1)$$

Knowing longitudinal field component E_z one can find F_x and F_y using Panofsky-Wenzel theorem:

$$\int F_x dz = \frac{1}{k}\frac{\partial E_z}{\partial x},\ \int F_y dz = \frac{1}{k}\frac{\partial E_z}{\partial y} \qquad (2)$$

where k is a wave number, E_z – longitudinal component of electric field.

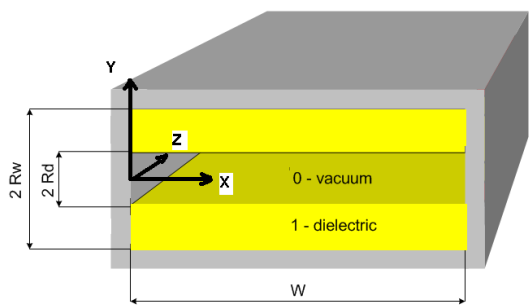

Figure 1.Rectangular Dielectric Loaded Accelerating structure with axial vacuum channel: $R_d = 0.5cm$, $R_w = 1cm$, $\varepsilon = 10$, $W = 2.3\,cm$

The complete $\vec{E}$ wakefield can be expressed in terms of *LSM* (Longitudinal Section Magnetic) and *LSE*

*Work supported by Ministry of Education and Science of the Russian Federation, the program "Scientific and scientific-pedagogical personnel of innovative Russia" and the Russian Foundation for Basic Research (09-02-00921)
#aaltmark@mail.ru

RF CAVITIES HOM LONGITUDINAL INSTABILITIES AT SR SOURCE SIBERIA-2 IN KCSR

V. Korchuganov, V. Moiseev, A. Smigacheva, A. Vernov, RRC KI, Moscow, Russia.

Abstract

The electron beam parameters stability and its lifetime depend on the resonant excitation by RF cavities HOMs. The instability rising links with the temperature change, the sequent tune of RF cavities and the synchrotron tune change. Besides that the different intensity bunch distribution along the orbit influences strongly on the instability appearance. For the instability study and their identification the spectrum analyzing is used. The results of instabilities study at SR source Siberia-2 are presented in the report.

INTRODUCTION

Electron beam instabilities at high order modes of oscillations in RF cavities can appear at any storage ring and even can be used for beam parameters manipulations. In this report, situation at Siberia-2 is described. The convenient analytic model of HOM instabilities is developed. The experience of instabilities suppression and control is derived. Siberia-2 is a storage ring dedicated for electron beam storage at injection energy level 450 MeV, acceleration up to 2.5 GeV and standing over a long period of time at high energy level to generate synchrotron radiation. The beam life time can reach at high energy level a few tens of hours. Weak beam instabilities can give here the positive effect – the bunch density decrease and as a consequence the beam life time increase. The same situation is observed sometimes at injection but more often the beam instabilities at injection lead to beam losses. Nevertheless, it is not easy to avoid the resonant conditions at injection. Wide band beam current spectrum (up to 7 GHz) consists of narrow lines spaced equidistantly by comparatively low revolution frequency 2.4 MHz. Storage ring RF system (181 MHz) is based on three RF cavities. Cavities are cooled by water in common cooling circuit without precision temperature stabilization. The fundamental modes of oscillations in cavities are tuned by feedback loops in accordance with beam loading and temperature changes. The HOM frequencies are not controlled automatically. Under these conditions, the HOM frequencies may appear near the lines of densely populated beam current spectrum.

ANALITIC DISCRIPTION OF LONGITUDINAL INSTABILITIES AT HIGH ORDER MODES OSCILLATIONS IN RF CAVITIES

To examine the longitudinal stability of rigid bunches circulating in the storage ring and interacting with one of the high modes of oscillations in RF cavities, the set of the linear equations for small phase deviations φ_m of bunches from synchronous values can be written as

$$\ddot{\varphi}_m+\Omega_0^2\varphi_m+\frac{\Omega_0^2}{V_{RF}\cos\varphi_{s0}}\cdot\mathrm{Im}\sum_{n=1}^{h}\frac{R_{shq}I_{qn}e^{iq\frac{2\pi}{h}(m-n)}}{1+i\eta_{qs}}\frac{q}{h}\times$$

$$\times\left(\varphi_m-\varphi_n+\frac{2\pi}{h\omega_s}(m-n)\left(\dot{\varphi}_m-\dot{\varphi}_n\right)+\frac{2Q_q}{\omega_q\left(1+i\eta_{qs}\right)}\dot{\varphi}_n\right)=0\,.$$

The set consists of h equations ($m=1,2,..h$) where h is the RF harmonic number, V_{RF} and Ω_0 are the RF voltage and correspondingly the synchrotron oscillations frequency in absence of high order mode excitation. For problem discussed, the dominant circumstance is that some harmonic $q\omega_s$ of beam revolution frequency ω_s is almost equal to frequency ω_q of some mode in RF cavities. For this mode, the shunt impedance R_{shq}, the quality factor Q_q and the detuning factor $\eta_{qs}=2Q_q\frac{q\omega_s-\omega_q}{\omega_q}$ are used in equations. The bunch intensities are introduced as the doubled bunch circulating currents I_{qn}, $n=1,..h$. The phase equations are worked out under the assumption that every n-th bunch excites in the cavity the field at the frequency $q\,\omega_n$ where $\omega_n=\omega_s-\frac{1}{h}\dot{\varphi}_n$ is the circulating frequency of the bunch in the ring. The complex (with respect to the bunch current) amplitude of bunch excited voltage $V_{qnn}=-\frac{R_{shq}I_{qn}}{1+i\eta_{qn}}$, where the detuning factor $\eta_{qn}=2Q_q\frac{q\omega_n-\omega_q}{\omega_q}=2Q_q\frac{q\omega_s-\frac{q}{h}\dot{\varphi}-\omega_q}{\omega_q}$. Thus the excited voltage for the bunch is fully braking if the bunch excites the cavity at its resonant frequency, $V_{qnn}=-R_{shq}I_{qn}$. The set of the phase equations presents the standard mathematical problem and can be solved by standard methods in general. At the same time, in particular cases equations allow the simple interpretations. For example, in the particular case for one bunch on the orbit (Robinson instability when $q=h$), the set of phase equations is reduced to one equation,

NONLINEAR ELECTRON BEAM DYNAMICS WITH LARGE ENERGY SPREAD IN THE MAGNETIC MIRROR

Ye. Fomin, V. Korchuganov, RRC Kurchatov Institute, Moscow, Russia

Abstract

One of the features of new injection system for Kurchatov source of synchrotron radiation is an energy doubling of electron beam in forinjector – linear accelerator. The magnetic mirror provides 180° turn of electron beam into acceleration structure of linac for twice beam energy increase [1]. This paper describes linear and nonlinear electron beam dynamics with energy 80 MeV and large energy spread in the magnetic mirror. The theoretical first order optical functions of the magnetic mirror and the results of computer simulation of electron beam trajectories taking into account large energy spread and curvature of trajectories are presented. The structure of the magnetic mirror providing the achromatic and isochronous 180° turn of electron beam with 7% energy spread is suggested. Mutual influence of "the head" and "the tail" of electron beam when colliding in a straight section spaced in between linac output and magnetic mirror on particle losses and on the longitudinal and transversal parameters are considered.

MAGNETIC MIRROR

The magnetic mirror is a main element of new upgraded forinjector (see Fig. 1). The magnetic mirror has to provide simultaneously the following: a) achromatic and isochronous bend, b) the saving spatial and angular beam size, c) the correction of beam position and angle. In addition, the design of magnetic mirror has to provide correction of electrons enters phase into linac after U-turn.

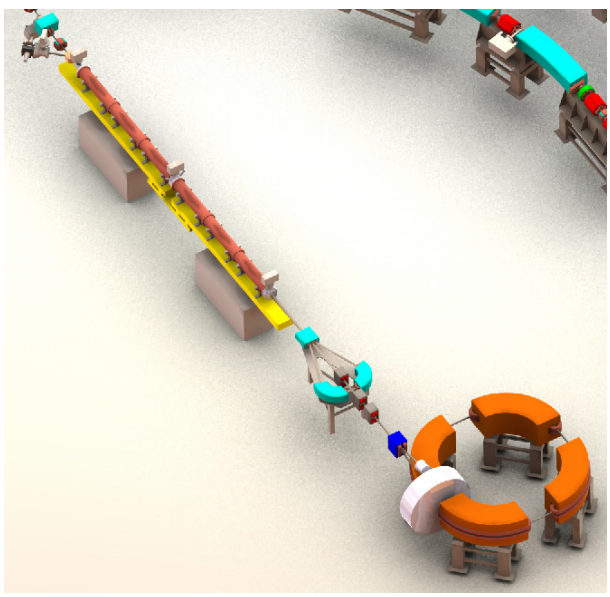

Figure 1: Upgraded forinjector.

The magnetic mirror consists from one 20° turn bending magnet and two complex mirror-symmetrical bending magnets with combined functions. This complex magnet has three components of the magnetic field (dipole, quadrupole and sextupole components) providing simultaneously 110° turn and beam focusing. Structurally the magnet consist from 3 part (see Fig. 2). The first part of magnet has all three components of magnetic fields. The central and the third parts have dipole and quadrupole components of magnetic fields. Dipole component of magnetic field in all three magnet parts is the same and quadrupole component is also the same, but has alternating values. The length of all three parts of the magnet is different.

The most important focusing property of complex bending magnet is the achievement of its length change in the sign of the dispersion function, which allowed to create on the basis of this magnet compact isochronous U-turn (see Fig. 3).

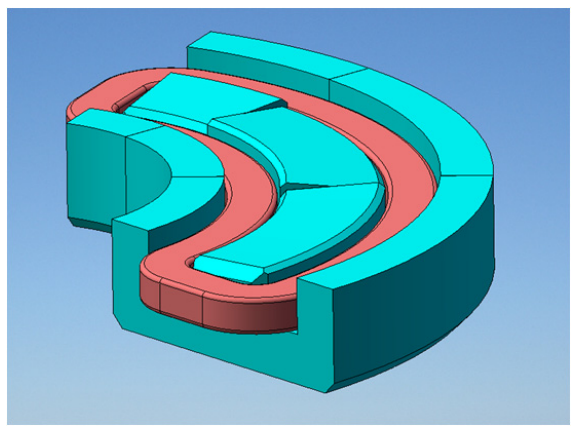

Figure 2. Bending magnet design.

The control of beam will be provided with help collimators, luminophor probes and correctors of trajectory.

LINEAR BEAM DYNAMICS

For magnetic mirror we choose mirror-symmetrical magnetic structure. This structure provides the coincidence of the initial and final values of the optical functions and their derivatives. In addition, in this structure the dispersion function and its derivative is zero and momentum compaction factor is almost zero. This provide achromatic and isochronous bend. The linear optical functions are shown in Fig. 3.

Made early calculations are not quite right for large energy spread (7%) of electrons, because they performed when electrons beam has small energy spread ($\Delta p/p \ll 1$) [1]. To improve our calculations, we take into account large energy spread into linear equations of

ELECTRON BEAM DYNAMICS WITH SPACE CHARGE IN LINEAR ACCELERATOR

Ye. Fomin, V. Korchuganov, RRC Kurchatov Institute, Moscow, Russia

Abstract

This paper describes electron beam dynamics with space charge in existing linear accelerator of Kurchatov source of synchrotron radiation. The linac structure operates with standing wave mode pulse power and without particle prebuncher. The results of comparison of electron beam parameters at the linac output with and without space charge consideration are presented. Electron beam shaping process starting from continuous beam to bunched beam on initial stage of acceleration under the action both of linac RF field and particle space charge field is considered. The main attention gives to calculate particle space charge field of the electron beam, which bring in essential contribution into beam dynamics on initial stage of shaping and accelerating electron bunches. The results of computer simulation of the electromagnetic field into linac structure taking with the help of ANSYS code are presented.

INTRODUCTION

Linac structure operates with standing wave mode pulse power. The pulsed diode gun with hot cathode is the electron beam source [1]. The main parameters of electron beam at the exit of a gun are given in Table 1.

Table 1: The main parameters of electron beam at the exit of a gun.

Parameter	Value
Beam current	4 A
Pulse duration	18 ns
Beam energy	40 keV
Microperveance	0.5 μA/V$^{3/2}$

Linac acceleration structure is made as biperiodic series of coupled cavities (DAW acceleration structure) [1]. It has 112 regular accelerating cells and 2 accelerating one half length cells. The special coaxial cavity, located in the center of linac, is the input of RF power. Along accelerating structure the aperture for the beam is small – a diameter of a diaphragm is 8.7 mm. The main parameters of linac are given in Table 2.

The electrons are accelerated due to stored energy which is reduced by ~10% after electron beam passage through acceleration structure.

The structure with washers and diaphragms has several advantages when working with stored energy:

- High shunt impedance.
- High coupling coefficient.
- High stored energy.

Table 2: The main parameters of linac.

Parameter	Value
RF frequency	2.797 GHz
Shunt impedance	95 MΩ/m
Q factor	28000
Time constant	1.8 μs
Length	6 m
Repetition rate	1 Hz

At Figure 1 we presented photo of existing linear accelerator of Kurchatov source of synchrotron radiation and at Figure 2 - photo and design of linac structure.

Figure 1: Linear accelerator.

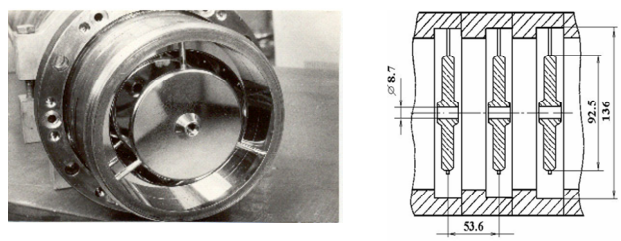

Figure 2. Linac structure.

RF FIELDS SIMULATION

For simulation rf electromagnetic field in acceleration structure we used ANSYS program code. Here we present the results of simulation.

Absolute value of electric field distribution into one cell of linac accelerating structure you can see at Figure 3. We can see that electric field has good uniformity in all volume of accelerating cell.

AN INCREASING OF ELECTRON BEAM LIFETIME AT INJECTION ENERGY IN SIBERIA-2 STORAGE RING BY REGULATING OF BETATRON COUPLING

A.Valentinov, V.Korchuganov, Yu.Krylov, Yu.Yupinov, RRC Kurchatov Institute, Moscow, Russia

Abstract

A dedicated synchrotron light source SIBERIA-2 operates at 2.5 GeV with more than 100 mA electron current. An electron beam lifetime at this energy is defined now by vacuum conditions and exceeds 15 hours for 100 mA. The lifetime at injection energy 0.45 GeV is much lower – less than half an hour for typical current value 3 – 4 mA in singlebunch mode.

An analysis of the lifetime value displayed a strong influence of Toushek effect in a presence of a horizontal aperture limitation. A dependence of the lifetime on different parameters (RF voltage, horizontal geometric and dynamic aperture, bunch current, betatron coupling value, electron energy) was analyzed.

A betatron coupling regulation was recognized the easiest way to increase lifetime value at injection energy. It was done by two families of skew-quadrupole lenses. A 30 – 40% increasing of the lifetime was observed for different values of a total current. Also a storing speed was raised because of slower decreasing of a stored current. The beam lifetime during energy ramping was also increased. It led to decreasing of current losses from 5 - 6% to 1.5 – 2% during energy rising from 0.45 GeV to 2.5 GeV.

INTRODUCTION

A dedicated synchrotron light source SIBERIA-2 [1] operates at 2.5 GeV with 100 – 150 mA electron current. An electron beam lifetime at this energy exceeds 15 hours for 100 mA that is quite enough for SR users. However the lifetime at injection energy 450 MeV is much less and not exceeds 30 minutes for typical current value 5 mA in singlebunch mode. It takes more than 30 minutes to reach 150 mA level, so current losses because of low lifetime during injection process strongly decrease injection speed. Low lifetime value is observed also at the beginning of energy ramping. It leads to additional current losses during this process. For these reasons methods of beam lifetime increasing at injection energy would be very useful. A regulation of betatron coupling is one of such methods.

BEAM LIFETIME AT 2.5 GEV

Beam lifetime $\tau(t)$ at 2.5 GeV depends on time t after energy ramping as follows:

$$\frac{1}{\tau(t)} = \frac{1}{\tau_0} + C \cdot I(t) \qquad (1)$$

where I(t) is electron current, τ_0 is lifetime for beam current close to zero and C is a constant. τ_0 is determined by vacuum level without the beam. Second term in (1) may be determined by Toushek effect or by SR stimulated gas desorbtion from vacuum chamber walls. In our case second effect is working because values of τ_0 and C depend on current integral at 2.5 GeV. This dependence continues at least to 300 A·hours.

The Toushek lifetime depends on many parameters (2):

$$\frac{1}{\tau_{Toushek}} \propto \frac{C(\zeta) \cdot I}{\gamma^3 \cdot \sigma'_x \cdot (\varepsilon_{acc})^2 \cdot V} \qquad (2)$$

where $C(\zeta)$ is a function of $\zeta = \left[\frac{\varepsilon_{acc}}{\gamma \sigma'_x}\right]^2$, I is bunch current, γ is relativistic factor, σ'_x is RMS horizontal angular spread, V is proportional to bunch volume: $V \propto \sigma_x \sigma_z \sigma_s$ ($\sigma_z \propto \sqrt{\frac{\varepsilon_z}{\varepsilon_x}} = \sqrt{k}$, $\varepsilon_{x,z}$ – horizontal and vertical emittances, $\sigma_{x,z,s}$ – RMS bunch sizes, k – betatron coupling coefficient), ε_{acc} is the smallest of the physical, dynamic and RF acceptance. Energy acceptance is determined by total RF voltage V_{RF}. If physical aperture X determines ε_{acc}, it will obey to $\varepsilon_{acc} = X/\eta_x$ (η_x – a dispersion function on aperture limitation azimuth). Because τ depends on machine functions it should be calculated as an average value around the ring.

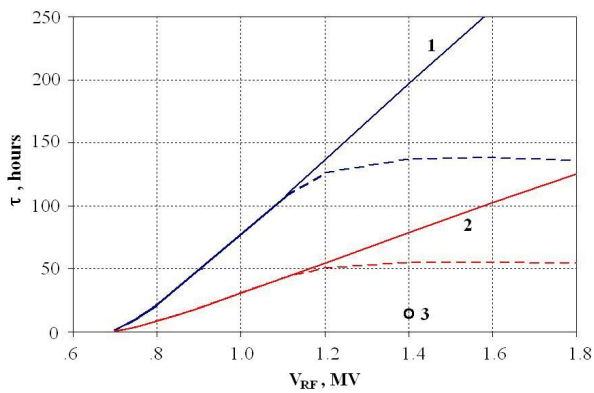

Figure 1: Calculated Toushek lifetime at 2.5 GeV as a function of the total RF voltage V_{RF}. Plots are given for two values of bunch current: **1** - 2 mA, **2** – 5 mA. An influence of horizontal aperture limitation X =20 mm is shown by dashed lines. A coupling coefficient k is equal to 0.01 (close to real value). **3** – measured lifetime value for 2 mA average bunch current and 80 A·hours total integral at 2.5 GeV.

CENTER REGION DESIGN OF THE SUPERCONDUCTING CYCLOTRON C400

Y. Jongen, M. Abs, W. Kleeven, S. Zaremba, IBA, Belgium
G. Karamysheva, O.Karamyshev, N. Morozov, E.Samsonov, JINR, Russia.

Abstract

Compact superconducting isochronous cyclotron C400 [1] has been designed at IBA (Belgium) in collaboration with the JINR (Dubna). This cyclotron will be used for radiotherapy with proton, helium or carbon ions. The ions extracted from the source and transported with the axial line are bent into the median plane of the cyclotron by a spiral inflector. The optimal design of the inflector and cyclotron center for acceleration of the ion beams in the 4th RF harmonic mode was studied. A computer model of the dee tip geometry with the inflector and inflector housing was created. The 3D magnetic field map and 3D electric field map were used for beam dynamics simulations. Comparison between field map created in electrostatic simulation and field map from RF simulation is given. Results of the beam tracking are presented.

C400 CYCLOTRON

The last years have seen increasing interest in the particle therapy based on $^{12}C^{6+}$ ions.

IBA, the world's industrial leader in equipment of the proton therapy centers, has designed a superconducting C400 cyclotron based on the design of the current Proton Therapy C235 cyclotron.

Most of the operating parameters of the C400 cyclotron are fixed: fixed energy, fixed field and fixed RF frequency (small main field and RF frequency changes are needed for switching species). It is relatively small (6.6 m in diameter) and cost effective.

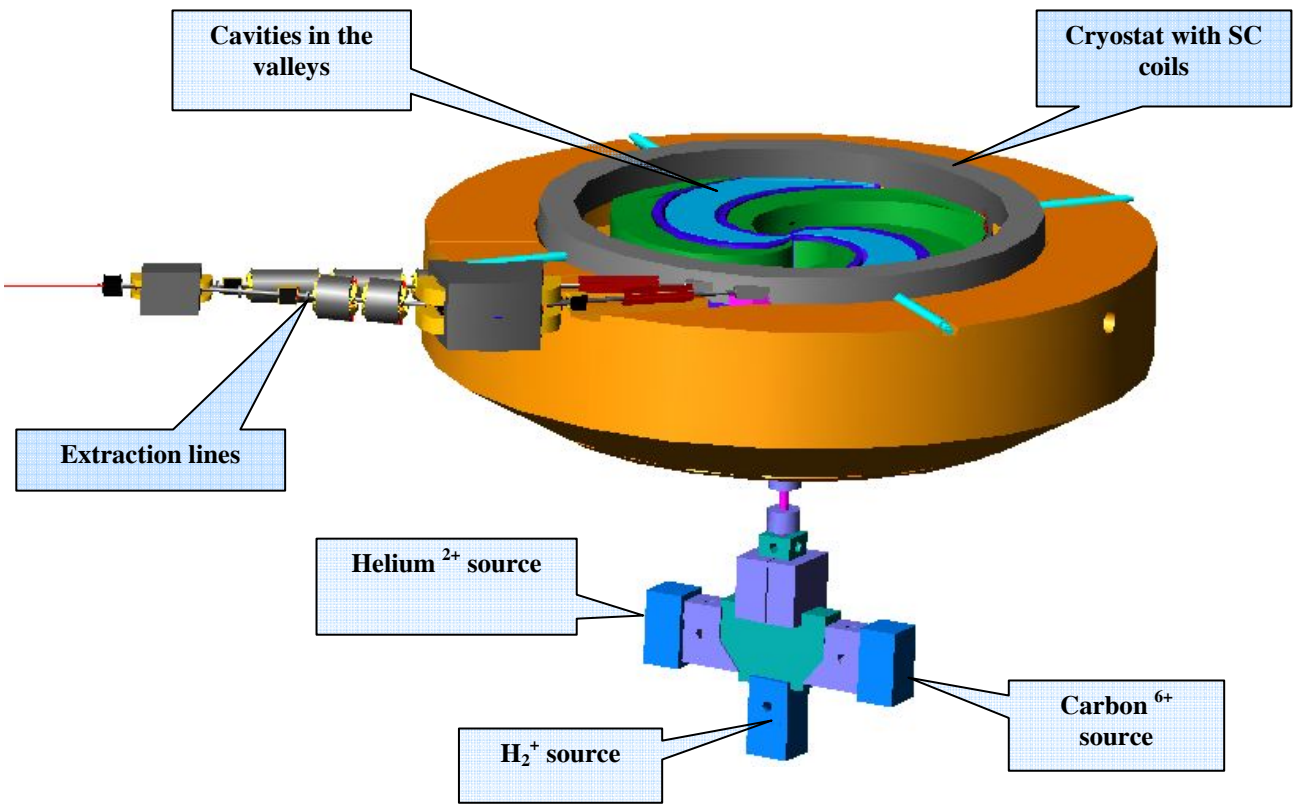

Figure 1: View of the median plane in the C400 superconducting cyclotron.

It offers very good beam intensity control for ultra-fast pencil beam scanning (PBS). But it requires an energy selection system (ESS) in order to vary the beam energy. The efficiency of the ESS for carbon is better than for

DIGITAL LONGITUDINAL FEEDBACK SYSTEMS IN SYNCHROTRONS

V. M. Zhabitsky, Joint Institute for Nuclear Research, Dubna, Russia

Abstract

The stability of a beam in synchrotrons with a digital longitudinal feedback system is treated. A longitudinal feedback system is required in synchrotrons to stabilize the high intensity beams against longitudinal instabilities and to damp the phase injection errors of a bunch. Damping rates of the digital longitudinal feedback system in dependence of its gain and delay are analysed.

INTRODUCTION

Longitudinal feedback systems are necessary in synchrotrons to reach the accuracy and stability required for reproducible beam performance [1, 2]. A digital bunch-by-bunch feedback [3] individually steers each bunch by applying electromagnetic kicks every time the bunch passes through the kicker (DK). The kick value is in proportion to the bunch deviation from the synchronus phase at the beam position monitor (BPM) location. The combiner (see Fig. 1) generates the wideband horizontal, vertical or sum signal, which is then demodulated to base-band by the detector. A stable beam rejection module removes useless

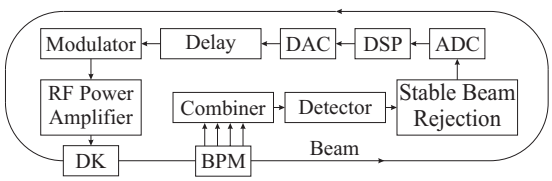

Figure 1: Block diagram of a digital feedback system

stable beam components from the signal, which is eventually digitized (ADC), processed (DSP), and re-converted (DAC) to analog by the digital processor. While in transverse feedback systems amplifier and kicker operate in base-band, longitudinal feedbacks require a modulator that translates the correction signal to the kicker operation frequency. The delay line adjusts the timing of the signal to match the bunch arrival time. Conditions for damping of the coherent synchrotron oscillations are discussed below.

BASIC NOTIONS

The RF system accelerates particles of a bunch in synchrotrons by producing a time-varying electric field in an accelerating station. The particle's energy growth per turn is given by [4, 5, 6]

$$E[n+1] - E[n] = q\widehat{V}_{\text{RF}} \sin\phi[n]\,, \qquad (1)$$

where q is the charge of the particle, $q\widehat{V}_{\text{RF}}$ is the maximal energy gain per turn and $\phi[n]$ is the phase of the RF when the particle crosses the middle of the accelerating station at the point s_{RF} of the orbit in the moment $t[n]$ at the n-th turn (the origin of time for the RF phase is taken at zero crossing of the RF voltage with positive slope; s is the coordinate along the orbit). It is also assumed in (1) that the electric field is the even function of $(s - s_{\text{RF}})$. Details of mode structure, geometry, transit time factor, etceteras are ignored in (1) by including these features in $\widehat{V}_{\text{RF}}$.

It will be assumed further that the particle with the energy $E[n] = mc^2\gamma[n]$ passes the n-th turn with the speed $c\beta[n]$ along the orbit with the circumference $C[n]$ so that the angular frequency $\omega[n]$ and the revolution period are $T[n] = 2\pi/\omega[n] = C[n]/(c\beta[n])$; here c is the speed of light, m is the particle mass, and $\gamma = 1/\sqrt{1-\beta^2}$. In accordance with these definitions the RF phase growth per turn can be written for the particle as follows:

$$\phi[n+1] - \phi[n] = \int\limits_{t[n]}^{t[n+1]} \widehat{\omega}_{\text{RF}}(t)dt = \omega_{\text{RF}}[n+1]\,T[n+1], \quad (2)$$

where $\omega_{\text{RF}}[n+1]$ is the average value of the angular RF frequency $\widehat{\omega}_{\text{RF}}$ during the turn $T[n+1] \equiv t[n+1] - t[n]$.

The phase $\phi[n]$ can be kept unchanged (modulo 2π) at the value ϕ_{s} when the particle returns to the same accelerating section after one revolution period. The phase ϕ_{s} is also called the synchronous phase. In what follows, the subscript "s" is used for synchronous quantities. The synchronous phase growth per turn in accordance with (2) is

$$\phi_{\text{s}}[n+1] - \phi_{\text{s}}[n] = \omega_{\text{RF}}[n+1]\,T_{\text{s}}[n+1] = 2\pi h_{\text{RF}}\,, \quad (3)$$

where $h_{\text{RF}} = (\omega_{\text{RF}}/\omega_{\text{s}})$ is the RF harmonic number. Let $\rho_{\text{s}}B_{\text{s}}$ be the momentum rigidity of the synchronous particle moving along the orbit with the circumference $2\pi R_{\text{s}}$. Then the synchronous particle's energy growth pur turn is

$$E_{\text{s}}[n+1] - E_{\text{s}}[n] = qV_{\text{RF}} \sin\phi_{\text{s}}[n] = q\,2\pi R_{\text{s}}\rho_{\text{s}}\dot{B}_{\text{s}}\,. \quad (4)$$

Eq. (3) and Eq. (4) are the system of difference equations for definition of $\phi_{\text{s}}[n]$ and $E_{\text{s}}[n]$. Let us assume that these solutions have been found. Therefore the motion of an arbitrary particle relative to a hypothetical synchronous particle can be examined.

Acceleration in presence of perturbations

Let $\delta E[n]$ and $\delta\phi[n]$ be small deviations of energy and phase of the particle from corresponding synchronous values at the n-th turn:

$$\delta E[n] \equiv E[n] - E_{\text{s}}[n], \qquad \delta\phi[n] \equiv \phi[n] - \phi_{\text{s}}[n]\,.$$

Let ΔV_{RF}, $\Delta\omega_{\text{RF}}$ and ΔB_{s} be small deviations of the accelerating voltage, the angular RF frequency and the magnetic

MULTP-M CODE UPGRADE

N.P. Sobenin, V.I. Kaminskii, S.V. Kutsaev, R.O. Bolgov, I.V. Isaev, M.A.Gusarova, M.V. Lalayan,
NRNU-MEPhI, Moscow, Russia
L.V. Kravchuk, INR, Moscow, Russia

Abstract

It is obvious that for all new RF devices all issues potentially influencing on their performance and operation must be considered at design stage. Multipacting discharge is known to be one of such phenomena. This discharge occurs in vacuum areas of RF devices in case resonant conditions for electrons are met and the secondary electron emission is strong enough. The problem of effective design of multipactor-free RF devices can be solved using powerful 3D numeric simulation tool Multp-M developed at MEPhI and INR. [1].

In this paper new features of this code are presented and illustrated by several common tasks solved. Multp-M code was upgraded so it is able to simulate the external magnetic and electric fields influence on discharge behavior and transient mode simulation. Code became more user-friendly thanks to new 3D interface.

INFLUENCE OF THE EXTERNAL FIELDS

There are a lot of ways for multipactor suppression known and used in microwave techniques. Use of external magnetic or electric field is one of the most widely implemented. Besides that a lot of RF devices like electron guns and injectors operate with magnetic field applied for beam focusing. This leads to sufficient change in multipactor properties. In order to simulate these conditions at early design stage Multp-M was expanded with new modules introducing static fields in model.

Algorithms added were tested and proved to yield correct results. As the initial test single electron dynamics was simulated in simple electric and magnetic fields pattern. More comprehensive research were done and their results compared to known data.

New features were used to evaluate external focusing magnetic field in PITZ photoinjector cavity and electric bias applied in “warm” coaxial line area commonly used in high power input couplers [2]. For instance latter having inner conductor radius equals to 14.4 mm and outer of 31 mm is used in Energy Recovery Linac.

Sample results obtained for PITZ photoinjector cavity illustrating Multp-M code simulation and visualization capabilities are presented on Fig.1. For research details refer to [3]. Multipactor trajectories in cell to circular waveguide transition area were found at 27.25 MV/m on-axis field strength.

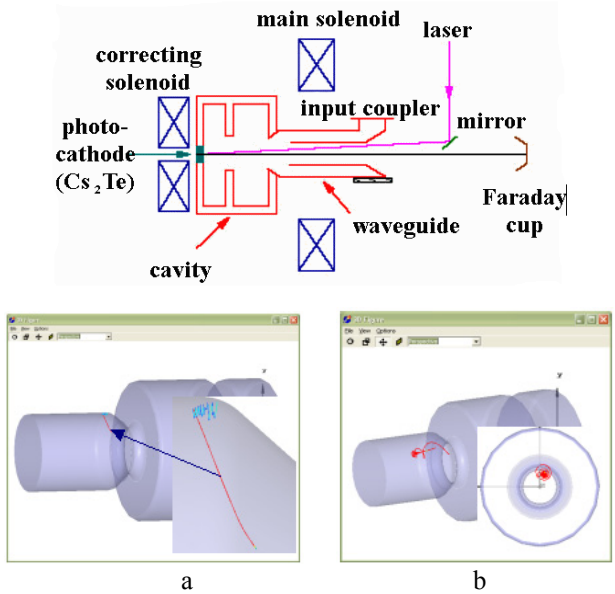

Figure 1: Sample multipactor electron trajectories a – without external field, b – with focussing magnetic field.

Multipactor could be a severe problem for coaxial lines operation. Its suppression could be done by applying DC high voltage bias between conductors. As an example the simulated multipactor in coaxial line used in ERL high power input coupler warm part [2] is shown on Fig. 2. Coaxial line model used for simulation has inner conductor radius equal to 14.4 vv and outer one 31 mm. Fig.2 illustrates raise of electrons number vs. transmitted power for different bias applied. RF power on charts is normalized: 1 unit equals to 33 MW.

One could see that applying 3...4 KV DC lead to multipactor suppression for transmitted power up to 250 KW CW. It covers full operating range for this coupler.

Thus new computation module implemented in Multp-M code allows to make correct simulation for devices with static magnetic or electric fields and to choose of bias parameters.

BOOSTER ELCTRON COOLING SYSTEM OF NICA PROJECT

E. Ahmanova, I. Meshkov, R. Pivin, A. Rudakov, A. Shabunov, V. Shokin,
A. Smirnov, A.Sidorin, N. Topilin, Yu. Tumanova, S. Yakovenko, JINR, Dubna, Russia

Abstract

Nuclotron-based Ion Collider fAcility (NICA) [1] is the new accelerator complex being constructed on the JINR site. A few cooling systems are considered for the NICA project – electron one for the Booster-synchrotron and for Collider rings – both electron and stochastic ones. The main goal of the Booster electron cooler is a decrease of the longitudinal emittance from the injection value to the necessary value for acceleration to Nuclotron. The designed electron cooling system for Collider rings have to prevent the emittance growth due to the intrabeam scattering and to keep the average luminosity on the constant value. The peculiarity of electron cooling systems is the using of superconducting solenoids to provide the beam transportation in cooling sections.

INTRODUCTION

The main goal of the Booster electron cooler is the decreasing of the longitudinal emittance from the injection value of about 7.5 eV·s to the necessary value of 2.5 eV·s. Cooling time is limited by the operation cycle of the Booster and can not exceed the value of 1 sec. For the transverse plane the cooling system has to keep the value of the normalized transverse emittances at the level of 1 π·mm·mrad (rms). For the stabilization of the transverse emittance the misalignment of electron and ion beam axes is proposed on the level of about 1 mrad in both transverse planes [2].

Ion energy in the Booster ranges from 6 MeV/u to 600 MeV/u that corresponds to the electron energy range 3.27 ÷ 330 keV. Choosing an optimal energy value for electron cooling one has to account the following effects:

1) beam lifetime limitation due to interaction with the rest gas ;
2) beam lifetime limitation due to recombination on the cooling electrons;
3) space charge effects appearing due to ion beam shrinking at cooling;
4) sufficiently short cooling time (≤1 sec);
5) space charge effect of electron beam on ion cooling;
6) an optimal use of the RF station;
7) cost of the electron cooler.

ELECTRON COOLER OPERATION

The maximum design ion energy of 4.5 GeV/u can be achieved in the Nuclotron with fully stripped ions only. To provide high efficiency of the ion stripping one has to accelerate them up to the energy of a few hundreds of MeV/u. For this purpose a new synchrotron ring – the Booster is planned to be used. Heavy ion injector-linac is designed for acceleration of Au^{32+} ions. The Booster has maximum magnetic rigidity of 25 T·m that corresponds to about 600 MeV/u of the ion energy, and the stripping efficiency is no less than 80%.

The Booster is equipped with an electron cooling system that allows providing an efficient cooling of the ions in the energy range from the injection energy up to 100 MeV/u.

The magnetic system of the Booster is superconducting. Its design is based on the experience of construction of the Nuclotron SC magnetic system [3] and SC magnetic system of SIS-100 developed later at FAIR project. Therefore to avoid connections between "warm" and "cold" sections in the ring the solenoids of the cooler located along the Booster circumference are designed in the SC version (Fig. 1). This is main difference of the Booster cooler from a conventional electron cooling systems.

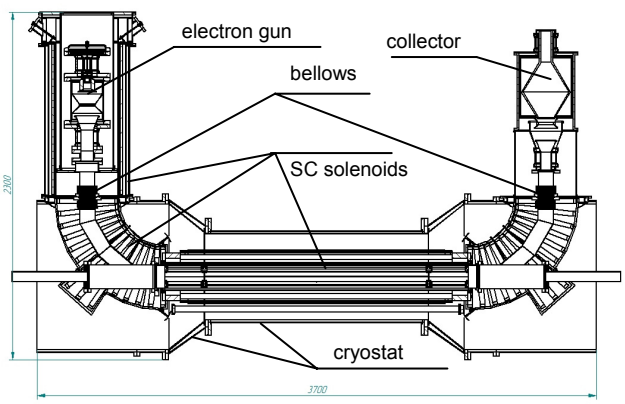

Figure 1: Booster electron cooler.

To cover total range of the ion energy in the Booster (600 MeV/u) the electron beam maximum energy has to be about 330 keV. However the cooling system at such energy is rather expensive, therefore the maximum electron energy (60 keV) is chosen as a compromise between the system price and its capability to fulfill the main project task – the ion colliding beams. A possibility to decrease the ion beam phase volume at injection energy is restricted by space charge limitations.

Another criterion for the electron energy choice is related to the frequency variation range of the Booster RF system. The ion acceleration in the Booster is proposed to be performed in two steps: on the 4^{th} harmonics of the revolution frequency up to the cooler energy and on the 1^{st} one after the cooling. If the cooling is performed at the ion kinetic energy ≥ 100 MeV/u, one can use the same RF system on both steps of the acceleration.

All other parameters of the Booster cooler (Table 1) are typical for conventional electron cooling systems. Design

ELECTRON GUN AND COLLECTOR FOR 2 MEV ELECTRON COOLER FOR COSY*

A.V. Ivanov#, M.I. Bryzgunov, A.V. Bubley, V.M. Panasyuk, V. V. Parkhomchuk, V.B. Reva
The Budker Institute of Nuclear Physics, Novosibirsk, Russia.

Abstract

COSY storage ring is planed to be upgraded in 2011 by installation of a new electron cooler [1]. Electron cooling will reduce energy spread of protons and so improve the precision of internal target experiments. Some of the most important parts of this new electron cooler are the electron gun and the collector, and they must satisfy several rigid requirements. Electron gun must provide high perveance electron beam with low transversal temperature and variable beam profile. The gun control electrode assembled of four separate sections will provide measurements of beam envelope along the transport section of the cooler. Displacement of corresponding part of the beam may be observed if alternating voltage is applied to each section. Collector should have high perveance, low secondary emission coefficient, and small dimensions. Wien filter is supposed to be installed before the collector to satisfy these requirements. In this case we can use high perveance small-scale collector with axially-symmetric magnetic field; secondary electrons will be absorbed in Wien filter. An additional vacuum pumping must be provided in the collector design.

ELECTRON GUN

The electron gun for COSY cooler is very similar to the guns for other BINP coolers, installed on CSR and LEIR rings [2]. This gun provides high-perveance electron beam with low transversal temperature. The gun design is shown in Fig. 1. The convex cathode 1 immersed into longitudinal magnetic field is used. To form the electron beam together with anode 4 control electrode 3 is used. This electrode is placed near the cathode edge and influences the emission from this area. By applying different potential on this electrode the beam with radial current density distribution from parabolic to hollow can be obtained.

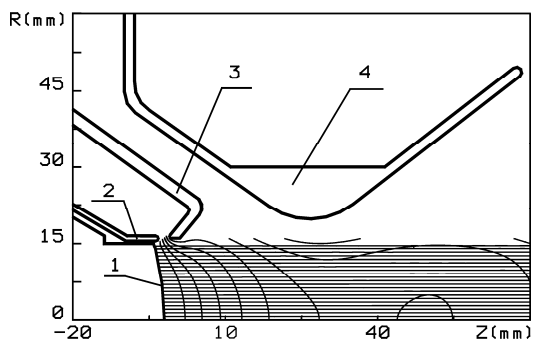

Figure 1: Electron gun for COSY cooler.

*Work supported by state contract P1198
#A.V.Ivanov@inp.nsk.su

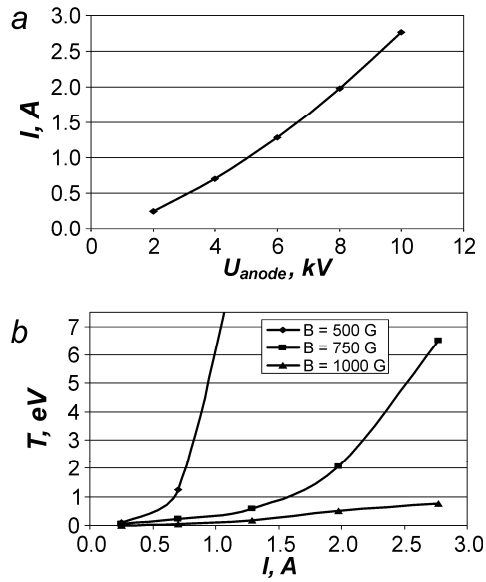

Figure 2: Current (a) and transversal temperature (b) of homogeneous electron beam.

To provide high efficiency of electron cooling at high energies one need to increase beam current density. The calculations of the homogeneous beam current as a function of anode potential (Fig. 2a) were made with UltraSAM code [3]. With the current increase the transversal temperature grows also (Fig. 2b). These calculations show that value of magnetic field should be at least 600 Gs to provide acceptable (< 2 eV) temperature of 1 A uniform beam.

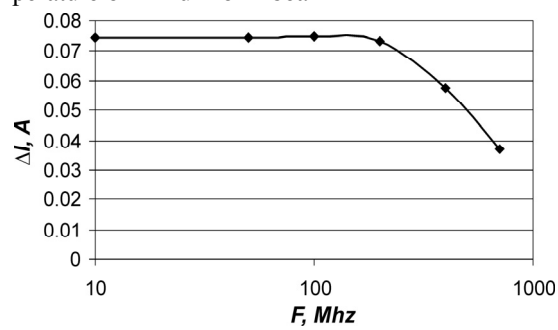

Figure 3: Electron beam current modulation at oscillation of the control electrode potential (ΔU= 50 V, U=600 V).

For beam diagnostic purposes the suggestion was made to reject axial symmetry and to divide control electrode into 4 segments. By applying small potential variation on one of these segments not only position of beam center but also beam sizes can be measured. Beam current modulation decreases at high frequencies of potential oscillation, thereby to realize this technique the cutoff

TRANSVERSE BUNCH-BY-BUNCH DIGITAL FEEDBACK FOR THE VEPP-4M COLLIDER

V.P. Cherepanov, V. V. Oreshonok , V.V. Smaluk, D.P. Sukhanov,
Budker Institute of Nuclear Physics, Novosibirsk, Russia

Abstract

The coupled-bunch instability is the base reason of the operating current limitation at the VEPP-4M electron-positron collider. For suppression any excited transverse mode of oscillation of the accumulated beam, the transverse bunch-by-bunch digital feedback has been installed. The paper reports on the current design and status of the feedback system. The available diagnostic tools and latest operational results and beam measurements is given.

INTRODUCTION

The single-bunch beam current in the electron–positron collider VEPP-4M at the injection energy of 1.8 GeV is limited by the instability of vertical betatron oscillations caused by the transverse mode coupling or fast head-tail. At the present time, use of the consistent bunch-by-bunch scheme for the transverse feedback systems is a conventional method for suppression of any excited transverse mode of beam oscillation [1, 2].

The digital feedback system to suppress the vertical betatron oscillation of each bunch independently has been developed for VEPP-4M.

Table 1: The general parameters of the VEPP-4M collider and feedback system

Parameter	Value
Revolution frequency, f_0	818.936 kHz
RF frequency, f_{RF}	181 MHz
RF harmonic, q	222
Injection energy, E	1.8 GeV
Experiment energy, E_b	5.2 GeV
Betatron tunes, n_x/n_y	8.56/7.58
Design bunch current, I_b	40 mA
Number of bunches	$2e^-$ x $2e^+$
Number of strip-line BPMs used	1
Number of kickers	4
Feedback system bandwidth	20 MHz
Power per kicker, P_k	400 W

Figure 1 shows the block-diagram of feedback system. The system configuration and specifications are mainly determined by necessity to suppress the TMC instability in the 2×2-bunch VEPP-4M operation mode. The beam position signals from strip-line BPM are prepared by the input front-end electronics, come to the signal processing board and are then digitized by the ADC. The kick signals formed by the digital board are converted by the DAC and, after amplification by the power amplifiers, come to the kickers.

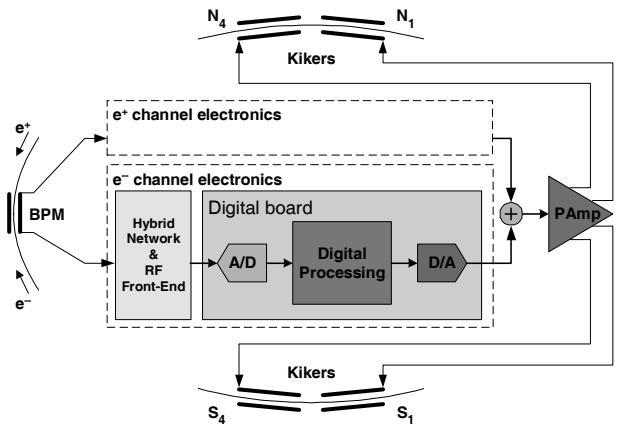

Figure 1: Block diagram of the Transverse Bunch-by-bunch Feedback system.

A more detailed description of the front-end electronics and of the power output devices is given in [3, 4]. Basic features of the presented system are the different digital part and use of the only BPM.

DIGITAL SIGNAL PROCESSING

Additional requirements for flexibility and availability of diagnostic tools have led to the development of the new digital board. The main feature of this device is use of an FPGA for the signal processing and controls (see Figure 2). The availability of several independent pipeline operations allows as to use the bunch-by-bunch feedback option and to organize different processing arrangements. This makes possible to fulfill completely the feedback system requirements and to use various diagnostic tools: detection of beam position and other possible variations of the beam parameters in real-time, betatron oscillations spectral analysis, etc. In addition, the device was developed for use in multi-bunch operation mode to satisfy the higher technical requirements in the future.

General Layout

The signal digitizing circuit includes two 12 bit pipeline ADC ADS5527, which are used to measure vertical position and intensity of the beam. Two Altera Cyclone III receive the beam position data from ADC, make DC rejection and necessary phase shift using the digital FIR filter. The correction kick data produced by the FPGA

TRANSVERSE FEEDBACKS IN THE U70 PROTON SYNCHROTRON OF IHEP

O. Lebedev, S. Ivanov, N. Ignashin, and S. Sytov
Institute for High Energy Physics (IHEP), Protvino, Moscow Region, 142281, Russia

Abstract

To handle the adverse effect of transverse injection errors and resistive-wall instability in the U70, two frequency-band-separated feedback circuits are routinely employed. The first one is a narrow-band (around base-band DC) local end-to-end-analog circuit terminated by an electrostatic kicker. The second is a wide-band band-pass circuit with a variable (–10% ca) digital delay line and low-level DSP units and an electro-magnetic kicker. Both the circuits were subjected to a deep renovation during the recent 5 years, which provided a better control over transverse motion of the beam. The paper reports on technical solutions implemented, problem-oriented R&D studies, and beam observations.

INTRODUCTORY FORMULAE

In the U70, like in most of proton synchrotrons worldwide, coherent transverse beam motion, if any, is quieted by means of a relatively slow multi-turn deflecting coercion on beam. In this context [1], one can apply to a wave-to-wave cross-talk approach that involves propagating waves $\propto \exp(ik\Theta - i\omega t)$ of deflecting Lorentz force field strength (whose wave amplitude is $S_k(\omega)$) and electric dipole moment of the beam ($D_k(\omega)$). Here, k is an integer wave number, $\Theta \propto \omega_0 t$ is azimuth along the ring, ω_0 is angular rotation frequency of on-momentum particle, t is time.

Electro-dynamical properties of beam environment, either passive or active (e. g., of beam feedback circuits), are commonly described in terms of a transverse coupling impedance $Z_k(\omega)$, in Ohm/m, that is tacitly defined via

$$S_k(\omega) = i\beta\omega_0 Z_k(\omega) D_k(\omega)/L \qquad (1)$$

where L is orbit length, β is reduced velocity. This Eq. implies reflection symmetry $Z_{-k}(-\omega) = Z_k(\omega)^*$. Given *passive* components of the vacuum chamber (resistive wall, deflecting HOMs, etc.), $\omega \cdot \mathrm{Re} Z_k(\omega) \geq 0$.

Adopt, for definiteness, the upper betatron side-band convention with series $\omega \cong (k + Q)\omega_0$ where Q is betatron tune (about 9.8–9.9 in the U70). In this case, a coherent mode observable at a frequency line that probes $\mathrm{Re} Z_k(\omega) < 0$ turns unstable.

Hence, design goal for a perfect damping beam feedback is to impose *active* coupling counter-impedance with

$$Z_k^{(\mathrm{FB})}(\omega) = A_k^2 + i0 \qquad \text{at} \qquad \omega = (k+Q)\omega_0 . \qquad (2)$$

Because of a comb nature of beam transfer function one must tailor out the appropriate function $Z_k^{(\mathrm{FB})}(\omega)$ only in a close vicinity of the frequency line (lines) $\omega = (k + Q)\omega_0$ of interest, rather than globally over the entire ω-domain, which simplifies the task from the technical viewpoint.

Let a (short) pickup electrode PU be mounted at azimuth Θ_{PU} and a (short) transverse kicker K be at Θ_{K}, their separation azimuthally being $\Delta\Theta_{\mathrm{K-PU}} = \Theta_{\mathrm{K}} - \Theta_{\mathrm{PU}}$. Following Eq. 1, one can put down

$$Z_k^{(\mathrm{FB})}(\omega) = -iG(\omega)\exp\left(i\omega\tau - ik\Delta\Theta_{\mathrm{K-PU}}\right). \qquad (3)$$

$\underline{G}(\omega)$ is in-out transfer function of electronics in the open feedback loop, reduced to units of Ohm/m,

$$G(\omega) = \frac{pc}{eJ_0}\left(\frac{\Delta y'_{\mathrm{K}}}{\Delta y_{\mathrm{PU}}}\right) = \frac{(El)_{\mathrm{K}}}{\beta(J_0\Delta y)_{\mathrm{PU}}} = \frac{c(Bl)_{\mathrm{K}}}{(J_0\Delta y)_{\mathrm{PU}}} . \qquad (4)$$

Here, y is transverse coordinate (vertical, horizontal), J_0 is average beam current, p is momentum, c is velocity of light, e is elementary charge, $(El)_{\mathrm{K}}$ and $(Bl)_{\mathrm{K}}$ are field strength integrals of electrostatic and magnetic kickers, optionally. Phase-frequency characteristic of $G(\omega)$ is assumed to have a vanishing slope averaged over the bandwidth. Time delay inherent in $G(\omega)$ (electronics + pure delay lines) is incorporated in the overall delay τ in Eq. 3.

NARROW-BAND FEEDBACK

It is a local system whose pickup, electrostatic kicker and signal-processing (analog) equipment are all housed in the same straight section SS#2 of the U70 lattice [2]. The system imposes a damping upon the dedicated spatial harmonic $-k_1 = [Q] + 1 = 10$ of beam perturbation where $[Q]$ is the integer part of Q. This harmonic is notable for the strongest destabilization by the resistive-wall wake.

The feedback signal-processing algorithm relies on tune Q being just below an integer value and reads

$$G(\omega) = -2\left(\frac{A}{1 - i\,\omega/\Delta\omega}\right)^2 \mathrm{HPF}(\omega) . \qquad (5)$$

Given (i) cut-off frequency (at –3 dB) of integrator circuit $\Delta\omega$ equal to $|k_1 + Q|\omega_0$, (ii) vanishing delay time $\tau = 0$, and (iii) negligible spatial separation $\Delta\Theta_{\mathrm{K-PU}} = 0$, Eq. 3 readily turns into a sought-for damping impedance of Eq. 2 at the frequency line $(k_1 + Q)\omega_0$ in question.

Last factor in Eq. 5 denotes a high-pass filter with a roll-off frequency $<< \Delta\omega$ that rejects a DC closed-orbit offset signal seen by the PU. Its higher-frequency translates at $\pm\omega_0$, $\pm 2\omega_0$, etc are safely smeared out by a cascade of two integrators in Eq. 5. The same mechanism suppresses residual self-excitation of the next neighbouring to k_1 base-band harmonic $k = -9$ that is inherently stable under the resistive-wall wake, with feedback off.

The system is in a routine service since 2007. Additional damping factor imposed is about 100 w. r. t. a natural decay time of harmonic k_1 due to de-coherence. Details of technical implementation are reported in [2].

USER INTERFACE IN THE DIAGNOSTIC SYSTEM OF THE EXTRACTED BEAMS OF THE U-70 ACCELERATOR

N. Ivanova, V.Kovaltsov, A.Koshelev, A.Lukyantsev
V.Milyutkin, Ju.Smirnov, A.Sotnikov, IHEP Protvino, Russia

Abstract

User interface in the diagnostic system of extracted beams is described. It was developed under Linux operating system on the personal computers used as workstations.

The considered program tools provide:

- the representation on operator consoles (workstations) information about beam profiles, intensity, displacement, root-mean-square error etc. in different forms;
- the dynamic adjustment of the diagnostic system;
- web presentation of the current information about the extracted beams;
- data transfer to physical setups;
- special beam characteristics calculation by the profilometer individual units data (for research purposes);
- data archiving and web facilities for data viewing.

INTRODUCTION

The diagnostic system for the beams extracted of U-70 accelerator is intended for beam profiles, intensity and position measurement. It is a three-level hardware-software complex [1]. The structure of the lower and middle levels is described in detail in [2]. The software for the middle and upper levels was developed by EPICS toolkit [2].

This report considers software for the upper level and its important part – the user interface. The users of the diagnostic system are the beam and the accelerator specialists, experimental physicists, hardware designers and operational staff. The user interface developed in the diagnostic system provides the interaction with the system in various forms. Functionality and convenience were the main aspects of the interface design.

UPPER LEVEL OF THE DIAGNOSTIC SYSTEM

The workstations and the server are the upper level computers. The workstations take the beam data from the middle level, which is composed of so called IOCs (Input Output Controller in EPICS terms). Each IOC is connected to the lower level of the system where the data is registered. The scheme of the upper level is shown in Figure 1. The computers are linked via Ethernet by TCP/IP protocol.

One IOC is usually used for a single beam channel. From experience, it is best when single workstation corresponds to one IOC. The workstation accepts the data from this IOC and it is responsible for initial loading and parameters adjustment of this IOC.

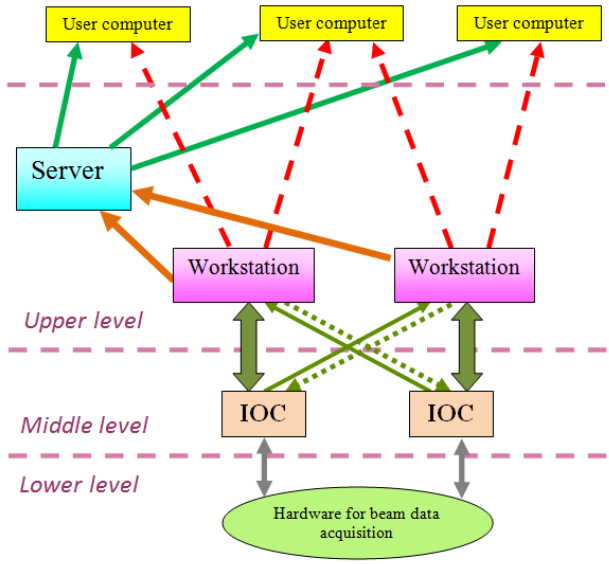

Figure 1: Upper level computers and their links. The dashed lines mean the restricted access.

However, the EPICS tools allow to monitor (and tune with small restrictions) any IOC from any workstation. For the system's reliability, we have supplied some redundancy measures. When one workstation is down another workstation is able to replace it. For this purpose the software for one workstation and "its" IOC is duplicated at another workstation and is in a non-active state. But this software can be activated if necessary and the workstation will work with two IOCs.

The current data from all workstations are transferred to the server which provides the access to information through a web-site. In addition to on-line data server keeps the information about the previous runs.

All computers of the upper level are running under Linux operating system. But user computers may be equipped with another operating system, for example, MS Windows. All one needs is a browser and an access to Internet.

SOFTWARE FOR USER INTERFACE

The upper level software includes the programs which directly realize the user interface, EPICS components needed for diagnostic system work, utilities, etc.

The main parts of the user interface software are shown in Fig. 2. The most important task of interface is to present beam data for on-line control. The appropriate software was developed by EPICS tools. It is shown by red color. This software is located on the workstation. The other part of the interface consists of utilities which are on

WIDEBAND BPM ELECTRONICS FOR THE VEPP-4M COLLIDER

E.A. Bekhtenev, G.V. Karpov, Budker Institute of Nuclear Physics, Novosibirsk, Russia

Abstract

New beam position monitor (BPM) FPGA-based electronics has been developed and tested at the VEPP-4M electron-positron collider. The VEPP-4M operates with two electron and two positron bunches. Compared to the old BPM electronics the new one can measure the position of each of four bunches with any BPM of storage ring including the BPMs near interaction point. Wide bandwidth of electronics (200 MHz) allows the separate measurements of electron and positron bunches with time interval between bunches up to 20 ns. BPM system works at two modes: slow closed orbit measurements and turn-by-turn measurements. We present details of system design and operation.

INTRODUCTION

The VEPP-4M is the modernized VEPP-4 collider, which had been commissioned for the first time in 1977 [1]. Conditions of high energy physics (HEP) experiments require continuous orbit measurements of electron and positron bunches. The present VEPP-4M Beam Position Monitor (BPM) system developed 25 years ago [2] can make orbit measurements only if one type of particles is circulating at storage ring: electrons or positrons. It is not capable to measure beam orbit during HEP experiments where both types of particles are at storage ring. The second disadvantage of the old BPM system is absence of turn-by-turn capability by each BPM. To satisfy modern requirements an internal R&D program has been started at BINP to develop new BPM electronics for VEPP-4M. Some of storage ring parameters are given in Table 1.

Table 1: Some parameters of the VEPP-4M collider

Beam energy	1-6 GeV
Revolution frequency F_0	0.819 MHz
RF frequency	181.8 MHz
Beam current	1-30 mA
Total number of electron and positron bunches	4
Total number of BPMs in storage ring	54
Minimal time interval between electron and positron BPM signals	20 ns

Precision requirements to BPM system are not so severe: relative accuracy of slow measurements has to be of order 50-100 microns, resolution of turn-by-turn measurements has to be of 20-50 microns.

The VEPP-4M collider operates with two electron and two positron bunches. Difference in arrival time of the electron and positron bunches is minimal for BPMs located close to places of meeting of bunches. For example for the BPMs NEP0 and SEP0 located close to interaction point (at opposite sides of interaction point) arrival time of the electron and positron bunches differs in ~22 ns. For NEP0 the first bunch arrived is positron bunch for SEP0 – electron bunch.

New electronics design utilizes signal peak sampling with high bandwidth digitizer as it was done for CESR [3]. At the end of 2009 new BPM electronics had been developed. In January 2010 two complete sets of BPM electronics had been fabricated and installed at VEPP-4M BPMs NEP0 and SEP0.

BPM ELECTRONICS DESIGN

Functional diagram of the new BPM electronics is presented in Fig.1.

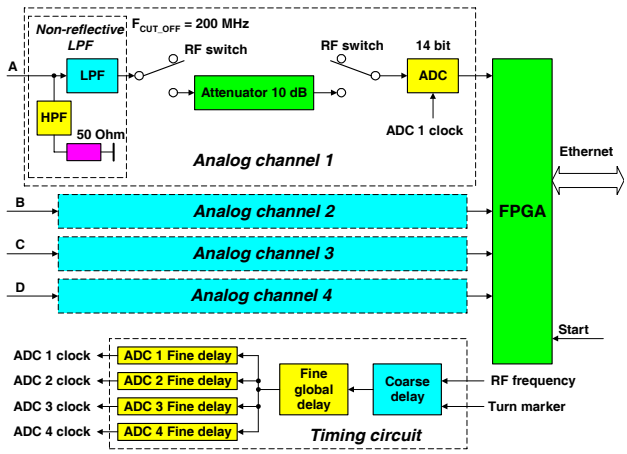

Fig.1. Functional diagram of new BPM electronics.

The electronics consists of four identical analog channels, FPGA, Timing circuit and Ethernet interface. All electronics occupies 1U 19" chassis.

In order to achieve separate measurements of electron and positron bunches the bandwidth of analog front-end electronics is chosen of 200 MHz. The bandwidth is defined by non-reflective Low Pass Filter (LPF) with cut-off frequency of 200 MHz. Pickup signal of electron bunch at the LPF output is shown in Fig2.

Amplitude of reflected from LPF signal is less than 1% of coming signal. "Tail" of the first bunch signal on the peak of second bunch signal is less than 0.5%. However such "tail" value can cause position measurement error of the second bunch up to 0.5 mm. To decrease this error program compensation of the "tail" is implemented in the system.

LOGGING ACTIONS OF OPERATORS IN THE IHEP U-70 ACCELERATOR COMPLEX CONTROL SYSTEM

V. Voevodin, IHEP, Protvino, Russia

Abstract

The control system (CS) of the U-70 accelerator complex supports distributed control rooms environment which are equipped by unified consoles. Using any console it is possible to request any action on any accelerator complex equipment in accordance with user's rights to access it. There are situations requiring knowledge of actions, was performed on some peace of equipment during defined time slot. To solve this problem the CS logs all operators' actions initialized from any consoles such as open/close session, change settings of accelerator parameters, restore settings from archives, etc.

The paper describes a logging software organization and functionalities, contents of the log files and information visualization tools.

LOGGING REASONS

The basic software architecture and organization of the CS was presented in [1]. The last steps of modernization towards homogenization of CS were discussed in [2]. As a result at present the control system supports a number of control rooms equipped with unified consoles on base of PC-compatible computers. The control rooms are distributed over different buildings and GUI is a separate software package dealing, on one side, with humans and, on other side, with descriptions in the data bases. That is why any changes and additions in the 'user–control system' interaction are made inside this package without influence on other CS software components, e. g. data processing.

Due to distribution of equal in rights consoles over number of control rooms there are necessities from time to time to know what actions on some accelerator equipment took place during the certain time slot. The knowledge helps significantly to understand complex difficult situations during simultaneous work of operators in a different control rooms with interconnected subsystems, e.g. ejection system of one accelerator and injection system of other.

We saw an acceptable decision of the problem in logging significant operator's actions with possibility of efficient visualization the information by any console of the CS. Control system users interact with it by the same unified GUI, realized as the data driven package of programs, which supports three main steps of actions:

1. User identification.
2. Menu tree - to select predefined set of parameters for observation and editing.
3. Tabular presentation of selected parameters values.

A password identifies the user and his rights to modify setting values.

'User – control system' dialogue session starts from root point of the menu tree and ends by closing the menu tree.

On selection of menu tree leaf the window with corresponding table of parameters' current values is opened. Current values of each parameter are presented by a row of a table. An operator may do next modifications on the values:

- Set new value to individual table cell.
- Set new value, add/subtract/multiply/divide all current values of selected rows or selected columns with some entered constant.
- Set new value, add/subtract/multiply/divide all current values of intersection cells of selected rows and columns with some entered constant.

So, it is possible to log most significant operator actions by modifying GUI programs only.

LOG FILES

Log files are placed in the fixed directory on the control system file server (Figure 1) and are accessed using NFS protocol inside of the CS.

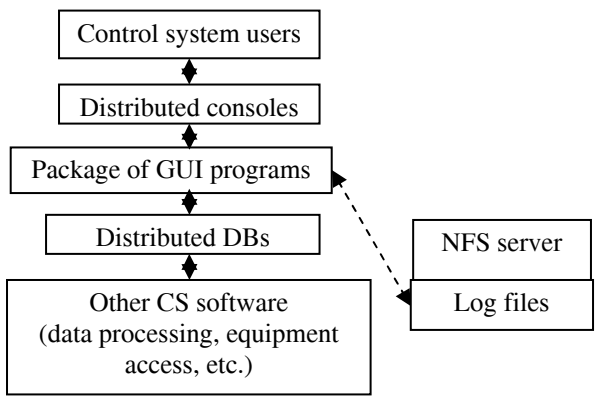

Figure 1: Location of the log files in the CS layout

There is a separate log file for each control system user containing descriptions of actins were performed by him. A log file is plane text file in Russian. A description of single action consists of two or three text lines and includes: consol computer name, date, time, menu tree path and concrete action.

A concrete action may be: open/close table corresponding to the menu tree path, restore settings from archive, one of modifications of values were listed in previous section. A table cells are addressed by row and column numbers. So, a value modification may be described like this:

pcstvn01.oku.ihep.su 09:38:40 Sat 24 Apr 2010

Table:

U1.5/ControlSystems/TimingSystem/Control/InjectionTimer/Reg.1:U-70High Intensity/Timing Delays

EXPERIENCE ON OPERATING HIGH-VOLTAGE ACCELERATORS DESIGNED IN NIIEFA ON INDUSTRIAL FACILITIES INTENDED FOR POLYMER MATERIALS' MODIFICATION

V.P. Maznev, V.P. Ovchinnikov#, M.P. Svinin, FSUE "D.V. Efremov Scientific Research Institute of Electrophysical Apparatus", Saint Petersburg, Russia
V.I. Alexandrov, Izhevsk Plastic-Production Plant, Izhevsk, Russia
E.M. Kolchin, "Insulating Polymer Materials (IPM)" Ltd, Saint Petersburg, Russia.

Abstract

High-voltage accelerators "Aurora-5" and "Electron-10" designed and manufactured in the D.V. Efremov Institute have been operated at the plastic-production plant in Izhevsk and the joint-stock company "Terma", St. Petersburg on facilities intended for production of polymer materials with specific properties due to radiation processing. The results of accelerators' operation are considered in the paper. The annual operating time of each facility is 5-7 thousand hours, which meets the requirements for industrial equipment.

At present, electron accelerators find more and more wide industrial applications: to modify physical and chemical properties of different materials and products, to eliminate bacterial and other types of pollution as well as for other purposes. From the data given in the IAEA review, nowadays more than 1400 high-power electron accelerators are commercially used throughout the world, and the cost of the products manufactured using these machines is more than 85 billions $ per year [1].

From the diagram shown below (see Fig. 1), it can seen that a significant part of the modern industrial electron accelerators is involved in the production of articles on the basis of polymer materials, such as wires and cables, heat-shrinkage pipes, sheets, tapes and gaskets.

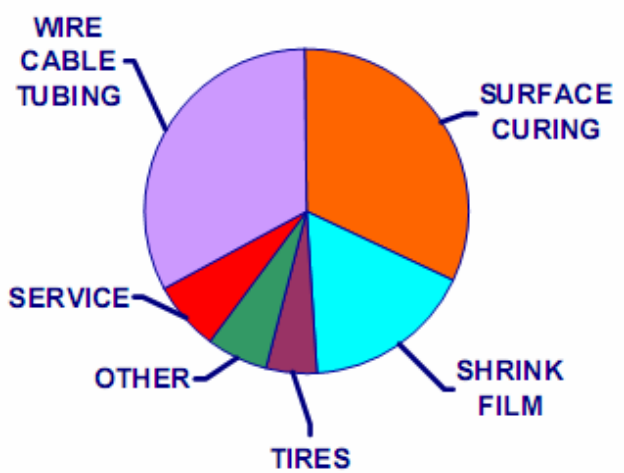

Figure 1: Industrial applications of electron accelerators

For many years, the development and manufacturing of high-voltage electron accelerators for radiation processing have been one of the traditional directions of activities in the D.V. Efremov Institute, NIIEFA. To date, more than fifty similar machines have been manufactured and delivered to different sites in Russia and abroad including eleven machines intended to operate in industrial processing lines for radiation curing of products made of polymers. Accelerators with an energy below 1 MeV are provided with a local radiation shielding and can be installed in conventional industrial buildings.

In 1985 the "Aurora-5" accelerator with the 400-600 keV electron energy, the beam current of 50 mA and the irradiation field width of up to 2 m was delivered to the Izhevsk Plastic-Production Plant to be used in the line producing sheets of foamed polyethylene using the manufacturing technique developed by the Japanese firm Sekisui Chemical (see Fig.2). The accelerator consisted of a separately located high-voltage generator and an irradiator with the local radiation shielding interconnected with a high-voltage cable. By using a special device, a component of the line, the material of up to 2 mm thickness was irradiated consequently from one and the other side; and the absorbed dose distribution was sufficiently uniform. The admixtures doped into the material resulted it its foaming under heating; the density decreased by 5-30 times and the heat conductance decreased as a result.

Figure 2: The "Aurora-5" accelerator in the line producing foamed polyethylene at the Izhevsk Plastic-Production Plant

The production rate of the line involving the "Aurora-5" accelerator was about one thousand tons of

#npkluts@niiefa.spb.su

SPECIFIC FEATURES OF AUTOMATIC CONTROL SYSTEMS FOR APPLIED CYCLOTRONS

V.P. Bagrievich, A.N. Kuzhlev, A.P. Strokach#, FSUE "D.V. Efremov Scientific Research Institute of Electrophysical Apparatus", Saint Petersburg, Russia

Abstract

A distributed automatic control system for the MCC-30/15 compact medical cyclotron has been built on the hierarchy principle. The lower hierarchical level consists of controllers for various systems of the cyclotron, which are networked on the basis of Profibus.

An industrial Advantech-type computer has been chosen as the host computer of the system. The upper hierarchical level also contains computers to control the RF system of the cyclotron and operator workstation.

Computers of the upper hierarchical level are networked on the basis of Ethernet. The number of computers for the operator workstation is limited only by the Ethernet bandwidth and the speed of the host computer.

To measure the beam current, a multi-channel high-precision measuring current amplifier has been developed, signals from which are sent to a high-speed ADC. It is possible to view current pulse oscillograms, which makes much easier the adjustment of the cyclotron modes.

A distributed automatic control system built on the hierarchy principle has been developed for the MCC-30/15 compact medical cyclotron [1].

The lower hierarchical level consists of controllers for various systems of the cyclotron: water cooling system, vacuum system, external injection system, power supply systems for the main electromagnet and ion guide magnets and system for control of mechanical devices of the cyclotron and ion guide. Controllers of the lower hierarchical level are networked with the host computer of the automatic control system via the Profibus DP. Controllers of the external injection system are networked with the host computer via the RS-485 interface. Programmable logic controllers (PLC) of the FX3U series (Mitsubishi) and ADAM-4501controllers (Advantech) are used as controllers of the lower hierarchical level.

A high-powered industrial Advantech-type computer with a 2.4 GHz Pentium 4 Celeron processor was chosen as the host computer of the automatic control system. In addition to the host computer, the upper hierarchical level also contains a computer to control the RF system of the cyclotron and computer(s) of the operator workstation. As the RF system is one of the most complicated and important system of the cyclotron, an industrial computer similar to the host computer is used for its control.

Any PC-compatible computers with the Windows XP operational system or higher may be used as the operator workstation computers. Computers of the upper hierarchical level are networked on the basis of Ethernet, for which purpose an industrial 8-port Ethernet-switch is applied. The number of operator workstation computers is limited only by the Ethernet bandwidth and the performance of the host computer. The use of the Ethernet network allows the operator workstation to be located both in the direct vicinity of the cyclotron and in any place, provided a computer network is available. The software of the automatic control system also allows several copies of the program for the operator workstation to be executed simultaneously on one and the same computer, which makes operation of the control system much more comfortable if several monitors are connected. The host computer performs arbitration of commands and transfer of the data on the status of the cyclotron systems to the operator workstation.

Fig.1 shows a simplified structure of the automatic control system.

The information is displayed on the operator workstation monitor(s) in the form of pages; each of these pages displays status of one of the cyclotron systems. The operator can arbitrarily choose a page to be displayed. If the operator workstation contains several monitors or computers, the operator can display several different pages simultaneously. The page shown in Fig.2 is the control of the vacuum system.

The software allows all the systems of the cyclotron to be controlled in two modes. In the "Manual Remote" mode, the operator performs on/off operations and adjustment of the cyclotron devices' parameters from one of the operator workstation computers on the basis of his own experience and design parameters of the mode. The "Choose and Control" principle is applied. By clicking the mouse, the operator chooses one of the cyclotron sub-systems on the mnemonic diagram displayed on the monitor and a panel to control this system is visualized. Current operating parameters and controls of this particular device are shown on the panel. The operator can either turn on/off the device or change the adjustment of its parameters (for example, the current of the main electromagnet or radial position / angle of the stripping device, etc). In so doing, the available ACS interlocking system does not enable any unallowable operations to be done. This ACS operating mode is used at the initial stage of the cyclotron operation until the data on the cyclotron operating modes has not been stored. Parameters of the actual mode can be stored in the data base. The second operating mode of the ACS is the automatic mode. In this mode, the operator chooses an operating mode among the modes previously stored in the data base and starts automatic procedures of turning on/off the sub-systems of the cyclotron. These procedures include production of the working vacuum in the cyclotron, external injection

#npkluts@niiefa.spb.su

LABVIEW CONTROL SYSTEM OF THE CRYOGENIC COMPLEX FOR THE KAON RF-SEPARATOR AT IHEP

A.Ageyev, V.Alferov, A.Bakay, V.Fedorchenko, A.Kholkin, V.Krendelev, A.Lutchev, D.Vasiliev,
Institute for High Energy Physics, Protvino, Moscow Region, 142281, Russia

Abstract

The superconducting RF separator is used for the separation of kaons at the OKA experimental setup at IHEP. The separator consists of two deflecting niobium cavities housed in the cryostats. Their cooling is provided by one large commercial helium refrigerator and two custom heat exchangers, located near cavities. The cryogenic complex for the separator provides liquid superfluid helium with the temperature of 1.8K as well as liquid nitrogen. The paper describes the arcvhitecture and the LabVIEW based software of the control system.

INTRODUCTION

The cryogenic complex comprises the vacuum system (CVS) and provides cooling of two deflecting niobium cavities RF1 and RF2 of the superconducting RF separator which is used for separation of kaons for the experiments at the OKA setup [1]-[4] at IHEP. The cryogenic helium plant KGU-500 is the main cold generating unit of the CVS. It produces both the cool and liquid helium of the same 4.6K temperature. The other parts of the cryogenic complex are: two heat exchangers located in the liquid helium baths (LHB) of intermediate cooling; large vacuum heat exchanger (HEX); heat exchangers at the entrances into the RF1 and RF2; pumping machine (PM). The control system provides measurements of about 500 analog parameters and 300 digital signals and generation of tens of commands.

ARCHITECTURE

On a lower level of the control system there are 40 custom equipment controllers based on Analog Device and Atmel programmable devices. They provide data acquisition, calculation of operating parameters, and generation of digital and analog commands for the following tasks:

- temperature measurements with various sensors;
- digital measurements of liquid Ni and He levels;
- analog measurements of He level;
- vacuum pump motors current measurements;
- vacuum measurements;
- turbine rotation speed measurements;
- controls of heaters power supplies;
- measurements of Ne contamination of gaseous He;
- valve position measurements;
- various measurements and generation of digital signals.

Equipment controllers are connected to three personal computers (PC) by means of CAN field buses. Each PC controls one of three physically separate groups of equipment: KGU, LHB, and HEX/RF. The fourth PC is used as a local Data Socket (DS) server. The PCs are connected by a dedicated Ethernet technology network (TLAN). Simplified block diagram of the control system is shown in Figure 1.

We use the Data Socket Connection program, which is a part of the LabVIEW package Developer Suite Core. All CAN masters are simultaneously clients and servers, so all the data are available on each console. The DS server is a client for the following users: three operator consoles; server for clients TLAN, a public LAN and SQL server hosting an archive of the CVS. As a result, all operators and other users of the TLAN can get data from both the DS and SQL servers.

CONTROLS AND DATA PRESENTATION

LabVIEW based software for control and monitoring consists of the following programs:

- **PK09.vi** installed on the KGU PC;
- **RF.vi** installed on the HEX/RF PC;
- **OM.vi** installed on the PM PC;
- **DS server.vi** installed on he DS server of TLAN;
- **CRYOVIEWER.vi** installed on computers of clients of the DS server of TLAN.

Every program presents the main window synoptic sirquit of the equipment group with sensors and actuators as well as a parameter values. One can change parameters by putting new data into an appropriate control field. Color is a status indicator. One can draw a time graph of any parameter. Additional windows permit tuning, calibration and other manipulations with various parameters. Graphical presentation of the HEX/RF group is shown in Figure 2.

DATA ACQUISITION AND CONTROL SYSTEM

The CVS data acquisition and control system developed at IHEP allows to display on the operator's console all the main parameters required for manual or remote control. After full commissioning the system shall provide control of the following parameters:

- temperature measurements of cryogenic components, of nitrogen and helium flows in 72 points;
- temperature measurements of pumps of the PM in 42 points;
- interstage pressure measurement of the PM by means of differential pressure transducers in 3 points;
- medium and high insulation vacuum measurements by PMT-6-3 and PMT-4 sensors in 32 points;
- liquid helium level measurement in 3 vessels;

UPGRADE OF THE U-70 PROTON SYNCHROTRON EXTRACTED BEAM LINES CONTROL SYSTEM: MULTIPLE ACCESS AND DATA PRESENTATION

V. Alferov, I. Lobov, A. Lutchev, Y. Bordanovski, V. Lagutin,
Institute for High Energy Physics, Protvino, Moscow Region, 142281, Russia

Abstract

The U-70 extracted beam lines system includes about 130 magnet dipoles and quadrupoles, with power provided by 112 power supplies (PS). Each PS is controlled by an individual Analog Device's based controller. Since a number of used magnets may vary and exceeds the number of available PSs, the commutation is used. Controllers are connected to a front-end computer by means of four CAN field buses. The software for the controllers is tuned to a specific type of the PS and a specific inductive load of the magnet. The Dell PowerEdge T710 server is used for the PS control with multiple access from several client workstations which controls PSs for a particular beam line. All client workstations along with the server and front-end computer are connected together with a dedicated LAN.

The server grants different users a different permissions to control their own PSs only. Every four seconds the measured data are stored into an archive. Operating commands are archived as well to keep a history of all user's actions. The software is based on the National Instruments Developer Suite Core and MS Office Web Components packages.

INTRODUCTION

The Extracted Beams on the Serpukhov 70 GeV Proton Synchrotron are spread for over 1 km. They include about 130 magnet dipoles and quadrupoles. The PSs (motor-generators, silicon rectifiers and thyristor rectifiers) are installed in the special building
500m away. The total number of PSs is only 112, so, as a result, the commutation is used. The PS are characterized with the following features:

- DC current stabilization time can be as long as several minutes;
- magnet hysteresis stipulates a special procedure of installation of current,
- imperfection of the PS feedback stabilization requires to adjust the DAC reference signal to get needed current of the magnet;
- current polarity can be changed.

Intel 8051 compatible custom PSs controllers (PLCs) are uploaded before a run with accordance to features of a specific "magnet-PS" couple [1]. The following data is uploaded;

- maximum value of current,
- DAC raising rate,
- matching delay,
- minimum making step,
- number of matching steps.

CONTROL SYSTEM CONFIGURATION

A block diagram of the control system is shown in Fig.1. Front-end computer (FEC) is used as a master for PLCs. FEC acts as a CAN master and can gain the access to controllers through 4 segments of 2 CAN field buses. The total length of each bus is about 600 meters. The data transmission rate of 20 Kbit/s is used because of heavy noise conditions in order to reduce information losses down to acceptable level.

FEC reads data from PLCs periodically, one read cycle accounts for about 15 ms. Due to large number
(100-120) of PLCs the polling period is 2 seconds.

FEC is a client of the MS SQL-server 2008, that is located in the beam control room on the main archive server. Any computer inside the both industrial and public LAN could be a client of this server. Each client has its own permissions. There are 3 levels in client's permissions hierarchy:

- The lowest level is occupied by «observers», who can only view the data and does not take part in any control operations. The observers may belong to both the industrial and public LAN;
- The middle level is reserved for the operators of the physical experimental installations. They are observers too, but in addition they can also operate their own magnets;
- The full permissions level is given to the operators in the main beam control room and at the PS building. They can control any magnet of any channel. In addition, they can generate a list of magnets for the current run.

  Both the middle and high level operators consoles can belong to an industrial LAN only.

SOFTWARE SERVICE FOR CRYOGENIC DATA REPRESENTATION AND ANALYSIS

I.Lobov, A.Lutchev, M.Stolyarov, S.Sukhov
Institute for High Energy Physics, Protvino, Moscow Region, 142281, Russia

Introduction

The Cryogenic and Vacuum System (CVS) for OKA experimental complex requires reliable, fast and convenient program facilities for cryogenic data analysis – temperatures of cryogenic components, liquid helium levels, helium mass flow rates. In order to achieve that goal the software complex was developed for remote analysis and supervision of the CVS parameters with data storing ability. MS SQL-server 2008 was used for data storage and archiving. For displaying the stored data in graphic and table forms, NI Developer Suit Core software package was used. For on-line displaying current CVS parameters the dedicated web-server with xml mimic panel engine was used. The engine was developed on the base of original software created in IHEP.

THE SOFTWARE COMPLEX STRUCTURE

CVS control system has three local control rooms, which corresponds to tree main CVS machinery subsystems: pump machine (PM), bubble cell (BC) and deflector (RF). Data is transferred from control rooms to local CVS server with 2 seconds periodicity, using Data Socket protocol (National Instruments DS technology). The local CVS server supplies DS-clients with current data and then put it into its own local temporary archive.

The main task of the local CVS server is to collect the data from all CVS subsystems, build full package and transfer it to the Central Database using Open Database Connectivity (ODBC) standard. The Central Database locates on the archive server machine (Zeus) and runs MS SQL-server.

Archive server sends the data to mimic panel server (Zerver) as well. The mimic panel server put incoming data into Microsoft Access DB table and the old data is replaced by new one. This DB is used as main data source for mimic panels.

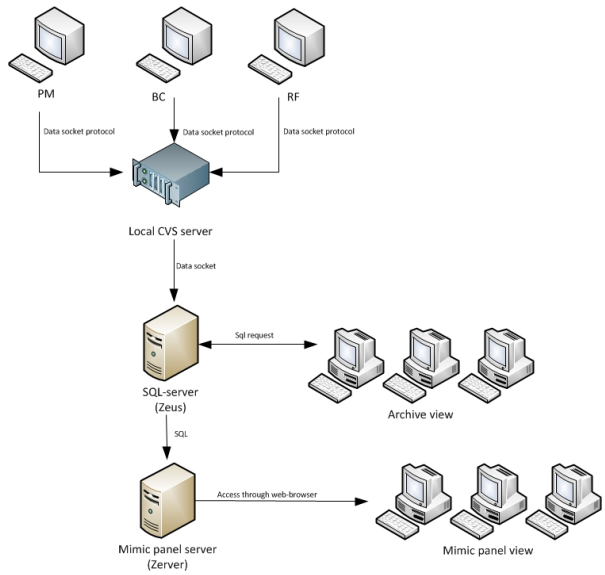

Figure 1: CVS data flow scheme.

SOFTWARE FOR CVS MIMIC PANELS

The CVS mimic panel is a web-page with graphical elements. All this web-pages are located on the mimic panel server (Zerver), and are available to users with any web-browser. The CVS operator has opportunity for supervising any parameter not only at CVS site but using any computer at IHEP site. There is no CVS control ability for mimic panels currently but it is a matter of future development.

The data for mimic panel comes from local CVS server to SQL-server as a string like:

'current data',T1,T2,T3,...Tn

where T - measured value. These original data array is represented on Figure 2.

CANOPEN CONNECTED POWER SUPPLY CONTROL SYSTEMS FOR THE ELECTRON LINACS

V.N.Boriskin, A.N. Savchenko, A.A. Sarvilov, D.L. Stepin, G.N. Tsebenko National Scientific Center "Kharkov Institute of Physics and Technology", 61108 Kharkov, Ukraine
A.S. Chepurnov, I.V. Gribov, Scobeltsyn Institute of Nuclear Physics, Moscow State University, 119899, Moscow, Russia
A.F. Shamarin, "MARATHON" Ltd., Mosfilmovskaja 17b, 117330, Moscow, Russia

Abstract

Power supplies, which feed magnetic systems of electron linac, together with the control system are very critical parts of any linac. The quality of power supplies and control software defines safety of the accelerator operation, stability and cost of operation. One of the today's tendencies in power supply system architecture is to use distributed CAN-connected power supplies with high level of local intellectual properties. These properties allow to achieve high stability, high safety of operation together with the specific features such as coil temperature check without any temperature sensors. Such programmable power supplies with the intellectual CAN-bus/CANopen controller have been designed for the specific accelerator applications. The control system software was adapted to operate with CANopen protocol. "Marathon IPP-1/100" and "Marathon IPP-4/35" power supplies with CANopen are used now within the control systems of LU-60m and LU-10 linacs. 3200 hours of continues operation were achieved since the year 2008.

INTRODUCTION

Power supply development was one of the important topic in particle accelerator instrumentation since particle accelerators appeared. Wide spread of different power supplies guarantee stable, safe and long term operation of any accelerator feeding directly magnet elements and feeding other electronic equipment such as vacuum pumps, RF systems and control system. A lot of efforts were made by different groups of accelerator specialists to improve mainly circuit technology in order to achieve the stability of the output values, high degree of efficiency, adjustable limitations of current, voltage and power stability of the output. In the meantime new types of power supplies have been developed – digital programmable power supplies, which could be directly interconnected and integrated into accelerator control system via different fieldbus interfaces such as CANbus.

There are two main approaches which are used today in distributed power supplies systems. The first one is based on modular architecture when control unit is independent and could process few different power modules [1, 2]. The control unit is usually equipped with one (or several different) fieldbus interfaces and realize control logic together with precise measurement and feedback control of power modules. The power modules in such approach are usually just high power (some time very high power) amplifiers of voltage or current, depending on application.

The second approach, that we have chosen, is to develop single channel power supply module as a separate device, based on modern power supply circuits and equipped with individual smart controller and digital interface. The controller provides measurements, stabilizing and locking capabilities. Due to standardized fieldbus interface CANopen, such devices could be combined together into separate power supply control system or with other CANopen compatible sensors and actuators.

To feed beam optic of the LU-60m linac [3,4] control subsystem based on intellectual power supplies "Marathon IPP-1/100" and "Marathon IPP-4/35" have been developed. Control system of the LU-10 linac was significantly improved by replacing existing powers supplies (B5-47/B5-49) with the new ones. All this power supplies systems are based on CANbus fieldbus with CANopen higher-layer protocol and form separate subsystem but naturally integrated in to the whole accelerator control system.

INTELLECTUAL POWER SUPPLY

There are several features in the accelerator magnet optics control tasks, which make impossible to use standard industrial DC power supplies "as is" without extra efforts and use of additional hardware and control software. These features are the following:

- high long term stability and repeatability together with high accuracy;
- bipolar operation with accurate zero crossing and "true zero";
- load check function (detection of shortage, open, impedance changes) and alarm generating;
- load with high inductance;
- operation in conditions of high level of external EMI;
- flexible interface for embedding the power supply in to the existing control
- parallel operation of multiply devices.

It is also important to have a possibility of stand alone operation and operation as lab instrument to check lenses

UNIVERSAL TIMER MODULE FOR THE TIMING SYSTEM OF THE ACCELERATING STORAGE COMPLEX ITEP-TWAC

A. Orlov, P. Alexeev, S. Barabin, D. Liakin, SSC RF ITEP Moscow, Russia

Abstract

A multipurpose synchronization module for renovating timing system of ITEP-TWAC accelerator facility is developed. A group of such modules is aimed to implement a sophisticated set of synchronization functions among four accelerators – proton LINAC I2, ion injector I3, buster synchrotron UK and accelerating and storage ring U10. This FPGA based module generates up to 16 output pulses related to timing scale (T), magnetic field scale (B), radio frequency, external events or their combination. The read back function allows controlling the pulses propagation on cycle-to-cycle basis. The structure of the module, a description of basic functions and IO interface are presented in details. Also an example of system configuration based on the developed module is discussed.

INTRODUCTION

The modernization of an accelerating complex in ITEP [1] lays new demands to the synchronization of the systems of accelerators. A new timing system should work with increasing number of synchronous elements providing more and more functionality and flexibility.

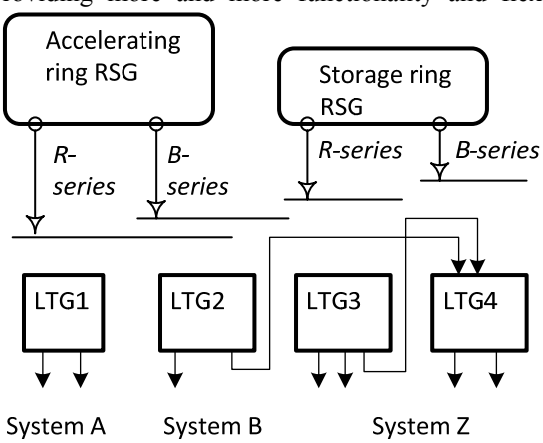

Fig. 1. A principle of organization of the timing system of the ITEP's accelerators

A principle of synchronization of the ITEP's accelerating complex shown on fig. 1.

Reference devices (reference signal generators RSG) generate **B**- and **R**- sequences of pulses synchronous to the magnetic field strength and zero phase of RF oscillations. Followed local timing generators LTGs are an assembly of properly commuted logical modules, modules of programmable time delays and fan-out modules as it shown on fig. 2. The system has a multiple hierarchy levels and distributed over the area. Some local generators are realized in the form of standalone units, synchronized by one or two pulses from higher-level LTG. Some of local generators are placed outside of the synchrotron's control room. There are, for instance, timing systems of proton or ion sources. This allows an independent work of linacs on their own targets.

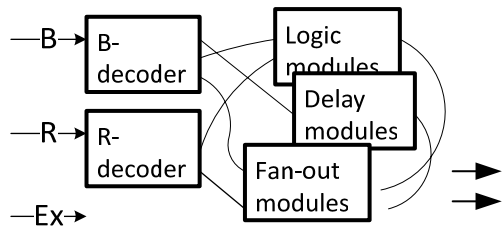

Fig. 2. A Local Timing Generator synchronizes devices with magnetic field (B), RF phase (R) and/or external events (Ex).

The tasks of the developing timing system are, in particular, unification of used modules, simplification of the process of the system setting up and extending of a system's functionality. The concept of the new timing system is based on the experience of the exploitation of the existing system in ITEP as well as other similar systems in GSI and CERN. A new timing system concept for CERN and FAIR so-called White Rabbit project [2] also has been examined. Similar to the White Rabbit the future timing system of ITEP presumed a possibility of precise delay compensation over Ethernet. But in opposition to White Rabbit, ITEP keeps a dedicated serial timing bus STB (fig.3b). The synchronized Ethernet (IEEE 1588) is an option, which is used when it is necessary without any modification of general standard. This way looks more reliable and budgetary which has the sense in present-day situation. Nevertheless, we are looking forward and in the case of successful realization of the White Rabbit project and the appearance of commercial accessible components there is a possibility of the essential incorporation of this new technology into the developed system.

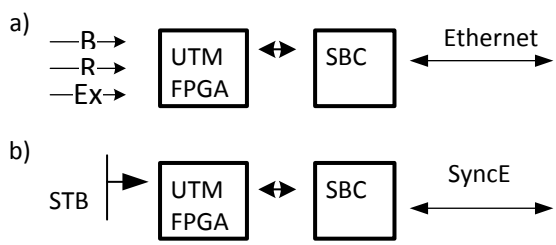

Fig. 3. Applications of the UTM: replacement of existing modules on top, using serial timing bus STB and synchronization over Ethernet on bottom.

A universal timing module UTM was developed as a key component of a new system. It intends to smoothly

CONTROL SYSTEM FOR THE NEW BEAM TRANSFER LINE AT IHEP

A.Matyushin, L.Kopylov, S.Merker, M.Mikheev, IHEP Protvino, Russian Federation

Abstract

New proton beam transfer line is study project to evaluate a possibility to use UNK injection line as an experimental facility. A wide set of accelerator equipment is involved in the test. The Control system is build on OPC and CAN technology using data driven and object oriented approach. The structure, key solution and operational experience are described in the paper.

INTRODUCTION

In IHEP on the basis of the beam transfer line (BTL) of not completed UNK ring the construction of installation for applied researches [1] is planned. Within the R&D study for finding-out of an opportunity of such decision the Prototype of such installation has been created using all spectrum of BTL equipment on the limited length of the channel: magnet optical elements, beam instrumentation, vacuum system, the radiating control. The beam, accelerated by proton synchrotron U-70 up to energy 50-70 GeV, is extracted into the channel, where it's demanded size (the maximal size allowed by the vacuum chamber) at a location of investigated object is formed.

The control system (CS) has been developed for management of the equipment, which is a subject of this report. As far as the most part of BTL equipment, and, in particular, operating electronics, has been inherited from UNK, the new CS shall be adapted for existing schemes, therefore, some of our solutions don't look very elegant. Meanwhile, as it is the prototype of essentially bigger installation, we aspired to realize CS with precise standard borders between levels. There are three such levels in our system (from bottom to top): the controller of the equipment (EqC), a front-end computers (FEC) and computer(s) in control room (CR).

As for the software solutions the object-oriented model driven by data has been chosen. It means that for all types of the equipment the corresponding data structures and methods for their handling have been designed. Corresponding objects have been developed for access to the equipment and the interface of the user.

Decisions made, experience of realization and two-year operation results are described further.

HARDWARE SOLUTIONS

The hardware of a BTL CS includes the centralized part, distributed controllers and communications (cables, repeaters, serial interfaces). The centralized part is located in CR, the embedded controllers - near to the process equipment. Communications between two parts are implemented via twisted pair cables supporting CAN protocol, timing pulses and signals of the dynamic interlocks.

Distributed part

The distributed part of a CS is based on three types of controllers: the universal controller of power supplies (PCC), the controller of the vacuum pumps (VC1) and those one for vacuum gauges (VC2). The PCC is constructed on two functional units: microcontroller CY8051F060 and programmed logic XC9536XL. Communication with upper level is carried out through microcontrollers CAN interface. There is a timing events receiver on the board as well as a driver of dynamic interlock. The controller has 16 inputs of status signals, 8 discrete outputs, two analogue inputs and one analog output.

The controller of ion pumps VC1 is embedded in a high voltage power supply. In each rack can be up to 3 high-voltage power supplies. The VC1 acquires the states of registers and transfers the status of pumps and their currents in predefined regular intervals.

Controller VC2 is used for vacuum measurement. It consists of 8-channel 24-digit sigma-delta ADC. The analogue signals proportional to pressure come from a power supply of gauges.

Means of data transmission, timing pulses and dynamic interlock of each building include repeaters boards, a twisted pairs main cable, as well as short cable taps.

The PCC develops a signal of the dynamic interlock if the current of a power supply is out of the window comparator thresholds. The inhibit signal in CAN terminology has a dominant level, and the permission signal – recessive one.

The timing controller carries out a number of service functions: calculation of number of cycles and distribution this information on CAN network, as well as management the dynamic interlock mode. The static interlock system is intended for supervision over a condition of doors of admission in a BTL tunnel, management of beam stopper and deliveries of the permission to the fast ejection system when safety requirements is fulfilled.

The BTL CS is located far away from the equipment of the proton beam fast ejection system. Communication between these two systems is done by means of timing signals generated by the fast ejection system and static interlock from BTL equipment.

BEAM TESTS OF THE LHC TRANSVERSE FEEDBACK SYSTEM

W. Höfle, G. Kotzian, E. Montesinos, M. Schokker, D. Valuch, CERN, Geneva, Switzerland
V. M. Zhabitsky, JINR, Dubna, Russia

Abstract

A powerful transverse feedback system ("Damper") has been installed in LHC in order to stabilise the high intensity beams against coupled bunch transverse instabilities in a frequency range from 3 kHz to 20 MHz and at the same time to damp injection oscillations originating from steering errors and injection kicker ripple. The LHC Damper has been also used for exciting transverse oscillations for the purposes of abort gap cleaning and tune measurement. The LHC Damper includes 4 feedback systems on 2 circulating beams (in other words one feedback system per beam and plane). Every feedback system consists of 4 electrostatic kickers, 4 push-pull wide band power amplifiers, 8 preamplifiers, two digital processing units and 2 beam position monitors with low-level electronics. The power and low-level subsystem layout is described along with first results from the beam commissioning of the LHC Damper.

INTRODUCTION

The powerful transverse feedback system ("Damper") for the Large Hadron Collider (LHC) is a joint project of the European Organization for Nuclear Research (CERN) and the Joint Institute for Nuclear Research (JINR) [1, 2]. To a large extent this project is based on the system in the SPS which has operated successfully for many years [3, 4].

The peak luminosity of 1.0×10^{34} cm^{-2}s^{-1} is achieved in the LHC with high intensity beams of low emittance. The ultimate intensities after injection into the LHC will be about 4.8×10^{14} particles for the proton beam with an energy of 450 GeV and 4.1×10^{10} ions for the $^{208}\mathrm{Pb}^{82+}$ beam with an energy of 177 GeV/u. These intensities can lead to coherent transverse instabilities. The theoretical prediction for the instability rise time τ_{inst}, dominated by the resistive wall effect, is about 18.5 ms or 208 turns [5] at injection energy for the proton beam, and a significant contribution of the LHC collimators at collision energy to τ_{inst} is also predicted [6].

The normalised transverse emittance ε is expected to be smaller than 3.75 mm·mrad at collision energy. The damping time τ_{d} of the LHC transverse feedback system (TFS) was chosen to limit the emittance growth due to injection errors [7, 8]:

$$\frac{\Delta\varepsilon}{\varepsilon} = \frac{e_{\mathrm{inj}}^2}{2\sigma^2} F_\varepsilon\,; \qquad F_\varepsilon = \left(1 + \frac{\tau_{\mathrm{dec}}}{\tau_{\mathrm{d}}} - \frac{\tau_{\mathrm{dec}}}{\tau_{\mathrm{inst}}}\right)^{-2}. \quad (1)$$

Here σ is the initial RMS beam size; $e_{\mathrm{inj}} \lesssim 4$ mm $= 3.5\sigma$ is the maximum assumed amplitude of a beam deviation from the closed orbit due to displacement and angular errors at injection where the betatron amplitude function is $\hat{\beta} = 185$ m; $\tau_{\mathrm{dec}} \simeq 750 \times T_{\mathrm{rev}} = 68$ ms is the assumed decoherence time (the revolution period of protons in the LHC is $T_{\mathrm{rev}} = 88.93$ μs after injection). These parameters lead to $\Delta\varepsilon/\varepsilon < 2.5\%$ the maximum admissible emittance blow-up in the LHC allocated to injection dipole errors [5] if $\tau_{\mathrm{d}} = 40 \times T_{\mathrm{rev}}$. Thus, the LHC TFS gain is $g = 2T_{\mathrm{rev}}/\tau_{\mathrm{d}} = 0.05$ and the overall damping time $(1/\tau_{\mathrm{d}} - 1/\tau_{\mathrm{inst}})^{-1}$ of the injection oscillations becomes about 50 turns or 4.4 ms.

The nominal LHC beam represents an unprecedented stored energy of 350 MJ [5]. The extremely high destructive power of such a beam imposes an external dump, where the beam must be extracted completely from the LHC, diluted to reduce the peak energy density and then absorbed in a dedicated system. A gap of 3 μs in the circulating bunch pattern is present to allow the horizontally deflecting extraction kickers to rise up to their nominal field. Since particles transiting the kickers during their field rise will not be dumped properly, the proton population in this interval must always remain below damage and quench limits. The control of the abort gap population is a problem common to high energy machines using superconducting magnets. Cleaning of the abort gap using the LHC transverse dampers should require no more than a few tens of milliseconds [9].

The LHC Damper will stabilize the beam against coupled bunch instabilities as well as damp the transverse oscillations of the beam originating from steering errors and kicker ripple. It will also be used for the purposes of tune measurement similar to the SPS system [10] and for abort gap cleaning.

GENERAL DESCRIPTION

The LHC Damper has 4 independent transverse feedback systems on 2 circulating beams (one feedback system per beam and transverse plane). Each system is a classical bunch-by-bunch transverse feedback system (see Fig. 1) [11]. It consists of 2 pick-ups (PU), a 4 section damper kicker (DK) and an electronic feedback path with appropriate signal processing and transmission from PU to DK. The DK corrects the transverse momentum of a bunch in proportion to its displacement from the closed orbit at the PU location. The digital signal processing unit (DSPU) ensures the adjustment of the feedback to the phase advance and the beam time of flight for optimum damping. The mixing of signals from 2 pick-ups allows adjustment of the betatron oscillation phase advance ψ_{PK} from the "virtual" PU to the DK to an odd multiple of $\pi/2$.

The total delay τ_{delay} in the signal processing of the feedback path from PU to DK adjusts the timing of the

THE NONLINEAR TRANSFORMATION OF A IONS BEAM IN THE PLASMA LENS

A.Drozdowskiy, N.Alexeev, S.Drozdowskiy, A.Golubev,
Yu.Novozhilov, P.Sasorov, V.Yanenko. ITEP, Moscow, Russia

Abstract

The focusing capabilities of a plasma lens depend on the stage of plasma development. Under certain conditions a magnetic field is linear, that allow focusing the beam to a very small spot. In other conditions, the magnetic field is nonlinear, that allow formation of hollow and others beam structures. Calculations and measurements were performed for a C+6 and Fe+26 beams of 200 MeV/a.u.m. energy. The obtained results and analysis are reported.

INTRODUCTION

The focusing properties of plasma lenses depend on the current density distribution along the radius of the

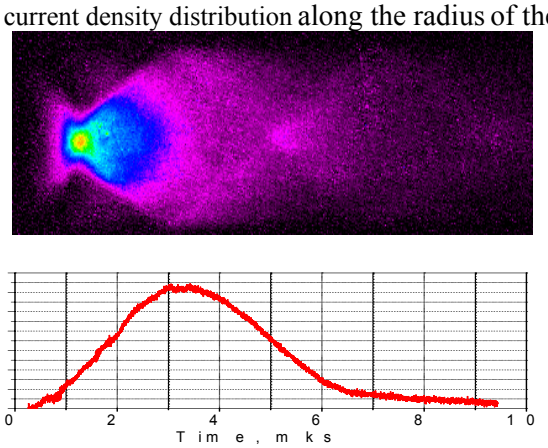

Fig. 1: Time scanning of the discharge luminescence and current.

plasma discharge [1]. Fig. 1 shows the time sweep of the luminosity of the plasma and the discharge current. The created magnetic field compresses the plasma-current cylinder. Expansion of the plasma column with a current takes place later and the discharge fills the whole tube. Current distribution across the tube changes significantly during the discharge. Therefore, plasma lens, in general, is nonlinear. Uniform current distribution longs for a limited time, so the plasma lens, as a device for sharp focusing, operates for about 1 microsecond or less. As a non-linear focusing device, the plasma lens can be used to produce beams of special shape. In particular, to create hollow beams, which can be used for the implosion of thermonuclear targets [2].

Test for sharp focusing of carbon ions has been conducted at ITEP in 2007-2008 [3]. These researches were continued in [4] to investigate possibilities of hollow beams formation. Lens parameters were as follows: capacitance - 24 μF; discharge current - 150 kA; current half-wave - 5 μs; argon pressure – 1-5 mbar; ion beam duration – 300 ns (fig. 2). The discharge tube has radius of R = 1 cm and length of L = 10 cm. The effect of beam focusing was detected by the luminescence of a thin quartz scintillator. Fig. 3 shows crossections of the beam at position of 30 cm behind the lens as function of time during injection of the beam.

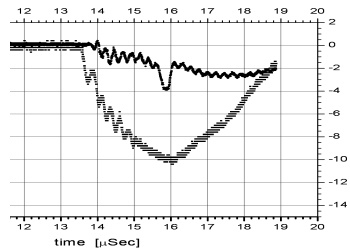

Fig. 2: Oscillograms of the discharge and the beam current.

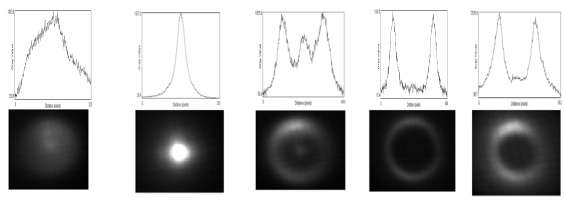

T=0 μs *T=0.5 μs* *T=1.5μs* *T=1.7μs* *T=2.3 μs*

Fig. 3: The light output from a scintillator and the distribution of ion Fe^{+26} density for T > 0 behind discharge switch

FORMATION OF HOLLOW BEAMS

Possibility of transformation of ion beams with such plasma lenses has been demonstrated experimentally in GSI [5]. Researches carried out on the ITEP plasma lens confirmed this opportunities in a wide range of operating modes lens.

The paraxial beam with zero emittance is converted to a tube beam, when the distribution of azimuthal magnetic field in the plasma lens is as follows

$$B = a + br, \qquad (1)$$

where a and b - constants. This distribution akes place, when distribution of the discharge current density is a superposition of a homogeneous distribution and a singular one, inversely proportional to radius r:

$$j = I_o/\pi R^2 + I_s/2\pi Rr. \qquad (2)$$

Here R - plasma lens aperture, within which there are a homogeneous current, Io and a singular one, I_s. In this notations

$$B = B_o\,(r/R + I_s/I_o), \qquad (3)$$

RECOVERY PROCESS STABILITY STUDY IN ENERGY RECOVERY ACCELERATOR

V.G..Kurakin, Lebedev Physical Institute, Moscow, Russia.

Abstract

Energy recovery technique in rf accelerator based applications allows to save rf power and reduce radioactive background as well. In this operation mode used beam is directed back to the accelerator in decelerating rf phase where it returns back its kinetic energy to rf field. Thus, rf generator that feeds linac covers cavities walls rf losses only and those part of beam kinetic energy that used for useful effects production as well. The sum of three fields – induced in the linac by an external rf source, accelerated and decelerated beams – determines energy and phase of the beam at linac exit, and together with beam return path optics amplitude and phase of decelerated bunches and hence third component of mentioned sum. In the case of positive sign of this feedback and sufficient amplification in the closed loop just described instability takes place.

The main equations that determine beam-rf cavity interaction in energy recovery rf accelerator are derived, single mode approximation being used. Expressions for small deviation from steady state are obtained followed by stability analysis. Results of calculations for increments of instability are presented and discussed.

INTRODUCTION

In some electron accelerator applications, only small fraction of kinetic beam energy is used, high brightness light sources of the next generation and free electron lasers being the typical examples. Keeping in mind large value of the beam energy in similar applications (it may be as large as hundreds megawatts) very fruitful idea to recover beam energy is widely discussed and already used in all over the world [1,2,3]. In recovery process used beam is guided back to the same accelerator in decelerating phase and for this reason reduces its kinetic energy along the accelerator. In other words, accelerated and decelerated bunches are spaced by half period of rf field, and in the case of lossless beam recirculation the first harmonic of total current is equal to zero and the total radiation field is equal to zero as well. The question arises whether the recovery process just described is stable in the sense that small perturbations of steady state result in such behaviour of the system that such perturbations tend to zero with the laps of time. Among the many one mechanism of feed back in the system beam – cavity may take place. Any change in beam energy results in phase shift of decelerated bunches if the longitudinal dispersion of return path is not equal to zero. This phase shift in turn results in phase shift of the voltage induced by decelerated bunches in accelerating cavity and thus in amplitude and phase of the total voltage at accelerating gap changing and as the result in energy changing acquired by the accelerated bunches. This feed back may result in instability in the case of its positive sign and sufficient amplification in the closed feed back loop.

Following is quantitative analysis of the processes just described. Single mode approximation is used in beam-cavity interaction equations. We limit ourselves by linear approach in stability analysis.

THE EQUATIONS OF BEAM-CAVITY INTERACTION

Fig.1 represents the main features of energy recovery linac. Electron beam from injector directed into the main accelerator consisting of rf cavities. Being accelerated electron bunches are rotated by two arcs consisting of bending magnets and entered the same linac in decelerating phase. Thus, electron bunches in two beams are shifted by the angle close to 180 degrees to each others.

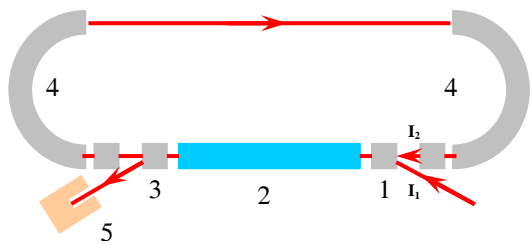

Fig.1. General layout of energy recovery linac. 1– magnet inflector, 2– main linac, 3 – magnet deflector, 4 – bending magnets, 5 – beam absorber.

While passing the main linac in decelerating phase the secondary beam looses its energy and with the help of deflector at the linac exit leaves accelerator and is directed into the beam absorber. In analysis that follows we will assume all voltage and currents being time dependent as complex exponent function $\exp(i\omega t)$ with the appropriate amplitudes which are slow functions of time t. Fig.2 represents these values on complex plane.

According to the superposition principle the total voltage $\hat{U}_\Sigma(t)$ at cavity gap is equal to the sum of three voltages – the first one $\hat{U}_e(t)$ excited by the external rf generator, while the second $\hat{U}_1(t)$ as well as the third one $\hat{U}_2(t)$ induced by the accelerated and decelerated beams:

$$\hat{U}_\Sigma(t) = \hat{U}_e(t) + \hat{U}_1(t) + \hat{U}_2(t), \qquad (1)$$

where t stands for time and "hat" symbols above letters denotes complex values. The primary (being accelerated) beam energy gain in the main linac is:

A BEAM LOSS SCINTILLATOR SYSTEM FOR BACKGROUND MONITORING AT THE LHCb EXPERIMENT

V. Talanov *, R. Dzhelyadin (IHEP, Protvino), A. Bobrov, A. Bondar (BINP, Novosibirsk),
F. Alessio, G. Corti, R. Jacobsson (CERN, Geneva), M. H. Lieng (TU Dortmund)

Abstract

The LHCb experiment at the Large Hadron Collider (CERN) has developed a complete high-speed and high-sensitivity background monitor based on a pair of plastic scintillators and a custom-made LHCb readout board to record fast LHC beam losses with time information. The system is installed close to the LHCb Vertex Locator and it has been operational since the LHC pilot run providing valuable information to the LHC Operations crew during beam commissioning and to the LHCb Control Room about the experimental conditions at the physics runs.

The system is able to record fast beam losses at a rate of 40 MHz, providing information regarding the bunch crossing of the loss and the intensity of the loss calibrated in number of Minimum Ionizing Particles. A full control and monitoring system has been developed as well within the framework of the LHCb Experimental Control System. A complete simulation of the system has been central in converting the response of the system into physical quantities.

In this paper we will describe the system in its components and functionalities, the commissioning phase, the simulation framework and the first results with real beam at the LHC.

INTRODUCTION

The Beam Loss Scintillator (BLS) detector is made of two cubic-like plastic scintillators installed 12 cm away at both sides of the LHC beam pipe on the horizontal plane, at $\sim$2 m from the LHCb Interaction Point in the opposite direction to that of the spectrometer. The initial scope of the scintillators was to look at injection problems [1]. However, the opportunities of using such scintillators as a continuous detector have been exploited. It is in fact, the only instrument within LHCb which is able to measure fast losses of the beam in the experimental area. Although the instrument is not able to protect the experiment, it is however able to predict possible incidents by analyzing the behavior of the beam and the evolution of the background. Eventually the system has proved his good performance and reliability as an independent source of luminosity measurement in LHCb.

The installed system comprises two scintillators of the size $4\times4\times3$ cm^3. Each scintillator is directly attached to a PhotoMultiplier, HAMAMATSU multi-mesh R2490-05 for one side and EMI pan-type 9839A for another side. The photocathode of each PMT is 40 mm diameter with a red light LED fast driver aside for calibration. Each scintillator itself is inserted in a steel tube and shielded against stray magnetic field. A TYVEK envelope is wrapped around each of the cubic scintillator in order to collect light. The whole tube is fixed with some rubber rings in the center of the PMT. Fig. 1 shows the position of the scintillators at the shielding wall between the LHCb Interaction Point and the accelerator tunnel.

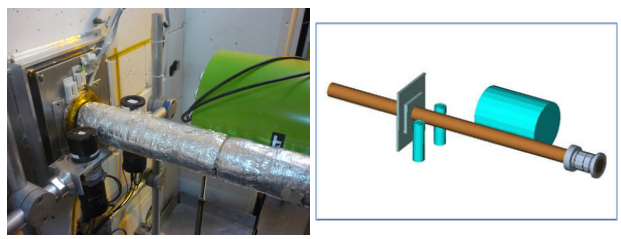

Figure 1: Left: the BLS system as installed in the LHCb cavern. The covered round pipe is the LHC beam pipe. Right: BLS model as implemented in the LHCb simulation.

The pulse generated from the PMT is then processed by an electronics limiter (LeCroy 612AM) which is able to limit the pulse between +0.2 and −5 V regardless of the input signal which can be as high as to −200 V. The limiter has two outputs that allow having the signal observed through an oscilloscope and a hardware readout system at the same time.

In view of the scope of the system as described earlier the readout of the BLS needs a hardware board which must be able to integrate and to read out the signal in short time scale ($\sim$25 ns clock cycle, 40 MHz). It is necessary to analyze the beam over a few turns ($\sim$5–10) at 25 ns time space just after each injection and also to monitor beam effects during a "stable" run, looking at the fine 25 ns structure of the beam. At injection, several problems — "marginal-over-injection" or "under-injection" effects, beam-beam effects (e.g. impedance effects) and misplaced bunches — can occur. It is therefore possible to predict wrong machine settings and injection timings or hardware failures. During circulating beam, misplaced bunches can surely lead to undesired effects as well as an undesired population of protons in the abort gap. LHCb is also the only detector really exposed to a possible dirty beam cleaning since the LHC betatron cleaning is located in one of the adjacent sectors.

Simulations of background estimates at injection and circulating beam are essential to know nominal rates from minimum bias p-p events and from beam halo enabling

*Corresponding author: talanov@ihep.ru. Work partly supported by the Russian Foundation for Basic Research grant No. 10-07-00435

STUDY OF THE INR RAS LINAC PULSED DUOPLASMATRON

A. S. Belov, O. T. Frolov, E. S. Nikulin, V. N. Zubets and V. P. Yakushev, INR RAS,
Moscow, 117312, Russia

Abstract

Results of numerical simulation and experimental study of hydrogen ion beam from a pulsed duoplasmatron with different plasma expansion cup geometry are presented. Intensive oscillations of hydrogen ion beam current with frequency of ~ 1 MHz and amplitude up to 70% from maximum value (~ 100 mA) of ion current were observed with plasma expansion cup of different shape. It was found by direct measurements that these oscillations are formed during plasma transport through the expansion cup. Noiseless mode of operation for the pulsed duoplasmatron has been obtained with a plasma expansion cup of new design. Results of measurements of current and emittance of the hydrogen ion beam are presented

INTRODUCTION

A duoplasmatron-type ion source initially developed at NIIEFA [1] is used for injector of linear accelerator of INR RAS. The ion source has pulsed mode of operation with repetition rate of 50 Hz, pulse duration of 200 μs and pulsed ion current of 50-120 mA. During several years we study the ion source with goal to improve its reliability and increase of brightness of ion beam produced [2]. Initially, ion beam formation system of the duoplasmatron consisted from cylindrical plasma expansion cup 60 mm in diameter and gridded extraction electrode. The grid of the extraction electrode has been made from tungsten-rhenium wires 0.1 mm in diameter [1]. Hydrogen ion beam with pulsed current up to 200 mA has been obtained with this beam formation system. However, significant sputtering of the wires of the grid by beam ions has been observed after long term operation of the ion source. Relative brakes of the wires occurred which reduce reliability of the ion source. Deformation of the grid was arisen also due to its heating by the ion beam.

Additionally, significant unavoidable emittance growth of the ion beam occurred in electric field of the grid cells. This is why several gridless ion beam formation systems were used after that. The gridless ion beam formation system had high reliability and produce formation of hydrogen ion beam with relatively small normalized emittance of 0.1 π cm mrad (for 67% of ion beam current) [2]. However, ion beam obtained with the gridless ion beam formation systems had "noise" (~ 1 MHz oscillating component) which reached in some cases 70% of average value of the ion beam pulsed current. The "noise" appearance was not controlled completely by parameters of the duoplasmatron discharge and extraction voltage. Some measurements were performed to determine the "noise" origination. Then a new ion beam formation system has been developed and tested. With this beam formation system the duoplasmatron produces "noiseless" hydrogen ion beam. Results obtained are outlined in the paper.

STUDY OF "NOISE" ORIGINATION

It was shown by direct measurements that oscillations of the ion beam current are arisen in a plasma expansion cup. Initially, total ion flux emitted from anode orifice to expansion cup has been measured. For that, a flat collector 38 mm in diameter was installed at distance of 16 mm from the anode orifice. The collector was biased by negative potential of ~ 200 V relative the anode to suppress electrons from plasma to come to the collector. The total ion flux current of 350-530 mA was recorded for the duoplasmatron discharge current of 30-50 A respectively. It was found that the ion flux current was noiseless, what means that the "noise" originated downstream the anode emission orifice. Then the ion beam current has been recorded immediately downstream the beam formation system by Faraday cup with suppression of secondary electrons and simultaneously ion beam current to the extraction electrode of the beam formation system has been recorded. It was found that oscillations already exist and that oscillations of ion beam current and of ion current to the extraction electrode are in the same phase. This result shows that oscillations of ion flux at emission plasma surface of the expansion cup are already existed. Thus, it was found that ion current oscillations arisen in the plasma expansion cup. A new ion beam formation system has been developed then with goal to eliminate the "noise" origination.

A NEW ION BEAM FORMATION SYSTEM

Extensive simulations of ion beam extraction from ion source and the ion beam transport in the proton injector were performed to optimize geometry of the ion beam formation system. Program code TRAK of Field Precision LLC [4] has been used for the simulations. The code makes possible simulation of a self-consistent emission plasma boundary of ion sources and ion beam transport with space-charge.

The new ion beam formation system designed is shown in Figure 1. A flat grid made of tungsten wires 0.1 mm in diameter is installed at output of the plasma expansion cup of the beam formation system. Diameter of the emission surface is 30 mm. A plasma electrode of the expansion cup has quasi-Pierce geometry (see Figure 1) with angle 23° relative to the emission grid surface for diameters between 30 and 40 mm. This allows to obtain flat surface of plasma with flat grid by respective choice of extraction voltage for given plasma ion flux and to minimize effective emittance growth connected with initial focusing of ions by curved emission plasma surface

SCRF DEVELOPMENT AT TRIUMF

V. Zvyagintsev, R.E. Laxdal, B. Amini, C. Beard, R. Dawson, T. Emmens, K. Fong, A. Grasselino, P. Harmer, D. Kishi, P. Kolb, A. Koveshnikov, D. Lang, M. Laverty, R. Leewe, C. Laforge, D. Longuevergne, M. Marchetto, A.K. Mitra, T. Ries, I. Sekachev, R. Shanks, B. Waraich, F. Yan, Q. Zheng, TRIUMF, Vancouver, Canada
R.S. Orr, W. Trischuk, University of Toronto, Ontario, Canada
R. Edinger, PAVAC Industries, Richmond, Canada

Abstract

TRIUMF started SCRF development with the superconducting heavy ion linear accelerator project, ISAC-II, in 2000. Since that time much work has been completed for development, prototyping and testing. The ISAC-II project was successfully completed and we now have in operation 40 superconducting bulk Nb QWR cavities assembled in eight cryomodules. The last twenty cavities, just completed, were produced by PAVAC Industries Inc. of Richmond BC; the first superconducting accelerator cavities produced in Canada.

In 2007 TRIUMF started development towards a 50MeV electron superconducting linear accelerator to be used as a driver to produce radioactive ion beams through photofission. The accelerator is based on TTF/ILC elliptical bulk Nb cavities technology.

Results, experience and plans of the SCRF program at TRIUMF will be discussed.

INTRODUCTION

Motivation for SCRF development at TRIUMF was the ISAC-II heavy ion accelerator project started in 2000 and required 20 106MHz medium beta (5.7 and 7.1%) and 20 141MHz high beta (11%) superconducting QWR cavities which provide an accelerating voltage of 40MV. Medium beta cavities were developed in collaboration with LNL and fabricated by Zanon (Italy). Five cryomodules with these cavities were successfully commissioned for operation in April 2006 [1]. High beta cavities were developed at TRIUMF and produced by PAVAC Industries in Canada. Three cryomodules with high beta cavities were successfully commissioned in April 2010 [2]. An SCRF infrastructure for SC development including SCRF test area, clean room and chemical laboratory (Fig. 1) was created at TRIUMF.

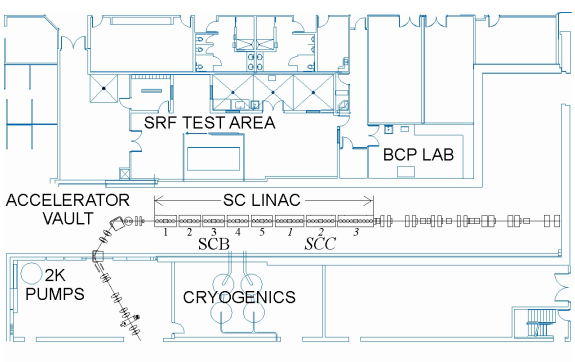

Figure 1: TRIUMF SCRF infrastructure

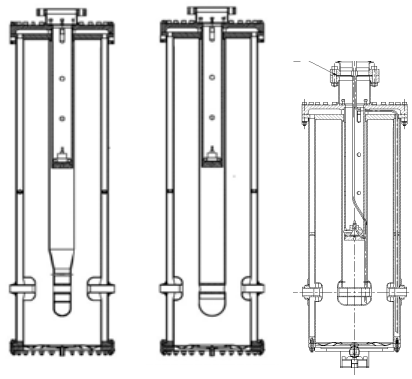

Figure 2: ISAC-II β =5.7,7.1 and 11% cavities

In 2007 TRIUMF has embarked on a 1.3GHz development program to support the construction of a 50MeV 10mA e-Linac for the production of radioactive ion beams through photo-fission. A prototype cryomodule and 9 cell cavity are in conceptual design. Two copper and two niobium single cell test cavities were fabricated, and one copper model of 7 cell cavity is in fabrication at PAVAC Industries.

ISAC-II RESULTS

ISAC-II commissioning and operation results [3] provide an example of bulk Nb QWR cavities in cryomodules with common vacuum. The cavities (Fig.2) are patterned after ALPI INFN-LNL are based on a coaxial line with inner and outer conductors with diameters of 60 and 180mm. The difference between the cavities is in the beam tube region of the inner conductor. The round inner conductor shape of the beta 7.1% 106MHz is modified by squeezing to attain the 5.7% beta cavity. To provide the structure with optimum beta of 11% we went to 141MHz with corresponding decreasing of cavity length. A beam tube is added to improve the transit time factor. All cavities are specified for CW operation at 7W power dissipation with acceleration voltage 1.08MV corresponding to 30MV/m electric and 60mT magnetic peak field. Tuning of the cavities is provided with deformation of Nb plates bolted to the bottom flange. A mechanical damper installed inside of the inner conductor provides >10dB attenuation of microphonics noise. The cavities operate in strong overcoupled regime (coupling ~50-100) to provide enough bandwidth to maintain stable

DEVELOPMENT AND PRODUCTION OF SUPERCONDUCTING AND CRYOGENIC EQUIPMENT AND SYSTEMS FOR ACCELERATORS BY IHEP

A. Ageyev, I. Bogdanov, S. Kozub, E. Kashtanov, K. Myznikov, A. Orlov, P. Slabodchikov, V. Sytnik, P. Shcherbakov, L. Shirshov, V. Sytchev, V. Pokrovsky, K. Polkovnikov, L. Tkachenko, S. Zinchenko, V. Zubko, IHEP, Protvino, Russia

Abstract

Superconducting and cryogenic programs at IHEP were got a powerful upsurge in the early eighties of the last century within the framework of the UNK project. More than hundred model superconducting magnets and the pilot batch of UNK superconducting dipoles and four quadrupoles were produced and tested with the help of cryogenic test facilities built for this purpose. Cooperation with international scientific accelerator centers was developed in last ten years. Two superconducting magnetic systems of Electron Lens for the Tevatron accelerator (USA) were developed, manufactured and successfully brought into operation. 42 cryogenic electrical feed boxes of various types for Large Hadron Collider (Switzerland) were developed, produced and put into commission. Results of the development of fast-cycling superconducting magnets for the FAIR project (European Research Centre of Ions and Antiprotons, Germany) are discussed. Description of the largest in Russia cryogenic system for cooling with superfluid helium of superconducting RF separator for the new beam channel of the U-70 accelerator (Russia) is presented. Design and test results of current leads as well as a dipole magnet on basis of High Temperature Superconductor are reviewed.

ITRODUCTION

In 1967 the 70 GeV proton machine of Institute for High Energy Physics (IHEP) has been commissioned. Experiments at high energies always required of cryogenic techniques (liquid hydrogen and deuterium targets, bubble chambers, cryogenic detectors). Special cryogenic plant and workshop were developed at IHEP.

RESULTS OF ACTIVITY

New generation of high energy proton accelerators is based on superconducting (SC) magnets. In the early eighties of the last century the special cryogenic and superconducting facilities have been created at IHEP in frame of UNK project (Fig.1 – 5). In collaboration with Bochvar's institute SC NbTi wire of 0.85 mm diameter with 8910 of 6 micron filaments was developed. More than 100 SC magnet models and 25 full scale 6 m dipoles (Fig. 6) and four quadrupoles were developed, produced and tested at IHEP [1] - [2]. The main characteristics of the magnets are presented in Table 1.

Figure 1: Machine for SC cable production. Nmax=28 strands of 0.3-1 mm diameter, V=1.5 m/min.

Figure 2: Machine for 6 m length SC coil winding.

Figure 3: Presses for collaring and curing of SC coil. 3800 tons, L = 7m, h = 0.67m.

DEVELOPMENT OF FAST-CYCLING SUPERCONDUCTING QUADRUPOLE AND CORRECTOR MAGNETS FOR THE SIS 300

L. Tkachenko, I. Bogdanov, S. Kozub, P. Shcherbakov, P. Slabodchikov, V. Sytnik, V. Zubko
Institute for High Energy Physics, Protvino, Moscow region, 142281

Abstract

IHEP participates in the development of superconducting fast-cycling magnets for the FAIR project. In the frame of this project IHEP has developed a prototype of the main quadrupole, assigned for using in the SIS300 ring. The main parameters of the quadrupole are: 45-T/m central gradient in 125-mm ID of the coil with the useful aperture of 105 mm; the gradient ramp rate is 10 T/m/c and the length of the prototype is 1 m. The main characteristics of the designed quadrupole magnet are discussed here. The correction system consists of multipole magnets, resonance and chromaticity sextupoles and steering dipoles. The multipole magnet contains octupole, sextupole and quadrupole coils and the steering magnet involves horizontal and vertical dipoles. Geometries of corrector and steering magnets are presented as well as their main magnetic parameters.

INTRODUCTION

During the past several years IHEP has took part in the FAIR project [1]. At the moment, IHEP's main tasks are to develop a design of the main quadrupole [2], [3], [4], as well as designs of the corrector and steering magnets [3] for the SIS 300 ring. The optimized 2D and 3D geometries of the quadrupole and the main magnetic characteristics of the magnet are presented. The preliminary designs of the corrector and steering magnets for the SIS 300 as well as their main characteristics are presented too. All magnetic characteristics were calculated with a help of computer programs MULTIC [5] and HARM-3D [6].

QUADRUPOLE; REQUIREMENTS

Main quadrupole requirements are: the central gradient (G_0) is equal to 45 T/m; the inner beam pipe diameter is 105 mm; the gradient ramp rate is 10 T/m/s; the injection gradient is 10 T/m. The region of good field quality is r_0 = 40 mm and the effective length of the magnet is 1 m. The temperature margin has to be at least 1 K. Alterations of lower multipoles of the integral field at r_0 should be less then 2×10^{-4}. Additional requirements are: minimal geometric length; simple and reliable design; low AC losses in the magnet; minimum risks; cost reduction.*

QUADRUPOLE; 2D GEOMETRY

The main characteristics of the superconducting wire are: 0.825-mm strand diameter; 3.5-μm filament diameter; a 5-mm filament twist pitch, a Cu/superconductor ratio of 1.4, a critical current density of J_c = 2.7 kA/mm^2 (at 5 T, 4.2 K). Ratio of ρ_{300}/ρ_{10} is more than 70. Superconducting strands will have Staibrite coating.

Numerical simulations showed that it is enough to have a cable with 19 strands in order to meet given requirements for the quadrupole. Such type of cable was used for the UNK magnets [4]. The cable will be fully keystone with a width of 8.45 mm and an average height of 1.56 mm (with insulation). The cable will be insulated by polyimide tape in three layers. The radial thickness of the insulation after assembly and cool down is 125 μm and azimuth thickness is 98 μm. It is estimated that the cable will have contact crossover resistance in 0.02 mΩ and transverse resistance in 20 mΩ [6].

The 1-layer coil is divided by three blocks, allowing suppress the first three multipoles in the approximation of an infinitely high permeability in an iron yoke with the inner cylindrical surface. The geometric parameters of the coil are presented in Table 1, where N is a number of turns; φ, α are the initial and final angles of the block. The operating current is 6.262 kA. The ID of the iron yoke, made from 2212 electric steel, is 190 mm and the iron thickness is 52 mm. The iron yoke has four notches with 17×30 mm^2 dimensions for location of bus bars placed symmetrically under 45° as well as four adjusting bolts for quadrupole arrangement in the cryostat (Fig. 1).

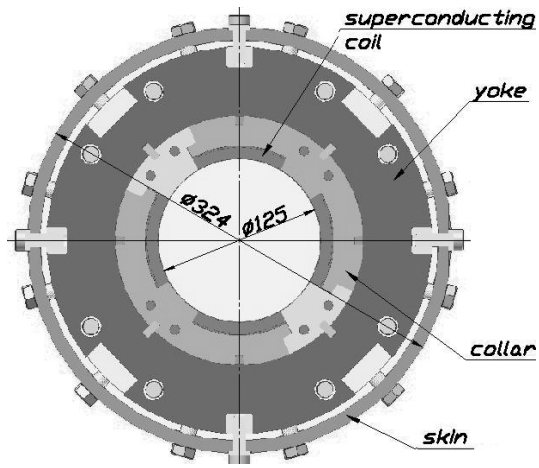

Fig. 1: General view of the cross section.

Table 1: Main Geometric Parameters of Coil Block

	N	φ	α
1	8	0.129	11.413
2	7	11.959	21.831
3	5	26.604	33.656

Field dependences for the normalized gradient and

* This work was completed with financial support from Rosatom, contract H4e45.03.10.1027

COOLING SYSTEM OF THE SIS300 ACCELERATOR

A. Ageev, S. Kozub, S. Zintchenko, V. Zubko, IHEP, Protvino, Russia

Abstract

The Facility for Antiprotons and Ion Research (FAIR) being under construction in Germany as an international project is a cascade of accelerators; two last accelerators from this cascade will be made with the use of superconducting magnets. The large volume of the executed work on the SIS300 superconductive equipment allowed to start the estimation of the basic parameters of SIS300 cooling system. On the base of many research notes and calculations the item-by-item heat load budget at the helium temperature level is composed. Cooling system flow diagram is proposed, the calculated single phase helium temperature profiles along the string of magnets are presented and discussed. Helium flow pressure drop along the string of magnets during cooling down is calculated on the basis of "temperature wave" model and cooling down time of the accelerator is estimated.

GENERAL COOLING SCHEME OF SC MAGNETS

According to [1], all SIS300 magnets will be divided into two equal cryogenic strings, each one to be supplied with separate flow of single-phase helium.

Based on this, following flow scheme is proposed for cryostating the string of superconducting (SC) magnets (Fig.1). In this scheme single-phase (supercritical) helium from the helium refrigerator is cooled in the subcooler and enters the string of the magnets, where it is heated due to the heat leaks and heat release, and simultaneously it is cooled in the heat exchangers located in the dipoles.

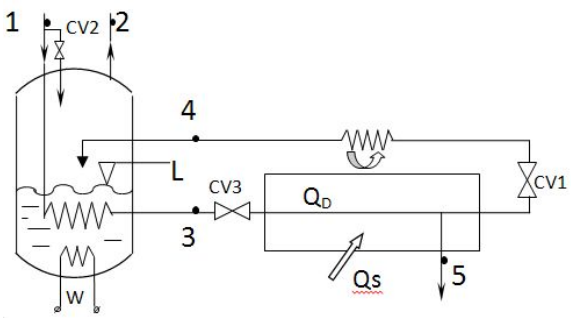

Figure 1: Flow scheme proposed for cryostating the string of SIS300 superconducting magnets.

At the end of the magnet string the single-phase helium is throttled in the J-T valve CV1, and it is converted into two-phase helium, which flows through the dipole heat exchangers of the magnet string into the subcooler. In the subcooler two-phase helium is separated to the vapor and liquid. Liquid helium is used for cooling single-phase helium in the heat exchanger of subcooler and helium vapor returns to the refrigerator.

The flow scheme is considered functional if one of the main conditions for the cryostating is satisfied: the quality factor x of the two-phase flow of helium at the exit from the magnet string is less than or equal to 0.95 (for Fig. 1 $x_4 \leq 0.95$). This is necessary for the stable heat exchange between the two-phase and single-phase flows of helium in the heat exchangers of dipole magnets.

Heat balance equations for the flow scheme in Fig. 1 at the conditions of maintaining the fixed level of liquid helium L by the control valve CV1 (CV2 is closed) and of zero flow rate through the current leads at point 5:

$$G_1 * i_1 + Q_D + Q_S = G_1 * i_2 \quad (1),$$

$$G_1 * i_3 + Q_D + Q_S = G_1 * i_4 \quad (2),$$

where i - enthalpy of helium flow; G_1 – helium mass flow rate; Q_D and Q_S – AC losses and static heat leaks.

From equations (1) and (2):

$$i_4 = i_3 + i_2 - i_1 \quad (3).$$

Equation (3) clearly shows that parameters of helium flow in point 4 at the exit from the magnet string, including its quality factor, do not depend on the heat leaks and heat release values, but depend only on the input/output parameters of the subcooler (points 1 and 2, Fig. 1). For the values given in table 10, using the thermodynamic properties of helium tables [2], one could obtain quality factor at the string exit $x_4=0.951$, which practically corresponds to the requirement of $x_4 \leq 0.95$. In fact, due to the presence of certain helium flow for cooling of current leads (point 5, Fig. 1), quality factor at the string exit will be below 0.95. This quality factor can be decreased by powering the electric heater W (Fig. 1).

The main part of SIS300 dipoles are about 8m length so for cooling the magnets it was decided to use single-phase (supercritical) helium, which directly washes the single-layer superconducting coil.

In the upper part of the cold mass this dipole magnet the heat exchanger is located, in which single-phase helium is cooled by two-phase helium. Thus, in each dipole magnet the heat released in the superconducting coil is removed by single-phase helium and the heat from the single-phase helium is removed by two-phase helium [3], [4].

Heat load on the cryogenic system from the cryomodules and the multipoles is considerably less in comparison with the load from the dipoles; therefore cooling of the single-phase flow by two-phase flow is not arranged in their designs. This means that in the cryomodules and in the multipoles both the heat release and the heat leak are removed only by single-phase flow.

HEAT LOAD OF SIS300 CRYOGENIC SYSTEM. PARAMETERS OF THE MAIN HELIUM FLOWS

Below we will consider the cryogenic system heat load at the helium temperature level (~4.5 K) only, as the thermal shields heat load at 50-80 K in the allowable range does not effect the functionality of SC magnets.

*Work supported by ROSATOM, contract H.4e.45.03.10.1027

A FAMILY OF TWENTY-AMPERES POWER SUPPLIES FOR MULTI-POLE CORRECTORS FOR ACCELERATORS AND STORAGE RINGS

O. Belikov, V. Kozak, A. Medvedko, BINP, Novosibirsk, Russia

Abstract

For decades, we at Budker Institute of Nuclear Physics SB RAS have developed precision power supplies for the electromagnets of accelerator facilities and storage ring complexes in broad range of output power. Some tasks, e.g. powering correctors, multipole magnets and low-current bending magnets, operate with up to 20A regulated current sources with an output power of about a few kilowatts [1]. Our long-term experience in the development and operation of power supplies resulted in the creation of the MPS-20 (Magnet Power Supply) family of three types of reversible power supplies. The output current of these supplies can be varied in the range of ±20A; the output voltage is ±50V, ±100V, and ±150V for MPS-20-50, MPS-20-100, and MPS-20-150, correspondingly. The power supplies developed meet the requirements of the up-to-date accelerator facilities.

INTRODUCTION

A magnetic system of the up-to-date accelerator and storage ring facilities requires a number of different regulated current sources, the large variety of which complicates the operation of a facility as a whole. That is why the goal of this work was to develop universal current sources which could be used at various accelerator facilities.

For instance, the precision experiments with colliding electron-positron beams requires a very stable magnetic field of the collider, which constrains the long-term instability of the output supply current for the magnets.

The acceleration of a charged particle beam requires good dynamic of magnetic field dynamics in an equilibrium orbit. Thus it is necessary to regulate the current in the windings of the magnetic elements in the parts of energy variation: during the energy boost in the acceleration mode and during the reduction to the injection energy. Since the impedance of corrector is the sum of the resistive impedance and the active impedance, a reverse polarity voltage is often required for regulation of the current decreasing. Thus current sources with a 4-quadrant current/voltage operation are required.

CURRENT SOURCE STRUCTURE

The circuit design was special subject to the possibility of realization of the required algorithms for the output current regulation with a high efficiency of the power supply for electromagnets. The design chosen is based on a circuit with double RF conversion (Fig. 1)

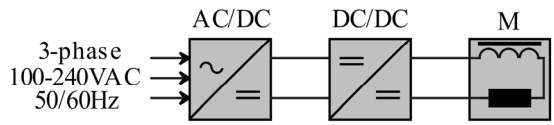

Figure 1: AC/DC and DC/DC are the Alternating current / Direct current and Direct current / Direct current convertors; M is the electromagnet.

AC/DC converters with isolated output voltage are used to get a DC buffer voltage. Those are usually conventional AC/DC converters, industrially manufactured voltage stabilizers. The output current is regulated with a DC/DC converter, a schematic diagram of which is given in Fig.2. The power part of the unit

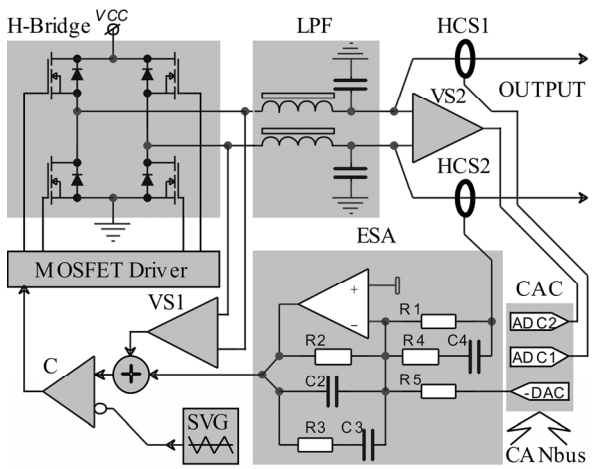

Figure 2: H-Bridge – H-Bridge inverter, LPF – Low-pass filter, HCS – Hall Current Sensors, VS – Voltage sensor, ESA – Error-signal amplifier, CAC – Controller with the CANbus interface, ADC – Analog-to-digital converter, DAC – Digital-to-analog converter, C – Comparator, SVG – Sawtooth-voltage generator.

includes the H-Bridge made on four MOSFET switches. The output current is regulated by the pulse width modulation of the output voltage of the bridge inverter. A second-order filter, LPF, is used to suppress voltage of the carrier frequency and its harmonics. Its suppression ratio is 60 dB or more.

The output current is measured with two identical noncontact Hall current sensors HCS1 and HCS2 of the current – compensating type. One sensor is used in the feedback loop; the other serves as an independent monitor for the control system.

The current-feedback loop provides the required quality of regulation. The mains ripple of 50÷360Hz is partially

FIRST RADIOCARBON MEASUREMENTS AT BINP AMS

S.A. Rastigeev, A.R. Frolov A.D. Goncharov, V. F. Klyuev, S.G. Konstantinov, E.S. Konstantinov, L. A. Kutnykova, V. V. Parkhomchuk, M.V. Petrichenkov, A. V. Petrozhitskii
BINP, Novosibirsk, Russia.

Abstract

Present status of the BINP accelerator mass spectrometry (AMS) facility is described. The results of experiments for beam selection and radiocarbon concentration analysis in trial samples are presented.

INTRODUCTION

The AMS is mainly dedicated for dating of archaeological, paleontological and geological samples by measurements of the ratio between carbon isotopes.

The BINP AMS facility [1] includes negative ion source, folded type vertical electrostatic tandem accelerator, magnesium vapors stripper [2], the high-energy and low-energy beam lines with analyzers, time-of-flight final detector [3].

The negative ion beam is horizontally extracted from the ion source. Then the beam is vertically injected into the low energy accelerating tube through injection channel with 90° magnet. The negative ions are accelerated to the positively charged high voltage terminal and stripped to charge state 3+ in magnesium vapors stripper. Then they pass through the 180^0 electrostatic bend and then again are accelerated vertically into the high energy accelerating tube to the ground potential. Then ions are horizontally put to the final detector through high-energy channel with 90° magnet.

The most distinguishing feature of our AMS machine is the use of additional electrostatic separator of ion beam, located inside the terminal. Interfering isobaric molecules are destroyed by collisions in the stripper into the terminal and are selected immediately after the stripping process. It is important to decrease the background from molecular fragments before the second stage of acceleration [4], because the energy of fragments is always less then the ion energy (at this moment). The next important distinguishing feature is magnesium vapours stripper instead of the gas stripper. The gas flow into the accelerator tubes leads to big energy spread in the beam thus limiting the sensitivity and accuracy of spectrometer. The molecular destruction and ion recharging by magnesium are localized into the hot tube of the stripper.

BINP AMS FACILITY MODIFICATIONS

Now the AMS facility created at BINP SB RAS is installed at CCU “Geochronology of the Cenozoic era”. The accelerator is placed into underground room with radiation shielding. The inner size of the room is 6 x 6 x 7.5 meters. The basic parts of electronic devices are located outside of the shielding room and connected with accelerator elements. The local equipment of the water cooling, compressed air and gas transfer system has been installed.

The 500 kV terminal voltage was achieved with 1 atm atmospheric air into pressure tank (without insulating gas). The equipment for gas filling and drying was not used, but the silica gel was placed directly into the tank. Initially, the terminal voltage was limited by the water vapor condensate on the cool surface of the gas turbine feeding dielectric tube, located along the accelerator column. This tube is used for terminal turbine feeding by compressed air. The electrical conductivity of condensed water distorts the electric fields, which can induce electrical breakdown. For prevention of water condensation, the lower part of the tube (outside of the tank) was heated. Now the electrical breakdowns are occurred only during the first start after tank closing, as we assume, due to the dust accumulation when the tank is open. Recently, 1 MV terminal voltage was achieved by using low cost air-gas mixture. The tank was pumped to the 0.8 atm air pressure, and then the tank pressure was increased to 1.6 atm by four nitrogen gas-cylinder. The 4 kg of SF_6 gas was added (+0.02 atm) to increase the electrical strength of the mixture. The 1 MV has been achieved without breakdowns.

The multi-cathode (for 24 samples) sputter ion source has been recently manufactured and installed. It's needed for synchronous analysis of the samples and for comparison of the tested samples with the reference one. The negative ions are produced by bombarding graphite target with positive cesium ions. The Cs+ ions are produced on a hot tantalum ionizer (1100^0C) by cesium vapor from the oven (180^0C). The cesium ion beam is focused on the carbon sample placed on the cathode, because the working surface of ionizer is a spherical-shape cup. The copper sample holder has the inner diameter of 2 mm. The holder is water cooled to reduce sample heating. The cesium ions leaving the ionizer are accelerated by 7 kV potential. The negative carbon ions are accelerated by the same potential and extracted through the hole 6 mm in diameter in the center of the ionizer. The power consumption of the ion source does not exceed 250 W. The test sample in ion source is selected by sample wheel rotation. The stepping motor with Pi/25600 rad/step resolution is used for sample changing. The process of rotation is controlled by motor driver and checked by optoelectronic sensor system (at every turnover) and by video camera (online).

The new magnesium vapors stripper has been manufactured and installed. All hot parts of striper are located in vacuum. It prevents corrosion of striper surface by the tank gas mixture. The power consumption is about 50 W.

HIGH POWER ELV ACCELERATORS FOR INDUSTRIES APPLICATION

N.K. Kuksanov, Yu.I. Golubenko, P.I. Nemytov, R.A. Salimov,
S.N. Fadeev, A.V. Lavruhkin, A.I. Korchagin, D.S. Kogut, A.M.Semenov
Budker Institute of Nuclear Physics SB RAS Lavrentyev av. 11, Novosibirsk, 630090, Russia

Abstract

Beginning from 1971, the Budker Institute of Nuclear Physics Siberian Branch of Russian Academy of Science (SB RAS) started its activity in the development and manufacturing of electron accelerators of the ELV-type for their use in the industrial and research radiation-technological installations. The ELV-type accelerators were designed with use of the unified systems and units enabling thus to adapt them to the specific requirements of the customer by the main parameters such as the energy range, beam power, length of extraction window, etc.. INP proposes a series of electron accelerators of the ELV-type covering the energy range from 0.3 to 2.5 MeV with a beam of accelerated electrons of up to 400 mA and maximum power of up to 400 kW. The design and schematic solutions provide the long term and round-the -clock operation of accelerators under the conditions of industrial production processes. The ELV accelerators are especially popular accelerators not only in Russia, but in China, Korea, and etc The cross-linking technologies are applied very widely in industries. While the improved maximum operating temperature was one of the initial attractions of cross-linking, there are other important product advantages as a results of cross-linking of the polymers, such as: reduced deformation under load, improved chemical resistance, increased abrasion resistance, improved impact properties, memory characteristics. At present the electron-beam technologies are extensively used in a cable industry for cross-linking of insulation made on the basis of polymer compositions. The use of these technologies enabled to develop the manufacture of a wide range of wires, cables and heat-shrinking goods for different markets (power plant, telecommunications, electronics, oil industry, nuclear power plant, submarine and aircraft, etc). All of them are of high reliability, when being mounted and during operation as under standard and extreme operating conditions.

INTRODUCTION

The use of electron-beam technologies gave an opportunity to develop the production of wide range of wires, cables, heat-shrinking products (heating cables, power and ship cables, airborne wires and cables, as well as atomic power plant (A-plant) wires). All of them are of improved reliability at assembly and operation as in regular service and in extreme conditions. The quality of radiation treatment depends on accelerator itself as well as on under-beam equipment. Thus, the accelerators should provide stability of electron beam parameters, such as energy, beam current and width of irradiation area. In order to enhance absorbed dose azimuthal homogeneity they should be provided by 4-side irradiation system.

The main specification of the system of cable transportation through radiation zone is transportation rate of speed, which should be proportional to beam current rate. Proportionality coefficient called “specific rate” depends on the type of irradiated product and accelerator parameters. Taking into account the information mentioned above, there was developed the high-automated systems for electron-beam treatment of cable isolation. Practically, there is no necessity in permanent presence of accelerator control panel operator. Effective visualization of irradiation process (energy, beam current, cable transportation speed) allows the operators of transportation line to control and set the treatment conditions directly at working place close by pay-off and take up machines.

ACCELERATORS

The main features of ELV-accelerators are as follows:

1. High power of electron beam in wide energy range, it means high productivity of EB processing;

Fig.1 Accelerator ELV-8

2. High efficiency of conversation of electricity power to electron beam power. The efficiency is limited by frequency converter and in case of transistors frequency converter efficiency is increased up to 80-92%;

55 MEV SPECIAL PURPOSE RACE-TRACK MICROTRON COMMISSIONING*

A.I.Karev, A.N.Lebedev, V.G.Raevsky, P.N.Lebedev Physical Institute, RAS, 119991 Moscow, Russia
A.N.Ermakov, A.N.Kamanin, V.V.Khankin, N.I.Pahomov, V.I.Shvedunov, SINP MSU, 119992 Moscow, Russia
N.P.Sobenin, MEPhI, Kashirskoe shosse 31, 115409 Moscow, Russia
L.Brothers, L.Wilhide, Valley Forge Composite Technology Inc. (VFCT) 50 East Rivercenter Blvd., Suite 820, Covington, KY, USA

Abstract

Results of Lebedev Physical Institute RAS 55 MeV special-purpose race-track microtron (RTM) commissioning are presented. RTM is intended for photonuclear detection of hidden explosives based on initiation of photonuclear activation and consequent registration of secondary gamma-rays penetrating possible screening substances.

INTRODUCTION

The purpose of the work consists in development of an effective photonuclear detector of hidden explosives to be used under stationary conditions and in mobile systems for searches of field mines. The detector consists of a source of high energy gamma - radiation and counters fixing the secondary radiation from decay of short-living isotopes formed in explosives due to reactions with nitrogen and carbon nuclei [1]. The gamma source is based on a specialized microtron (RTM) for energy of 55 MeV. A RTM photo is presented in Fig. 1, main RTM A RTM photo is presented in Fig. 1, main RTM parameters reached by commissioning are listed in Table 1.

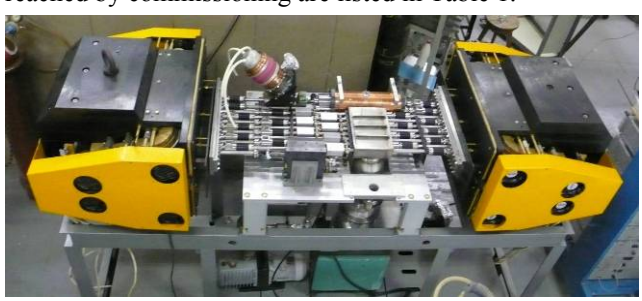

Figure 1: RTM photo.

Table 1: RTM parameters

Output energy	55 MeV
Output pulse current	10 mA
Repetition rate	5 – 50 Hz
Number of linac passages	11
Energy gain / turn	5 MeV
Current pulse length	5 μs
Operating frequency	2856 MHz
End magnet field	1.0 T
Maximum RF power	2.5 MW
Orbit circumference increase / turn	1 λ

RTM has been built following a classical scheme with two 1 T end magnets and a standing wave linac between them providing 5 MeV energy gain per pass. A 50 keV beam from an electron gun is injected into linac through a 45^0 magnet and a solenoidal lens. The 5 MeV electron beam after the first acceleration is reflected by the end magnet field back to the linac axis and is accelerated up to 10 MeV - the energy sufficient to bypass the linac at the next turn. The beam is extracted from the last orbit *with a dipole of 17.5^0 deflecting angle. More details about the RTM scheme can be found in [2].

RTM SYSTEMS

RF system

The RF system is based on a multibeam klystron KIU-168 [3] with a rare earth permanent magnet focusing system providing 6 MW/6 kW pulsed/average power at 2856 MHz. The klystron is compact, its high voltage pulse amplitude is only 54 kV, so it does not need oil insulation and can be installed under the RTM table. A pumping port, a vacuum window, and a circulator are installed between the linac and the klystron.

The non-vacuum part of the waveguide tract is filled with SF_6 at 2 bars. Parameters of the vacuum window and the circulator by commissioning restricted the maximum RF power transported to the linac by 2.5 MW and thus restricted a maximum exit pulsed beam current by 10 mA. The klystron is fed by a "hard" modulator [4] with pulse duration up to 15 μs. To simplify the RF system we use a self-oscillation mode of operation with linac structure included in a feed-back loop [5]. Optimal conditions for self-oscillations and for RF power level regulation are controlled with a phase shifter and an attenuator installed in the feed-back loop. In Fig. 2 the klystron current, the high voltage and RF field pulses are shown. The 8 μs high voltage pulse duration is set externally. The delay of about 3 μs between the high voltage front and RF pulses is the time required for building-up self-oscillations from the noise. This time can be decreased by adding a low power "igniting" RF signal to the feed-back loop.

* This work was supported by CRDF Grant #RP0-10732-MO-03 (LLNL)

MAGNETIC COUPLED DISK-LOADED WAVEGUIDE

N.P.Sobenin, S.V.Kutsaev, M.A.Gusarova, M.V.Lalajan ,D.S.Kamenschikov, A.Yu.Smirnov
R.O.Bolgov
Moscow Engineering-Physics Institute, Russia.

Abstract

The results of numerical simulations of electrodynamical parameters (EDP) of magnetic coupled disk-loaded waveguide (DLS) with negative dispersion are presented in this article. Different structure variants for high and low phase velocity were considered. High order modes and multipacting discharge issues were also regarded.

INTRODUCTION

The most common accelerating structure for electron linacs is DLS at travelling wave (TW) and biperiodic accelerating structure (BAS) at standing wave (SW)

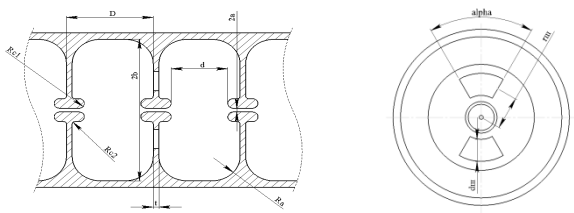

a) longitudinal section b) transversal section

Figure 1: Magnetic coupled disk-loaded structure

TW magnetic coupled accelerating structure (DLSM) presented at Fig.1 unites the advantages of both electric coupled DLS (small fill time) and BAS (high shunt impedance). This structure is able to work in backward wave regime at the modes less than π [1].

STRUCTURE OPTIMIZATION

To design a linac which use DLSM as an accelerating structure it is necessary to find its optimal dimensions in order to obtain the best electrodynamical parameters. These parameters are the following: shunt impedance r_{sh}, normalized electric field strength $E\lambda/P^{1/2}$ and attenuation α. It is important to know their dependences on operating mode θ, group velocity β_{gr} and coupling coefficient k_c. This optimization was done for the frequency equal to 5712MHz.

Aperture Radius Optimization

First, electro-dynamic parameters dependences on aperture radius to wavelength ratio a/λ were found. At each value of a/λ the coupling holes dimensions were adjusted to make either coupling coefficient or relative group velocity equal to 1%.

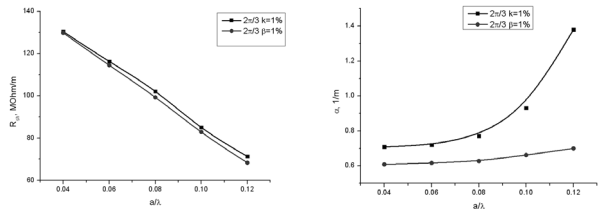

a) shunt impedance b) attenuation

Figure 2: Parameters dependences on aperture radius

The larger aperture radius means the larger acceptance but also the larger electric coupling. To retain the chosen coupling coefficient it is necessary to increase the magnetic coupling. Besides, the large aperture reduces the electric field concentration near the axis, thus leading to shunt impedance decrease and overvoltage coefficient K_E increase. The results are presented at Fig.2. The $2\pi/3$-mode was chosen as an operating mode for DLSM.

Operating Mode Optimization

Second, it is necessary to optimize the operating mode of the structure, in order to obtain the maximum shunt impedance and normalized field strength. Also, the coupling coefficient and group velocity should be reasonable. The group velocity has the most influence on electric field among all other parameters. Thus, the coupling holes dimensions were adjusted to make β_{gr} equal to 1%.

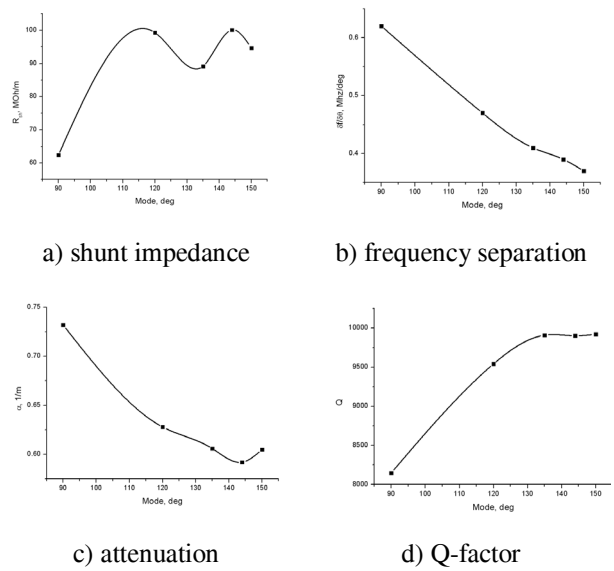

a) shunt impedance b) frequency separation

c) attenuation d) Q-factor

Figure 3: Parameters dependences on the operating mode for DLSM

FEASIBILITY OF ALTERNATIVE PHASE FOCUSING FOR A CHAIN OF SHORT INDEPENDENTLY-PHASED RESONATORS

V.V. Kapin*, A.V. Nesterovich, MEPhI#, Moscow, Russia.

Abstract

Alternative phase focusing (APF) is usually realized in a long drift-tube structure with multiple acceleration gaps. The synchronous phase alternates periodically gap-by-gap according to either sinusoidal or square-wave laws. The period of synchronous phase oscillations depends on charge-to-mass ratio of accelerated ions and increases with beam energy. One period may include up to 10-20 accelerating gaps. In the case of square-wave law, the sets of 5-10 neighbouring gaps have the same synchronous phase, while whole structure consists of continuous chain such gap-sets with a constant value of synchronous phases. Therefore, every such gap-set can be formed into a separate resonator. As result a long multiple gap structure is converted into a chain of short independently-phased resonators. Such realization of APF linac allows more flexibility in a phase variation, while additional focusing-matching lenses can be set up in betweens of resonators. In this report possible parameters of such linac are evaluated and discussed.

INTRODUCTION

The APF belongs to the wide class of focusing methods by axially symmetrical RF fields provided in sequences of drift-tubes with axially symmetrical cross-sections. The original APF idea of beam focusing by a periodical alternating a synchronous phase in a sequence of the drift-tube gaps has been developed and modified since the early 50's by many authors. In the papers [1-5], there are comprehensive lists of references to the most known recipes of generating the APF drift-tube structures.

In the APF linac, the synchronous phase alternates periodically gap-by-gap according to either sinusoidal or square-wave laws. The period of the synchronous phase oscillations may include up to N_g=10-20 accelerating gaps which forming up one focusing period.

Usually, APF is considered for long multiple-gap resonators containing several tens of drift-tubes. However, APF linac also can be realized as a chain of short independently-phased resonators similar to superconductiong heavy-ion linacs [6]. For example, APF linacs consisting of the chain of *identical* short independently-phased resonators had been analyzed in Ref. [7,8], while S.A. Minaev [7] considered resonators with one and two gaps and increasing N_g along linac, and E.S. Masunov [8] considered 4-gap "fork" structures with a constant N_g=4.

The main feature of both concepts is constant number of gaps in every short resonator. It is known [1,2], that in order to preserve a position of working point on the stability diagram, it is necessary to increase N_g along the linac. For example the approach of Ref. [7] uses an increasing number of N_g along the linac (up to 10-20). Alternatively, in the approach of Ref.[8], operating point can be stabilized by an additional focusing force.

In this paper, it is suggested to use a chain of short independently-phased resonators with increasing number of the gaps in every short resonator along a whole linac. This feature may minimize the total number of short independently-phased resonators, while preserving a position of working point on the stability diagram without an additional focusing force.

APF IN CHAIN OF RESONATORS

Method for stability analysis

The stability analysis is based on the methods developed for the asymmetrical alternative phase focusing (A-APhF), which has been proposed by V.V. Kushin in more than 30 years ago [1,2]. In the report [9], stability conditions had been extended for an arbitrary law of the synchronous phase oscillations.

Following Ref. [9], the synchronous phase sequence can be written as the step-wise function $\varphi_s(\tau) = \overline{\varphi} + \widetilde{\varphi}(\tau)$, which is the sum of the constant and varying functions $\overline{\varphi}$ and $\widetilde{\varphi}(\tau)$, respectively, while $\widetilde{\varphi}(\tau)$ is constant within every accelerating period. The focusing period of APhF linac L_f coincides with the period of phase excursions. With independent variable $d\tau = dZ_s / L_f$, small phase deviations of particle phase ψ and a linear radial motion ρ can be expressed by the following Matiew-Hill equations:

$$\begin{cases} d^2\psi/d\tau^2 + P_\psi(\tau)\cdot\psi = 0 \\ d^2\rho/d\tau^2 + P_\rho(\tau)\cdot\rho = 0 \end{cases}. \qquad (1)$$

where the periodical step-wise functions $P_\psi(\tau) \equiv P_\psi(\tau+1)$ and $P_\rho(\tau) \equiv P_\rho(\tau+1)$, are given by the following equations

$$\begin{cases} P_\psi(\tau) = 2B\cdot\sin[\overline{\varphi} + \widetilde{\varphi}(\tau)] \\ P_\rho(\tau) = -B\cdot\sin[\overline{\varphi} + \widetilde{\varphi}(\tau) + \psi] \end{cases}, \qquad (2)$$

The focusing strength B [1,2] is given by

*kapin@mail.ru
#National Research Nuclear University "MEPhI"; http://www.mephi.ru

DEVELOPMENT OF WIRE-MESHED ELECTROSTATIC LENSES FOR PROTON LINAC

V.V. Kapin*, B.Yu. Bogdanovich, A.V. Nesterovich,
V.V. Yanenko, MEPhI#, Moscow, Russia

Abstract

The 2-MeV 150-MHz proton RFQ linac is set up at the Radiation-Acceleration Center (RAC) of Moscow-Engineering Physics Institute (MEPhI). Its output beam-line contains doublet of the electrostatic focusing lenses with a novel design featured by the two-dimensional electric field and wire-meshed beam apertures. Every lens provides a transverse focusing effect only in one plane, while does not affect on the beam in a perpendicular plane. In this report, the analytical and numerical analysis of this lens is presented. The optics of output beam-line including these lenses is evaluated with TRACE-3D code. The experimental construction of the lens doublet is presented.

INTRODUCTION

The 2-MeV 150-MHz proton RFQ linac [1] is set up at RAC of MEPhI. It serves as a base system for the applied research works. Its output beam-line consists of doublet of the electrostatic focusing lenses, the post-accelerating 7-gap two-ridge interdigital H-resonator and a magnetic C-shaped spectrometer with vertical magnetic field.

Initially, the output beam-line with focusing doublet of two magnetic quadrupoles (instead of electrostatic lenses) had been simulated with TRACE-3D code [2]. It was shown [3] that the beam transmission is less than 10% without a focusing doublet, and it can reach 100% at the optimal magnetic field gradients of 6-7 T/m.

Although these gradients are quite moderate for a modern technology, a fabrication of quadrupoles may require impermissible efforts and resources for our small experimental setup. Therefore, the alternative focusing system based on wire-meshed electrostatic lenses had been proposed. In this report, the features and status of doublet of the electrostatic focusing lenses are presented.

WIRE-MESHED ELECTROSTATIC LENS

General Scheme of the lens

An unconventional design of the electrostatic lens featured by the two-dimensional electric field and wire-meshed beam apertures is proposed. Figure 1,a shows the ideal 2D-layout of such lens, which consists of two plane electrically-grounded wire-meshes located at planes $z=\pm l/2$ and two (upper and lower) high-voltage (U_m) cylindrical electrodes of radius R located at distance a from z-axis. The 3D model of the lens and the distribution of electric potential in the lens cross-section at $x=0$ are shown in Fig.1,b and Fig.1,c, respectively.

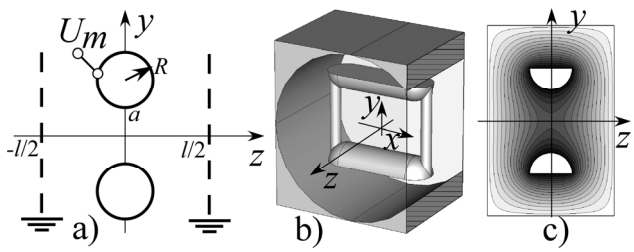

Figure 1: Layout of wire-meshed electrostatic lens: a) 2D ideal layout; b) 3D model; c) potential at $x=0$.

Such lens provides a transverse focusing effect only in one plane (the Y0Z-plane in Fig.1), while does not affect on the beam in a perpendicular plane (the X0Z-plane in Fig.1). The pair of such lenses rotated by 90-degree relatively each other can provide an independent focusing in both transverse planes.

Focal distance evaluation

Let's evaluate the focal distance in a this-lens paraxial approximation according to the formulae

$$f_y = y_0 / \mathrm{tg}(\alpha_y) \approx y_0 / \alpha_y , \qquad (1)$$

where y_0 is the transverse particle coordinate at the lens center and $\alpha_y \approx \Delta v_y / v_z$ is the angle kick provided by the lens. Let's neglect deviations of the longitudinal velocity v_z. Then, the increment of the vertical velocity Δv_y can be expressed as

$$\Delta v_y = \frac{q}{m_0 \gamma v_z} \int_l E_y \cdot dz , \qquad (2)$$

where the integral can be treated as a transverse lens voltage U_y. Note, that the transverse voltage can not exceed the electrode potential

$$U_y = \int_l E_y \cdot dz \le U_\mathrm{m} . \qquad (3)$$

Finally, the angle kick α_y is expressed as

$$\alpha_y = U_y / (W \beta_z^2), \qquad (4)$$

*kapin@mail.ru
#National Research Nuclear University "MEPhI"; http://www.mephi.ru

INPUT COUPLERS FOR THE DIPOLE MODE PERIODIC STRUCTURES

A. Anisimov, M. Lalayan, A. Smirnov, N. Sobenin,
National Research Nuclear University – MEPhI, Moscow, Russia
A. Zavadtsev, D. Zavadtsev, S. Kutsaev
Nano Invest, Moscow, Russia
L. Kravchuk, V. Paramonov
Institute for Nuclear Research of Russian Academy of Sciences, Moscow, Russia

Abstract

Three variants of the input coupler for the periodic deflecting structure, operating at hybrid dipole E_{11} mode, with the phase velocity equal to the light speed are considered: non-symmetric design and two symmetric designs with auxiliary rectangular waveguide and shorting plates in it along with auxiliary cut-off rectangular waveguide. The reflection coefficient dependences on the coupling window width and on the coupling cell diameter was been investigated for all these coupler variants. The reflection coefficient has been calculated in the whole dipole mode pass-band. The field asymmetry in the beam area has been investigated. The eigen frequency of the coupling cell has been calculated.

INTRODUCTION

Three input coupler designs have been developed for Transverse Deflecting System. 16-cell deflecting structure is shown on Fig.1 with three input coupler versions: non-symmetric coupler (a), symmetric coupler with shorting plates in additional waveguide (b) and symmetric coupler with cut-off additional waveguide. Three variants of the disk loaded waveguide (DLW), operating at 2997.2 MHz frequency and $2\pi/3$ mode, as a deflecting structure are considered: with two holes stabilizing the deflecting plane position, with two recesses at periphery cylindrical surface and with elliptical aperture hole [1].

SIMULATION MESH CHOICE

The simulation accuracy of the deflecting structure with two couplers in traveling wave operation depends on mesh used. The calculation of the TDS cell geometry has been done using 3-cell model with two coaxial couplers (Fig.2). The electric field distribution at $2\pi/3$ mode in resonant model and the tetrahedron simulation mesh in the traveling wave model are shown in Fig.2. The calculation has been done frequency band 2996.2 - 2998.2 MHz with frequency step df=0.05 MHz.

Figure 3 shows the number of mesh cells (a), reflection S_{11} (b) and tuning quality ratio K (c) depending on the number of simulation iterations for 16-cell deflecting structure with two couplers. The tuning quality ratio shows uniform distribution of the transverse electric field in the iris planes. The same mesh in 3-cell and in 16-cell models is equivalent to 64949 and 407464 tetrahedrons correspondently.

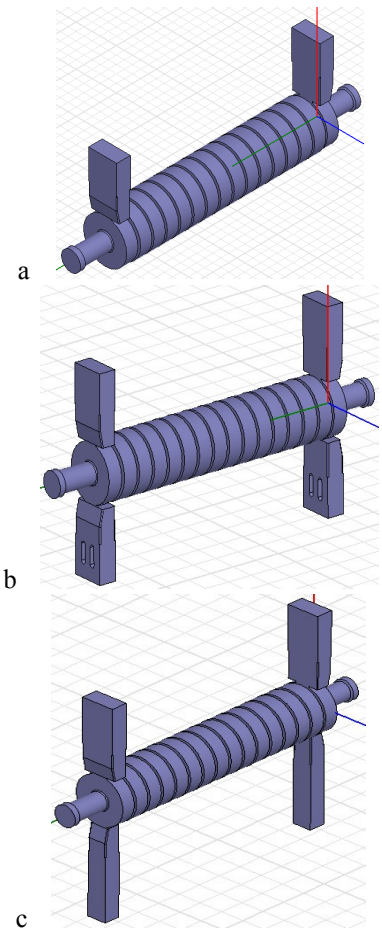

Figure 1: The deflecting structure with three input coupler variants.

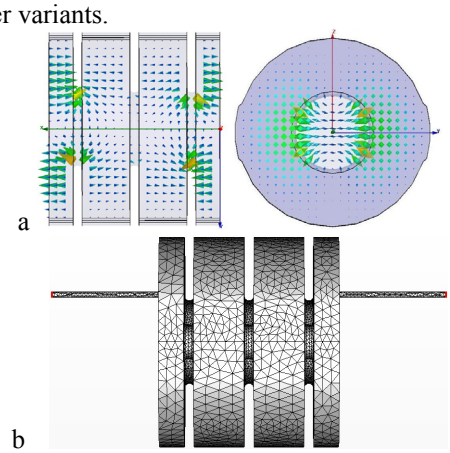

Figure 2: The field distribution in resonant model (a) and the mesh in the traveling wave model (b).

MATERIALS FOR FAST CYCLING ACCELERATOR SUPERCONDUCTING MAGNETS

P. Shcherbakov, I. Bogdanov, S. Kozub, L. Shirshov, P. Slabodchikov, V. Sytnik, L. Tkachenko, V. Zubko, Institute for High Energy Physics, Protvino, Moscow region, 142281

Abstract

Development of fast-cycling superconducting magnets with high field amplitudes and ramp rate makes severe requirements especially to material properties in order to improve field quality and to reduce AC losses. Analysis of experimental and literature data is fulfilled for magnetic characteristics of electric steels at different temperatures. Susceptibilities of stainless steels of different grades are examined as well as a tolerance on the value of the magnetic permeability. Mechanical, thermophysical and technological properties at room and cryogenic temperatures are presented. Comparison of steel characteristics, selected for the SIS300 quadrupole prototype, with the steels, used in the SIS300 dipole and steels, applied in the SIS100 prototype magnets is carried out. General advices to the choice of materials for electrical and stainless steels, used in a design of fast-cycling magnets, are given. *

INTRODUCTION

IHEP takes part in the development of SC magnets for SIS300 from 2001 year [1]. The substantiation of steel selection for fast cycling magnets of FAIR SIS300 and SIS100 was the one of IHEP task. Accelerator dipoles work at the field ramp rates 1 T/s and 4 T/s correspondently. The main materials of SC magnet design beside the superconductor are yoke electric steels and stainless steels for collars, vacuum pipes and other elements.

In 2003 in IHEP and GSI the study of magnetic properties of steels with 1-4% Si at different temperatures have been carried out. The anisotropy of magnetic properties has been determined and hysteresis loss have been measured in symmetric, unipolar and partial cycles [2].

Main conclusions of R&D are: a) the reducing of temperature up to 4.2 K effects on magnetic properties less than in low carbon steels; b) anisotropy, obtained on the strips of one direction (in the rolling direction and transverse one) is averaged in the ring samples, and the properties of isotropic and anisotropic steel with similar Si content are approximately the same.

In this paper the emphasis is made on the technology and possibilities of industry

The selection of stainless steels for the FAIR magnets is similar to the choice in big "slow" SC projects (Tevatron, SSC, LHC). The enormous experience in the development and study of stainless steels has been obtained during magnet development for LHC. This experience is valid for fast cycling magnets of FAIR with taking into account eddy currents at 4.2 K.

In this paper the magnetic properties of stainless steels, acceptable for the production of the collars, vacuum chambers and other elements at 300 and 4.2 K are presented.

IHEP is developing the SIS300 quadrupole, models of SIS100 magnets are developing in JINR, BINP and GSI.

ELECTRIC (ET) STEELS FOR YOKE

Severe requirements for yoke steels of SIS100 and SIS300 are given to field quality and AC losses, determined by coercivity H_c and saturation magnetization M_s, which in turn depend on Si content: H_c have to be less than 40 A/m for dipoles and 70 A/m – for quadrupole of SIS300 magnets; M_s have to be greater than 2.0 T and be as high as possible.

The carried out measurements of magnetic properties of Si steels together with analysis of literature data and steel maker catalogs allowed us to make the list of steels, which can be used as yoke material for dipole or quadrupole of the SIS 300 and SIS 100 magnets, depending on demands to field quality or acceptable AC losses. The short and full scale models of the SIS 300 and SIS 100 magnets have been made during R&D using the steels from the candidate list. The testing of these models and comparison of field quality and AC losses as well calculations with detailed models and obtained steel magnetic properties give the possibility of problem understanding and greater certainty in steel choice.

In Table 1 the steels with Si content 1.5-3% are presented [3, 4, 5]. Coercive force H_c lies in the range of 20-65 A/m, specific hysteresis loss W_h in unipolar cycles with B_{max} = 2 T at 4. 2 K is in the range of 30-60 mJ/kg, saturation magnetization Ms is in the range of 2.0-2.1 T.

Table 1: Steels with 1.5-3 % of Si content

Grade	Type	Si, %	Thickness, mm	Country
M250-50	Isotropic	3	0.5	Germany
M350-50	Isotropic	1.5	0.5	Germany
2412	Isotropic	3	0.5	Russia
2212	Isotropic	1.5	0.5	Russia
M600-100	Isotropic	3	1	Germany
M700-100	Isotropic	2.4	1	Germany
M800-100	Isotropic	1.5	1	Germany
3413/3414	Anisotropic	3	0.5	Russia

* This work was completed with financial support from Rosatom, contract H4e45.03.10.1027

STUDY OF ELECTRODYNAMIC AND THERMODYNAMIC MECHANISMS INFLUENCING STABILITY OF SUPERCONDUCTING RUTHERFORD CABLE

V. Zubko, S. Kozub, I. Bogdanov, L. Tkachenko, L. Shirshov, P. Shcherbakov
Institute for High Energy Physics (IHEP), Protvino, Moscow region, Russia, 142281

Abstract

Stability for superconducting fast-cycling dipoles and quadrupoles plays an important role. A feature of a complex network of strands and strand-to-strand contacts, current distribution in the network has to be taken into account for superconducting cables. The coupled numerical simulation of electromagnetic and thermal processes in Rutherford superconducting cables during the initiation of a quench was carried out. The network model has been combined with thermal analysis, which allows one to model quench dynamics, including the effects of a current redistribution in strands, discontinuities and inhomogeneity, the initial heating in strand, and as a result occasional quench recovery or runaway quench propagations.

Results for the minimum quench energy for cables with core are presented and dependence the minimum quench energy from various parameters of cable is discussed.

INTRODUCTION

Russia expressed interest in the international project FAIR participation [1]. At the moment, IHEP's main tasks are to develop a design of the main quadrupole [2] for the SIS300 ring.

The main quadrupole requirements are as follows: 45 T/m central gradient; 10 T/m/s the field ramp rate; 10 T/m injection field. Maximal magnetic field in the coil is 3.5 T, the operating current I_{op} is 6.26 kA [2], working point at 70% along the load line.

As the given magnet is fast-cycling, it is necessary to have a cable with low losses and simultaneously with a good redistribution of currents between strands of the cable at a quench. For this purpose Rutherford cable has a core decreasing losses in a perpendicular magnetic field and strands, coated by a 0.5 μm thick Staybrite with low resistance for good redistribution of currents between strands.

The thickness of the core is 25 μm and the width is 6 mm. The core is made from an annealed 316L stainless steel foil. The cable with 19 strands is fully keystone, it has the 8.25 mm wide and the average thickness of 1.447 mm. The transposition length is 60 mm, all parameters are presented in [2].

The stability of the superconducting cable against local disturbance is described in general by a curve, presenting the Minimal Quench Energy MQE, as a function of the current I or ratio the current to the critical current I/I_c. If there is current redistribution between strands of cable, normally these curves exhibits a sharp 'kink', separating two distinctive stability regimes. The current, at which the 'kink' occurs, is called I_{kink} [3, 4, 5]. Above the 'kink' MQE of the cable is equal to the single strand MQE. Below I_{kink} MQE of the cable can be more than two orders of higher than the MQE of a single strand, this current redistribution increases stability. In order to improve the stability, a shift of the 'kink' to higher current and an increase of the quench level left from the 'kink' is highly desirable. This can be achieved by increasing heat transfer to helium and the Residual Resistance Ratio of the copper RRR, and decreasing contact adjacent resistivity R_a and thermal contact.

APPROACH FOR ANALYSIS OF MQE

For the study of MQE the cable was fabricated with properties, almost the same as the original cable of quadrupole has. The cable used three types of strands with different critical current density: 2548, 2632 and 2406 A/mm^2 (5T, 4.2K), Cu/NbTi ratio of the cable is 1.45, RRR differs from 110 to 200.

Further for MQE analysis the current of the cable is used instead of the ratio I/I_c as strands have the different critical currents, so it is difficultly to calculate correctly the ratio of the current to the critical current of the cable. Other reason is impossibility to compare the working point on the load line with I_{kink}/I_c, as MQE measurements were carry out at a constant magnetic field. MQE is possible to study numerically as a function of magnetic field for turn in the high magnetic field of the magnet [5]. In this case one can compare the working point on the load line with $I_{kink}/I_c(B)$ but it is difficult to compare with measurement dates I_{kink}/I_c (constant magnetic field, therefore constant I_c)

The measurements of MQE were carried out in liquid helium (pressure of 1 atm., temperature of 4.3 K), so it is necessary to compare measured and calculated results. General experimental arrangements are described in [6].

Simulations of MQE were performed with code, developed in IHEP [7] and the CUDI program, developed in CERN [8].

These codes consist of electrodynamics and thermal parts. For electrodynamics part basic input parameter is a contact resistivity, which can be measured. For cable with core the contact adjacent resistivity R_a is about 0.2 mΩ and the crossover resistivity R_c is larger than 20 mΩ [9].

In thermal part the most difficult is correctly to define a heat transfer through thermal contact resistance between contacting strands and between strands and helium.

* This work was supported by Russian Foudation for Basic Research, project number **09-08-00528-a**.

SUPERCONDUCTING TRANSFORMERS FOR STUDY OF HIGH-CURRENT SUPERCONDUCTING CABLES

L. Shirshov, I. Bogdanov, E. Kashtanov, S. Kozub, P. Shcherbakov, P. Slabodchikov, L. Tkachenko, V. Zubko, Institute for High Energy Physics (IHEP), Protvino, Moscow region, Russia, 142281

Abstract

A facility for measurement of the critical current and minimal quench energy of Rutherford-type superconducting cables for accelerator magnets is created. The current in the sample is energized by a superconducting transformer circuit, using an inductive method, where the sample conductor is a part of the secondary circuit. Two superconducting transformers have been built; one of them is a solenoid type coil. The transformer consists of two concentric solenoids; the secondary coil is placed inside the primary coil. External magnetic field up to 6.5 T is provided by a superconducting solenoid with the aperture diameter of 60 mm. The second superconducting transformer with race-track coils has been designed and taken into operation. Short-circuited sample, fixed on a special holder, is placed in the aperture of a superconducting dipole magnet such way that the plane of sample loop is perpendicular to direction of external magnetic field, which can reach up to 6 T. The critical current of the secondary superconducting coil is 18 kA. The equipment for measurements of characteristics of a superconducting cable versus magnetic field is described.

INTRODUCTION

One of the main tasks in a development of superconducting magnets is measurements of current carrying characteristics of a superconducting (SC) cables and wires. Some equipment for measurement of the critical currents and minimal quench energy (MQE) has been development and produced in IHEP.

A direct powering of the sample by a power supply causes high losses in current leads at a level of 10 кА, what leads to large losses of liquid helium in a cold zone. The inductive method of a current input is applied for reduction losses of liquid helium and achievement of high values of currents in samples.

The description of the SC transformer design, with a help of which a study of SC cables with different coating of SC wires has been carried out, is presented in [1]. The hairpin sample and the secondary winding of transformer are fixed on the cryostat insert, can be placed into the cryostat with liquid helium, where the superconducting solenoid and primary transformer winding are fixed stationary, thus allowing one to make a fast replacement of the sample. This equipment allows one to measure characteristics of usual Rutherford type cables. The current carrying element with the stainless steel core between two layers of Rutherford type cable (cored cable) [2] will be used for the SC coils of quadrupole magnets of the SIS 300 ring [3]. New equipment, developed and produced in IHEP, gives a possibility to study samples of different types of SC cables in an extended region of uniform magnetic fields.

Two designs of SC transformer are tested; one of them consists of solenoid coils. One of them is used a SC dipole for a creation of an external field, another one is based on a solenoid magnet.

TRANSFORMER WITH RACE-TRACK COILS

The design of equipment is shown in Fig.1 and its basic parameters are presented in Table 1. An external magnetic field with an enough large region of homogeneity is necessary for study of SC cable characteristics. From the technological reasons this magnetic field is created by SC dipole, placed into the boiling cryostat.

The part of the sample, which is being studied, is the secondary coil of the SC transformer. The measuring section of the sample is fixed in the holder at the length of 830 mm under the pressure 80 MPa. The secondary SC contour has one joint, located above the coils. The detachable insertion is put and fixed in the aperture of the dipole with a diameter of 80 mm.

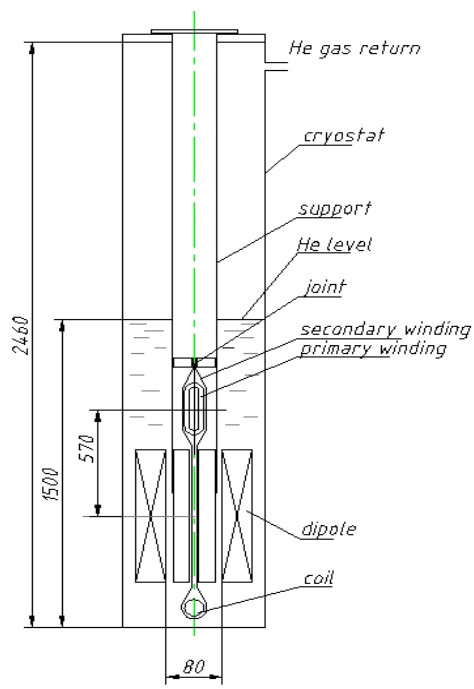

Fig.1. The general view of the equipment with SC dipole.

EXPERIMENTAL STUDY OF CHARACTERISTICS OF CABLE FOR FAST-CYCLING SUPERCONDUCTING MAGNETS

I. Bogdanov, E. Kashtanov, S. Kozub, P. Shcherbakov, L. Shirshov,
P. Slabodchikov, L. Tkachenko, V. Zubko
Institute for High Energy Physics, Protvino, Moscow region, 142281.

Abstract

Fast-cycling magnetic fields, produced by superconducting magnets of the SIS300 accelerator, generate cable losses, which should be reduced by increase of contact resistances between wires in the cable. For this purpose various methods of cable interstrand resistance increasing are used successfully. But the values of contact resistances have strong influence on a stability, which could be characterized by minimum quench energy (MQE).

From this point of view at IHEP it was carried out the experimental study of Rutherford type 19-strand superconducting cable with high value of contact resistances. Contact resistances and MQE measurements were performed. The description of features of samples, the measurement scheme and procedure are presented along with the experimental results.

INTRODUCTION

Last years IHEP developed the superconducting magnets for modern particle accelerators using fast-cycling magnetic fields. IHEP participates actively in FAIR project. In particular it is responsible for the development of superconducting correctors, quadrupole magnet of accelerator ring SIS300, and also for the choice of its design current carrying element [1]. Maximum magnetic field in this quadrupole coil is 3.5 T and field ramp rate is about 0.8 T/s [2].

The high and fast-ramping field in superconducting magnet generates large AC losses. For the purpose of reduction of losses try to make cable with relatively high value of the adjacent resistance Ra, which is the side-by-side resistance between adjacent pairs of strands, and the crossover resistance Rc, which is the resistance of each crossover contact. The knowledge of these resistances values, and also the ways of their control has great value already at a magnet design stage.

Two years ago we reported the results of study of cables with Ni or Cr coated surfaces of strands and it was shown that AC losses in the SIS300 quadrupole can be effectively suppressed by increasing of interstrand contact resistances by such coating. In recent time for quadrupole the cable design was chosen with stainless steel core. For such cable the interstrand resistances can be controlled independently by means of a high-resistance metallic core (Rc) and by proper oxidation of the wire surface (Ra).

Main task of this work was the study of the influence of cable curing parameters on the interstrand resistances value. Due to profound effect of these resistances on stability against short point heat pulses the minimum quench provoking energy of cable was measured too.

* This work was supported by Russian Foudation for Basic Research, project number **09-08-00528-a**.

INTERSTRAND RESISTANCES

The tested cable consists of 19 NbTi strands with diameter of 0.825 mm. The strands are coated by a 0.5-μm thick Staybrite. The cable has a core with thickness of 25 μm and width of 6 mm, which is made from an annealed 316L stainless steel foil. The cable is fully keystoned and it is 8.25 mm wide and has average thickness 1.447 mm without insulation. The transposition length is 60 mm.

All tested samples were made from the same original cable. The preliminary heat treatment was done in order to form the high resistive oxide layers on the surface of cable strands. The pieces of original bare cable were heat treated in air under no pressure at 200ºC during 2 and 4 hours. Then cable was insulated be three layers of polyimide tape. The last layer was PIXEO adhesive tape.

Four cable pieces were stacked with the alternation of keystone angle direction. This package was placed into the fixture mould, which consists of two massive iron block equipped by electrical heaters and temperature sensors. After the mould was placed into the hydraulic press and the curing was performed according to regime, shown in Fig. 1.

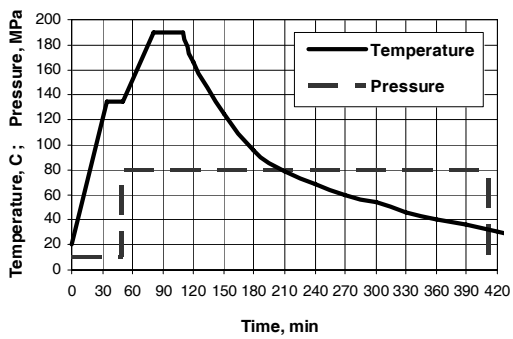

Figure 1: Curing cycle of stack of samples.

From the cured stacks the testing samples were cut, placed into sample holder and were compressed at room temperature once again up to 80 MPa on the length of 60 mm (one transposition length) and were fixed with help of bolts. Two inner layers in stack were equipped by potential taps and were used for measurement with the help of the VI method [3]. Current up to 100 A was fed into two opposite strands of cable sample (strands 1 and 10 in our case, Fig. 2 a), which was immersed into liquid helium bath. Voltage drop on strands 3, 5, 7, 9, and 10 was measured relative to strand 1. For example, the resulting profile of normalized voltage versus strand

THE ELECTRON LINEAR ACCELERATOR LUE-200 – DRIVER THE IREN FACILITY

Boettcher Ju., Zamriy V.N., Kayukov A.S.,
V.V. Kobets, I.N. Meshkov, V.F. Minashkin, V.G. Pyataev, A.V. Skripnik, A.P. Sumbaev,
V.G. Shabratov, V.A. Shvets, V.N. Shvetsov, JINR, Dubna, Moscow region, 141980, Russia
P.V. Logachev, V.M.Pavlov, BINP, Novosibirsk, 630090, Russia

Abstract

It is reported on startup of the first stage of the Intense REsonance Neutron source installation (IREN) at the Frank Laboratory of Neutron Physics of the Joint Institute for Nuclear Research. The general scheme and current status of the electron linear accelerator with accelerating structure on a S-band traveling wave (f = 2856 MHz) are presented. Results of adjustment of the basic functional systems of the linac and the measured parameters of the beam (pulse current of a beam – 3,0 A, electron energy - 30 MeV; duration of a pulse current - 100 ns; rep, rate - 50 Hz) are reported. The integral neutron yield from nonmultiplying target reaches $(3\div5)\cdot10^{10}$ n/s.

INTRODUCTCTION

Linear electron accelerator LUE-200 [1, 2] was designed at the Budker Institute of Nuclear Physics of Siberian branch of RAS (Novosibirsk) as the driver for intense resonance neutron source IREN [3].

Accelerator consists of the pulsed electron gun, accelerating system, RF power supply system based on 10-cm range klystrons with modulators, beam focusing and transport system including wide aperture magnetic spectrometer and vacuum system. Accelerator is allocated vertically inside 3-floors building. Its designed parameters are listed in table 1. At the beginning the nonmultiplying neutron producing target will be used.

Table 1: LUE-200 designed parameters

Parameter	**Value**
Maximal electron energy, MeV	200
Pulse beam current, A	1.5 – 2.0
Accelerated electron pulse width, ns	≤ 250
Repetition rate, Hz	150
Accelerating rate, MeV/m	35
Beam power, kW	9 – 12

IREN FACILITY COMPONENTS

Electron sourse

LUE-200 electron source is the 2-electrode electron gun with 12 mm diameter oxide thermocathode. Cathode is fed by 200 kV pulsed transformer. The anode – wall of the vacuum chamber with hole 43 mm in diameter closed with wire frame made of stainless steel. Electron gun provides pulsed electron beam with 8 A peak current, 250-300 ns duration, 50 Hz repetition rate and ≤ $0.01\cdot\pi\cdot$cm·mrad emittance.

Accelerating system

Accelerating system consists of the RF buncher and 2 short (3 meters long) accelerating sections with high acceleration rate. Accelerating sections were designed and manufactured at BINP (Novosibirsk). Accelerating section represents the circular blinded waveguide with constant impedance fed by RF power. RF power comes from klystrons – RF power amplifiers of 10-cm frequency range (2856 MHz). The prototype of the accelerating system was tested at foreinjector of the VEPP-5 complex of BINP. During the tests the maximal electric field 45 MV/m and average accelerating rate 35 MeV/m were achieved [4].

Full scale accelerator project foresees two accelerating sections. At present one accelerating section is used the second one is replaced with drift section surrounded by two quadruple lenses doublets.

RF power supply

As the optimal RF power supply for LUE-200 accelerator the SLAC 5045 were chosen providing peak RF power 60 MW at average level 45 kW. RF power compression system is introduced to provide 3-4 times gain in RF power transfer to the accelerating section providing average accelerating rate up to 35 MeV/m. Main components of the RF system of the accelerator are: two-channel high frequency driving generator with possibility to set 180 degrees phase shift between channels and fast phase reversal; two RF preamplifiers for klystrons actuation; two power compression systems; waveguides, couplers etc.

At present due to the absence of SLAC 5045 klystrons only one accelerating section was put into operation with TH2129 (Thomson) klystron providing 20 MW peak power.

Beam focusing and transport system

Beam focusing and transport system provides beam transporting and trajectory correction on the way from electron gun to the nonmultiplying neutron producing target. From electron gun to the RF buncher 3 short solenoidal magnetic lenses are focusing electron beam.

INVESTIGATION ON THE ELECTRON BEAM FORMATION IN THE MAGNETRON GUN WITH A SECONDARY-EMISSION CATHODE USING THE MAGNETIC SYSTEM BASED ON PERMANENT MAGNETS

A. N. Dovbnya, V.V. Zakutin, N.G. Reshetnyak, N. I. Aizatsky, V. N. Boriskin, V. P. Romas'ko, I. A. Chertishchev, N. A.Dovbnya, National Science Center "Kharkov Institute of Physics & Technology", 1 Akademicheskaya St., Kharkov, 61108, Ukraine

INTRODUCTION

The interest in the physics of processes with crossed electric and magnetic fields is aroused in connection with their wide application in the high-power vacuum electronics. Of a particular interest is the use in such devices of electron magnetic guns with secondary-emission cathodes as electron sources [1-3]. In the investigations of magnetron guns used were relatively long [1, 3] secondary-emission cathodes placed in the longitudinal magnetic field formed by the solenoid.

The present paper gives the results of investigations on the electron beam formation in the magnetron guns with secondary-emission cathodes having small longitudinal sizes in the magnetic system based on the permanent annular magnets made of NdFeB material.

EXPERIMENTAL SETUP AND INVESTIGATION METHODS

Experiments aimed to the investigation of the electron beam formation and its parameters were carried out at the facility schematically shown in Fig.1. For the electron beam powering a long (~50 μs) pulse generator was used. The present system uses a complete discharge of the storage capacitor C_1, advancing through the correcting circuit L_2R_2 to the pulse transformer. Using the low-resistance circuit: L_2 = 134 μHn and R_2 ~ 3 Ohm it is possible to decrease the voltage pulse drop during the high-current electron beam generation. The discharge of the capacitor C_2 provides a top-surge voltage pulse transmitted to cathode 4. The surge amplitude is from 10 to 45 kV, and the pulse repetition rate is from 3 to 7 Hz. Anode 5 is earth-connected via the resistor. The magnetron gun was placed in the vacuum chamber with a pressure maintained to ~10^{-6} Torr. The beam parameters were studied by means of Faraday cup 6 with 12-channel computer-assisted measuring system 7.

The investigations were carried out using the digital storage oscillograph Tektronix TDS-2014.

The cross-sectional dimensions of the beam were measured by making an indentation on the targets made of different materials.

The experiments on the electron beam formation in the magnetron gun with secondary-emission cathodes were realized using a magnetic system based on permanent annular magnets 8.

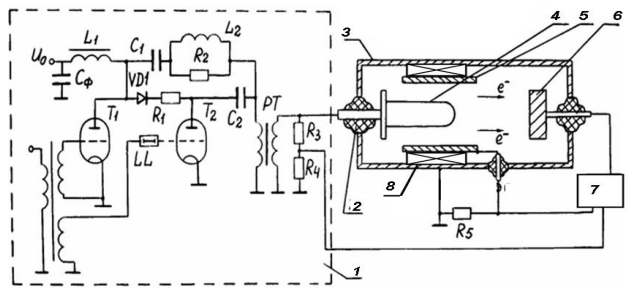

Fig.1. Schematic representation of the experimental setup: 1 – pulse generator, 2 – insulator, 3 – vacuum chamber, 4 – cathode, 5 – anode, 6 - Faraday cup, 7 – computer measuring system, 8 – permanent annular magnets.

EXPERIMENTAL RESULTS AND DISCUSSION

For experiments permanent annular magnets of NdFeB having internal diameter of 60 mm, external diameter of 80 mm and thickness of 10 mm were manufactured. The distribution of longitudinal (H_z) and radial (H_y) magnetic field components for magnetic assemblies was studied depending on the number of rings in the system. The most optimum field for the beam forming magnet system, with relation to the field homogeneity of ±5 % and its amplitude of ~750 Oe, is the magnetic system of 10 rings having 10 cm in length (Fig.2).

Since we have selected a magnetic system having the longitudinal magnetic field amplitude of ~ 750 Oe, it was necessary to select the magnetron gun geometry for realization of experiments and electron beam generation.

In the previous experiments [1] investigations were carried out using the magnetron beam with the cathode of 5 mm in diameter, the anode of 50 mm in diameter, and the maximum cathode voltage of 60 kV in the solenoidal magnetic field with amplitude of 200 Oe. It has been shown that the beam generation is reached with the drift velocity V_D ~ cE/H~0,15c . At lower cathode voltages of 26…27 kV, the electron beam was formed in the magnetic field of 900…950 Oe, and the radial component was ~10 Oe.

The estimates show that in the experiments using the magnetron gun with the anode of 56 mm in diameter and cathode of 5 mm in diameter at the cathode voltage of 20 kV it is necessary to have a magnetic field of ~750 Oe for electron beam forming. The investigation of electron beam formation and its parameters was carried out for two geometries of magnetron guns: anode diameter of

ONE ASPECT OF THERMAL STABILITY FOR 4-VANE RFQ OPERATION WITH HIGH HEAT LOADING

V.V. Paramonov*
Institute for Nuclear Research of the RAS, Moscow, Russia

Abstract

Due to dispersion properties, 4-vane RFQ cavity without resonant coupling is a thermally unstable structure. With deterioration of balance for local detuning, especially near cavity ends, there is a possibility for runaway in the field distribution and related thermal-stress effects. It can, in principle, finish with irreversible plastic deformations and cavity frequency shift. Both the increment and the threshold of instability are proportional to the average dissipated RF power. This possibility increases for long RFQ cavities. Also particularities for the cavity ends design are important. Some general features of this effect are discussed and illustrated with simulations.

INTRODUCTION

The Normal Conducting (NC) RFQ cavity is now the imprescriptibly part of the hadron's linac. For proton linac 4-vane RFQ with operating TE_{210} mode is now prevailing. The sensitivity of the field longitudinal distribution to the shape deviations in such cavities strongly depends on the relative RFQ length $\frac{L_c}{\lambda_0}$, where L_c is the RFQ length and λ_0 is the operating wavelength. To reduce it for long RFQ cavities, $\frac{L_c}{\lambda_0} \geq 5$ the resonant coupling with special coupling cells was proposed [1], providing for RFQ properties of compensated structure in the field distribution sensitivity and stability. The shorter RFQ cavities, $\frac{L_c}{\lambda_0} \leq 5$, as a rule, are without coupling cells. It this report the stability of the longitudinal field distribution in time for RFQ without resonant coupling is considered with respect thermal induced geometry perturbations.

OPERATING REGIME STABILITY

In modern proton linac's RFQ operate with the frequency $f_0 \sim (324 \div 402.5)MHz$, maximal electric surface field $E_{sm} \sim 1.8E_k \approx (25 \div 32)\frac{MV}{m}$, which corresponds to the maximal magnetic field at the regular RFQ surface $H_{sm} \sim 5.2\frac{kA}{m}$. It results in the pulse heat dissipation is of $P_p \approx 100\frac{kW}{m}$. Even for operation with duty factor $d_f \sim (1 \div 6)\%$ the average heat dissipation $P_a \sim (1 \div 6)\frac{kW}{m}$ is significant for thermal effects. The temperature of the cavity increases and f_0 decreases due to the cavity expansion. For the fixed cooling conditions the cavity frequency shift df_0 is linearly proportional to P_a.
Suppose a steady-state high RF power operation with a reference field distribution in the cavity is achieved. Let us suppose a small local temperature deviation $\delta T > 0$ at the cavity surface due to some reasons. It may be either cooling fluctuation or electric discharge. This local temperature deviation leads to the local cavity expansion and local frequency change δf. The local frequency change δf immediately results in the change of the field distribution along the cavity and the change of the field in place of local heating. Depending on the cavity dispersion properties, two options, shown in Fig. 1, are possible.
In the first case, Fig. 1a, the local field relatively decreases.

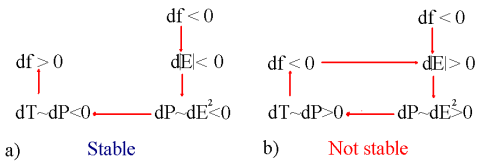

Figure 1: Thermal stable (a) and unstable (b) chain.

The local RF power dissipation decreases, the local temperature decreases, the local frequency increases, canceling or reducing initial frequency deviation δf. It is the stable case. After some time the cavity returns to operation with the reference field distribution.
In the second case, Fig. 1b, the local field, together with the local RF power dissipation, relatively increases, the local temperature increases, the local frequency decreases, amplifying initial local frequency deviation δf. Self-amplifying runaway starts and in the cavity itself there is no physical mechanism, which can stop it.
As it is shown in [10], without resonant coupling 4-vane RFQ cavity is thermal unstable.

$$\vec{E} = \vec{E}_0 - \sum_n \sqrt{8}\vec{E}_0 \frac{\delta f_0}{f_0}(1 + \frac{4L_c^2}{n^2\lambda_0^2})cos(\frac{n\pi z_0}{L_c}). \quad (1)$$

As one can see from (1), the negative local frequency deviation $\delta f_0 < 0$ at the cavity end leads to the local field increasing $\delta|\vec{E}| = |\vec{E} - \vec{E}_0| > 0$.
Most dangerous is the detuning of the cavity ends, $z = 0, L_c$. This effect linearly rises with the cavity length $\frac{L_c}{\lambda_0}$, because the relative detuning $\frac{\delta f_0}{f_0}$, caused the same absolute local deviation δf_0 is inverse proportional to L_c.

RFQ ENDS DETUNING

The RFQ vanes have undercuts in the cavity ends to return magnetic field flux, to tune the cavity frequency and tune longitudinally the field distribution. Different shapes are known - the undercut with a small tip ($N1$ in Fig. 2a,

* paramono@inr.ru

THE DETECTION OF THE LEAKS LOCATION IN THE VACUUM CHAMBER ACCORDING TO SPUTTER-ION PUMPS CURRENT MEASUREMENTS

K.G. Mirzoev, A.M. Kiver, V.G. Lapygin, A.V. Larionov.
Institute for High Energy Physics (IHEP), Protvino, Moscow Region, Russia.

The present work is focused on developing methods to determine the locations of leaks in the extended vacuum chamber what is similar to chamber proton synchrotron U-70. This refers to small leaks that are difficult to detect by leak detector. Leak location is determined by measuring the air pressure in the chamber near the connectors of the diode-type sputter-ion pumps which pump out the chamber. The pumps discharge currents were used as the pressure gauges, as described in [1]. The main components of residual gas in the chamber are hydrogen and air, which come from gassing at the walls and above mentioned uncontrolled leakages, respectively. The flow and the pressure of hydrogen in the chamber were determined as described in [2], and the current of discharge corresponding to this pressure was determined as described in [1]. The discharge current corresponding to the air was determined by subtracting the current required for pumping out hydrogen from the total pump discharge current. Air pressure can be determined by the formula:

$$P = 1.67 \times 10^{-4} I^{0.92} \quad (1)$$

where the discharge current is expressed in amperes and the pressure in mm Hg. We assume that the sections of the ring between two adjacent pumps are the separate chambers. During a number of sessions of the accelerator we carried out measurements of currents in the process of alternate shutdown of neighboring pumps in six chambers. For some of these chambers the locations of leaks and air flows through them were known [3]. These observations allowed us to determine the empirical coefficients, showing what fractions of air pressure at pump connections to the chamber are the partial pressures of air components - nitrogen, oxygen and argon, as well as what are the fractions of flow of air components in the chamber and their fractions of total air discharge current. This allowed us to develop a methodology to detect a leak at its arbitrary location.

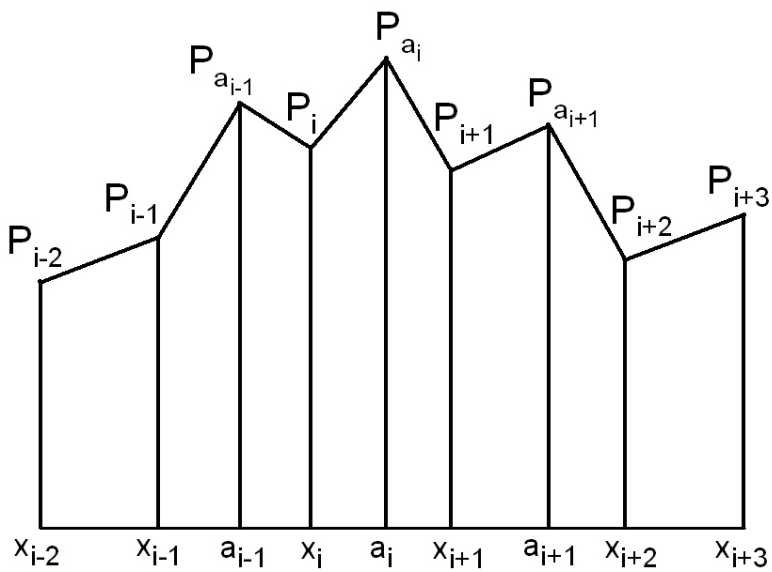

Figure.1. The diagram of pressure changes from the sites of leaks to the sites of pumps in the case of an area of three chambers having leaks, when the chambers at the beginning and the end of the area are without leaks.

HIGH-VOLTAGE SOURCE WITH OUTPUT VOLTAGE UP TO 60 KV WITH OUTPUT CURRENT UP TO 1A

Gusev I.A., Medvedko A.S., Protopopov A. Yu., Pureskin D.N., Senkov D.V.,
BINP Novosibirsk Russia

Abstract

The presented report contains the description of high-voltage source with output voltage up to 60kV and output current up to 1A. The source consist of the chopper with IGBT switches working with a principle of pulse-width modulation and the fill H-bridge converter with IGBT switches , both working on programmed from 15 to 25 kHz frequency, and the high voltage sectioned transformer with the rectifier and additional capacity filter. The transformer is made in oil tank with silicon oil. The additional capacity filter decreases the ripple and noise level in working range of output currents. The design of the high-voltage transformer provides preservation of working capacity at voltage up to 100kV. A nominal output voltage of the source is 60kV. The source can operate with series of high-voltage breakdowns in output voltage without risk of damage the components of source. In the high-voltage breakdown the released in load and matching circuit energy is less than 15J at maximum operating voltage 65kV. The efficiency of system is more than 80% at the nominally output power 60kW. The controller of the source is developed with DSP and PLM, which allows optimizing operations of the source. For control of the source serial CAN-interface is used. The description of the source and the test results are presented.

DESCRIPTION

The presented source was designed for some different applications at the BINP tasks. That was reason for some specific terms like: short time interval for voltage rise up to 60 kV after high-voltage breakdown, strong reliability to high-voltage breakdown, low voltage ripple for maximal power operation. The energy is dissipated in components of source and in the load during the high voltage breakdown less than 15J for 60 kV operation. The basic characteristics of high-voltage source are shown in Table1.

Overview

The circuit diagram of power part of high-voltage source is shown in Fig.1. The high-voltage source consists of the 20 kHz power converter with insulated gate bipolar transistors (IGBT) as switches (part A) and high-voltage sectioned transformer with the rectifier (part B). The power converter consists of 3-phase rectifier VD1, electromagnetic (EMI) filter F1, switch SW1, rectifier's filter capacitors C1-C2, 20 kHz chopper with IGBT switches Q1-Q2, 20 kHz inverter with IGBT switches Q3-Q6, impedance matching design L2 C5, and isolation transformer T1.

Table 1. Basic parameters of high-voltage source.

Parameter	**Unit**			
		Min	**Nom**	**Max**
Output voltage	kV	10	60	70
Output current	mA	0.1	1000	1100
Output power	kW		30	
Voltage ripple	%			0.5
Voltage stability	%			0.2
Transient time	ms		5	
Inverter frequency	kHz	15	20	25

Input rectifier

EMI filter is used to eliminate high-frequency noise to the power line from the source. 3-phase rectifier and filter C1-C4 are used to convert input AC 3-phase voltage 380V 50Hz to DC 550-600V voltage. Switch SW1 is used for soft start of converter and its consists two groups of contacts (not shown of sheet). First group of contacts is switched ON and the filter's capacitors C1-C2 are charged with 10A current. When the voltage on filter is up to 450 volts level the second group of contacts is switched ON and the rectifier is connected directly to 3-phase AC line.

Chopper

The chopper's switches Q1, Q2 are connected in parallel and operates one by one in working circle. As a result, the working frequency of each switch is the half of operated frequency of source. The chopper switches are operated with principle of pulse-width modulation on programmed from 15kHz to 25kHz frequency. The working frequency of inverter is the same. The operating frequency is selected depending on the characteristics of high-voltage transformer and the requirements to the spectrum of output high voltage ripple. The output voltage of chopper is changed from 10 to 450 volts DC by control circuit to obtain the required output high voltage of source.

Inverter

Full-bridge inverter Q3-Q6 converts DC voltage from chopper's capacitors C3-C4 to AC voltage with programmed from 15 to 25kHz frequency.

POWER SOURCE FOR HIGH-VOLTAGE COLUMN OF INJECTOR TO PROTON SYNCHROTRON WITH OUTPUT POWER UP TO 5KW

Golubenko Yu.I., Medvedko A.S., Nemitov P.I., Pureskin D.N., Senkov D.V.,
BINP Novosibirsk Russia

Abstract

The presented report contains the description of power source with output voltage of sinusoidal shape with amplitude up to 150V, frequency 400Hz and output power up to 5kW, operating on the primary coil of high voltage transformer - rectifier of precision 1.5MV electrostatic accelerator – injector for proton synchrotron. The source consists of the input converter with IGBT switches, transformer and the synchronous rectifier with IGBT switches also. Converter works with a principle of pulse-width modulation (PWM) on programmed from 15 to 25 kHz frequency. In addition, PWM signal is modulated by sinusoidal 400Hz signal. The controller of the source is developed with DSP and PLM, which allows optimizing operations of the source. For control of the source serial CAN-interface is used. The efficiency of system is more than 80% at the nominal output power 5kW. The description of the source and the test results are presented.

DESCRIPTION

The presented source was designed as part of high-voltage power source for proton synchrotron injector, developed in BINP. The high voltage source consists of 1.5MV high voltage column with input matching circuit, operated on 400Hz frequency, and the power source with 400Hz 150V harmonic output. The block-diagram of high voltage source is shown on Fig.1. The matching circuit is necessary due to the high voltage column design feature, such as series inductance of high voltage transformer is compatible with magnetizing inductance, the capacitance of high voltage transformer calculated to primary side organize with the inductance the oscillatory circuit with 1.5kHz resonant frequency [1]. But the maximal working frequency of high voltage column consisting of sectioned transformer with rectifier is 600Hz. So the capacitor bank C1 decrease the resonance frequency of contour to operating frequency. The inductance L1 organize the partial including of the Harmonic 400Hz PS into resonance circuit, protecting the PS from large reactive currents from resonance circuit. Also L1 and C1 together are low-pass filter, which preventing the high voltage column from high frequency harmonics, from power source, where they are generated by converter and synchronous rectifier under the PWM. The basic characteristics of high-voltage source are shown in Table1.

Overview

Design of the power part of the source is shown on Fig.2. The power source consists of the 20kHz power converter with insulated gate bipolar transistors (IGBT) as switches (part A) and the isolation transformer with synchronous rectifier (part B). The design of power converter consists of 3-phase diode rectifier VD1, electromagnetic (EMI) filter F1, switch SW1, rectifier's filter L1 C1-C8, 20 kHz inverter with IGBT switches Q1-Q4, isolation transformer T1, synchronous rectifier O5-Q8, output low-pass filter L2 C9 and three current sensors: U1, U2 and U3.

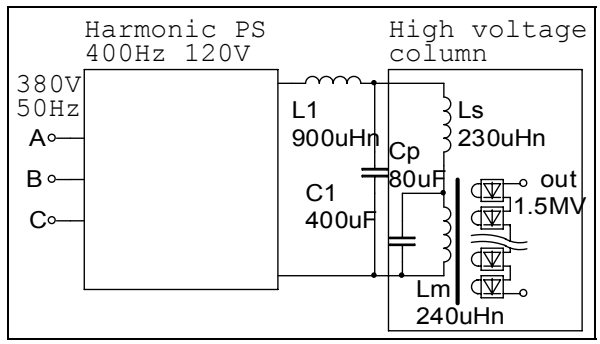

Fig. 1 High voltage source block-diagram

Table 1. Basic parameters of power source.

Parameter	Unit	Value		
		Min	Nom	Max
Output voltage	V r.m.s.	10	120	150
Output current	A r.m.s.		65	80
Output power	kW		5	7
Output voltage long time stability	%			0.1
Power source output frequency	Hz	200	400	600
Inverter frequency	kHz		20	

Input rectifier

EMI filter is used to prevent high-frequency noise from the power line from the PWM source. 3-phase diode rectifier and filter C1-C4 are used to rectifier input AC 3-phase voltage 380V 50Hz and to get DC 550-600V voltage. Switch SW1 is used for converter soft start.

COMPACT CYCLOTRON AS A PROTON SOURCE FOR THE DETECTION OF EXPLOSIVES BASED ON NUCLEAR RESONANCE ABSORPTION IN NITROGEN

L.M. Onischenko #, S.B. Vorozhtsov, A.S. Vorozhtsov, Yu. G. Alenitsky, E.E. Perepelkin, A.A. Glazov, JINR, Dubna, Russia
T.J.T. Kwan, R.E.Morgado, T.F.Wang, Los Alamos National Laboratory, Los Alamos, NM, USA

Abstract

In the proposed operational implementation of the Nuclear Resonance Absorption (NRA) method for explosives detection, the inspected object is scanned by a beam of 9.17-MeV gamma rays of a precise energy to determine the fraction of the beam resonantly absorbed in the nitrogen nuclei of the explosive in the reaction, ^{14}N (gamma, p) ^{13}C. The 9.17-MeV gamma rays are most readily generated in the inverse reaction, ^{13}C (p, gamma)^{14}N, in which a 1.747-MeV proton is resonantly captured by C^{13}, followed by the emission of gamma rays from the recoiling N^{14} nucleus. To achieve the stringent requirements of a 1.747-MeV proton beam with an intensity of several milliampere and with as small as possible energy spread and angular divergence, a compact isochronous cyclotron with internal H^- ion source and current of ~2mA was considered as a stand-alone source or as an injector (with a current of ~200 microA) into a storage ring. This report describes the main cyclotron design consisting of an internal ion source, magnet, acceleration system, extraction system, and beam delivery system.

BACKGROUND

Earlier investigations [1], [2], [3], [4], [5], [6] of the beam dynamics in a cyclotron with an external H^- source resulted in the following characteristics:
maximum current (~1.8 MeV): 2.2-2.5 mA,
transverse emittances: 150-300π mm·mrad,
energy spread, □E/E: ±8%.
Since these beam parameters do not meet the proton source requirements for nuclear resonance absorption, a cyclotron with a reduced current of ~200 □A with the transverse emittances and the energy spread reduced by an order of magnitude was proposed. This tailored beam could then be injected into a small storage ring in which the desired final beam parameters could be achieved.

To simplify the design and reduce costs, an internal ion source was examined with 6 mA of H^- ion current into the continuous mode of the cyclotron. Due to the 30-fold decrease of the average captured beam current for acceleration (from 6 mA to 200 □A), delimited by a diaphragm on the first turn, it became possible to reduce the transverse emittances and the energy spread. Calculations were performed taking into account the 3-D distributions of the electric fields of beam space charge as well as the field of the accelerating system.

BASIC CYCLOTRON PARAMETERS

The basic cyclotron parameters are listed in Table 1. The general view of the cyclotron is shown in Fig. 1

Table 1. Basic cyclotron parameters

Type of ion	H^-
Extraction energy, keV	1747
Average magnetic field, T	0.64
Number of sectors	4
Number of dees	2
Betatron frequencies, Qr , Qz	1.1, 0.85
Angular span of dees, (°)	45
RF voltage, kV	60
Orbital frequency, MHz	9.76
Harmonic number	4

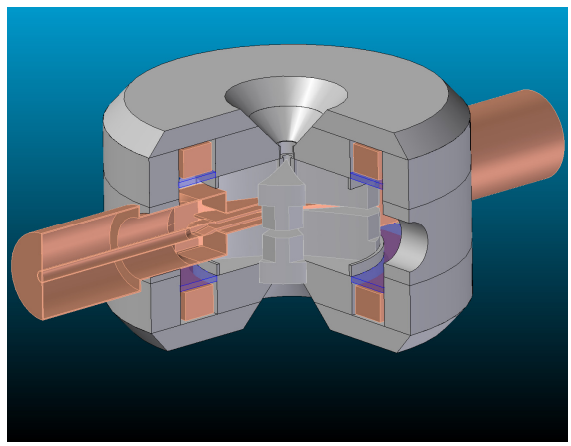

Fig. 1. Magnet and RF structures

MAGNET

The 4-fold type magnet with all-round yoke chosen for the cyclotron (Refs [2] and [7]) is shown in Fig. 1. The magnet poles and yoke shape the vacuum chamber for this design. The parameters of the magnet are given in Table 2.

Table 2. parameters of the magnet

magnet height	89 cm
magnet outer radius	70 cm
pole outer radius	35 cm
final orbit radius	30 cm
hill field at final radius	1.35 T
valley field	0.2 T
hill gap	3 cm
valley gap	40 cm
sector angular width	10º-30º
power consumption	10 kW

IMPROVING OF THE DTL CAVITY RF VOLTAGE STABILITY BY MEANS OF ANODE MODULATOR FEEDBACK

A.I.Kvasha, Institute for Nuclear Research, RAS, Moscow, Russia

Abstract

In the DTL RF systems of ion pulse accelerator, operating at frequencies up to 300 MHz, are used vacuum tubes power RF amplifiers (PA). At that, the vacuum tube discharger has to be used in anode pulse modulator regardless of the PA output RF power mode of operation: RF driving or PA vacuum tube plate supply. Just these modes allow supporting an accelerating RF voltage stability by means of amplitude control system. The efficiency of the system, in particular, depends on the modulator speed of response and time delay in the feedback. The simplest and cheapest way of modulator speed of response improving is a modulator feedback.

INTRODUCTION

The subject of this paper investigation is the amplitude control system (ACS) of an accelerating RF voltage in the DTL tanks, operating at frequencies below 300 MHz. The point is that at these frequencies RF system includes in her structure vacuum tube amplifiers with the RF output power amplifier (PA), operating in B or C mode. It means that any changes of PA vacuum tube RF driving result in changes of the dc component of the anode current. Moreover, nearly all now in use powerful triodes like RCA 7835, GI-54A, GI-71A can be controlled by means of plate voltage only. As an example in fig.1 control characteristic of the INR DTL RF power amplifier are presented for cavity voltage (U/Uo) and RF power (P/Po), dissipated inside of cavity; Uo and Po correspond nominal values of cavity voltage and RF power.

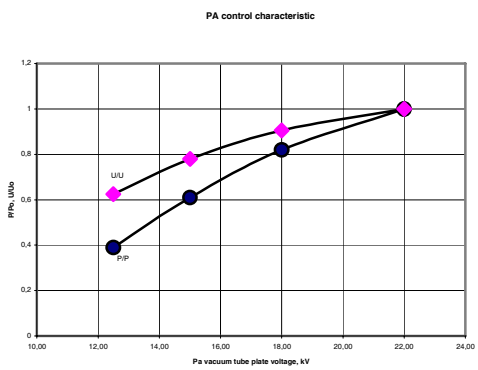

Fig.1. INR DTL power amplifier control characteristic.

That is why vacuum tube as an actuator of the DTL tank RF voltage amplitude control system is available in the PA anode pulse modulator.

At that, series connection of the modulator vacuum tube and the load (inner resistance of the PA vacuum tube over the dc component of the anode current) takes place. Obviously, in this case the modulator vacuum tube fulfills two functions: discharge of energy storage device (capacity battery or artificial forming line) at the load and control of the discharge voltage value at the load. In turn, there are two ways of the series connection of modulator vacuum tube and load:

- The load (PA) is connected to the anode of modulator vacuum tube (MVT) by means of pulse transformer
- The load is connected to the cathode of modulator vacuum tube.

The last case opens possibilities of high-speed modulator development without powerful pulse transformer. For that it is necessary to solve a problem of the control signal transmitting at the modulator vacuum tube grid. The point is that the MVT cathode is under pulse high voltage and, hence, the control signal also has to be put up at the pulse high voltage platform. Some decisions were considered in [1, 2], and they had shown their operability.

Designers of the INR DTL RF system had chosen the simplest decision: the load connected to the cathode of MVT also, but separation of control circuit from high voltage platform was realized by means of step down pulse transformer (see fig.2) with high voltage isolation between primary and secondary windings.

In that case the modulator speed of operation is, in the main, determined by the pulse transformer parameters (leakage inductance and parasitic capacitances of transformer winding) which, in turn, depend on pulse transformer overall dimensions and passing pulse power. Certainly, the pulse transformer operation at low-resistance load – MVT grid current, allows reducing the primary inductance and, hence, the leakage inductance too. However, remarkable reducing of the primary inductance results in modulator pulse tilt, which is additional inner disturbance for the amplitude control system ACS. It isn't true as the control system has been developed to cope with outside accidental disturbances, the main of which is beam loading.

ANODE MODULATOR OF THE INR DTL RF SYSTEM

In fig.2 simplified scheme of the PA anode modulator is presented. As one can see the pulse transformer is placed directly in front of MVT that simplifies the modulator structure: with the exception of the pulse transformer only two transformers – bias and filament ones are under output pulse high voltage. On the other hand a pulse power value that comes through the transformer at the MVT grid achieves tens of kW. At that level of the pulse power it is difficult to design the pulse transformer (and the modulator as a whole) with high response speed. The simplest and cheapest way of the modulator bandwidth

DEVELOPMENT AND APPLICATION OF ELECTRON LINAC ELECTROMAGNETIC DEVICES FOR RADIOTECHNOLOGIES

A.N. Dovbnya, A.E. Tolstoy, V.A Shendrik,. Yu.I. Akchurin
National Science Center "Kharkov Institute of Physics and Technology", Kharkov, Ukraine

The creation and subsequent service of modern electron linear accelerators at the NSC KIPT have brought evidence for possible successful introduction of radiotechnology processes using electron irradiation. A further extension and complication of physical problems solvable on the basis of radiotechnologies have put forward new and increased requirements for the systems of beam scanning, extraction and formation on the targets and extended irradiated objects. The results of applying our methods developed for prompt measurement of the kinetic energy of the scanned electron beam are presented. For measurement and continuous control of the electron energy the hodoscope magnetic spectrometer technique has been used. The spectrometer includes only one deflecting magnet and has no magnetic focusing. If the real field topography in the magnet is known in detail, then using the input and output coordinates of deflected particles it is possible to determine their energy, and also the chromaticity of electron beam. The step-pulse scanning of the beam is realized through the use of an air-core short-pulse electromagnet. Development and tests of separate units of the device are under way.

To realize a system of discrete-pulsed separation of the electron linac beam it was necessary to develop a series of new devices and units for electro physical equipment. The present paper considers devices of linac excitation and synchronization and a previously developed air-core short-pulse electromagnet magnet (EM). The requirements to the systems of excitation and synchronization impose that at a linac pulse repetition rate in the range from 3.125 to 300 Hz the beam-bending magnet and the accelerator were operating strictly synchronously. This condition is reached when, into the excitation source mounted by the Larionov circuit, the linac pulses of a selected frequency arrive. In the excitation source the rectified voltage transforms into the meander and then into the two-polar current pulses incoming into the bending magnet by the time of beam arrival (Fig.1).

The system of excitation and synchronization operates as is shown in Fig.2. Similarly to the linac synchronization device [1] in the source of EM excitation the positive and negative half-waves of all the three phases of the mains are rectified and fed into the amplifier-converter. At the same time in the triggering generator of the synchronization device the rectangular pulses of 2.5 μs duration are formed and fed into the injector and accelerating sections; here the excitation pulses are delayed and transformed by means of the

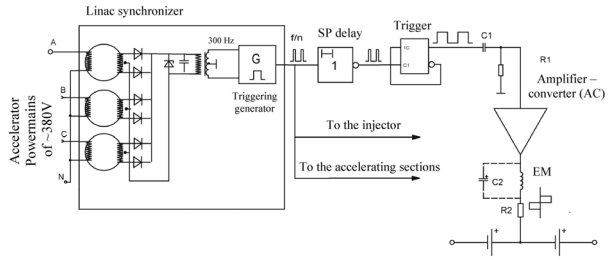

Fig.1. Block diagram of the device of excitation and synchronization

trigger into the meander of a pulse repetition frequency selected for all the linac systems, then they are amplified, transformed into the two-polar ones and enter in the bending EM. Thus, the conditions are created for, by the time of beam entering in the deflecting device (DD), the magnetic field in it be completely formed.

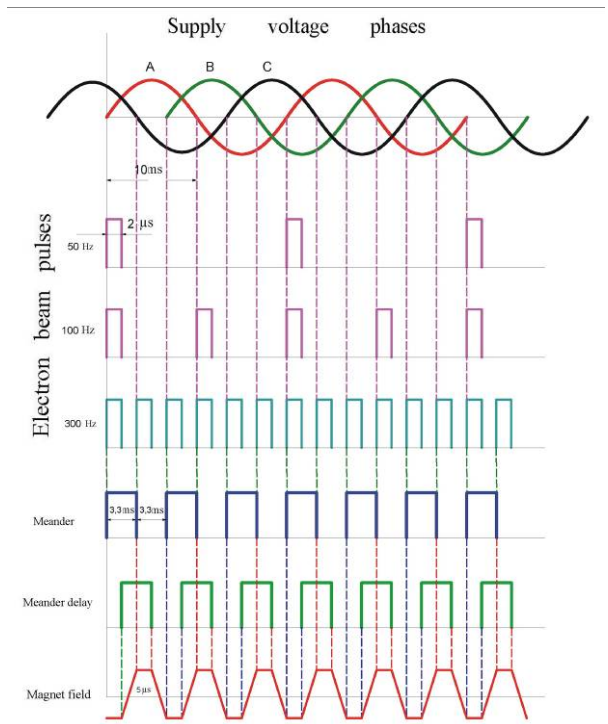

Fig.2. Diagrams of excitation system pulses.

The last state is illustrated by Fig.3 showing the magnetic field diagram in the DD at the linac pulse repetition frequency of 50 Hz.

For the DD one can apply a previously developed air-core electromagnet-transversely flat solenoid (TFS)

BEAM ABSORBER FOR TUNING ACCELERATOR IN THE BEAM LAYOUT OF THE EXPERIMENTAL COMPLEX

M.I. Grachev, V.A. Fedchenko, L.V. Kravchuk, E.V. Ponomareva, INR RAS, Moscow, Russia

Abstract

The absorber of a beam without moving parts in vacuum volume for tuning the high current linear accelerator is described.

INTRODUCTION

Since 2006 both the Linear accelerator and the Experimental complex at the INR have started operating with the proton beam of the current up to 100 μA [1]. The beam absorber for tuning of the accelerator, located at the beginning of the Experimental complex, was put through an upgrade. The old absorber contained by construction several moving absorbing elements in the vacuum (the copper cylinders the diameter of 20cm and the length 20cm), which required direct maintenance by people. A new beam absorber, without moving absorbing elements in vacuum, has been designed, mounted and set up in the beam tunnel.

BEAM ABSORBER

At the moment tuning of the parameters of the acceleration beam before its transport to the physical facilities in the Experimental complex is accomplished in the new beam absorption region (Fig.1). This region consists of a deflecting magnet and an absorbing part of vacuum cell, surrounded by biological shielding. The shielding decreases the level of radiation fields around the tunnel of the accelerator and surrounding rooms.

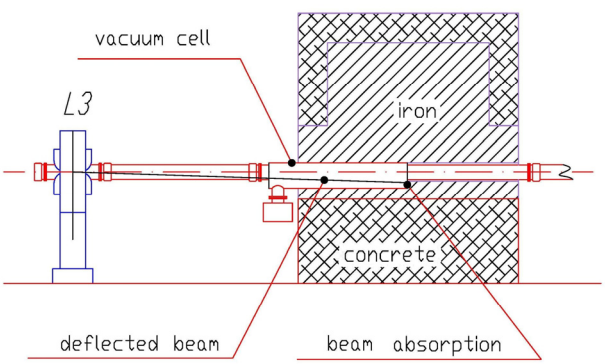

Figure 1: The beam absorber.

Beam of protons is deflected vertically downwards from the axis of the beam “red arrow” for the purpose of beam absorption during the tuning of the accelerator in the vacuum cell (as shown on Fig. 2).

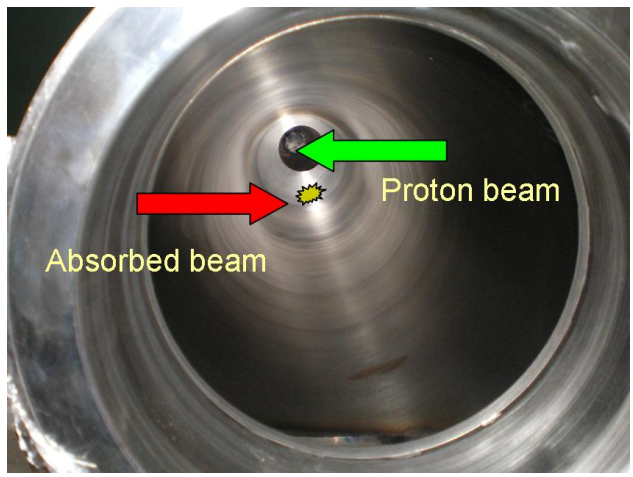

Figure 2: Inside view of the vacuum cell.

For the purposes of deflecting the beam some structural changes were made to the quadrupole lens L3 of the dipole magnet (in particular switching of lens’s coils has been carried out). During the tuning of the accelerator lens L3 is used as a dipole magnet. The beam is absorbed inside a special vacuum cell, surrounded by shielding. Shielding consists of the blocks of iron and of concrete with the following dimensions: length of 4m x height 3m x width 2.5m. This ensures sufficient protection from the activation of the equipment and the air in the tunnel.

Design features of the magnetic core of this type of lens allow effective vertical deflection of the proton beam. The angle of deflection from the beam axis is 2 degrees.

Thermal calculations of absorption of the beam in the wall of the vacuum cell are implemented by JSC “N.A. Dollezal Research and Development Institute of Power Engineering” [2]. Maximum temperature of the region absorption of the beam in the vacuum cell after 16 hours of continuous work was 120C, while the maximum temperature of the near iron blocks – no more than 30C. Analysis of results of the calculations allows us to come to the conclusion of possibility of using the beam absorber without a water-cooling system.

The main factors of radiation hazard to people when the beam absorber is active are the beams of secondary photons and neutrons. These arise during interaction between proton beam and equipment of the beam absorber and channel of transportation of the beam in the Experimental complex.

Radiation safety while the beam absorber is in operation is provided by biological shielding, system of blocking doors of the Experimental complex, system of blocking of the beam of the Linear acceleration from the signal of readiness of the absorber of the proton beam of

LOW LEVEL RF CONTROL OF ITEP-TWAC FACILITY

P. Alekseev, S. Barabin, A. Milyachenko, V. Zavodov, ITEP, Moscow.

Abstract

Digital LLRF control system was developed to improve the RF system mobility in multimode operation of the ITEP-TWAC booster and main synchrotrons. High precision mapping of the magnetic field derivative signal to the reference function of accelerating frequency f(B) allows to accelerate ions of any type in both rings up to relativistic energies even without feedback loops. The first modification of the LLRF control module is based on a fixed point DSP, which operates with the frequency lookup table to calculate the accelerating frequency. This module is now used in the booster synchrotron. Upgraded module has a floating point DSP, which allows calculation of the accelerating frequency "on the fly". This module is in operation in the main ring. Short description of the systems is given. Some results and experience obtained at operation with the number of types of particles, such as protons and ions of carbon, aluminium, iron and silver, are presented.

INTRODUCTION

ITEP-TWAC Accelerators facility consists of two synchrotrons: УК booster and У-10 main ring [1]. At present we have two injectors:

- И-2 – for protons which are transported directly to the У-10 where they are accelerated up to 10 GeV. This is the classic mode of ITEP accelerator.
- И-3 – for ions injection into the booster. The Ions are accelerated and transported to the main ring where they may be stored or additionally accelerated up to the relativistic energies.

The RF system of the booster synchrotron consists of two accelerating cavities [2]. The first cavity operate in the range from about 700 kHz to 2.5 MHz, after that the second cavity continues operation up to 12 MHz. All five accelerating cavities of У-10 operate in the range from 1 MHz to 5 MHz. The frequency provided for each of the accelerating cavities should correspond to the beam energy at each moment of the acceleration process. The dependency is described by well known formula (see Eq. 1) that should be reproduced by the master oscillator from the available diagnostic signals.

$$f(B) = \frac{h \cdot c}{L} \cdot \frac{p}{\sqrt{\left(\frac{m_o A}{Z}\right)^2 + p^2}}, \qquad (1)$$

where h - harmonic number, c – velocity of light, L – the length of the equilibrium orbit, m_0 – atomic mass unit, A – atomic weight, Z – ion charge and p is momentum per unit charge of the ion.

Additionally independent control of phase and amplitude of the accelerating voltage should be provided for each cavity. All of the functions described are provided by digital LLRF control system of the ITEP-TWAC facility.

MASTER OSCILLATOR

The core part of the LLRF system is the master oscillator unit (see Fig. 1) based on a digital signal processor. We are using standard Texas Instruments DSK boards available on the market. Originally the master oscillator unit was based on TMS320C6211DSK with processor clock frequency of 150 MHz and 4 MB of on-board memory. Self-designed daughter board is connected to the DSK. It contains an ADC circuit and control logic for six DDS submodules.

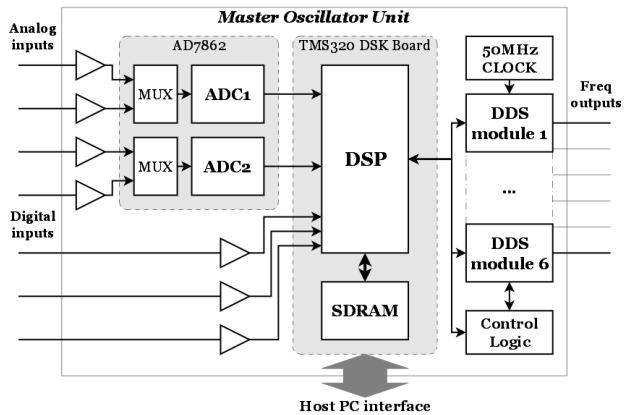

Figure 1: Master Oscillator block diagram.

All the DDS modules are connected to the common data bus. Common clock source of 50 MHz is used for all the DDS modules. All the modules could accept write commands simultaneously (on the same clock pulse) but only selected modules will store the data. Operational mode of each DDS could be selected individually by the software.

The signal of the derivative of the magnetic field induction is used as source information for producing the RF function of the magnetic field. This signal is presented in a digital form by an analog-to-digital converter with sampling frequency of 50 kHz and is integrated by a signal processor. Calculated value of the magnetic field induction then used as an address in the frequency lookup table. The table of 256 kB size should be calculated on the host computer software and stored in the SDRAM. Output frequency value is calculated by linear interpolation of the nearest tabulated values. DSP algorithm is illustrated on the figure 2.

STATUS OF HITS INJECTOR

V.G. Cherepkov, V.F. Kluev, E.S. Konstantinov, E.A. Kuper, V.R. Mamkin, A.S. Medvedko, P.I. Nemytov, V.V. Repkov, V.B. Reva, R.A. Salimov, A.V. Semenov, D.V. Senkov, V.A. Vostrikov. BINP, Novosibirsk, Russia.

Abstract

Ion injector for cancer therapy facility HITS was designed and assembled at BINP. Injector is based on electrostatic tandem accelerator with 1.25 MV at the high voltage terminal. The negative ion beams are injected into tandem and charge exchanged in the vapor-magnesium target with vacuum heat insulation. The results of injector tests and working with carbon ion beam are presented.

INTRODUCTION

In the BINP the facility for ion therapy of cancer based on the synchrotron with electron cooling is developed. Facility generates the therapeutic beam of carbon ions with energy up to 430 MeV/u [1, 2].

The tandem electrostatic accelerator with 1.25 MV at the high voltage terminal is used as the injector. The source of sputtering type is used for the generation of negative carbon ions C^- beam. The 10 keV beam of negative ions is transported along the low energy transport channel into the tandem accelerator. After acceleration in the first accelerating tube, negative ions charge exchange while passing the vapor-magnesium target and accelerated again at the same voltage in the second accelerating tube. Then carbon ions C^{+3} with the energy 0.417 MeV/u are injected through the transport channel into the booster synchrotron.

TANDEM ACCELERATOR

The electrostatic tandem accelerator is designed on the base of the ELV-type industrial accelerators developed in BINP [3]. The tandem assembled in a vessel with the following overall dimensions: a height is H = 3.64 m, a diameter is D = 1.346 m. The vessel can be operated at pressure up to P = 1.0 MPa (10 bar) of SF_6.

The tandem accelerating system consists of two ELV accelerating tubes located vertically at the vessel axis and the magnesium vapor charge exchange target between them. Operating vacuum $p = 1 \cdot 10^{-6}$ Torr in the accelerating tubes is provided by two vacuum systems placed at ground potential up and down of the vessel.

The source of high potential is the ELV type cascade voltage generator with magnetic link located in the bottom part of vessel. The alternate magnetic flux is produced by the primary winding (35 turns of double copper pipe) coiled on the cone frame. The winding is shielded by stainless steel thin strips. The shield protects the winding turns against high voltage breakdowns from the rectifying column.

The power supply voltage with the frequency 400 Hz is provided by the transistor frequency inverter. The high voltage column consists of 38 rectifying sections connected in series. Each section consists of the coil (3000 turns), rectifying circuit doubling voltage and supports for putting sections one onto another. The column outer diameter is 750 mm. The distribution of voltage among the accelerating tube sections is provided by the resistive divider.

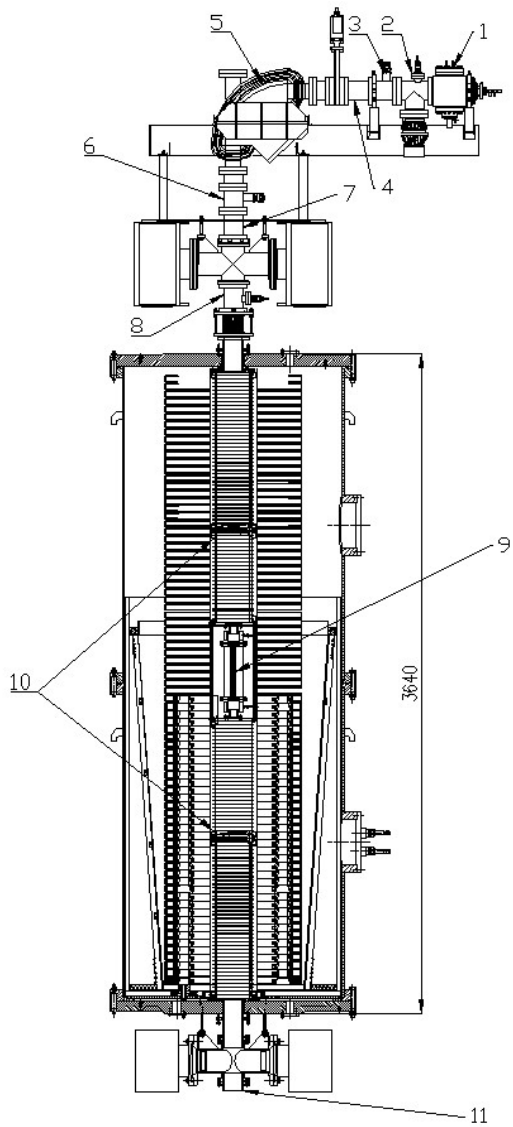

Figure 1: Injector layout: 1 – source of negative carbon ions C^- (10 keV); 2, 8 – electrostatic lenses; 3, 6 – electrostatic correctors; 5 – 90^0 bending magnet; 4, 7, 11 – Faraday cups; 9 – charge-exchange target; 10 - accelerating tubes.

In the high voltage electrode the charge exchange magnesium vapor target, the target power supply, the power supply winding for electronics, control and

DUBNA PROJECT OF CYCLOTRON C250 FOR PROTON THERAPY APPLICATION

Yu.G. Alenitsky, A.A. Glazov, G.A. Karamysheva, S.A. Kostromin, L.M. Onischenko, E.V. Samsonov, S.B. Vorozhtsov, O.V. Karamyshev, O.E. Lepkina, N.L. Zaplatin, JINR, Dubna, Russia

Abstract

Project of the C250 – cyclotron for proton therapy is considered. Energy of the extracted from cyclotron beam was increased according to medical requirements up to 250 MeV. 4-fold and compact types of magnet yoke were studied by 3D computer magnetic field calculations. The ability of optimal combination of the magnet yoke, new form of HF systems of the cyclotron based on the dynamics of the proton beam in calculated magnetic and accelerating field is under discussion. Dubna scientific medicine canter is under development since 1967 on the base of the proton beam of LNP JINR Phazotron. Proton beam with energy Ep ~170 MeV and intensity I ~0.1 mkA is used for patients irradiation. Proposal of the cyclotron with the same beam characteristics was reported earlier at the RUPAC04 [1] ICAA05 [2], printed in the "Applied Physics" magazine [3], RUPAC06 [4], RUPAC08 [5].

Computer model of the double gap delta RF cavity with 2 stems was developed in a general-purpose simulation software CST STUDIO SUITE. Necessary resonant frequency and increase of the voltage along the gaps were achieved.

CACLOTRON MAGNETIC SYSTEM

In work [4] the various types of yoke are considered, is shown, that the magnet with four opposites yoke is more convenient for service, such design is accepted in the present project. As a material of a magnet it is supposed to use steel - 10. On the Fig. 1 one can see the lower part of magnet system of the cyclotron C250p plane view.

The magnetic system consists of sectors, poles, horizontal and vertical yokes, current coils, the circuit of a magnet is shown on Fig. 1. In opposite valleys through 90° the high-frequency resonators are located, it one can see on the Fig. 3. The key parameters of the proton cyclotron are listed in Table 1.

The variation of a magnetic field creates four pairs flat sectors located symmetrically on poles from above and below. A gap between sectors is constant size of 40 mm. The average magnetic field, growing with radius, is created at the expense of increase of the azimuth extent of sectors. The vertical stability is reached at the expense of high sectors and them spirality, the extent of sectors spirality is increased at the expense of internal border, thus, increasing spirality and, accordingly, frequency of axial fluctuations.

For the consumer the important characteristics of installation are both the sizes and a technology of manufacturing of the project, and both operational conditions - consumed energy and cost of service. We propose on the base of our results, that the offered project C250p with four symmetry return yoke (Fig. 1) is optimum and that such installation can be created as a pilot project of our institute.

Modeling of the cyclotron magnetic system was carried out by means of the code *Radia ver. 4.098* [6], which works under *Mathematica* platform and calculates magnetic field of the three-dimensional magnetic systems by a method of the integrated equations. As a material of the magnet the steel - 10 was used.

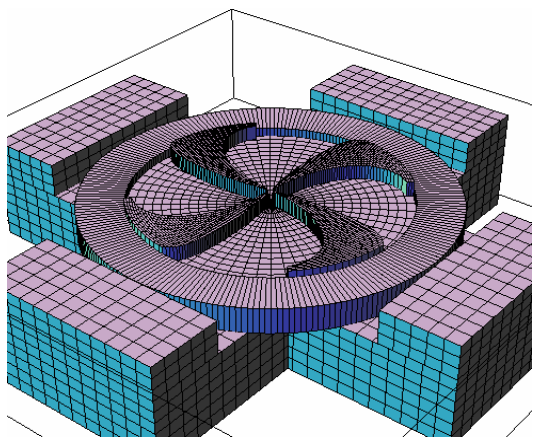

Figure 1: Magnet system of proton cyclotron C250p plane view (four symmetry return yoke).

The dynamic characteristics of beam in the magnetic field was calculated, one of them you can see on Fig. 2, all of them are in allowable limits [1, 2, 3, 4].

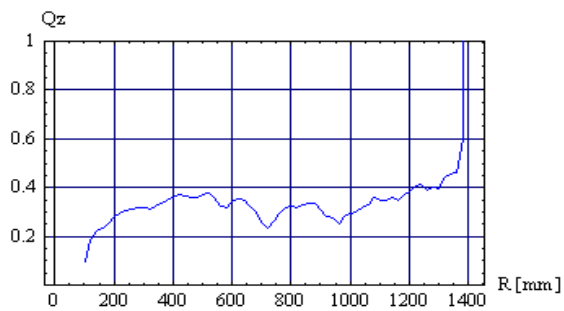

Figure 2: Dependence of frequency of axial fluctuations on radius.

UEL-10-D NEW LINEAR ELECTRON ACCELERATOR FOR NON-DESTRUCTIVE TESTING

V.A. Alexeev, I.Yu. Vakhrushin#, M.F. Vorogushin, L.Z. Kavalerchik, A.P. Klinov, A.S. Krestianinov, K.N. Maslov, Yu.P. Schepin, FSUE "D.V. Efremov Scientific Research Institute, of Electrophysical Apparatus", Saint Petersburg, Russia

Abstract

A compact accelerator UEL-10-D intended for radiographic inspection of steel products of up to 500 mm thickness has been designed and manufactured.

The accelerator provides the 10 MeV energy of accelerated electrons and the X-ray dose rate 1 m from target of 30 Gy/min.

The accelerator consists of an irradiator mounted on a special yoke, a heat-exchanger unit and an industrial panel-type computer. Practically all the equipment of the accelerator is mounted inside the irradiator including the HV power supply system, magnetron modulator and control system blocks. Using this yoke, the irradiator is installed on a bridge crane, which ensures its high manoerability necessary to test products of complicated geometry. Size of the irradiator without yoke is: 2040×950×950 mm.

In 2010, the accelerator was put into operation at the "Izhorskie Zavody", St.Petersburg.

The UEL-10-D accelerator can be also used in radioscopic and tomographic systems.

Requirements for reliability effective in nuclear, chemical and shipbuilding industries make necessary the non-destructive testing of large products including detection and identification of different defects such as cracks, cavities, foreign inclusions, etc. For example when manufacturing atomic reactors, 100% inspection of weld seams is necessary in compliance with requirements of Gosatomnadzor and IAEA. As the thickness of products inspected can be up to 600 mm for steel, charged particle accelerators are the only tool ensuring the required inspection quality.

A series of accelerators for NDT with energies from 2 up to 16 MeV and the photon dose rate (1 m from target) from 20 up to 120 Gy/min has been developed in the D.V. Efremov Institute [1]. Technical performances of these accelerators provide necessary quality of radiographic inspection at the 1-1T level in compliance with the international standard ASTME 142 for products with an equivalent thickness for steel up to 450 mm.

To date, more than thirty similar accelerators have been delivered to industrial enterprises in Russia and abroad. However, technological progress makes necessary updating of the delivered equipment in 10-15 years after its development. Unfortunately, in Russia deliveries of many domestically-produced component parts and units have been stopped, which impedes the process of updating. In particular, has been stopped the production of the power klystron KIU-111 (pulse power up to 6 MW), which served as a source of the RF power in our accelerators for non-destructive inspection with an energy higher than 6 MeV. Taking into account the fact that the only our competitor in the development of accelerators for industrial radiography, VARIAN (the USA), can supply accelerators to Russia only provided a special permission of the USA government, there has been taken a solution on the designing and manufacturing a practically new domestic machine for NDT, namely UEL-10-D.

This accelerator provides the following radiation parameters: the maximum average X-ray dose rate 1m from target on the central axis is 30 Gy/min at the 10 MeV energy; the pulse repetition rates are 50 and 200 Hz; the time for the beam stabilization after its turn-on is 5 s; the range of inspected thickness for steel is 50-500 mm.

The irradiator 2040×950×950 mm in size and of 1160 kg weight is installed on the bridge crane using a specially designed yoke. The yoke enables changes of its location relative to an object under inspection: in the horizontal plane from $+180^0$ (rightwards) to -135^0 (leftwards) and in the vertical plane from $+45^0$(upwards) to -95^0 (downwards). The irradiator is made as a support frame of aluminum section, inside which is installed practically all the equipment of the accelerator including the high-voltage power supply system, in contrast to the previous layout [1].

An electron beam with an injection energy of 50 keV is accelerated up to 10 MeV. A biperiodic standing-wave accelerating structure with axial coupling cells is applied in the accelerator. The buncher of the accelerating structure provides focusing of the electron beam under the action of accelerating RF-field, and as a result there is no need for the focusing solenoid and centering coils. The beam of accelerated electrons focused to 2 mm in diameter strikes the target wherein X-rays are produced. A water-cooled target is made of tungsten-rhenium (WRe). To measure the beam current, the target is insulated from the casing by a ceramic insulator. At the accelerator output, a collimator with a cone angle of 17^0 is installed. A laser is used to point the irradiator to a section inspected.

The MG-6090 magnetron with a power of 3 MW per a 3 μs pulse (the maximum average power is 2.5 kW) produced by an English firm is used as a source of the RF energy. The modulator of the magnetron forms the high-voltage pulse voltage up to 50 kV with a current of 100 A.

The modulator works with complete discharge of a storage device. A PFN, which is discharged through a

#npkluts@niiefa.spb.su

THE USE OF THE ELECTRON BEAM FROM THE MAGNETRON GUN-BASED ACCELERATOR FOR ZIRCONIUM SURFACE MODIFICATION

A.N. Dovbnya , V.V. Zakutin , N.G. Reshetnyak , S.D. Aksyonova, S.D. Lavrinenko, N.N. Pilipenko, V.N. Pelykh, NSC "KIPT", Kharkov, Ukraine, 1 Akademicheskaya St., Kharkov, 61108, Ukraine

INTRODUCTION

The paper reports the results from studies on metal surface irradiation with an electron beam of the accelerator based on the secondary-emission cathode magnetron gun. Presented are the results of examination of flat zirconium sample surfaces after their irradiation with an electron beam of the accelerator having the following parameters: electron energy 70 to 80 keV, pulse length – 15 μs, pulse rate – 2 pulses/s for two regimes of energy density on the samples, namely, 10 J/cm^2 and 20 J/cm^2. Experiments have been made to explore possibilities of irradiating inner surfaces of tubular items.

EXPERIMENTAL SETUP AND METHOD OF STUDIES

To irradiate zirconium surface, we have used the electron beam of the accelerator based on the magnetron gun having a secondary-emission cathode [1, 2] of diameter 40 mm and a stainless-steel cylindrical anode with a diameter of 78 mm. The accelerator diagrammatic sketch is presented in Fig. 1.

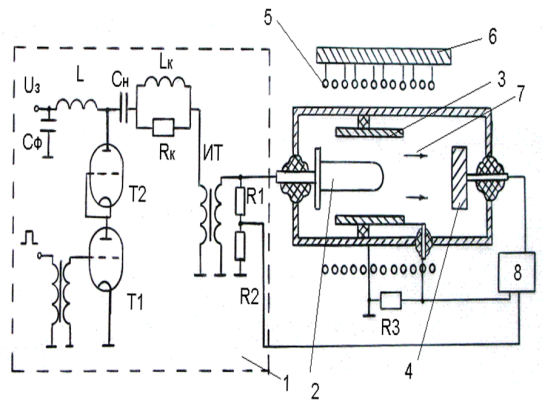

Fig. 1. Full diagram of the accelerator. 1 – impulse generator, 2 – cathode, 3 – anode, 4 – Faraday cup, 5 - solenoid, 6 - solenoid power supply, 7 – electron beam, 8 – computerized measurement system.

The accelerator consists of the following main units: an energizing high-voltage pulse generator 1; a magnetron gun with a secondary-emission cathode 2 and anode 3, located in the vacuum chamber; solenoid 5 that generates a longitudinal magnetic field; a target device with a Faraday cup (FC) 4; a computerized measurement system 8 for measuring beam parameters. The supply voltage pulse from the impulse generator 1 was applied to the magnetron gun cathode.

The impulse generator 1 provided voltage pulse shaping with a pulse overshoot amplitude of 190 kV, a pulse overshoot decay time of ~ 0.6 μs to provide the development of secondary-emission multiplication processes, and an amplitude of the voltage-pulse flat part of ~ 150 kV; the pulse length was 15 μs, the pulse-repetition rate was 2 Hz. In the impulse generator circuit, use was made of the full discharge of the storage capacitor Cs via a correcting circuit L_2R_2 to the pulse-transformer (ИТ) primary winding through two series-connected thyratrons for increasing the commutation voltage. The voltage surge was provided due to spurious inductance and capacitance of the pulse transformer.

The electron source (C – cathode, A – anode) is arranged in the vacuum chamber with an inside pressure of about 10^{-6} Torr. To produce the electron beam, the magnetron gun is used. The latter has a copper cathode (40 mm in diameter, 85 mm in length) and a stainless steel anode (78 mm in inner diameter and 140 mm in length).

The magnetic field for electron beam shaping and transport is generated by the solenoid 5 consisting of four sections, which are energized by dc sources 6. The amplitude and longitudinal distribution of the magnetic field can be controlled by varying the current value in the solenoid sections.

The measured data on the parameters of the voltage pulse, the beam current traversing the Faraday cup and their stability were processed by a computerized measuring system 9. The measurement error ranges within 1 % to 2 %. The processed data were displayed on the monitor.

EXPERIMENTAL RESULTS AND DISCUSSION

The parameters of the accelerator under discussion were investigated for the case of material surface irradiation.

The experiments have demonstrated that the maximum parameters of the beam were attained in a uniform magnetic field at a cathode voltage of ~ 120 kV. The magnetron gun formed an electron beam of current 125 A with a power density on the target ~ 4 MW/cm^2 at a pulse length of 10 μs.

The bandwidth of electron beam generation was determined by varying the magnetic field and was found to be ΔH~200 Oe. This beam generation bandwidth is of great importance in the accelerator adjustment for technological purposes.

It has been shown that at a constant cathode voltage the change in the magnetic-field amplitude and

ION SCANNING SYSTEM IN BEAM LINE OF U-400M CYCLOTRON FOR ELECTRONIC COMPONENTS TESTING†

A. Fateev††, E. Gorbachev, G. Gulbekyan, I. Kalagin, N. Kazarinov, V. Kazacha, E. Muravyova
JINR, Dubna, Moscow region, Russia

Abstract

The beam line of the U-400M cyclotron is designed for irradiation of chips by beams of accelerated ions to determine their radiation resistance. The results of the beam transport calculations for various ion types taking into account the beam parameter changes on passing a collimator and degrader are presented. The resulting beam sizes on a target are obtained for all beam variants. The calculated beam size on the target varies in the range from 15 cm up to 30 cm. An analysis of three variants of the magnetic scanning system is carried out. The working scheme, construction and main technical characteristics of the optimal variant are presented.

INTRODUCTION

The beam line of the U-400M cyclotron is intended for the chip irradiation by flows of the accelerated ions for determination of the radiation influence upon chip work. Parameters of the ions that are supposed to be used in this beam line are presented in Table 1**[1]**.

Table 1: Parameters of the ions

Ion	W_0 [MeV/amu]	A	Z_{ext}	A/Z_{ext}
Ne	9.2	22	+10	2.2
Ar	7.8	40	+17	2.35
Kr	8.8	86	+33	2.61
Xe	8.8	136	+49	2.78

Calculations of the beam tracing in the beam line for the beam parameters, specified in Table 1, were carried out in this work. The turned out beam dimensions on the target were defined. The different variants of the scanning system for getting demanded uniformity of the beam density distribution on the target were investigated.

BEAM LINE SCHEME

The beam line scheme is shown in Figure 1. The main beam line elements are: the correcting magnet B5CMV1 (B5CMH1), the horizontal scanning magnet B5SMH1, the vertical scanning magnet B5SMV1, the diagnostics block B5BD1 and device in the beam line end where the target is placed. The iris is placed between corrector and horizontal scanning magnet. The length of both scanners is equal to 600 mm; their bore diameter is equal to 90 mm. In the diagnostics block there is a device having the set of tantalum foils. The energy of the accelerated and extracted from the cyclotron ions can be diminished with

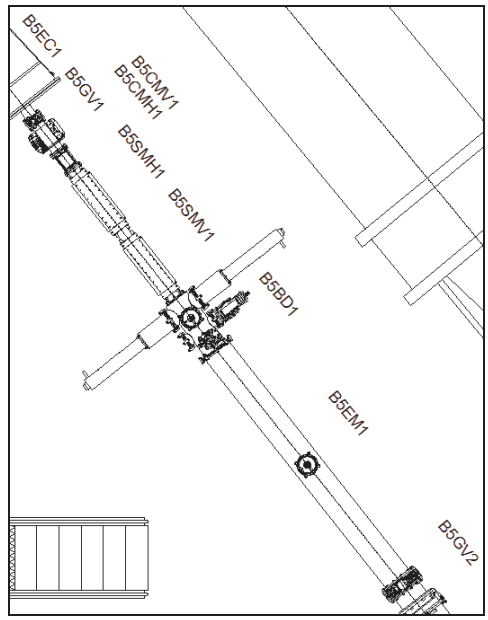

Figure 1: Scheme of the beam line

the help of these foils down to three chosen intermediate values of 6 MeV/amu, 4.5 MeV/amu and 3 MeV/amu.

Calculation of the ion movement in the beam line was carried out with the help of the code COSY INFINITY **[2]** in assumption that the beam has the Gaussian density distribution in its cross-section. One considered also that the magnetic fields of the scanners were switched off and the particle movement from the extraction point to the target occurs in a free space. In this case the initial data for COSY INFINITY code were calculated from the initial values of the second order moments $\overline{x^2}$, $\overline{(x')^2}$, $\overline{xx'}$, $\overline{y^2}$, $\overline{(y')^2}$ and $\overline{yy'}$ **[1]**. All dispersions and their derivatives were considered to be equal to zero. The magnitudes of the initial moment values for the set of ions specified in Table 1 are presented in Table 2. The value of the initial relative root-mean-square spread of the ion longitudinal momentums δ_0 is equal to 2.49 10^{-3}

The total length of the beam line is equal to 622 cm. There is an iris at the distance of 139 cm from the point of the beam extraction. The tantalum foil having the diameter of 90 mm is placed at the distance of 155 cm from the iris.

Evaluations show that maximum beam deviation on the foil, when the scanners are turned on, amounts ~30 mm. Therefore the beam radius before the foil must not exceed 15 mm in order the beam will not exceed the foil bounds on scanning. From these considerations the iris diameter was chosen equal to 20 mm.

†Work was supported by ROSKOSMOS structure
††fateev@sunse.jinr.ru

COMPROMISE SYSTEMS FOR TRANSPORT PROTON AND ION BEAMS IN MEDICAL AIMS

Mark Kats, ITEP, 25, B.Cheremushkinskaya, Moscow, Russia

Abstract

A center of treatment by proton and ion beams must be equipped by a few (4-6) treatment rooms and in most of them must be used equipment for choose optimal directions of irradiation. Usually it is gantry. In gantry patient is immovable and any directions of irradiation are possible. But any modern gantry are so large, complex and expensive, that it is necessary to suggest new solutions – more compact, less heavy, less expensive, but with enough wide choose of direction of irradiation. Similar system can be designed only with compromises: with displacement of treatment coach at horizontal position of the patient and at limited directions for irradiation. Planar systems are seems as most suitable for treatment centers. Layouts of proton and ion centers with 5-6 treatment rooms equipped by planar systems at hot magnets are suggested.

INTRODUCTION

The number of patients requiring beam therapy is very high. Future centers for medical irradiation by proton or ion beam should be highly effective and it requires 5-6 treatment rooms that use one accelerator and are able to have high quality irradiation for every room.

It is necessary for successful treatment in most cases to choose direction of irradiation and change this direction several times within one fraction of treatment. The second important condition of optimal irradiation is to use active dose distribution on the target volume (3-D scanning by the narrow beam).

Equipment used today to provide these conditions is called gantry. Gantry consists of a beam transport channel with magnets for beam scanning placed on the rotatable frame. Classical gantry, according to the medical requirements, assumes that horizontally fixed patient is placed immovable with center of the target at center of irradiation, at the axis of frame rotation Any directions of irradiation are available via frame rotation. But any modern gantry are so large, complex and expensive, that it is necessary to suggest new solutions – more compact, less heavy, less expensive, but with enough wide choose of direction of irradiation. Similar system can be designed only with compromises: with displacement of treatment coach at horizontal position of the patient and at limited directions for irradiation. It is important to highlight that availability of any direction (as it is using gantry) is not necessary. Three versions of compromise solutions were observed.

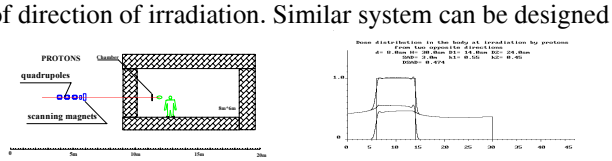

Figure 1. Scheme of treatment room with horizontal beam and scheme of doses distribution at irradiation from two opposite directions.

EQUIPMENT WITH FIXATED DIRECTIONS OF THE BEAM

Simplest equipment with fixated direction is a horizontal beam. There is clear defect of similar system. Doses level in healthy parts of the body is comparable to doses into the target at irradiation in only one direction targets with large sizes. So, it is very useful to produce irradiation from two or three directions. At horizontal beam doses level can be decreased two times at irradiation by two opposite directions after rotation of treatment table around of vertical axis (see Figure1). But volume of irradiated healthy parts of the body will be increased more then two times. Sometimes the second direction of irradiation at horizontal beam is closed by value of maximal range (30cm) or by medical reasons.

There are systems with beam transport to patient from vertical or bent directions. Sometimes the beam can be transport from two directions in one room, in one common iso-center. Two directions have more possibilities in comparison with one direction, but quantity of possible directions are small and magnetic channel for similar system has magnetic optic and volume of the room comparable to gantry. Increasing of quantity of transport channels with different fixated directions of irradiation to one iso-center does not seem as optimal solution.

ECCENTRIC GANTRY

For decreasing diameter of rotated heavy equipment in gantry it was suggested to rotate it around of the axis which pass through center of heavy mass and displaces treatment table with horizontally fixated patient around of magnets in order to direction of bended beam pass through the target center (see Figure 2).

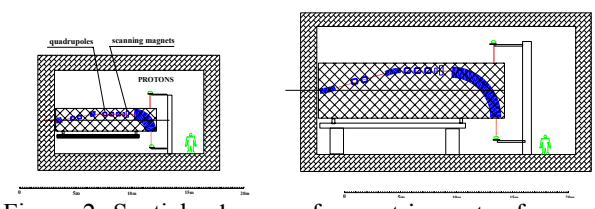

Figure 2. Spatial schemes of eccentric gantry for proton and ion beams.

In such eccentric gantry design diameter of heavy rotated equipment is like to radius of particles bend in magnetic field (at 1.6Tl R=1.4m for protons and R=4m

COMPACT SUPERCONDUCTING SYNCHROCYCLOTRONS AT MAGNETIC FIELD LEVEL OF UP TO 10 T FOR PROTON AND CARBON THERAPY

A.I.Papash, G.A.Karamysheva, L.M.Onischenko,
Joint Institute for Nuclear Research, Dubna, Russia

Abstract

Based on brief analysis of accelerators widely used for proton-ion therapy and patient cure during last 20 years the feasibility and importance of compact superconducting synchrocyclotrons operating at magnetic field level up to 10 T is outlined. The main component of modern commercial facility for proton-ion therapy is an isochronous cyclotron with room temperature or superconducting coils accelerating protons up to 250 MeV as well as synchrotron accelerating carbon ions up to 400 MeV/A. Usually ions are delivered from accelerator into the treatment room by transport lines. Irradiation is done by system of pointed to the patient magnets, collimators, energy degraders which are attached to the rotating Gantry. To greatly reduce price of facility (almost one order of magnitude) and to simplify operational conditions of hospital personal it is proposed to provide iso-centric rotation of compact superconducting synchrocyclotron around the patient. Main physical and technical parameters are described in the paper.

INTRODUCTION

During 60 years proton beams are being used for radiation therapy[1]. Proton resistive tumours are treated by carbon beams [2]. Dedicated commercial facilities for proton/ion therapy are based on 250 MeV synchrotron build by FERMILAB [3] and 400 MeV/A carbon synchrotron HIT [4]. Room temperature cyclotron C235 from Company IBA [5] and superconducting isochronous cyclotron SC250 built by ACCEL [6] are basic accelerator units on the international market. The field level of C235 magnet is 2.17 T and weight is 200 tons while field of SC250 is 3 T and weight is 90 tons. Modern commercial proton therapy complex includes accelerator, beam lines, rotating Gantries and auxiliary equipment. Basic price of Complex is 100-150 M$ and cyclotron cost is only 15% of total price. Special buildings and services are required for such Facility for extra cost.

COMPACTNESS LIMIT FOR 250 MEV ISOCHRONOUS CYCLOTRONS

If one could locate accelerator on rotating carousel platform then ions might be delivered to patient directly – without beam lines and gantry. Compact neutron therapy system with superconducting cyclotron on the rotating platform has been built at NSCL MSU [7,8]. Weght of 50 MeV Deuteron cyclotron is 20 tons. Main condition for rotation of 250 MeV proton machine is the reduction of cyclotron dimensions and weight. Of course one may build rotating platform with 100 tons accelerator on it but there is no commercial interest on such equipment.

Beam energy in cyclotron is $T_k \sim (B_{ext} \cdot R_{ext})^2 Q^2/A$. Magnet weight is $\sim R^2$ (coefficient $\sim R^3$ leads to overstated results). Increasing of field will reduce magnet pole radius and weight. Magnet for 250 MeV cyclic accelerator is weighting 65 tons at field level B=5.5 T and only 20 tons at level B=9 T. Magnet is saturated at high field levels and maximum contribution from iron sectors is ~2 T. Thus flutter is inversely proportional to $F \sim B_{av}^{-2}$ and at the field level of 10 T flutter is only F=0.01.Using of sectors with high spirality $\delta \approx 80°$ ($tg\delta \approx 5$) to improve focusing properties might cause nonlinear instabilities. It is hardly possible to build compact 10 T isochronous cyclotron.

SYNCHROCYCLOTRONS FOR PROTON/ION THERAPY

Main operational principles of synchrocyclotron with weak focusing $0<n<1$ do not impose any limit on the level of magnetic field. In contrast to isochronous cyclotrons there is a possibility to operate synchro-cyclotron with superconducting colis (SC-SC) at high fields. Prof.H.Blosser has proposed to install 5.5T SC-SC on rotating platform [9] and theoretical studies have been performed in NSCL MSU [10,11]. In 2007 Dr. T.Antaya has proposed design of the SC-SC at significantly higher level of magnetic field – up to 10 T (Fig.1) [12]. Private company "Still River" has built "single room" unit for proton therapy "Monarch250" (Fig.2) where compact 9T SC-SC roundabout patient (Fig.3) [13]. The first beam was extracted in May 2010 [14].

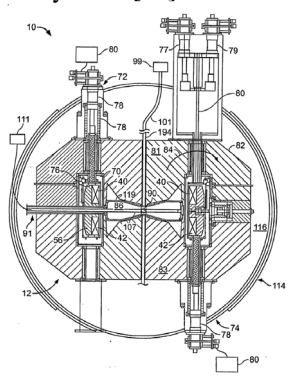

Fig.1. Vertical cross-secion of 9T Synchrocyclotron **[12]**: (81,82,83)–magnet, (40)–Superconducting coils from Nb_3Sn, (70)–cryostat, (119)–Dee, (114)–magnetic shield.

TUNING OF THE INR THERAPEUTIC PROTON BEAM

S.V. Akulinichev, V.N. Vasiliev, Yu.K. Gavrilov, M.I.Grachev, E.V. Ponomareva, INR RAS, Moscow, Russia
V.N. Zapolsky, IHEP, Protvino, Russia

Abstract

The medical proton beam channel of the INR Experimental Complex and the therapeutic beam formation system are described (see also Refs. [1,2]). Parameters of the 209 and 160 MeV proton beams were investigated and dose distributions in matter were measured.

MEDICAL PROTON BEAM CHANNEL

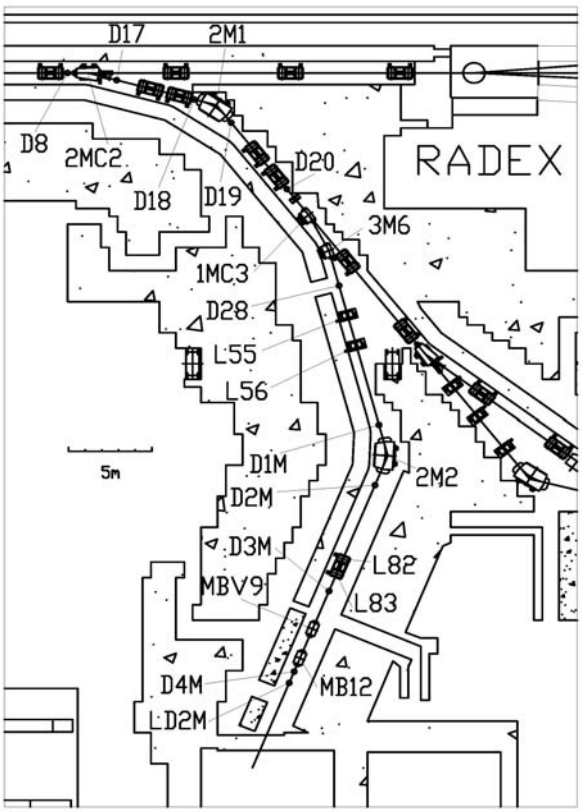

Figure 1: The layout of the proton beam channel for proton therapy. 2MC2, 2M1, 1MC3, 3M6, 2M4, MBV9, MBV12 – bending magnets; L55, L56, L82, L83 – quadrupole lenses; D8, D17, D18, D19, D20, D28, D1M, D2M, D3M, D4M, LD2M – profile detectors.

A special channel of INR Experimental Complex was built for radiotherapy needs [3]. The layout of the optical elements and profile detectors along this proton beam channel is illustrated in Fig.1. The length of this channel is about 50 metres [4].

The distinguishing feature of optics, operated during the last session in April 2010, is that only 4 quadrupole lenses have been used in the channel. Five magnets ensure beam bending on 112 degrees. The lenses L55, L56 are responsible for compensation of angular and linear dispersion of the beam after the bending magnet 2M4. The lenses L82, L83 form a beam on the scatterer with the required angular divergence of less than 2mrad and the dimensions $\sigma_x=\sigma_y=5$mm. Alignment of the beam with the axis of the treatment room is provided horizontally by magnets 3M6 and 2M4, and vertically by magnets MBB9 and MBB12. Each element in the channel is supplied by its own power source with the current fluctuations of ~ 10^{-4}. The electrical power consumption of the channel with the proton energy of 209MeV is equal to ~ 87.5kW. This amount is just a small fraction of the total energy consumption of both the accelerator and the experimental complex.

For the purposes of beam tuning there are ten 16-channel secondary-emission profile detectors, with a step of 2 and 4mm [3]. Profile detectors allow us to measure the position and the spot size of the proton beam during the tuning of a channel. A luminescent detector (item LD2M in Fig. 1) is installed at the end of the channel, just before the treatment room. This detector enables us to monitor on-line position and dimensions of the beam.

The principal aim of the tuning of the channel during the April 2010 session was the analysis of the parameters of the beam with proton energies of 160 and 209 MeV. This has been carried out with the aid of the profile detectors. As it follows from the analysis, the energy spread of protons was very small, approximately 10^{-3}. Therefore a strict achromaticity of the channel is not necessary for the required parameters of the beam. This eliminates the constraints on the regimes of the lenses L55-56 that are used for the focusing of the beam. Fig.2 shows the profiles of the beam at the entrance to the channel (distance from the accelerator is about 150 m), before the magnet 2M4 and at the end of the channel.

It is worth highlighting the details of the profile of the beam in front of the magnet 2M4. We have managed to focus the beam into dimensions $\sigma_x=1.6$mm, $\sigma_y=1.5$mm by means of the lenses L55-56.

The profile of the beam, at the end of the channel and before the scatterer, is obtained using the adjusted regime of lenses L55-56 for the beam focusing of lenses and the computed value of the regimes of the lenses L82, L83. This beam was used for forming the dose field.

One of the main properties of the medical channels is the time required to tune the channel. In the last session the tuning process took 1.5 hours. Similar time was required for the tuning of the beam during the transfer to another beam energy (without taking into account the time of re-tuning of the accelerator).

THE HIGH-CURRENT DEUTERON ACCELERATOR FOR THE NEUTRON THERAPY

V. Skorkin, S. Akulinichev, A. Andreev, INR RAS, Moscow, Russia.

Abstract

Physical project of neutron sources for the neutron therapy and neutron activation analysis is proposed. The neutron sources are based on beam provided by the high-current deuteron accelerator. The fast neutrons with intensity up to $5 \cdot 10^{12}$ n·s^{-1} are produced using T(D,n)^{4}He reaction at the energy of deuteron beam about 430 keV and average current up to 20 mA. Neutron source can be used for the fast neutron and neutron capture therapy. Liquid-crystalline DNA-Gd nanoparticles, as a potential biomaterial for the neutron capture therapy were investigated on a thermal neutron beam.

INTRODUCTION

Progress in the physics and technology of linear accelerators ion promotes the wider use in various sectors of the linear accelerators of protons and deuterons at low energies. In particular, such accelerators are used for the production of medical radioisotopes, neutron activation analysis, fast neutron therapy and neutron capture therapy of cancer [1]. Creation of fast and thermal neutrons through nuclear reactions (d, n), (p, n) without the use of fissile materials is a safe alternative to nuclear reactors. At low deuteron energy for high intensity neutron fluxes is most preferable DT and DD fusion reactions.

Currently in Russia powerful neutron generators (NG) using DT reaction produces NIIEFA. One of them, NY-12-2, provides a flow of 14 MeV neutrons of about $2 \cdot 10^{12}$ n·s^{-1} at an accelerating voltage of 250 kV and a current of 10 mA of deuterium ions. From foreign producers should be noted the firm "IRELEC" (France), which produces NG with fast neutron flux of about $5 \cdot 10^{12}$ n·s^{-1} at an accelerating voltage of 430 kV and a deuteron current of 20 mA. In the INR, was assembled and tested a NG based on high-current accelerator of deuterons (HCAD). The impact of a 20 mA deuteron beam accelerated at 430 kV on tritium target produces a neutron flux of $2 \cdot 10^{11}$ n·s^{-1}·cm^{-2} for a neutron output of $5 \cdot 10^{12}$ n·s^{-1}.

DEUTERON ACCELERATOR

The machine consists of: an electrostatic particle accelerator, supplying a 20 mA/430 kV beam of monoatomic deuterium ions, a target assembly, an ISU type high voltage DC power supply, providing the 400 kV acceleration voltage, a control and monitoring system.

The electrostatic particle accelerator consists of a high voltage electrode with the injector and associated power supplies, accelerating tube, quadrupole focalization double, an extension tube, leading to the targets assembly (see Fig. 1). The high voltage (HV) electrode is mechanical assemble designed to house the high voltage components (400 kV) and supported by three insulated legs.

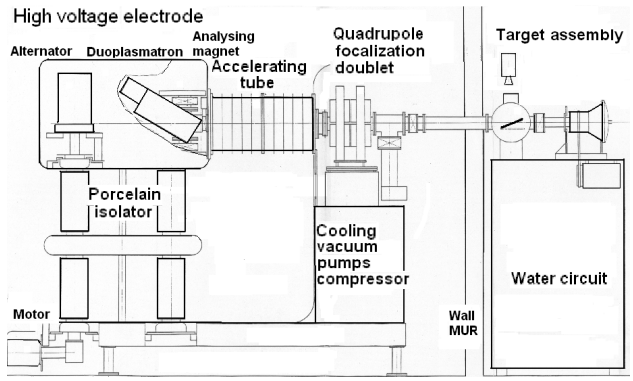

Figure 1: Deuteron accelerator.

The HV electrode includes the vacuum chamber of the injector with deflecting magnet and associated power supplies, the magnet enclosure auxiliaries, the ion source equipment, the alternator supplying power to the HV electrode. The injector has the ion source (the duoplasmatron type), beam extraction optics, atomic ion analysing magnet. A low pressure discharge is created between a hot cathode and an anode. The plasma expands through the anode into a expansion cup. Oven-heated oxide cathode has lifetime greater than 300 hours for discharge current of 15 A and discharge voltage of 150 V. The beam extraction optics (the pierce type) has maximum deuterium beam current of 55 mA.

Accelerating tube fixed to the high voltage head and consists of two half-length tubes, each made up of 5 porcelain rings and electrodes bonded together, providing a 12.5 kV/cm outside the accelerating space. A rated voltage, diameter and length of the tube are 400 kV, 0.5 m and 1.03 m respectively. The beam hits the target at a distance of 3.3 m. To compensate for divergence and to adjust the impact dimension, a quadrupole doublet is located. A throat diameter and a nominal gradient of the doublet are 102 mm and 1.9 T/m respectively.

The target assembly consists of the retractable target designed for beam adjustment, the rotating target containing the tritiated layer, representing the neutron source, a cryopump, the target water cooling system.

The retractable target used to focus the beam by examining the impact dimension on a tantalum network through a window using a video camera. The power of the beam is determined by a calorimetric measurement of the cooling water. Considering the angle of 18° between the target and the horizontal plane, it can receive a maximum power of 8.6 kW for a 20 mm beam diameter.

DEVELOMPENT OF ACCELERATORS AND DETECTOR SYSTEMS FOR RADIACIAN MEDICINE IN DLNP JINR

E.M. Syresin*, N.V. Anphimov, G.A. Chelkov, G.A. Karamysheva, M.Yu. Kazarinov, C.A. Kostromin, G.V. Mytzin, N.A. Morozov, A.G. Olshevsky, V.M. Romanov, E.V. Samsonov, N.G. Shakun, G. D. Shirkov, S.G. Shirkov, Joint Institute for Nuclear Research, Dubna, Russia.
M.Abs, A. Blondin, Y. Engen, S. Zaremba, D. Vandeplassche, IBA, Belgium.

Abstract

The DLNP JINR activity is aimed at developing two directions in radiation medicine: development of accelerator technique for proton and carbon treatment of tumors and new types of detector systems for spectrometric computed tomography (CT) and combined magnetic resonance tomography (MRT)/positron emission tomography (PET).

JINR-IBA realized the development and construction of proton medical cyclotron C235-V3. At present time all basic cyclotron systems were constructed. During 2011 we plan to assemble this cyclotron in JINR and in 2012 perform tests with extracted proton beam.

A superconducting isochronous cyclotron C400 has been designed by IBA-JINR collaboration. This cyclotron will be used for radiotherapy with proton, helium and carbon ions. The $^{12}C^{6+}$and $^{4}He^{2+}$ ions will be accelerated to the energy of 400 MeV/amu, the protons will be extracted at the energy 265 MeV. The C400 construction was started in 2010 in frame work of the Archarde project (France).

Modern CT require modification to allow determining not only density of a substance from the X-ray absorption coefficient but also its chemical composition (development of spectrometric CT tomographs with colored X-ray imaging). JINR develops the principle new pixel detector systems for the spectrometric CT. A combined MRT/PET is of considerable interest for medicine, but is cannot be made with the existing PET tomographs based on detectors of compact photomultipliers. Change-over to detectors of micropixel avalanche photodiodes (MAPDs) developed in JINR allows making a combined PET/MRT .

PROTON THERAPY

Dubna is one of the leading proton therapy research centers of the in Russia [1]. The modern technique of 3D conformal proton radiotherapy was first effectuated in Russia in this center, and now it is effectively used in regular treatment sessions [1-2]. A special Medico-Technical Complex was created at JINR on the basis of the synchrocyclotron (phasotron) used for proton treatment. About 100 patients undergo a course of fractionated treatment here every year. During last 10 yeas were treated by proton beams about 660 patients .

PROTON CYCLOTRON C235-V3

A cyclotron C235–V3, superior in its parameters to the medical proton cyclotron IBA C235 installed in 10 proton treatment centers of the world, has been design and manufactures by JINR-IBA collaboration. This cyclotron design is an essentially modified version of IBA C235 cyclotron [3-4] (Table 2).

Table 2 JINR-IBA cyclotron C235-V3

Parameter	C235	C235-V3
Optimization of magnetic field at modification of sector		Modification of sector azimuthal angle at R>80
Vertical betatron frequency at R>80	Qz=0,25	Qz=0,45
Vertical coherent beam displacement related to median plate effects	6-7 mm	1,5-2 mm
Beam losses at proton acceleration	50%	15%
Beam losses at extraction	50%	25%
Reduction of radiation dose of cyclotron elements		by 2-3 times

The one goal is to modify the sectors spiral angle at R>80 cm for improving of the cyclotron working diagram (Fig.1) and reduction of coherent beam losses at acceleration. The coherent beam displacement z from median plane is defined by vertical betatron tune Q_z: $z \propto Q_z^{-2}$. At $Q_z \approx 0.2$ the coherent beam displacement

ELLUS-6M LINEAR ELECTRON ACCELERATOR FOR RADIOTHERAPY

A.A. Budtov, M.F. Vorogushin, V.A. Shyshov#, FSUE "D.V. Efremov Scientific Research Institute of Electrophysical Apparatus", St. Petersburg, Russia
S.V. Kanaev, N.N. Petrov Scientific Research Oncology Institute, Pesochny, St. Petersburg, Russia

Abstract

"ELLUS-6M", a compact medical accelerator of new generation, has been designed and manufactured for radiotherapy by 6MeV photons in the multi-static and arc modes. The gantry of the accelerator can be rotated through $\pm 185^0$ and ensures setting accuracies of the irradiator rotation velocity and positioning sufficient for the IMRT mode. The computerized control system is compatible with the treatment planning system and allows upgrading by adding new modules.

To realize the conformal radiotherapy, the following additional medical equipment has been developed: a multi-leaf collimator, a portal vision system for the dose field verification during irradiation and an upgraded treatment table made as a semi-pantograph.

In 2010, it is planned to finish clinical tests of the "ELLUS-6M" accelerator with the additional medical equipment carried out in the N.N. Petrov Scientific Research Oncology Institute, Pesochny, St.Petersburg.

In countries with a highly-developed economics, radiotherapy is used for treatment of more than 70% of oncological patients, and more than 60% of such patients are usually successfully cured of cancer. In Russia, this method is used for treatment of less than 20% of the whole number of oncological patients, which mainly depends on insufficient up-to-date radiotherapeutic equipment available in oncologic institutions in our country Linear accelerators, which can be used for the conventional beam therapy, are about 80 in number, and only 20 machines are used for the conformal treatment. It is highly insufficient to satisfy the needs for these machines; for comparison, the international standards are 1 machine for 250-300 thousand people.

Nowadays in Russia have appeared all necessary prerequisites to change critically the status of radiotherapy. The Government of the Russian Federation has taken a decision on the financial support of activities aimed at the advancement of oncological treatment of the population and fitting out of oncological clinics with up-to-date equipment.

Development of electrophysical equipment for radiotherapy is one of high-priority lines of activity of FSUE "D.V. Efremov Scientific Research Institute of Electrophysical Apparatus". Several generations of accelerators and cyclotrons for medicine have been developed since the foundation of the Institute [1, 2]. A new generation of linear electron accelerators for radiotherapy has been developed by specialists of the Institute, one of these machines is a 6 MeV "ELLUS-6M" shown in figure 1.

Figure 1: The "ELLUS-6M" accelerator under technical tests; dose fields are being measured in a water phantom

The new accelerator is equipped with a computerized control system, demountable multileaf collimator to form bremsstrahlung fields with a high accuracy and a portal image-based verification system. The system for radiotherapy developed on the basis of the "ELLUS-6M" accelerator allows the most advanced technologies of the radiation oncology to be realized.

The main block of the accelerator is an irradiator, which includes systems and units for an electron beam generation and acceleration, its transport and forming in compliance with a particular treatment plan, as well as dose monitoring and verification of treatment prescription.

The beam is generated in a three-electrode electron source and injected into the accelerating structure, which is a chain of coupled cavities. A standing-wave accelerating structure is used in the "ELLUS-6M" accelerator. Simultaneously, the RF energy is supplied to the accelerating structure by a magnetron via the waveguide line.

#npkluts@niiefa.spb.su

MCC-30/15 CYCLOTRON – PARAMETERS, ADJUSTING WORKS AND THEIR RESULTS

P.V. Bogdanov, M.F. Vorogushin, A.V. Galchuk, V.G. Mudrolubov, A.P. Strokach#,
FSUE "D.V. Efremov Scientific Research Institute, of Electrophysical Apparatus",
Saint Petersburg, Russia

Abstract

The Medical Compact Cyclotron MCC-30/15 is intended for acceleration of hydrogen and deuterium negative ions in the energy control range. The Cyclotron was designed in the frame of the Contract for the delivery of the MCC-30/15 cyclotron equipment to the Accelerator Laboratory of the Jyvaskyla University, Finland.

The Cyclotron is built up on the basis of a shielded-type electromagnet with a pole diameter of 140 cm. The Cyclotron is equipped with the external injection system of negative hydrogen and deuterium ions.

Particles are accelerated at a fixed frequency (the 2nd and 4th harmonics). The beam current of 30-18 MeV protons and 15-9 MeV deuterons extracted into two beam lines is more than 100 μA and 50 μA, respectively.

The Cyclotron equipment has been delivered to the Buyer; the commissioning works were finished on April 30, 2010.

THE MAIN DESIGN FEATURES OF THE CYCLOTRON

The designing of the MCC-30/15 cyclotron was started in 2007 after signing the Contract for the cyclotron delivery to the Jyvaskyla University, Finland. The main cyclotron characteristics were agreed upon with the Customer: the cyclotron must be equipped with an external ion injection system, the negative ions of hydrogen and deuterium must be accelerated up to an energy of 30/15 MeV with an energy control range of 60-100% of the ions maximum energy, the cyclotron beam are to be extracted by negative ion stripping on thin carbon foils to two beam lines with a possibility to irradiate two targets simultaneously. The maximum beam current was defined to be 100 microamperes for protons and 50 microamperes for deuterons.

When designing the cyclotron, the positive experience gained when designing and commissioning the CC-18/9 cyclotron at the Abo Academy PET Center (Turku, Finland) in 2006 was used. A series of basic engineering solutions were applied, in particular, the external multicasp source of negative hydrogen and deuterium ions, the RF field frequency similar for both types of ions, the vertical location of the beam acceleration and extraction plane, which gives an operator an easy access to in-chamber units and injection system for maintenance/repair in the process of exploitation. A software package previously applied on the CC-18/9 cyclotron was used for 3D calculations of the cyclotron magnetic and accelerating RF systems.

While elaborating the Technical Project, a Planning Information document for the layout of the cyclotron equipment was worked out. On the basis of this document, the works on elaboration of construction documentation and on building the rooms to house the cyclotron equipment have been finished by the Finnish side for two years.

THE CYCLOTRON MAGNETIC FIELD

3-D calculations of the cyclotron magnetic field were performed to provide isochronous magnetic fields required for the acceleration of two particles, hydrogen and deuterium ions. The calculations were carried out by the method of successive iterations. The magnet pole geometry and corresponding magnetic field in the acceleration area were defined from the beam dynamics calculations [1].

Two magnetic fields needed for isochronous acceleration of hydrogen and deuteron ions were formed in the following way. The rotating shims placed into two cyclotron valleys free of dees were used when changing from one accelerating mode to another. In the acceleration mode of deuteron ions, these shims were placed completely inside the magnet pole. The pole sector sides were provided with plates of small azimuth length, which shape was chosen when forming the isochronous field for the deuteron ion acceleration. If hydrogen ions are accelerated, the magnetic shims are rotated so that the magnetic masses enter the magnet gap thus providing the magnetic field increase along the radius. The required isochronous radial dependence was provided by adjusting the shim generatrix.

Use of the shims located in two cyclotron valleys free of dees results in the appearance of the 2nd harmonic of the magnetic field. To decrease its value, two fixed shims were additionally placed into two other valleys. In the deuteron ion acceleration mode with these fixed shims, the 2nd harmonic of the magnetic field appeared and the 2nd harmonic in the hydrogen ion acceleration mode decreased respectively.

The carried out calculations of the beam dynamics have shown that the 2nd harmonic of the magnetic field of the 500 Gs amplitude does not affect the accelerated beam stability and does not increase the radial emmitance of the beam.

Radial distributions of the measured average magnetic field are shown in figs. 1-2.

#npkluts@niiefa.spb.su

STATUS OF ILU-14 ELECTRON ACCELERATOR

V.S.Podobaev#, V.V. Bezuglov, A.A. Bryazgin, K.N. Chernov, V.G. Cheskidov, B.L. Faktorovich, V.A. Gorbunov, I.V. Gornakov, A.V. Ivanov, E.N. Kokin, M.V. Korobeynikov, A.N. Lukin, I.G. Makarov, N.V. Matyash, S.A. Maximov, G.N.Ostreiko, A.D. Panfilov, V.M. Radchenko, N.D. Romashko, G.V. Serdobintsev, A.V. Sidorov, V.V. Tarnetsky, M.A. Tiunov, V.O. Tkachenko
BINP SB RAS, 630090, Novosibirsk, Russia.

Abstract

A new high power (up to 100 kW) industrial linear electron accelerator ILU-14 for energy of 7.5–10 MeV is under construction at Budker INP. The accelerator operates at 176 MHz with total efficiency of 26 %, its modular structure allows the electron energy and beam current to be varied within certain limits by changing the modular arrangement. The 5 MeV prototype of the accelerator was created and successfully tested in 2009. The designed average beam current of 600 mA with pulsed power of 2.5 MW and accelerating structure electron efficiency of 68 % were obtained during experiments. Applying an additional RF voltage to the electron gun cathode-grid gap allowed a beam current passing of 96 % with minor beam energy spread. The paper presents results of the numerical and experimental study of the accelerator systems together with the latest tests on the accelerator prototype.

INTRODUCTION

A new powerful (up to 100 kW) industrial electron accelerator with energy range from 7.5 to 10 MeV was designed in BINP SB RAS [1-3]. This model was named ILU-14 and can be used in electron and bremsstrahlung modes. This accelerator has all basic features of ILU-type accelerators like internal injection type and using of autogenerator for RF power feeding, but has also some its own features. On the base of ILU-14 it planned to produce a line of simple and effective accelerators, which can compete with existent industrial accelerators in this energy range.

IDEA OF ILU-14 ACCELERATOR

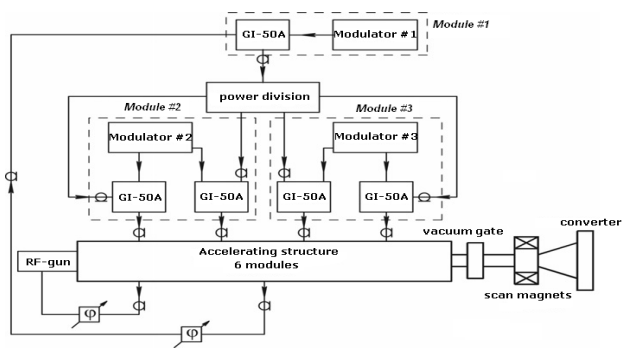

Fig.1. Block scheme of ILU-14

The main elements of the accelerator are: accelerating structure, triode RF-gun, two-cascade autogenerator, feeder system, RF power inputs, modulators, scan magnets system and converter (in the case of bremsstrahlung mode operating) (Fig.1).

In ILU-14 (in comparison with other powerful impulse linear accelerators) some features were realized.

The first feature of it is using of low-frequency many-resonator structure on standing wave with coupling resonators on the axis. The accelerating structure is assembled from separate modules with using of indium vacuum seals. The module consists of one coupling resonator and two half accelerating resonators (Fig. 2-A). Accelerating structure, used for electron accelerating to the energy up to 10 MeV, consists of 6 such modules (Fig.2-B).

The structure is excited by autogenerator, based on powerful pulse triodes GI-50A, which provide competitive efficiency to the accelerator.

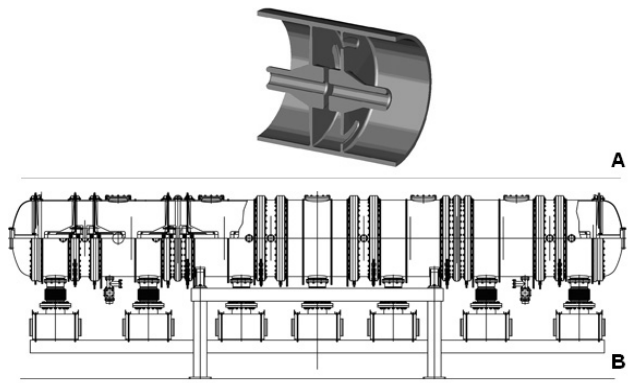

Fig.2. ILU-14 units. A-The module of accelerating structure. B-General view of accelerating structure

The second feature of the low-frequency accelerator is the using of triode RF-gun with specially designed for it grid with high transmissivity as an injector. RF-gun is placed directly in the first accelerating gap. Narrow energy spectrum of electron beam, which is necessary for effective conversion its power to bremsstrahlung and beam conducting through the structure with small losses are provided by feeding of grid-cathode unit of the RF-gun by additional RF-voltage.

The third feature is using of two-cascade autogenerator with feedback through accelerating structure. This feature allows operating of the accelerator without frequency stabilization system of structure or generator. As a result, the generator and accelerator control system are simple enough.

The fourth feature is the module construction of ILU-14. Separate modules are assembled by using of serial units, designed in the experimental plant of BINP.